319.11

UNCLASSIFIED

3466 (3807

3466 (3807)

1A

[redacted]

DO NOT CIRCULATE
Retention Copy

LA - 1021

[redacted]

August 13, 1947 [redacted]

VOLUME VII

BLAST WAVE

Part II

Chapters 5 through 10

Edited by

Hans A. Bethe

UNCLASSIFIED

[redacted]

1694
17

VOLUME 7

BLAST WAVE

Volume Editor: H. Bethe

TABLE OF CONTENTS

Part II (LA -1021)

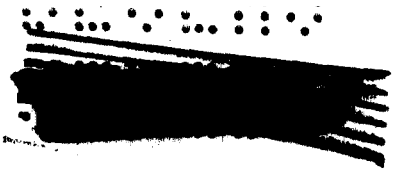

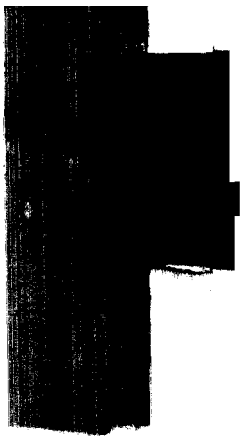

CHAPTER 5

APPROXIMATION FOR SMALL $\gamma - 1$

H. A. Bethe

5.1 GENERAL PROCEDURE

The solution given in Chapter 2 is only valid for an exact point source explosion, for constant γ, for constant undisturbed density of the medium and for very high shock pressures. It is very desirable to find a method which permits the treatment of somewhat more general shock wave problems and thereby comes closer to describing a real shock wave. The clue to such a method is found in the very peculiar nature of the point source solution of Taylor and von Neumann. It is characteristic for that solution that the density is extremely low in the inner regions and is high only in the immediate neighborhood of the shock front. Similarly, the pressure is almost exactly constant inside a radius of about .8 of the radius of the shock wave.

It is particularly the first of these facts that is relevant for constructing a more general method. The physical situation is that the material behind the shock moves outward with a high velocity. Therefore the material streams away from the center of the shock wave and creates a high vacuum near the center. The absence of any appreciable amount of material, together with the moderate size of the accelerations, immediately leads to the conclusion that the pressure must be very nearly constant in the region of low density. It is interesting to note that the pressure in that region is by no means zero, but is almost 1/2 of the pressure at the shock front.

The concentration of material near the shock front and the corresponding

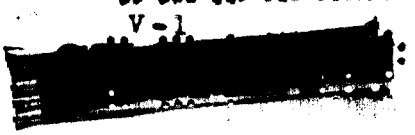

evacuation of the region near the center is most pronounced for values of the specific heat ratio γ close to 1. It is well known that the density at the shock increases by a factor

$$\frac{\rho_s}{\rho_0} = \frac{\gamma + 1}{\gamma - 1} \tag{1}$$

This becomes infinite as γ approaches unity. Therefore, for γ near 1 the assumption that all material is concentrated near the shock front becomes more and more valid. The density near the center can be shown to behave as $r^{3/(\gamma-1)}$.

The idea of the method proposed here, is to make repeated use of the fact that the material is concentrated near the shock front. As a consequence of this fact, the velocity of nearly all the material will be the same as the velocity of the material directly behind the front. Moreover, if γ is near 1, the material velocity behind the front is very nearly equal to the shock velocity itself; the two quantities differ only by a factor $2/(\gamma+1)$. The acceleration of almost all the material is then equal to the acceleration of the shock wave; knowing the acceleration one can calculate the pressure distribution in terms of the material coordinate, i.e., the amount of air inside a given radius. This calculation again is facilitated by the fact that nearly all the material is at the shock front and therefore has the same position in space (Eulerian coordinate).

The procedure followed is then simply this. We start from the assumption that all material is concentrated at the shock front. We obtain the pressure distribution. From the relation between pressure and density along an adiabatic, we can obtain the density of each material element if we know its pressure at the present time as well as when it was first hit by the shock. By integration of the density we can then find a more accurate value for the

position of each mass element. This process could be repeated if required; it would then lead to a power series in powers of $\gamma - 1$.

The method leads directly to a relation between the shock acceleration, the shock pressure and the internal pressure near the center of the shock wave. In order to obtain a differential equation for the position of the shock as a function of time, we have to use two additional facts. One is the Hugoniot relation between shock pressure and shock velocity. The other is energy conservation in some form: in some applications such as that to the point source solution itself, we may use the conservation of the total energy which requires that the shock pressure decreases inversely as the cube of the shock radius (similarity law). On the other hand, if there is a central isothermal sphere as described in the last chapter, no similarity law holds, but we may consider the adiabatic expansion of the isothermal sphere and thus determine the decrease of the central pressure as a function of the radius of the isothermal sphere. If we wish to apply the method to the case of variable γ without isothermal sphere we may again use the conservation of total energy but in this case the pressure will not be simply proportional to $1/r^3$.

As has already been indicated, the applications of the method are very numerous. The case of not very high shock pressures can also be included; in this case the density behind the shock wave does not have the limiting value of Equation (1) but depends itself on the shock pressure. This does not prevent the application of our method as long as the density increase at the shock is still very large so that most of the material is still near the shock front.

The only limitations of the method are its moderate accuracy and the possible complications of the numerical work. The accuracy seems satisfactory up to γ about 1.4. For the point source, a direct comparison with the

exact solution is possible.

5.2 GENERAL EQUATIONS

We shall denote the initial position of an arbitrary mass element by r, and the position at time t by R. The position of the shock wave will be denoted by Y. The density at time t is denoted by ρ, the initial density by ρ_0. The pressure is $p(r,t)$ and the pressure behind the shock is $p_s(Y)$.

The continuity equation takes the simple form

$$\rho R^2 \, dR = \rho_0 \, r^2 \, dr \tag{2}$$

From this we have

$$\frac{\partial R}{\partial r} = \frac{\rho_0}{\rho} \frac{r^2}{R^2} \tag{3}$$

The equation of motion becomes simply

$$\frac{d^2R}{dt^2} = -\frac{1}{\rho}\frac{\partial p}{\partial R} = -\frac{R^2}{\rho_0 r^2}\frac{\partial p}{\partial r} \tag{4}$$

The pressure for any given material element is connected with its density by the adiabatic law (conservation of energy). The particular adiabat to be taken is determined by the condition of the material element after it has been hit by the shock. If we assume constant γ the adiabatic relation gives

$$p(r,t) = p_s(r)\left(\frac{\rho(r,t)}{\rho_s}\right)^{\gamma} \tag{5}$$

We shall use this relation mostly to determine the density from the given pressure distribution. Using Equation (1) for the density behind the shock ρ_s, and the continuity Equation (2), we find

$$\frac{\partial R}{\partial r} = \frac{r^2}{R^2}\frac{\rho_0}{\rho} = \frac{\gamma-1}{\gamma+1}\frac{r^2}{R^2}\left(\frac{p_s(r)}{p(r,t)}\right)^{1/\gamma} \qquad (6)$$

The three conservation laws, (2), (4) and (6), must be supplemented by the Hugoniot equations at the shock front which are known to be, themselves, consequences of the same conservation laws. These relations give for the density at the shock front the result already quoted in Equation (1), for the relation between shock pressure and shock velocity $\dot{Y}$:

$$\frac{p_s(Y)}{\rho_0} = \frac{2}{\gamma+1}\dot{Y}^2 \qquad (7)$$

and for the relation between the material velocity behind the shock, $\dot{R}$, and the shock velocity, $\dot{Y}$:

$$\dot{R} = 2\dot{Y}/(\gamma+1) \qquad (8)$$

The problem will now be to solve these eight equations for particular cases with the assumption that γ is close to 1. Then Equation (4) reduces to

$$\frac{1}{r^2}\frac{\partial p}{\partial r} = -\rho_0\frac{\ddot{Y}}{Y^2} \qquad (9)$$

On the right hand side of this equation we have used the fact discussed in the last section that practically all the material is very near the shock front. Therefore the position R can be identified with the position of the shock Y, and the acceleration $\ddot{R}$ with the shock acceleration $\ddot{Y}$. Since the right hand side of Equation (9) is independent of r, it integrates immediately to give

$$p(r,t) = p_s(Y) + \rho_0\frac{\ddot{Y}}{3Y^2}(Y^3 - r^3) \qquad (10)$$

If we use the Hugoniot relation (7) and put $\gamma = 1$ in that relation we find further

$$\frac{p(r,t)}{\rho_0} = \dot{Y}^2 + \frac{\ddot{Y}}{3Y^3}\left(Y^3 - r^3\right) \qquad (11)$$

This equation gives the pressure distribution at any time in terms of the position, velocity and acceleration of the shock.

Of particular interest is the relation between the shock pressure and the pressure at the center of the shock wave. This relation is obtained by putting $r = 0$ in Equation (10). Then we get

$$p(o,t)/\rho_0 = \dot{Y}^2 + Y\ddot{Y}/3 \qquad (12)$$

The pressure near the center is in general smaller than the pressure at the shock because $\ddot{Y}$ is in general negative.

It can be seen that the derivation given here is even more general than was stated. In particular, it applies also to a medium which has initially non-uniform density. It is only necessary to replace $\rho_0 r^3$ by the mass enclosed in the sphere r (except for the factor $4\pi/3$).

From the pressure distribution (11) we can obtain the density or the position R using Equation (6). The remaining problem is now to calculate this density distribution explicitly, and to determine the motion of the shock wave in particular cases.

5.3 THE POINT SOURCE

The simplest application of the general theory developed in the last section is to a point source explosion. In this case, the theory of von Neumann and G. I. Taylor is available for comparison.

Equation (12) gives a relation between various quantities referring to the shock and the pressure at the center of the shock wave. To make any further progress we have to use the conservation of total energy in the

Table 5.3

γ =	1	1.1	1.2	1.4	1.67	2
$p(0)/p_s$ =	.500	.462	.424	.368	.306	.251
$(\gamma-1)\, E/\rho_0 A$ =	2.094	2.152	2.148	2.144	2.05	1.96

With the relation of internal and shock pressure known, we can now calculate the total potential energy content. We know that the potential energy per unit volume is $p/(\gamma-1)$. We further know from Equation (11) that the pressure is constant and equal to $p(0)$ over the entire region which is nearly free of matter. Moreover, we know that all the matter is concentrated in a very thin shell near the shock front. Therefore, with the exception of a very small fraction of the volume occupied by the shock wave, the pressure is equal to the interior pressure. The total energy is then

$$E = \frac{4\pi}{3}\,\frac{Y^3\, p(0)}{\gamma-1} = \frac{2\pi}{3}\,\frac{Y^3 p_s}{\gamma-1}$$

$$= \frac{2\pi}{3}\,\frac{\rho_0}{\gamma-1}\, Y^3 \cdot Y^2 = \frac{2\pi}{3}\,\frac{\rho_0 A}{\gamma-1} \qquad (17)$$

(cf. Equation (13))

In the last line of Table 5.3, above, we give the exact numerical factor in last expression in (17), according to calculations of Hirschfelder. It is seen that this factor is very close to $2\pi/3$, for all values of γ up to 1.4. This is due to a compensation of various errors. The internal pressure is actually less than 1/2 of the shock pressure, but this is compensated by the fact that the pressure near the shock front is higher than the internal pressure. Indeed, the ratio of the volume average of the pressure to the shock pressure is much closer to 1/2 than the corresponding ratio for the internal pressure (cf. Equations 31a, 31b). A further error which has been made in Equation (17) is that the factor $2/(\gamma+1)$ has been neglected in

shock wave. Since there is no characteristic length, time, or pressure involved in the problem, the blast wave from a point source explosion must obey a similarity law as has been pointed out by Taylor and von Neumann. In other words, the pressure distribution will always have the same form; only the peak pressure and the scale of the spatial distribution will change as the shock wave moves out. Now the energy is mainly potential energy (1)

(1) This assumption is not necessary for the validity of the following equations.

if γ is close to 1; the potential energy per unit volume is $p/(\gamma - 1)$ and therefore the total potential energy will be proportional to $p_s Y^3/(\gamma - 1)$. Therefore p_s and $\dot{Y}^2$ (cf. Equation (7)) will be inversely proportional to Y^3. This gives immediately the equation

$$\dot{Y}^2 = AY^{-3} \tag{13}$$

where A is a constant related to the total energy. Integration gives

$$Y = (5/2)^{2/5} A^{1/5} t^{2/5} \tag{14}$$

and differentiation gives

$$Y \ddot{Y} = -(3/2) \dot{Y}^2 \tag{15}$$

Inserting this in Equation (12) we find immediately

$$\frac{p(0,t)}{\rho_0} = \frac{1}{2} \dot{Y}^2 = \frac{1}{2} \frac{p_s}{\rho_0} \tag{16}$$

Therefore in the limit of γ close to 1, the internal pressure is just 1/2 of the shock pressure. This can be compared with the numerical result of von Neumann's theory which gives the following values for the ratio of internal pressure to shock pressure:

Equation (7). On the other hand, the kinetic energy has been neglected. This kinetic energy is very nearly equal to

$$E_{kin} = \frac{2\pi}{3} \rho_0 \quad Y^3 \dot{Y}^2 \quad = \quad (\gamma - 1) \quad E \tag{18}$$

because all the material moves almost with the shock velocity $\dot{Y}$. It is seen that this kinetic energy is small compared with the potential energy by a factor $\gamma - 1$; this justifies our neglect of the kinetic energy along with a large number of other quantities of the relative order $\gamma - 1$. It is, of course, only an accident that there is almost exact compensation of all these neglected terms up to values of γ as high as 5/3.

We can now use our result to obtain the density distribution of the matter behind the shock front. We need only apply Equations (6) and (11) to (16) and find

$$\frac{\rho_e}{\rho} = \frac{\gamma - 1}{\gamma + 1} \left(\frac{p_s(r)}{p(r,Y)} \right)^{1/\gamma} = \frac{\gamma - 1}{\gamma + 1} \left(\frac{2}{x(1+x)} \right)^{1/\gamma} \tag{19}$$

with

$$x = r^3/Y^3 \tag{19a}$$

Setting also

$$y = R^3/Y^3 \ , \tag{19b}$$

Equation (6) becomes

$$\frac{dy}{dx} = \frac{\gamma - 1}{\gamma + 1} \left(\frac{2}{x(1+x)} \right)^{1/\gamma} \tag{20}$$

to integrate this equation, it is convenient to distinguish two cases:

(1) If x is not too small, more precisely for

$$x \gg e^{-1/(\gamma - 1)} \tag{20a}$$

we may consider the exponent in (20) as equal to 1 since $\gamma - 1$ is assumed small. Then, neglecting quantities of order $(\gamma - 1)^2$, integration of (20) gives

$$y = \frac{R^3}{Y^3} = 1 - (\gamma - 1) \log \frac{1 + x}{2x} = 1 - (\gamma - 1) \log \frac{Y^3 + r^3}{2r^3} \qquad (21)$$

(2) If

$$x \ll 1 \qquad (21a)$$

we may neglect x compared to 1. Then, neglecting quantities of relative order $\gamma - 1$, we get

$$\begin{aligned} dy &= (\gamma - 1)\, x^{-1/\gamma}\, dx \\ y &= x^{(\gamma - 1)/\gamma} + A \end{aligned} \qquad (22)$$

where A is a constant. The regions defined by (20a) and (21a) overlap very considerably. Comparing (21) and (22) we find that

$$A = 0, \qquad (22a)$$

neglecting a small term of order $\gamma - 1$. This value of A will make (22) sensible for small values of x. Inserting (19a), (19b), we get

$$R = Y^{1/\gamma} r^{1 - (1/\gamma)} \qquad (23)$$

or

$$R/Y = (r/Y)^{(\gamma - 1)/\gamma} \qquad (23a)$$

From the position of any point we can deduce the velocity by a simple differentiation with respect to time. In this process, the material coordinate r should be kept constant. Equation (23) gives for the material velocity

(neglecting terms of order $\gamma - 1$)

$$\dot{R} = \frac{\dot{Y}}{\gamma}\left(\frac{r}{Y}\right)^{\frac{\gamma-1}{\gamma}} \approx \dot{Y}\,\frac{R}{Y} \qquad (24)$$

Over most of the volume the material velocity is nearly linear in R which is borne out by the numerical integrations of the exact solution (see Chapter 2). Over most of the mass the material velocity is nearly equal to the velocity of the shock wave.

5.4 COMPARISON OF THE POINT SOURCE RESULTS WITH THE EXACT SOLUTION.

The results obtained in the last section can be compared with the exact solution described in Chapter 2. The results of that chapter can very easily be applied to the special case when γ is very nearly 1.

In going to this limit one should keep the exponent of θ correct because this quantity goes from 0 to 1, and if it is close to 0 a factor $\theta^{\gamma-1}$ will matter. In all other factors the base of the power becomes $(\theta + 1)/2$ in the limit $\gamma = 1$, which goes over the range from 1/2 to 1 and therefore never becomes very small. Consequently $\gamma - 1$ may be neglected in the exponent of these other factors except if higher accuracy is desired.

Neglecting small quantities in this manner, Equation (2.37) reduces to

$$r/Y = Z = \theta^{\frac{\gamma}{2\gamma+1}} \approx \theta^{1/3} \qquad (25)$$

Z and θ being the notations used in Chapter 2.

(25) may be rewritten

$$\theta = Z^3 = (r/Y)^3 \qquad (25a)$$

Equation (2.38) becomes then

$$R/Y = F = \theta^{\frac{\gamma-1}{2\gamma+1}} = (r/Y)^{\frac{\gamma-1}{\gamma+1}} \qquad (26)$$

This result for the Eulerian position is identical with that obtained from

our approximate theory in Equation (23a). A more accurate evaluation, keeping terms of relative order $\gamma - 1$ throughout, gives

$$F = \left(\frac{2\theta}{\theta + 1}\right)^{\frac{\gamma-1}{2\gamma+1}} \tag{26a}$$

For the pressure we find from Equation (2.41) in the limit $\gamma \to 1$ the result

$$p = p_s \frac{\theta + 1}{2} + \frac{1}{2} p_s \left[1 + \left(\frac{r}{Y}\right)^3\right] \tag{27}$$

This again is identical with the result of our approximate theory given in Equation (11) and Equation (15). Again, a more accurate evaluation, neglecting only terms of relative order $(\gamma - 1)^2$, gives:

$$\frac{p}{p_s} = \frac{\theta + 1}{2} \left[1 + 2\delta \ln \frac{\theta + 1}{2} + \delta\left(\frac{1}{\theta + 1} - \frac{1}{2}\right)\right] \tag{28}$$

with the abbreviation

$$\delta = \gamma - 1 \tag{28a}$$

Of particular interest is the relation between the total energy and such quantities as the shock pressure. We shall therefore calculate this relation including terms of relative order $\gamma - 1$. First of all, we shall calculate the potential (heat) energy:

$$E_{pot.} = 4\pi \int_0^Y R^2 \, dR \; p/(\gamma - 1) \tag{29}$$

$$= \frac{4\pi}{3} \frac{Y^3 p_s}{\gamma - 1} \int_0^1 d(F^3) \frac{p}{p_s}$$

Using (26a) and (28a), we have

$$d(F^3) = d\left(\theta^\delta \left(\frac{\theta+1}{2}\right)^{-\delta}\right)$$
$$= \left[d(\theta^\delta) - \delta \frac{d\theta}{\theta+1}\right]\left(1 - \delta \ln \frac{\theta+1}{2}\right) \qquad (29a)$$

neglecting[2] terms of relative order δ^2. Inserting (29a) and p from (28) into (29), we get

$$I = 2\int_0^1 d(F^3)\frac{p}{p_s} = \int_0^1 \left[d(\theta^\delta) - \delta\frac{d\theta}{\theta+1}\right](\theta+1)\cdot$$
$$\cdot\left[1 + \delta\left(\ln\frac{\theta+1}{2} + \frac{1}{\theta+1} - \frac{1}{2}\right)\right] \qquad (30)$$

This integral can be evaluated very easily. We note that θ^δ changes from 0 to 1 at very small values of θ so that in first approximation for this part of the integral, the integrand should be taken at $\theta = 0$. (This corresponds to the physical fact that most of the material is near the shock front, $F^3 = \theta^\delta$ becomes close to 1 already for relatively small values of θ or of the material coordinate $Z = \theta^{1/3}$). Evaluation of (30) gives

$$I = 1 + \delta\left(\ln\frac{1}{2} + 1 - \frac{1}{2}\right) + \delta - \delta \qquad (30a)$$

or

$$E_{pot.} = \frac{2\pi}{3}\frac{p_s Y^3}{\gamma-1}\left[1 + \delta\left(\frac{1}{2} - \ln 2\right)\right] \qquad (31)$$

This result, except for the last factor, is identical with the result

---

(2) It is permissible to set the factor θ^δ which should appear in the second term in the square bracket, equal to one; the error in (29) is only of order of δ^2.

of our approximate theory, Equation (17). The last factor is seen to differ only very slightly from 1, the factor of δ being only -0.2. It is of some interest to define the average pressure (volume average); this is according to (31):

$$p_{A0} = \frac{1}{2} p_s \left[1 + \delta \left(\frac{1}{2} - \ln 2 \right) \right] = \frac{1}{2} p_s \left[1 - .193\, \delta \right] \tag{31a}$$

This may be compared with the central pressure (cf. (28))

$$p(0) = \frac{1}{2} p_s \left[1 + \delta \left(\frac{1}{2} - \ln 4 \right) \right] = \frac{1}{2} p_s \left[1 - .886\, \delta \right] \tag{31b}$$

The average pressure is, of course, higher than the central pressure; it differs from it only in the order δ as is to be expected; and it is much closer to one-half the shock pressure than the central pressure is.

Now let us calculate the kinetic energy. According to (2.46), the ratio of kinetic to potential energy in any mass element is θ, therefore

$$\begin{aligned} E_{kin} &= \frac{4\pi}{3} \frac{Y^3 p_s}{\gamma - 1} \int_0^1 d(F^3) \frac{p}{p_s} \theta \\ &= \frac{2\pi}{3} \frac{Y^3 p_s}{\gamma - 1} \int_0^1 \delta \; d\theta \left(\frac{1}{\theta} - \frac{1}{\theta + 1} \right) (\theta + 1) \theta \\ &= \frac{2\pi}{3} Y^3 p_s \end{aligned} \tag{32}$$

The simplifications in this integral, i.e. neglect of the last square bracket in (30) and replacement of $d(\theta^\delta)$ by $\delta d\theta/\theta$, are possible because of the factor θ in the integrand. This also makes the integral of order δ. The result (32) agrees with that of the approximate theory, (18).

Adding (31) and (32), we find for the total energy

$$E = \frac{2\pi}{3} \frac{p_s Y^3}{\gamma - 1} \left[1 + \delta \left(\frac{3}{2} - \ln 2 \right) \right] \tag{33}$$

This gives the shock pressure as a function of the radius including terms of relative order $\gamma - 1$ which will be useful for the calculation of the waste energy. We may also replace p_s by the shock velocity $\dot{Y}$ according to (7):

$$E = \frac{2\pi}{3}\rho\frac{Y^3\dot{Y}^2}{\gamma-1}\left[1+\delta\left(1-\ln 2\right)\right] \tag{33a}$$

Here again the correction factor in the square bracket differs only slightly from 1, in agreement with the numerical results reported in Table 5.3.

A further quantity of interest is $\partial R/\partial r = dF/da$ for which Equation (2.37) gives the result

$$\frac{\partial R}{\partial r} = F' = \frac{\gamma-1}{\gamma+1}\,\theta^{-1/3}\left(\frac{\theta+1}{2}\right)^{-1} \tag{34}$$

From this expression or directly from Equation (2.39) we can find the density which turns out to be

$$\frac{\rho}{\rho_0} = \frac{\gamma+1}{\gamma-1}\,\theta^{\frac{3}{2\gamma+1}}\,\frac{\theta+1}{2} = \frac{\gamma+1}{\gamma-1}\,z^{3/\gamma}\,\frac{1+z^3}{2} \tag{35}$$

We can also express this density in terms of the Eulerian position in which case we get from (26)

$$\frac{\rho}{\rho_0} = \frac{\gamma+1}{\gamma-1}\left(\frac{R}{Y}\right)^{3/(\gamma-1)}\frac{1}{2}\left(1+z^3\right) \tag{35a}$$

This equation shows that the density becomes extremely low for all points away from the shock front even if they are only moderately close to the center of the explosion. This is in agreement with our basic assumption that most of the material is concentrated near the shock front.

Finally combining (2.38) and (2.40) we find in the limit $\gamma = 1$

$$\frac{u}{R} = \frac{2}{5t} \tag{36}$$

However, from the similarity solution we know that

$$Y = a\, t^{2/5} \tag{36a}$$

where a is a constant, and therefore

$$\frac{u}{R} = \frac{\dot{Y}}{Y} \tag{36b}$$

This result is again identical with the result of our approximate theory given in Equation (24).

We see, therefore, that our approximate solution is identical with the limit of the exact solution of the point source for $\gamma = 1$ if terms of the relative order $\gamma - 1$ are consistently neglected.

5.5 THE CASE OF THE ISOTHERMAL SPHERE

We shall now consider the somewhat more complicated problem of the production of a shock wave by a sphere which is initially heated to a high uniform temperature and then exerts pressure on its surroundings. The relevance of this problem of the isothermal sphere has been discussed in Chapters 1 and 4 and is connected with the great influence of energy transport by radiation.

The problem now no longer permits the application of similarity arguments. For this reason we can no longer use the conservation of total energy to advantage. Instead of this we can now assume adiabatic expansion of the isothermal sphere. This is completely equivalent to an application of the energy conservation law because the adiabatic law itself is based on the assumption that there is no energy transport out of the isothermal sphere.

Let us assume that the material coordinate of the surface of the isothermal sphere is r_o. The initial position of this surface is then equal to r_o. At a later time when the isothermal sphere has expanded to R_o its average density has decreased by a factor $(r_o/R_o)^3$. If we assume that the

density and pressure in the isothermal sphere are uniform, the pressure will be equal to

$$P_0 = P\,(r_0 / R_0)^{3\gamma} \tag{37}$$

where P is the initial pressure in the isothermal sphere which is related to the total energy by the equation

$$E = \frac{4\pi}{3} \frac{P r_0^3}{\gamma - 1} \tag{37a}$$

We shall now proceed in two steps. First of all we shall consider the case when the radius of the shock wave is not extremely great compared with the initial radius of the isothermal sphere, more precisely

$$Y/r_0 \ll e^{1/(\gamma-1)} \tag{37b}$$

We shall show that with this assumption the solution with an isothermal sphere approaches the point source solution as Y/r_0 increases. Afterwards, for large values of Y/r_0 where (37b) is not valid, the approximations used in the first part of our calculation will break down; but we can then use the results of the last section to obtain R_0/Y for the surface of the isothermal sphere, and this will enable us to solve the problem for the case of large values of Y/r_0.

(1) Case I: Y/r_0 Moderate

If Y/r_0 is not very great we can replace the exponent 3γ in Equation (37) by 3. At the same time we can use our general assumption that practically all material is close to the shock front and that, therefore, R_0 is very nearly equal to Y. With this approximation we find from Equation (12)

$$\dot{Y}^2 + \frac{Y\ddot{Y}}{3} = \frac{P r_0^3}{\rho_0} Y^{-3} \tag{38}$$

This equation can be integrated without difficulty by setting

$$\dot{Y}^2 = \varphi(Y) \tag{39}$$

and

$$P r_o^{3\gamma/\rho_o} = A = \frac{3(\gamma-1)}{4\pi} \frac{E}{\rho_o} \tag{39a}$$

Then

$$\ddot{Y} = \frac{1}{2} \frac{d\varphi}{dY} \tag{39b}$$

Then Equation (38) becomes

$$\varphi + \frac{1}{6} Y \frac{d\varphi}{dY} = A Y^{-3} \tag{40}$$

This can be integrated and gives

$$\varphi Y^6 = 2 A Y^3 + B \tag{41}$$

where B is a new constant.

Now the initial condition is, for $Y = r_o$:

$$\frac{p_s}{\rho_o} = \dot{Y}^2 = \frac{P}{\rho_o} \tag{42}$$

or, with (39) and (39a):

$$\varphi(r_o)\, r_o^3 = A \tag{42a}$$

so that

$$B = -A r_o^3 \tag{42b}$$

and finally

$$p_s = \rho_o \dot{Y}^2 = \rho_o A \left(\frac{2}{Y^3} - \frac{r_o^3}{Y^6} \right) \tag{43}$$

$$= \frac{3(\gamma-1)}{2\pi} \frac{E}{Y^3} \left(1 - \frac{r_o^3}{2 Y^3} \right)$$

Equation (43) shows that for large values of Y/r_o, the shock pressure p_s approaches the value given in Equation (17), i.e. the value corresponding to the point source solution. This result appears rather important because it shows: (1) that the point source solution is stable and is approached even under conditions which initially deviate strongly from those assumed in the point source solution, and (2) that the simple and well-known point source solution can be used at late times for our problem including the isothermal sphere.

(2) Case II: Y/r_o Large

We know from the discussion of Case I that our solution approaches the point source solution as soon as $Y/r_o \gg 1$. We can then use Equation (23) for the position R_o of the surface of the isothermal sphere, and obtain, neglecting terms of second order in $\gamma - 1$:

$$p_o = p \frac{r_o^{3\gamma}}{Y^3 r_o^{3\gamma-3}} = p\left(\frac{r_o}{Y}\right)^3 \qquad (44)$$

This is the same expression which we used in Case I and which we then justified simply by neglecting γ in the exponent of (25). Therefore the further development is identical with that leading to Equation (43).

We have thus shown that Equation (43) is valid both for small and for large expansions of the isothermal sphere. It is possible to derive the density distribution, the position and the velocity, as we did in the previous section for a point source case. However, the analytical expressions are fairly involved and there does not seem to be any particular application for them. The ratio of the shock pressure to the central pressure in the isothermal sphere is according to (43) and (35):

$$p_s/p_o = 2 - r_o^3/Y^3 \qquad (44a)$$

It changes from 1 in the very early stages to 2 in the late stages. At any reasonably late stage the energy in the blast is related to the velocity of the shock front in the same way as for the point source solution.

5.6 VARIABLE GAMMA

The theory developed here can be used to solve the problem of a shock wave in a medium with variable γ. The assumption is, of course, that $\gamma - 1$ still remains small throughout. We also assume that the shock pressure is high enough so that the Hugoniot relations hold in their limiting form.

We shall make the further simplifying assumption that γ is a function of the entropy only, so that it remains constant for any given mass element r as soon as that element has been traversed by the shock. This assumption is fairly well fulfilled by air, with the value of γ decreasing from 1.4 to about 1.2 with increasing entropy, and later on increasing again to 1.67. The more general problem in which γ is a function both of the entropy and the density can also be solved by the same method, but the algebra becomes so involved that it seems hardly worth-while to use the present method instead of direct numerical integration.

The pressure distribution Equation (11) will still be valid. However, the relation between Y, $\dot{Y}$, and $\ddot{Y}$ will no longer be given by Equation (15). We introduce the pressure at the front and the pressure at the center of the shock wave separately by writing

$$p_s = \frac{3}{2\pi} \frac{E}{Y^3} \alpha$$

$$p(0) = \frac{3}{4\pi} \frac{E}{Y^3} \beta \qquad (45)$$

where α and β are slowly variable with the shock radius Y. In the case of constant γ we have (cf. 17)

$$\alpha = \gamma - 1 \tag{46}$$

It is our aim to calculate α and β for a given variation of γ with the material coordinate r.

Using Equation (11) we have

$$\frac{p(0)}{\rho_0} = \dot{Y}^2 + \frac{1}{3} Y \ddot{Y} = \varphi + \frac{1}{6} Y \frac{d\varphi}{dY} \tag{47}$$

where φ is an abbreviation for $\dot{Y}^2$. Inserting the expression (45) and remembering (7) we get the following relation between α and β.

$$\beta = \alpha + \frac{1}{3} \frac{d\alpha}{d \log Y} \tag{48}$$

It will be shown in the following that α changes very slowly with log Y; in fact $d\alpha/d \log Y$ is of the order $\gamma - 1$ relative to α itself. Therefore, in our theory in which $\gamma - 1$ is considered as small, we have

$$\beta = \alpha \tag{49}$$

Therefore, even with variable γ the ratio of the shock pressure to the internal pressure is equal to 2.

In order to find α for a given function $\gamma(r)$ we use the fact that both the geometrical and the material coordinate must be equal to Y at the shock front. We shall calculate the geometrical coordinate R as a function of r with the help of the density distribution. The required condition is then

$$R^3(r - Y) = \int_0^Y d(r^3) \frac{\rho_0}{\rho} = Y^3 \tag{50}$$

As in Equation (6), the density of the material element r at the time when the shock wave is at Y, is given by

$$\frac{\rho}{\rho_0} = \frac{\gamma+1}{\gamma-1}\left(\frac{P(r,Y)}{P_s(r)}\right)^{1/\gamma} = \frac{\gamma+1}{\gamma-1}\left(\frac{P_0(Y)\,(1+r^3/Y^3)}{P_s(r)}\right)^{1/\gamma}$$

$$= \frac{2}{\gamma(r)-1}\,\frac{\alpha(Y)}{2\alpha(r)}\left(1+\frac{r^3}{Y^3}\right)\left(\frac{r}{Y}\right)^{3/\gamma} \qquad (51)$$

In this equation we have made use of the pressure distribution (11) and also of (45) and (49). Furthermore, we have put γ in the exponent equal to 1 in all those terms where this makes an error of the order $\gamma - 1$. Inserting (51) we find R as a function of r as follows

$$R^3 = \frac{1}{\alpha(Y)}\int_0^r d(r^3)\left(\frac{Y}{r}\right)^{3/\gamma\left[\gamma(r)-1\right]}\alpha(r)\left(1+\frac{r^3}{Y^3}\right)^{-1} \qquad (52)$$

No appreciable error is made by neglecting the last factor in this expression because it is different from 1 only over a region in R of the order $\gamma - 1$. In fact, only by neglecting this last factor do we get the correct result for constant γ, owing to other neglected terms in our theory. In any case, this last factor is no different for constant and variable γ and can, therefore, not be relevant for the theory of variable γ.

With this simplification we obtain

$$R^3 = \frac{1}{\alpha(Y)}\int_0^r \frac{d(r^3)}{r^{3/\gamma(r)}}\,Y^{3/\gamma(r)\left[\gamma(r)-1\right]}\alpha(r) \qquad (53)$$

and in particular for $r = Y$ we find, after dividing by Y^3

$$\alpha(Y) = \int_0^Y \frac{d(r^3)}{r^{3/\gamma(r)}}\,Y^{-3\left(1-\frac{1}{\gamma(r)}\right)}\left[\gamma(r)-1\right]\alpha(r) \qquad (54)$$

This is the desired equation determining $\alpha(Y)$. It is seen to be a linear integral equation.

Let us first consider the case of constant γ. In this case, Equation (54) reduces to

$$\alpha(Y) = \int_0^Y \alpha(r) \quad d\left(\frac{r}{Y}\right)^{3(\gamma-1)} \tag{55}$$

which is solved by α = constant, with the value of the constant arbitrary. From previous considerations, particularly Equation (17), we know that in this case $\alpha = \gamma - 1$.

Let us now assume that γ is constant and equal to γ_1, for all values of r up to r_1; then $\alpha = \alpha_1 = \gamma_1 - 1$ in that region. Further, for $Y > r_1$ the integral Equation (54) reduces to

$$\alpha(Y) = \alpha_1 \ (r_1/Y)^{3(\gamma_1-1)}$$

$$+ \int_{r_1}^{Y} \frac{d\, r^3}{r^{3/\gamma(r)}} \ Y^{-3+3/\gamma(r)} \cdot \left(\gamma(r) - 1\right)\alpha(r) \tag{56}$$

In order to solve this equation we proceed in two steps, similar to the calculations in Section 5.5. In the first step we shall consider Y/r_1 as moderate so that the $\gamma - 1$ power of the quantity can be considered equal to 1. In this case we shall be able to obtain a general and rather simple differential equation for α which can be solved by quadratures. As a second step we shall then admit large values of Y/r_1; in this case we shall obtain a solution only in the special case of having a step-wise variation of γ.

(1) Case I: Y/r_1 Moderate

In this case we may replace the exponent $3/\gamma$ in Equation (56) by 3. Also we shall expand the first term on the right hand side of that equation in a Taylor series. Then Equation (56) reduces to

$$\alpha(Y) = \alpha_1 - 3(\gamma_1 - 1)\alpha_1 \log (Y/r_1) \tag{57}$$

$$+ 3 \int_{r_1}^{Y} d \log r \ (\gamma(r) - 1)\alpha(r)$$

To solve this integral equation we need only differentiate with respect to Y or better with respect to

$$X = 3 \log (Y/r_1) \tag{58}$$

Then we obtain

$$\frac{d\alpha}{dX} = -\alpha_1(\gamma_1-1)+\alpha(X)(\gamma(X)-1) \tag{59}$$

This equation can be integrated with the result

$$\alpha(X) = e^{\int_0^X (\gamma(x')-1)\,dx'} \alpha_1 \left[1-(\gamma_1-1)\int_0^X dx' e^{-\int_0^{x'} [\gamma(x'')-1]\,dx''}\right] \tag{60}$$

The result (60) as well as the differential Equation (59) show that α does not have a discontinuity at a point at which γ has one, but only $d\alpha/dX$ has a discontinuity. This may be set even more in evidence by solving (59) for small values of X; i.e. for points just beyond the place at which γ begins to change. In this case we find

$$\alpha(X) = \alpha_1 \left[1+\int_0^X dX' \,(\gamma(X') - \gamma_1)\right] \tag{61}$$

A special case which is of some interest because it is the simplest possible model of a substance with changing γ, is obtained by assuming that γ has the value γ_2 for all values of $r > r_1$. In this case (59) can be solved explicitly with the result

$$\alpha = \frac{\gamma_1-1}{\gamma_2-1}\left[(\gamma_2-\gamma_1)e^{(\gamma_2-1)X} + \gamma_1 - 1\right] \tag{62}$$

For small values of X this reduces to

$$\alpha = (\gamma_1-1)\left[1+(\gamma_2-\gamma_1)\,X + \cdots\right] \tag{63}$$

Another result which follows from Equation (59) is that $d\alpha/dX$ is of the

order $\alpha(\gamma-1)$. This result has been used above in obtaining the relation $\beta = \alpha$.

(2) Case II: Y/r_1 Large

We shall consider this problem only in the particularly simple case when γ has the constant value γ_2 for all values of $r > r_1$. In this case Equation (56) reduces to

$$\alpha(Y) = \alpha_1 (r_1/Y)^{3(\gamma_1-1)} + \int_{r_1}^{Y} d\left(\frac{r}{Y}\right)^{3(\gamma_2-1)} \alpha(r) \tag{64}$$

Similarly, as in Case I, we solve this equation by differentiating with respect to X. Then we obtain

$$\frac{d\alpha}{dX} = -(\gamma_1-1)\alpha_1 \left(\frac{r_1}{Y}\right)^{3(\gamma_1-1)} + (\gamma_2-1)\alpha(X) - (\gamma_2-1) \int_{r_1}^{Y} d\left(\frac{r}{Y}\right)^{3(\gamma_2-1)} \alpha(r) \tag{65}$$

The integral in this equation can be expressed by means of Equation (64). Neglecting terms of higher order in $\gamma-1$ we get then

$$\frac{d\alpha}{dX} = \alpha_1(\gamma_2-\gamma_1) \left(\frac{r_1}{Y}\right)^{3(\gamma_1-1)} \tag{66}$$

This equation is actually even simpler than the differential Equation (59) which we obtained in the approximate theory of Case I. Using the boundary condition $\alpha = \gamma_1 - 1$ for $Y = r_1$ Equation (66) integrates immediately to

$$\alpha = \gamma_2 - 1 - (\gamma_2-\gamma_1)(r_1/Y)^{3(\gamma_1-1)} \tag{67}$$

For small values of X this reduces to

$$\alpha = (\gamma_1-1)(1 + 3(\gamma_2-\gamma_1)\ln Y/r_1) \tag{68}$$

which is identical with the result (63).

Equation (67) shows that the value of α goes gradually from the original value γ_1-1 to the value γ_2-1 which corresponds to the new value of γ. It is seen that this asymptotic value is reached only for extremely large values of Y/r_1. As long as Y/r_1 is moderate, the shock pressure is still influenced largely by the previous value of γ instead of by the present one. For air in particular we may take $\gamma_1 = 1.2$ and $\gamma_2 = 1.4$. The shock pressure in a substance with γ constant $= 1.4$ should be twice as great as that for γ constant and equal to 1.2, for the same radius Y of the shock wave and the same energy E. Actually, when the shock pressure falls low enough so that γ increases to 1.4 the coefficient α does not immediately increase by a factor 2, but increases very slowly. Physically the reason for this is that the interior part of the shock volume still has the low value of γ and therefore has a high internal energy for a given pressure. Only when the hot gases which possess the low γ fill a small part of the volume included in the shock wave will the γ in the outer regions of the shock determine the shock pressure.

5.7 THE WASTE ENERGY

G. I. Taylor has introduced the concept of the waste energy, i.e. the energy which remains in the hot gases traversed by the shock wave after an adiabatic expansion to a pressure of 1 atmosphere. The knowledge of this waste energy is useful because it permits one to calculate the energy which remains available to the shock wave at small overpressures.

The waste energy can be calculated very simply for the point source solution. Let us consider a material element which is traversed by the shock at a shock pressure p_s. When this element has been expanded adiabatically to atmospheric pressure p_o, its density will be

$$\rho = \rho_o \frac{\gamma+1}{\gamma-1} \left(\frac{p_o}{p_s}\right)^{1/\gamma} \tag{69}$$

Its temperature will be $p_o/\rho R$ and its energy content per unit mass:

$$\mathcal{E} = \frac{\gamma p_o}{\rho(\gamma-1)} = \frac{\gamma}{\rho_o(\gamma+1)} \left(p_o\right)^{\frac{\gamma-1}{\gamma}} \left(p_s\right)^{\frac{1}{\gamma}} \tag{70}$$

In calculating the energy content, we have used the specific heat at constant pressure; the reason for this is that our final state is obtained from normal air by heating it at constant pressure p_o to the temperature p_o/ρ. Strictly speaking, in order to get the waste energy, we should subtract from (70) the expression $\gamma p_o/\rho_o(\gamma-1)$, but we shall confine our discussion to the case when $p_s \gg p_o$.

The total energy wasted in the shock wave is then

$$W = 4\pi\rho_o \int_0^\infty Y^2 \, dY \, \mathcal{E} \tag{71}$$

We can now use the relation between shock pressure and radius, (33). We are using this fairly exact relation because it will turn out that we have to know the waste energy including terms of relative order $\gamma-1$. We solve (33) for Y; inserting the result and (70) into (71) we obtain

$$W = C \; E \left(p_o\right)^{\frac{\gamma-1}{\gamma}} \int_{Kp_o}^{\infty} \left(p_s\right)^{1/\gamma} \frac{dp_s}{p_s^2} \tag{72}$$

with

$$C = 2(\gamma-1)\left[1-(\gamma-1)\left(\frac{3}{2}-\ln 2\right)\right]\gamma/(\gamma+1) \tag{72a}$$
$$\approx (\gamma-1)\left[1-(\gamma-1)\left(\frac{1}{2}-\ln 2\right)\right]$$

neglecting terms of relative order $(\gamma-1)^2$. Equation (72) gives the energy wasted up to the time when the shock pressure has fallen to the value Kp_o.

Equation (72) can be integrated immediately and gives

$$W = \frac{\gamma}{\gamma-1} \; C \; E \left(\frac{p_o}{Kp_o}\right)^{\frac{\gamma-1}{\gamma}} \tag{73}$$
$$= \left[1+(\gamma-1)\ln 2\right] E \; K^{-\frac{\gamma-1}{\gamma}}$$

Subtracting this expression from the total energy E we obtain the energy which is still available:

$$E_{eff.} = E\left[1 - (K/2)^{-\frac{\gamma-1}{\gamma}}\right] \tag{74}$$

It is clear that for small values of $\gamma - 1$ and moderate K, this expression is proportional to $\gamma - 1$. This shows the necessity of knowing the relation between p_s and E up to terms of the order $\gamma - 1$; i.e. of using (33) rather than (17).

It is somewhat problematic what to use for K. Clearly the relation (33) will break down at too low values of p_s; namely, when the limiting form of the Hugoniot relations ceases to be valid. This requires

$$K \gg \frac{\gamma+1}{\gamma-1} \tag{75}$$

Setting

$$K = 2n/(\gamma-1) \tag{76}$$

then $n \gg 1$

and using the fact that $\gamma - 1$ is small, Equation (74) reduces to

$$E_{eff.} = E\ (\gamma-1)\ \log\frac{n}{\gamma-1} \tag{77}$$

Of course the available energy will be further reduced as the shock pressure is reduced closer to atmospheric pressure. In fact, Penney has shown that the dissipation of energy continues indefinitely as the shock wave expands (see Chapter 8, Section 8.7). It is therefore not possible to give any accurate

definition of the percentage of energy wasted but it would be necessary to specify the shock pressure for which this statement is made. In order to obtain the percentage wasted for shock pressures of the order of one atmosphere, it would be necessary to follow the shock wave through the region of intermediate pressures which can adequately be done only by numerical methods (see Chapter 7).

However, it is clear from our Equation (77) that the energy available for the shock wave is smaller the smaller $\gamma - 1$. The fact that the air has a small value of γ at high temperatures leads to increased dissipation of energy at the shock and, therefore, to a relatively smaller blast wave at large distances. This is the main reason why the blast wave from a nuclear explosion is less strong at a given distance than from a TNT explosion liberating the same total energy. In the latter case the temperatures reached are only moderate, and the energy wasted is, therefore, less than for the nuclear explosion.

The greater wastage of energy for smaller γ is also related to the result obtained in Section 5.6; namely, that the shock pressure after a sudden change of γ does not correspond to the new value of γ but is rather close to the value for the original value of γ. This slow variation of the shock pressure is in turn important if one wants to calculate the waste energy for a gas with variable γ. In fact, if it were not for this gradual change, gases might occur in which the waste energy would be greater than the total energy available which would be obvious nonsense. The change of α derived in Section 5.6 is just sufficiently gradual to keep the waste energy always below the total available energy.

CHAPTER 6

EFFECT OF VARIABLE DENSITY ON THE PROPAGATION OF THE BLAST WAVE

K. Fuchs

6.1 INTRODUCTION

We have seen in preceeding chapters that there is a considerable range in which fairly reliable predictions about the propagation of the blast wave may be made. The range extends from somewhat below one million degree shock temperature to about 5,000 degrees. Above 1,000,000 degrees the isothermal sphere extends up to the shock front. If r_o is the radius of the shock front at the time when the isothermal sphere separates from the shock, then the shock pressure at a given radius $Y > r_o$ is proportional to (see Equation 5.43)

$$(1 - r_o^3/2Y^3) \qquad (1)$$

and therefore the effect of the isothermal sphere is negligible even for moderate values of Y/r_o.

Below 5,000 degrees the formation of an opaque layer at a slight distance behind the shock front may lead to absorption of radiation which might otherwise escape, and therefore radiation transport of energy has a considerable effect on the propagation of the shock. Furthermore, below 5,000 degrees the luminosity comes from some distance behind the shock front and this makes photographic observation of the shock front difficult.

Between about 200,000 degrees and 20,000 degrees shock temperature the ionization of the L-electrons proceeds and within this range the variation of γ is not very pronounced. This, therefore, appears to be the most useful

range.

The corresponding shock pressures are

T	1,000,000°	200,000°	20,000°	5,000°
P_s	350,000	50,000	1,600	200 atmospheres

Observing that the shock radius is roughly proportional to the inverse cube root of the shock pressure, this gives a fairly comfortable range of useful observation.

However, there are some factors which limit the range. One factor is the height at which the explosion takes place. When the shock reaches the ground a reflected shock goes back and only those parts of the shock sphere which have not been reached by the reflected shock, can be compared directly with the theory. This was particularly serious at Trinity, but would also present some limitation in future tests, since it is impracticable to raise the gadget to a great height without interfering with other experiments. At Trinity the gadget was set off at a height of 30 meters.

The other limitation arises from the fact that initially the propagation of the shock is affected by the material of which the gadget is composed. Although the dimensions of the gadget are rather small, the effect persists over a considerable distance, since it is the mass in the gadget compared to the mass of air engulfed by the shock which matters.

In particular, with a view toward an evaluation of the energy release in the Trinity test, we shall attempt in this Chapter to get over the second limitation. We consider a blast wave originated by a point source, travelling through material of variable density. We shall make some simplifying assumptions:

(1) The density is supposed to depend on the radius only, and the variation of density is assumed to be continuous. We disregard,

therefore, any asymmetry in the construction of the gadget and the exact details of the transmission of the shock from the gadget into air are neglected. Neither of these two factors can have appreciable effect at a sufficiently large distance.

(2) We assume that $\gamma - 1$ is small compared to 1 and use the essential ideas on which the approximation of small $\gamma - 1$, discussed in Chapter 5, is based. Insofar as this approximation can be compared with exact calculations of a point source it was found to be very good, even if γ is 5/3. However, it does not necessarily follow from this fact that the approximation is equally good in more general cases. At present we have no means of estimating the error.

(3) We assume that γ is constant. This is not a bad assumption, since we are mainly interested in the region from about 200,000 degrees to 20,000 degrees, where γ does not vary too much.

6.2 METHOD OF ESTIMATING ENERGY RELEASE BY OBSERVATION OF THE SHOCK RADIUS

Before proceeding to the analysis of the problem with variable density, let us consider the application of the method of estimating the energy release in the simplest case when the similarity solution for constant density holds. The derivation given below is due to Bethe.

If $\gamma - 1$ is small, the kinetic energy may be neglected and the total energy is given by

$$E = \int \frac{p}{\gamma - 1} \, dv \qquad (2)$$

as pointed out in Chapter 5, the pressure is constant and equal to 1/2 the shock pressure p_s over the greater part of the volume. Hence (1) can be replaced by

$$E = \frac{1}{2} \frac{p_s}{\gamma - 1} \frac{4\pi}{3} Y^3 \tag{3}$$

where Y is the shock radius. Using the Hugoniot condition for strong shocks

$$p_s = \frac{2}{\gamma + 1} \rho_o U^2 \tag{4}$$

we obtain for $\gamma = 1$

$$E = \frac{2\pi}{3} \frac{\rho_o U^2 Y^3}{\gamma - 1}, \quad U = \dot{Y} \tag{5}$$

Here U is the shock velocity and ρ_o the normal density of air.

Since E is constant, we can integrate (5) and find

$$t = \frac{2}{5} \left\{ \frac{2\pi \rho_o}{3E(\gamma - 1)} \right\}^{\frac{1}{2}} Y^{5/2} \tag{6}$$

If the finite value of $\gamma - 1$ is taken into account, the factor $2\pi/3$ should be replaced by a constant $B(\gamma)$ which differs but little from $2\pi/3$. $B(\gamma)$ is the quantity tabulated in the last line of Table 5.3, Chapter 5.

If, therefore, we plot the observed values of $Y^{5/2}$ against the time t, they should lie on a straight line and from the slope of the line we can immediately derive the total energy.

6.3 INTEGRATION OF THE EQUATIONS OF MOTION.

We shall now turn to the case of variable density. If $\gamma - 1$ is small the kinetic energy is small compared to the internal energy. The internal energy per unit volume is

$$p / (\gamma - 1) \tag{7}$$

Now p is practically constant over the larger part of the volume of the shocked sphere; it varies appreciably only in the region where most of the mass is accumulated, i.e. near the shock front. If we integrate (7) over the volume, we can disregard the small shell of variable pressure near the shock front and identify p with the pressure $p(o,t)$ at the center of the sphere. Then the total energy E is given by

$$E = \frac{4\pi Y^3}{3} \frac{p(o,t)}{\gamma - 1} \tag{8}$$

Using Euler variables R, and Lagrange variables r, the equation of motion is

$$\rho(r) r^2 \ddot{R} + R^2 \partial p / \partial r = 0 \tag{9}$$

where ρ is the original density of the mass element which was at the radius r, before the shock reached it. Integration of (9) yields

$$p(r,t) = p_s + \int_r^Y \left(\frac{\ddot{R}}{R^2}\right)_t \rho(r) r^2 \, dr \tag{10}$$

where $\ddot{R}/R^2$ is to be considered as function of r for fixed time t. p_s is the shock pressure and Y the shock radius. Now, nearly all mass is near the shock front. Hence $\ddot{R}/R^2$ is practically identical with $\ddot{Y}/Y^2$. This will no longer be true if r becomes very small, but then the contribution to the integral (10) will be small. Hence we may write approximately

$$p(r,t) = p_s + \frac{\ddot{Y}}{Y^2} \int_r^Y \rho(r) \, r^2 \, dr \tag{11}$$

In particular at the centre

$$p(o,t) = p_s + \frac{\ddot{Y}}{Y^2} M \tag{12}$$

where

$$M(Y) = \int_0^Y \rho(r)\, r^2\, dr \tag{13}$$

is the total mass per unit solid angle within the shock radius.

The shock pressure is given by the Hugoniot condition

$$P_s = \frac{2}{\gamma+1}\, \rho\, U^2 \tag{14}$$

and U is the shock velocity

$$U = \dot{Y} \tag{15}$$

Since we assumed γ near 1, we may omit the factor $2/(\gamma+1)$ in (14). Considering U as function of Y, we have

$$\ddot{Y} = U\, \frac{dU}{dY} \tag{16}$$

Substituting (14) and (16) into (12) one finds

$$p(o,t) = \rho U^2 + \frac{U}{Y^2}\, \frac{dU}{dY}\, M = \frac{1}{2MY^2}\, \frac{d}{dY}\, (U^2M^2) \tag{17}$$

Combining this equation with (8), we find

$$\frac{d}{dY}\, (U^2M^2) = \frac{3}{2\pi}\, (\gamma-1)\, \frac{M}{Y}\, E \tag{18}$$

and therefore

$$U^2 = \frac{3}{2\pi}\, (\gamma-1)\, \frac{E}{M^2} \int_0^Y \frac{M(Y)}{Y}\, dY \tag{19}$$

The lower limit in the integral is derived as follows:

If Y is small, ρ may be considered constant and equal to its value at the center. Then (19) reduces to

$$U^2 = \frac{3}{2\pi}\, (\gamma-1)\, \frac{E}{\rho Y^3} \tag{20}$$

which is the Equation (5) derived for a point source and constant density, as it should be. If a constant of integration were added to the integration in (19) we would not obtain the correct behavior for small shock radii. In addition, the kinetic energy $4\pi M U^2$ would become infinite for $Y \to 0$ contrary to the assumptions made.

6.4 EFFECT OF VARIABLE DENSITY NEAR THE CENTER ON THE AIR SHOCK

We assume next that the density has an arbitrary distribution $\rho(Y)$ up to a certain radius Y' and constant density ρ_o beyond. We wish to know the propagation of the shock, after it has reached the region of constant density.

If $Y > Y'$, we have

$$M = \int_0^Y \rho(Y)\, Y^2\, dY = \frac{1}{3}\, \rho_o\, (Y^3 + Y_o^3) \qquad (21)$$

where Y_o is the radius of a sphere occupied by the excess material at the center, if it were spread out at the density ρ_o; i.e.

$$\frac{1}{3}\, \rho_o\, Y_o^3 = \int_0^{Y'} \left\{\rho(Y) - \rho_o\right\} Y^2\, dY \qquad (22)$$

Similarly

$$\int_0^Y \frac{M(Y)}{Y}\, dY = \frac{1}{9}\, \rho_o\, Y^3 + \int_0^{Y'} \frac{dY}{Y} \int_0^Y \left\{\rho(Y) - \rho_o\right\} Y^2\, dY \qquad (23)$$

Partial integration yields

$$\int_0^Y \frac{M(Y)}{Y}\, dY = \frac{1}{9}\, \rho_o\, Y^3 + \frac{1}{3}\, \rho_o\, Y_o^3 \left\{\ln Y - \ln \bar{Y}\right\} \qquad (24)$$

where $\bar{Y}$ is the logarithmic average radius of the excess material

$$\ln \bar{Y} = \int_0^{Y'} \ln Y\, (\rho(Y) - \rho_o)\, Y^2\, dY \Big/ \int_0^{Y'} (\rho(Y) - \rho_o)\, Y^2\, dY \qquad (25)$$

Substitution of (21) and (24) into (19) yields

$$U^2 = \frac{3E(\gamma-1)}{2\pi\rho_0 Y^3} f(Y)^2 \qquad (26)$$

where

$$f(Y)^2 = \frac{1 + 3(Y_0/Y)^3 \ln(Y/\bar{Y})}{\left\{1 + (Y_0/Y)^3\right\}^2} \qquad (27)$$

If $f = 1$, the formula (26) reduces to the equation (5) for constant density. f, therefore, is the correction factor by which the shock velocity is changed.

It is of interest that the factor f depends strongly on the radius Y_0. The latter depends only on the total mass of excess material at the center, but not on its distribution. This is rather fortunate, because the distribution of matter in the gadget is changed during the implosion and it would not be simple to calculate the correct distribution. The radius $\bar{Y}$ on the other hand depends on the distribution of matter. However, since it is only a logarithmic average, it is not very sensitive to small errors in the assumed distribution of matter.

For the Trinity test the gadget was located on a tower and we are most interested in the expansion of the shock before it hit the ground. The effect of the tower on the average shock radius may be bracketed between two limits. On the one hand we may neglect it. On the other hand, we may assume that the matter in the tower is spread with spherical symmetry around the gadget. This leads to the following problem:

The density distribution is arbitrary up to a radius Y' as before. Beyond that radius the density is given by

$$\rho(Y) = \rho_0\left\{1 + Y_1^2/Y^2\right\} \text{ for } Y > Y' \qquad (28)$$

The formulae can be evaluated for this case in a manner similar to that employed above; one finds for the correction factor f

$$f^2 = \frac{1+\frac{3}{Y^3}\left\{\ln(Y/\bar{Y}) + \frac{Y_1^2}{Y_o^2}\left[\frac{Y}{Y_o} - \frac{Y'}{Y_o}\left(1+\ln\frac{Y}{Y'}\right)\right]\right\}}{\left[1+\frac{Y_o^3}{Y^3}\left\{1+\frac{Y_1^2}{Y_o^2}\left(\frac{Y}{Y_o}-\frac{Y'}{Y_o}\right)\right\}\right]^2} \quad ? \qquad (29)$$

In order to be able to neglect the effect of the tower, we require that in the region in which measurements are used, the formula (29) should be for practical purposes identical with the formula (27).

If Y is sufficiently large compared to Y_o, the excess mass near the center becomes negligible compared to the total mass within the shock radius and the solution must approach asymptotically the similarity solution. This is indeed the case since f tends to 1 for large Y.

For the similarity solution we have the exact formula valid for any value of γ. It can be written in the form

$$U^2 = \frac{E(\gamma-1)}{B(\gamma)\rho_o Y^3} \qquad (30)$$

where $B(\gamma)$ differs only little from the value $2\pi/3$. B as function of γ is tabulated in Chapter 5. It is identical with the quantity given in the last line of Table 5.3.

It seems reasonable to fix up the formula (26) in such a way that it gives the correct asymptotic behavior; i.e. we put

$$U^2 = \frac{E(\gamma-1)}{B(\gamma)\rho_o Y^3} f^2 \qquad (31)$$

In particular, if the formula is used in the region where f approaches 1, the effect of a finite $(\gamma-1)$ on f will be a small order effect and then it is perfectly justified to include the finite $(\gamma-1)$ in the main term but to neglect it in f.

6.5 APPLICATION TO THE TRINITY TEST

The correction factors f have been evaluated for the conditions in the Trinity test. Four functions f have been calculated as follows:

In the first instance only the material in the gadget itself was included. For the second curve the X- unit was included. This unit does not have spherical symmetry. However, the difference between the two curves was found to be small.

Next, the platform on which the gadget was located was taken into account, and finally the tower. Again these two curves did not differ appreciably from each other.

However there was quite an appreciable difference between the curves which did or did not include the platform. Since the platform has no spherical symmetry, the difference between the two curves represents an unavoidable experimental error. Clearly for future tests it would be desirable to eliminate this source error.

Values of the shock velocity on an arbitrary scale calculated with the help of these four correction factors are shown in Figure 1. For comparison a curve which neglects the variable density is also shown. The numerical data for these curves are:

Gadget only: $Y_o = 8.58$ m, $\overline{Y} = 0.36$ m

Gadget and X-unit: $Y_o = 8.75$ m, $\overline{Y} = 0.37$ m

Gadget, X-unit and platform: $Y_o = 11.9$ m, $\overline{Y} = 1.9$ m

Tower: $Y' = 2$ m, $Y_1 = 5.3$ m.

It will be noticed that the correction factor f is below 1 for small shock radii and above 1 for large radii. The explanation is as follows: When the shock passes from the gadget into air, the shock velocity increases rapidly. The gadget material, which was shocked by a slow shock, must now

Figure 1

Shock Velocity as Function of Radius

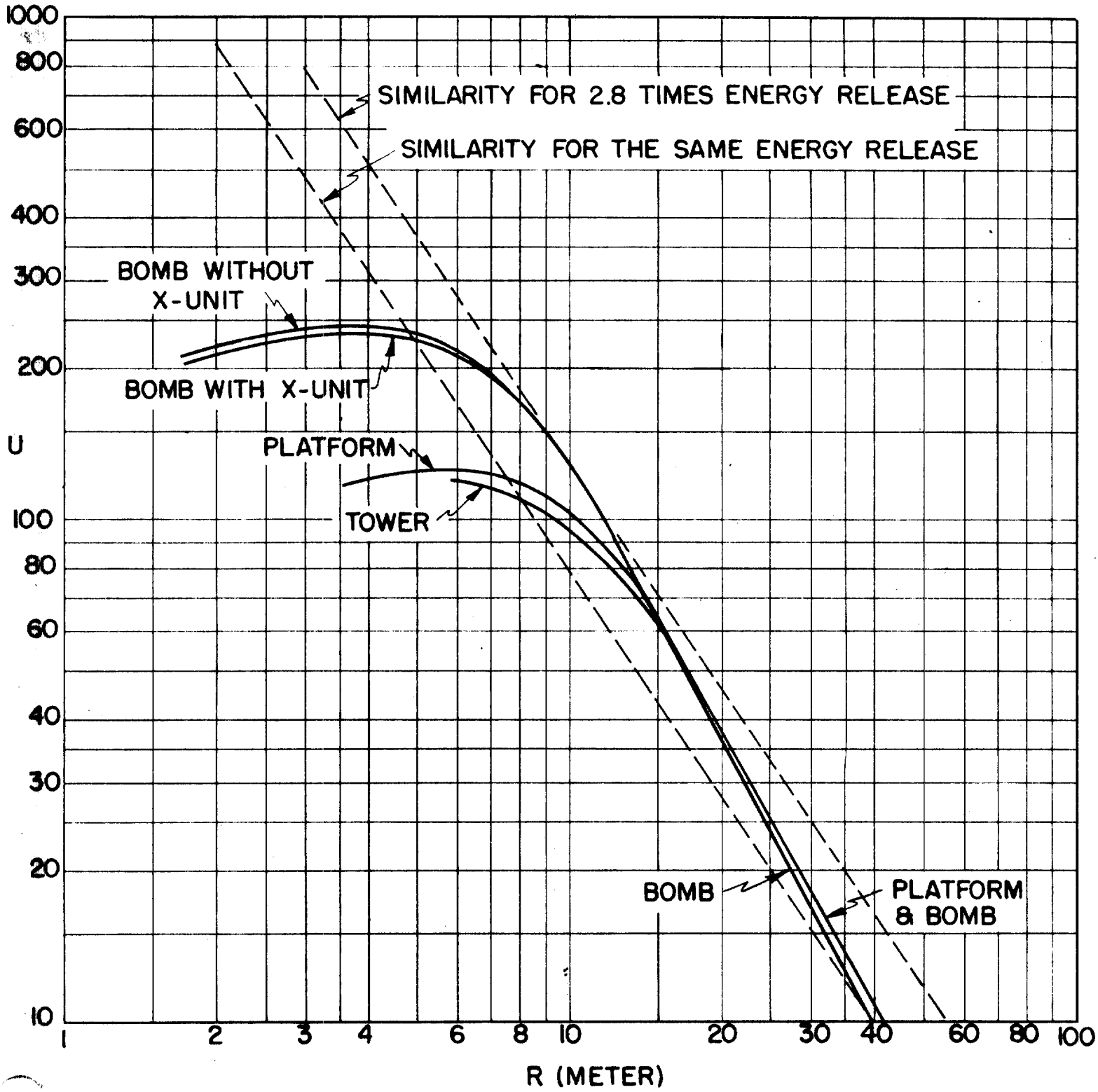

be speeded up and this requires that the pressure gradient behind the shock be reversed. Thus the average pressure, instead of being one half the shock pressure, (see equations 5-16), will now be higher than the shock pressure. Eventually, as the air shock slows down, the gadget material must again be decelerated. Since there is now more material, the pressure gradient required to do so must be larger and the average pressure drops below one half the shock pressure. Hence the equation (8) may be written in the form

$$E = \frac{4\pi}{3} \frac{Y^3}{\gamma - 1} \quad p \text{ average} = \frac{2\pi}{3} \frac{Y^3}{\gamma - 1} \quad p_s / f^2 \qquad (32)$$

where $f < 1$ at small distance and $f > 1$ at large distance. With the help of (14), it is found immediatley that f as defined here is identical with the correction factor f.

In the early stages the heavy material at the center has, therefore, the tendency of holding the shock back, until it is accelerated sufficiently to follow the shock. In this stage the assumptions on which the theory is based are not very well satisfied. Combining (31) and (27) one finds for $Y \ll Y_o$

$$U^2 = \frac{3E(\gamma - 1)}{B(\gamma) \rho_o Y_o^3} \quad \ell n \left(\frac{Y}{Y}\right); \quad \text{for } Y \ll Y_o \qquad (33)$$

and the shock velocity varies little with the shock radius. However, the essential reason for the accumulation of matter near the shock front lies in the rapid decrease of shock velocity with radius, which is accompanied by a corresponding decrease in entropy. Hence, there is normally a region of high entropy and low density in the inside of the sphere. This is no longer correct if the shock velocity remains constant over an appreciable distance. For this reason the theory is not reliable until the second phase is reached, and the shock slows down again. In this phase the heavy material continues to press outward and, therefore, raises the shock velocity above the value expected from the similarity theory. The magnitude of this effect

can be judged from Figure 1 by the fact that the shock velocity curve at one point touches the similarity curve for 2.8 times increased energy release. It is, therefore, easily possible that the energy release be overestimated by a factor of this order, if the effect of the gadget on the propagation of the shock is neglected.

From the shock velocity we obtain the shock radius as function of time by means of one integration. Using the factor (27) we find

$$t = \int^{Y} \frac{1}{U}\, dY = \left\{\frac{B(\gamma)\ \rho_o\ Y_o^5}{E\ (\gamma-1)}\right\}^{1/2} F\left(\frac{Y}{Y_o}, \frac{\bar{Y}}{Y_o}\right) \qquad (34)$$

$$F(z, z_o) = \int^{z} \frac{1 + z^3}{(z^3 + 3 \ln z/z_o)^{1/2}}\, dz \qquad (35)$$

If z is large compared to 1, we obtain asymptotically the formula for the similarity solution

$$F = \frac{2}{5}\, z^{5/2}, \quad \bar{t} = \frac{2}{5}\left\{\frac{B(\gamma)\ \rho_o\ Y^5}{E\ (\gamma-1)}\right\}^{1/2} \quad ; \text{ if } z >> 1 \qquad (36)$$

The function F has been evaluated by numerical integration for two values of z_o, obtained if either the effect of the gadget only is included or if the platform is also taken into account. They are shown in Figure 2 where $Y^{5/2}$ is plotted against t for an energy release of 21,000 tons of TNT. $1/(\gamma-1)$ was assumed to be 4.3. The value of 21,000 tons was chosen in order that the experimental points for shock radii between 20 and 30 meters should lie between the two theoretical curves. In this region the experimental points lie on the dotted straight line shown in Figure 2.

The experimental data were obtained by Mack's group from photographs of the ball of fire by means of Fastax cameras (see Chapter 18).

The shock pressure is obtained from (14) as soon as the shock velocity

Figure 2

$Y^{5/2}$ as Functions of t.

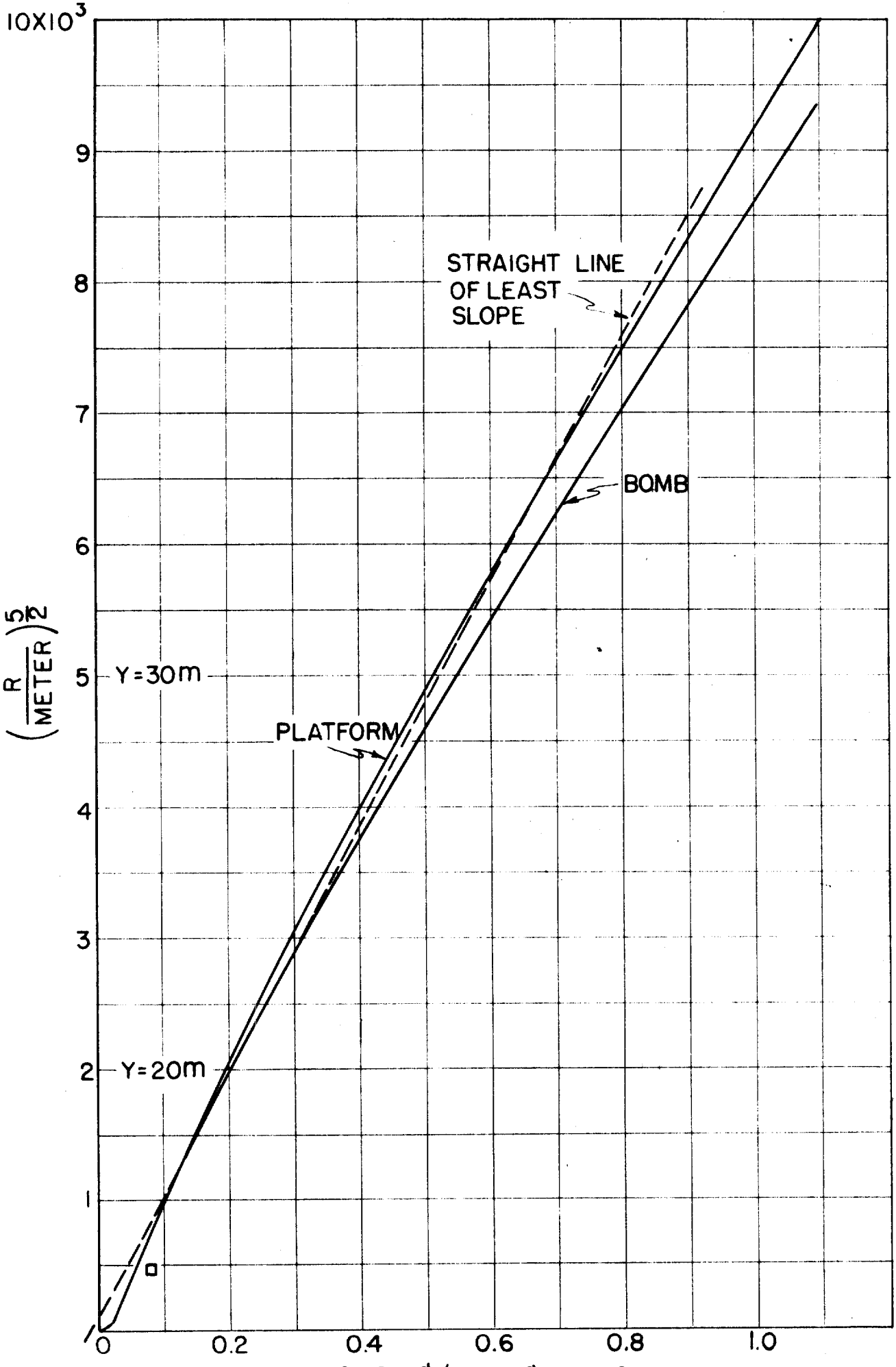

is known. It varies between 15,000 - 25,000 atmospheres at Y = 20 meters to 4,000 - 5,000 atmospheres at 30 meters and is, therefore, well within the range postulated in the introduction.

CHAPTER 7

THE IBM SOLUTION OF THE BLAST WAVE PROBLEM

K. Fuchs

7.1 INTRODUCTION

The discussion in the preceding chapters shows that the problem of the propagation of the blast wave from a nuclear explosion is quite complicated. Even if we disregard any transport of radiation, appreciable complications arise in view of the large variations in temperature and entropy. We may roughly divide the range of shock temperatures into two regions. Firstly, the region from about one million degrees to about three thousand degrees absolute. Here dissociation of molecules and ionization of the atoms takes place. Consequently $\gamma - 1$ is fairly small but varies with temperature. Below 3000° γ is less variable and approaches eventually the value 1.4 in normal conditions.

The temperature varies of course also along an adiabatic. However, the total variation between the shock pressure and one atmosphere is not excessive - about a factor 2 at shock temperature of 3000° and slightly more than a factor 10 for a shock temperature of 1,000,000°. The effect of decreasing temperature along the adiabatic on the degree of ionization or dissociation is partly balanced by the decrease in density. For this reason the variation of γ along an adiabatic is not as pronounced as one might expect from the change in temperature. For this reason qualitative statements made about the conditions at the shock front hold to a large degree also for the subsequent expansion behind the shock.

A temperature of 3,000° K is reached in the shock when the shock pressure is about 80 atmospheres. (For an energy release of 10,000 tons of TNT the shock radius is then 80 meters). We are however more interested in the pressure region from about one atmosphere down (corresponding to shock radii of 500 meters and more). It was felt that the exact energy distribution at this early

stage could not have an appreciable effect on the pressure distribution in the later stages as long as the energy distribution is at least roughly correct. For this reason it was decided to start an IBM calculation at this point and to calculate the initial conditions for this instant by means of the approximations developed in the preceding chapters. The approximations made include: (for details see section 2)

(1) An approximate treatment of the isothermal sphere. In actual fact the isothermal sphere at this late stage has no significant influence on the propagation of the shock. However, in the first instance we were interested in the isothermal sphere as such; in the second instance the isothermal sphere greatly facilitates numerical computations, since it reduces the total range of temperatures and entropies which exist at any given moment, and eliminates the singularity at the centre.

(2) γ was assumed to be constant and an average value of 1.25 was assumed. This is probably the least satisfactory of the assumptions made; but in view of the fact that we did not require a very accurate estimate of the initial conditions, and that a calculation with variable γ is hardly feasible without IBM machines or a great amount of computation, this assumption seemed justified.

(3) $\gamma - 1$ was assumed small. This assumption is not essential, but the error introduced thereby is small and it has the advantage that the isothermal sphere can be included as an integral part of the calculation.

For the IBM run it is of great advantage if the variation of the pressure along an adiabatic is a simple function of the density, though the variation from one adiabatic to another may be given in numerical form. The reason is that in this case the adiabatic of each mass point is given by one or two constants and we require only a table of these constants as functions of one variable. (Problems in which the equation of state is given completely in numerical form have not yet been tried on the IBM machines).

It would be difficult to find a simple presentation of the equation of state covering the whole region of adiabatics between the shock pressure curve and normal pressure. However, with the limitation to shock pressure below 80 atmospheres the demand of a simple representation becomes feasible. In particular this is true for the adiabatics which start at shock pressures below 80 atmospheres, since then no ionization or dissociation occurs. We require of course also the adiabatics of the inner mass points, which were shocked by stronger shocks. However we require only the tail end of these adiabatics. Furthermore, the highest entropies are eliminated by the equalisation of entropy inside the isothermal sphere. The equation of state which has been used is discussed in Chapter 3.

The requirement of a simple equation of state is the principal reason for starting the IBM run at such a comparatively late stage.

Although radiation transport has been taken into account insofar as it is responsible for the formation of the isothermal sphere, no allowance has been made for the radiation transport from the isothermal sphere into the region in which NO_2 is formed. As explained in Chapter 4, Section 4, this transport of energy becomes important when the shock radius has reached about 100 meters and it should affect the propagation of the shock shortly thereafter. The opacity data required for the purpose of calculating this transport are not sufficiently well known. In neglecting the radiation transport altogether we are pessimistic, since it is of advantage to have the energy close to the shockfront. Then the shock pressure decreases less rapidly than it would otherwise. The increased shock pressure would naturally lead to a greater degree of dissipation of energy by the shock so that at larger distances the shock pressure might drop again more rapidly and at sufficiently large distances the effect of the radiation transport on the shock pressure would be reversed. At present we are not in a position to make any definite statement about this possibility.

The IBM run was intended for an energy release of 10,000 tons of TNT. Owing to some unfortunate circumstances related in Section 3, no definite energy can be attributed to the run throughout its whole history. At sufficiently large distances the energy should be assumed to be 13,000 tons. Other energies can, of course, be obtained by the usual scaling laws.

7.2 THE INITIAL CONDITIONS OF THE IBM RUN

The initial conditions of the IBM run were prepared by Hirschfelder and Magee. The principal data are summarized below without going into the details of the calculation. All data are for an energy release of 10,000 tons of TNT.

7.2-1 The Isothermal Sphere

The Lagrange radius r_o of the isothermal sphere is given in terms of the shock radius Y by Equation 4 of Chapter 4, Section 3. It can be written in the form

$$r_o = \left[11.85\ Y'^{.7326} - 601.5 \right]^{1/3} 100 \text{ cm} \qquad (1)$$

Here both r_o and Y are given in centimeters. It was convenient to choose a simple value of Y/r_o and the value 4 was chosen, which corresponds to a shock pressure very near to 80 atmospheres. Then

$$r_o = 1997 \text{ cm}, \quad Y = 7987 \text{ cm}, \quad Y/r_o = 4 \qquad (2)$$

The actual radius R_o of the isothermal sphere is obtained from the conservation of mass. Since we assume constant density ρ and constant pressure in the isothermal sphere one has

$$\rho_o r_o^3 = \rho R_o^3 \qquad (3)$$

r_o as function of Y is shown in Figure 1 of Chapter 4. It will be seen that r_o varies very slowly after the shock radius has reached about 10 meters and the effect of the isothermal sphere on the shock is negligible a short while thereafter. Beyond a shock radius of 80 meters r_o varies very slowly indeed.

According to Figure 2 of Chapter 4, it increases from 20 meters to 27 meters as the pressure in the sphere decreases to 1 atmosphere (the analysis is no longer valid for such small pressures, but it indicates the order of magnitude).

For this reason it is a good assumption to assume that r_o is constant. The actual radius R_o then varies in accordance with Equation 3 only because the air in the isothermal sphere expands. The initial value of R_o is 60 meters (see Figure 1 Chapter 4).

The initial condition of the isothermal sphere is given by the following quantities:

Temperature = 49,000°K

Pressure = 37.0 atmospheres

Density = 0.0392 x normal density

Entropy $\Delta S/R$ = 85

Internal energy and enthalpy $E/R = 1.487 \times 10^6$, $H/R = 1.782 \times 10^6$

R_o = 60.23 meters, r_o = 19.97 meters.

These data were obtained from a calculation indicated below.

7.2-2 Initial Pressure and Density Distribution

It has been shown in Chapter 5, Section 5 that the isothermal sphere can be treated on the assumption of small $\gamma - 1$. The small $\gamma - 1$ approximation has been checked for a point source solution (see Chapter 5, Sections 3 and 4) and it was found satisfactory in the region in which we are interested. Since the solution which we require is in any case very close to the point source solutions except in the neighborhood of the isothermal sphere, the error of the small $(\gamma-1)$ approximation is small.

We shall not go into the details of the calculation. The analysis is rather involved, but the lines along which it proceeds are sufficiently indicated in Section 5 of Chapter 5. The resulting equations had previously been evaluated for two values of γ in order to see how sensitive they were to a change in γ. The values chosen were $\gamma = 1.2$ and $\gamma = 1.3$.

The values for $\gamma = 1.25$ were then obtained by interpolation. In this way we find the initial pressure and density distribution as well as the velocities and the Euler coordinates of all mass points.

Some adjustments had to be made on the initial conditions. A minor adjustment arose from the fact that the small $\gamma - 1$ treatment of the isothermal sphere does not agree exactly with the treatment given in Chapter 4 Section 3. The error, which may be due to either method, may be seen from the values of R_0/Y; the small $\gamma - 1$ treatment gives $R_0/Y = 0.850$ compared to 0.761 by means of the other method. The latter value was assumed to be more reliable.

Furthermore, at the start of the IBM calculation the value of γ at the shockfront is larger than 1.25; instead of a compression ratio in the shock $\rho_s/\rho_0 = 9$, as would be expected for $\gamma = 1.25$, the value obtained from the correct Hugoniot curve for a pressure of 77.25 atmospheres is $\rho_s/\rho_0 = 7.24$. The density contour was, therefore, adjusted to give the correct compression ratio at the shock, and the correct radius of the isothermal sphere. This required also an adjustment in the Euler coordinates R, since it is essential that the initial conditions satisfy the equation of continuity:

$$\frac{\rho_0}{\rho} = \frac{R^2}{r^2}\,\frac{dR}{dr} \tag{4}$$

where r is the Lagrange coordinate.

The initial velocities were then calculated directly from the equation

$$u = \frac{\dot{Y}}{(\gamma+1)^{1/3}}\,\frac{1+(r/Y)^{3(\gamma-1)/\gamma}}{\left[1+\gamma(r/Y)^{3(\gamma-1)/\gamma}\right]^{2/3}} \tag{5}$$

which follows from the small $\gamma - 1$ approximation. Here the correct shock velocity $\dot{Y}$ for the given shock pressure was used.

7.3 THE TOTAL ENERGY

The methods used to establish suitable initial conditions are in parts somewhat arbitrary. For this reason it is not surprising that the total energy corresponding to these conditions turned out to deviate appreciably from the assumed value of 10,000 tons of TNT. Unfortunately the energy was recalculated from the initial conditions only after the IBM-run had been completed. It was then found that the total energy was 13,500 tons TNT.

Since the initial shock pressure of 77.25 atmospheres at the initial shock radius of 79.9 meters corresponds to an energy release of 10,000 tons, we have no remedy for the discrepancy. All that can be said, is that the shock pressure versus distance curve corresponds to 10,000 tons up to 80 meters shock radius and to 13,500 tons for large radii. For intermediate radii it should slowly change between these values.

Actually the discrepancy is slightly less. A check of the total energy at a shock radius of 2000 meters gave only 13,100 tons. The "loss" of 400 tons is entirely due to errors of the IBM-run and is of the order of magnitude to be expected from this source.

For most purposes the total energy in the IBM-run should be assumed to be about 13,000 tons, except at small shock radii, where 10,000 tons is more appropriate.

7.4 THE IBM-RUN

The hydrodynamical equations are

$$\rho_0 \frac{\partial^2 R}{\partial t^2} + \frac{R^2}{r^2} \frac{\partial P}{\partial r} = 0 \qquad (6)$$

$$\rho_0 / \rho = \frac{R^2}{r^2} \frac{dR}{dr} \qquad (7)$$

In addition we have the equation of the adiabatics, which were put in the form

$$\frac{P}{P_0} = \varepsilon \left(\frac{\rho}{\rho_0}\right)^{1.5} + \eta \frac{\rho}{\rho_0} \qquad (8)$$

where g and h are numerically known functions of the entropy.

The boundary conditions are that the velocity $\partial R/\partial t$ vanishes at the center and that at the shockradius the Hugoniot conditions are satisfied. The latter determine also the entropy of any mass point as it passes through the shock front. The entropy is assumed to remain constant, so that essentially g and h are given functions of the Lagrange variable r.

The methods employed in solving the system of partial differential equations by means of the IBM machines are explained in Volume 2 of this series. The method used first was suitable as long as the shock pressure differed appreciably from one atmosphere, but it became erratic as the overpressure became small. The method was therefore changed, so as to calculate changes in density and pressure rather than their absolute values. This change of procedure quickly suppressed the erratic behavior of the pressure.

The run was continued until the shock radius had reached a value of 6,270 meters. At that instant the overpressure in the shock was 0.0251 atmospheres. The positive pulse was 290 meters long and the negative pulse 760 meters. Since the further propagation of the shock is influenced at these low overpressures only by the positive pulse, the approximations on which the semi-acoustic theory of the next chapterare based, are well satisfied. They are (1) that the overpressure be small compared to 1 atmosphere, and (2) that the length of the pressure pulse be small compared to the shock radius. Even the application of the semi-acoustic theory to the negative phase is not bad. Hence, the IBM-run was discontinued and the semi-acoustic theory was used for the purpose of continuation.

7.5 RESULTS

The shock pressure as a function of the distance of the shock front from the center of the explosion is shown in figure 1.

In this graph all data have been collected from the various chapters. From a shock radius of 10 to 80 meters the similarity solution has been used. The

Figure 1

Shock pressure versus distance for nuclear explosion. Time is given in seconds, T = 0 is 0.012 after start of explosion.

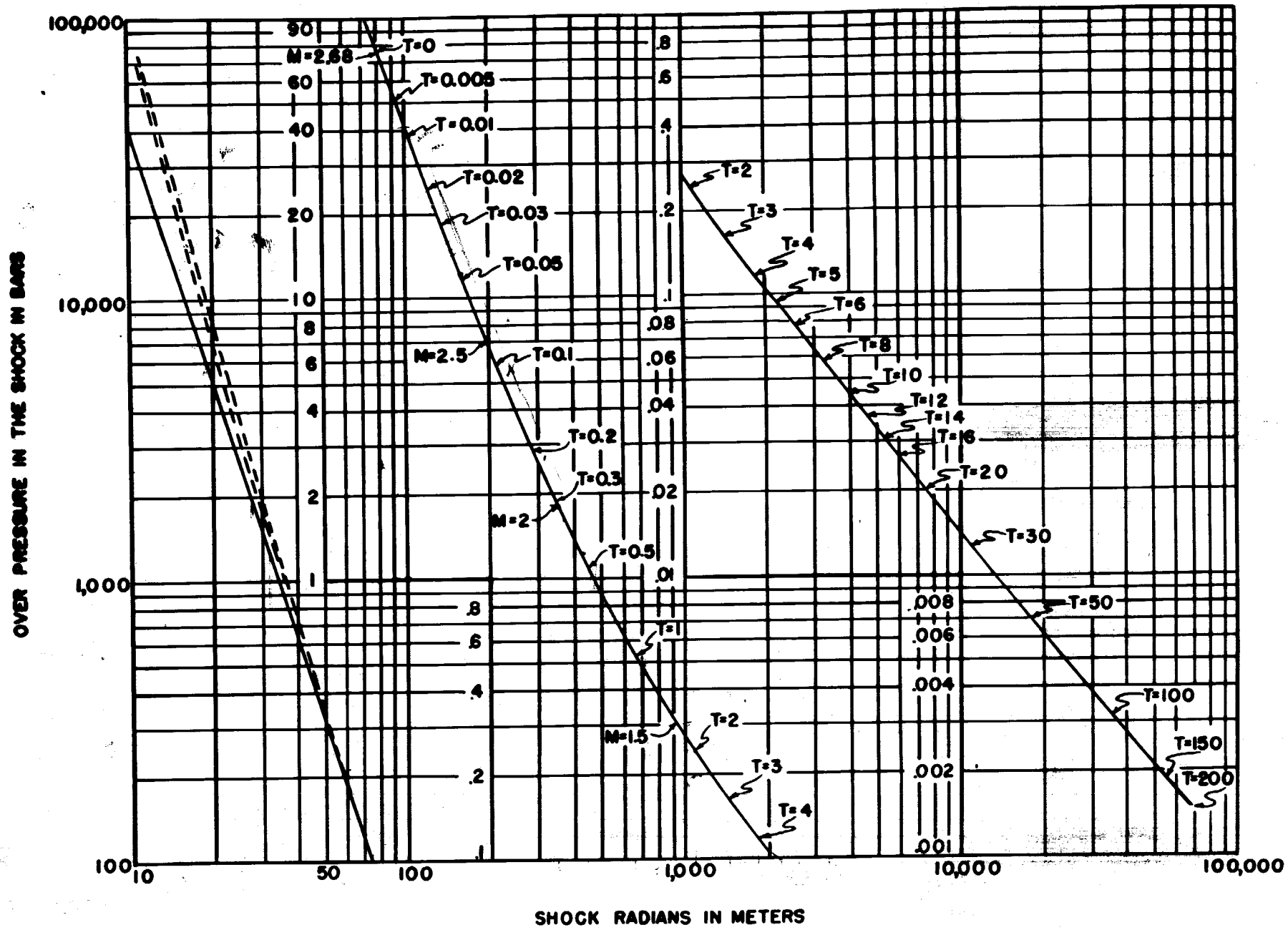

dotted lines show upper and lower limits for the effect of the gadget material on the propagation of the shock, as calculated for the Trinity gadget (sealed down to 10,000 tons of TNT). In this region the curve corresponds to an energy release of 10,000 tons.

For shock radii from 80 to 6300 meters, the shock pressures are obtained from the IBM run. Here the total energy is between 10,000 and 13,000 tons, the upper value being correct at sufficiently large distances. The time of arival of the shock is indicated at various points. $t = 0$ is the start of the IBM run which was 0.012 second after the explosion.

Beyond a radius of 6300 meters up to 67,000 meters, the semi-acoustic theory of the next chapter has been used.

A number of curves showing the pressure at a fixed distance as function of time are shown in Figures 2 to 9. Graphs of the pressure versus distance at a fixed time are shown in Figures 10 to 18.

The duration of the positive phase of the pulse as function of the shock pressure is given in Figure 19.

For comparison with measurements at Trinity we have also made a graph of the arrival time of the shock at various distances. It is most convenient to plot the shock radius divided by the arrival time as function of the shock pressure divided by the normal pressure, since such a graph is independent of the energy release. This graph is included in Chapter 19. It depends, of course, on the normal velocity of sound in the given circumstances, c_o. For the IBM-run $c_o = 347$ centimeters per second.

Finally, there are shown in Figure 20 the positive impulse $I+$ and the fraction of the total energy which is left in the blast as functions of the shock pressure divided by the normal pressure. The latter is independent of the energy release. The positive impulse has been scaled to an energy release of 40,000 tons in free air (or 20,000 tons on the ground) for the purpose of comparison with observations at Trinity.

Figure 2

Pressure versus Time for Radius 170.7 meters

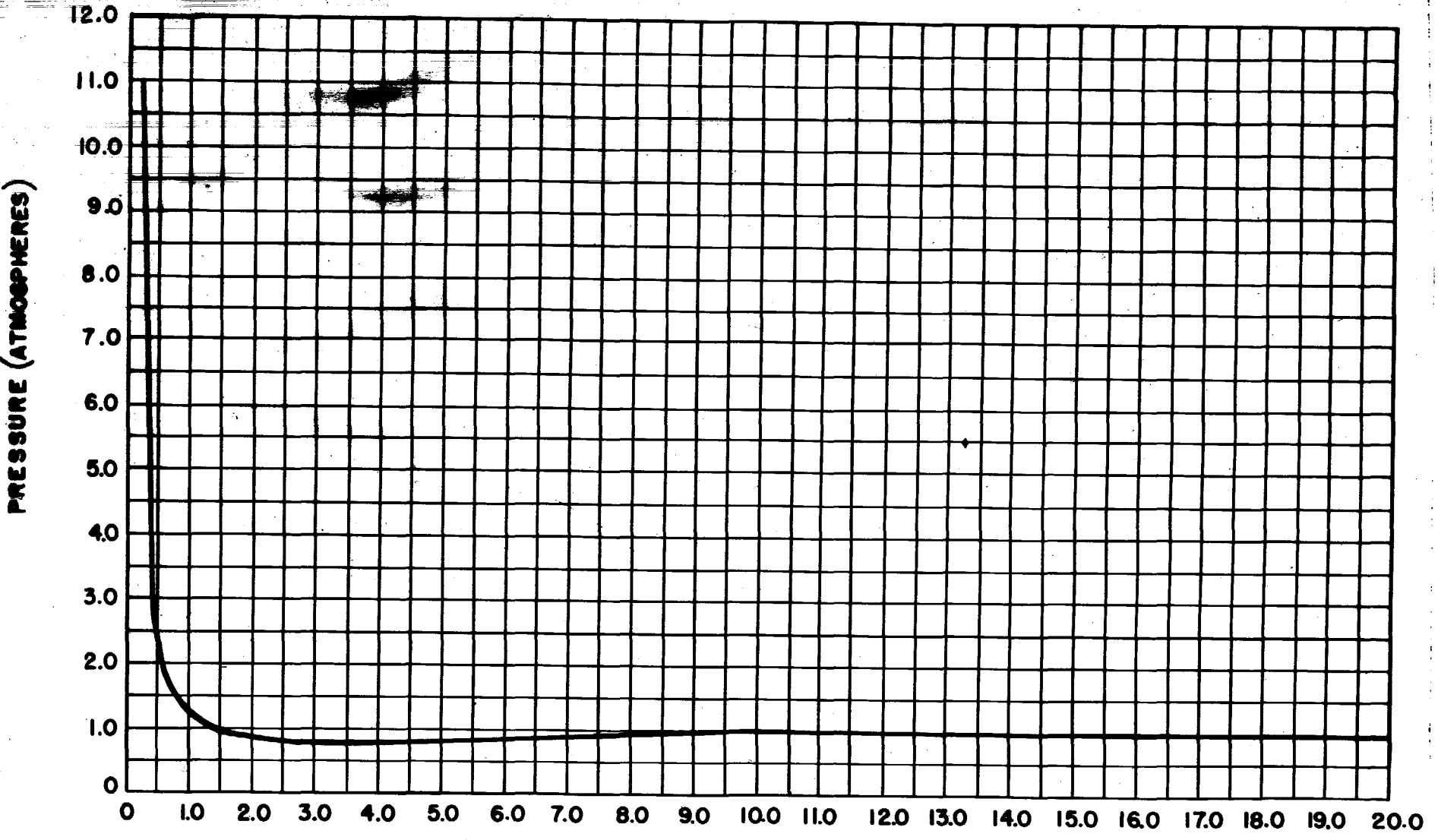

APPROVED FOR PUBLIC RELEASE

Figure 3

Pressure versus Time for Radius 223.4 meters

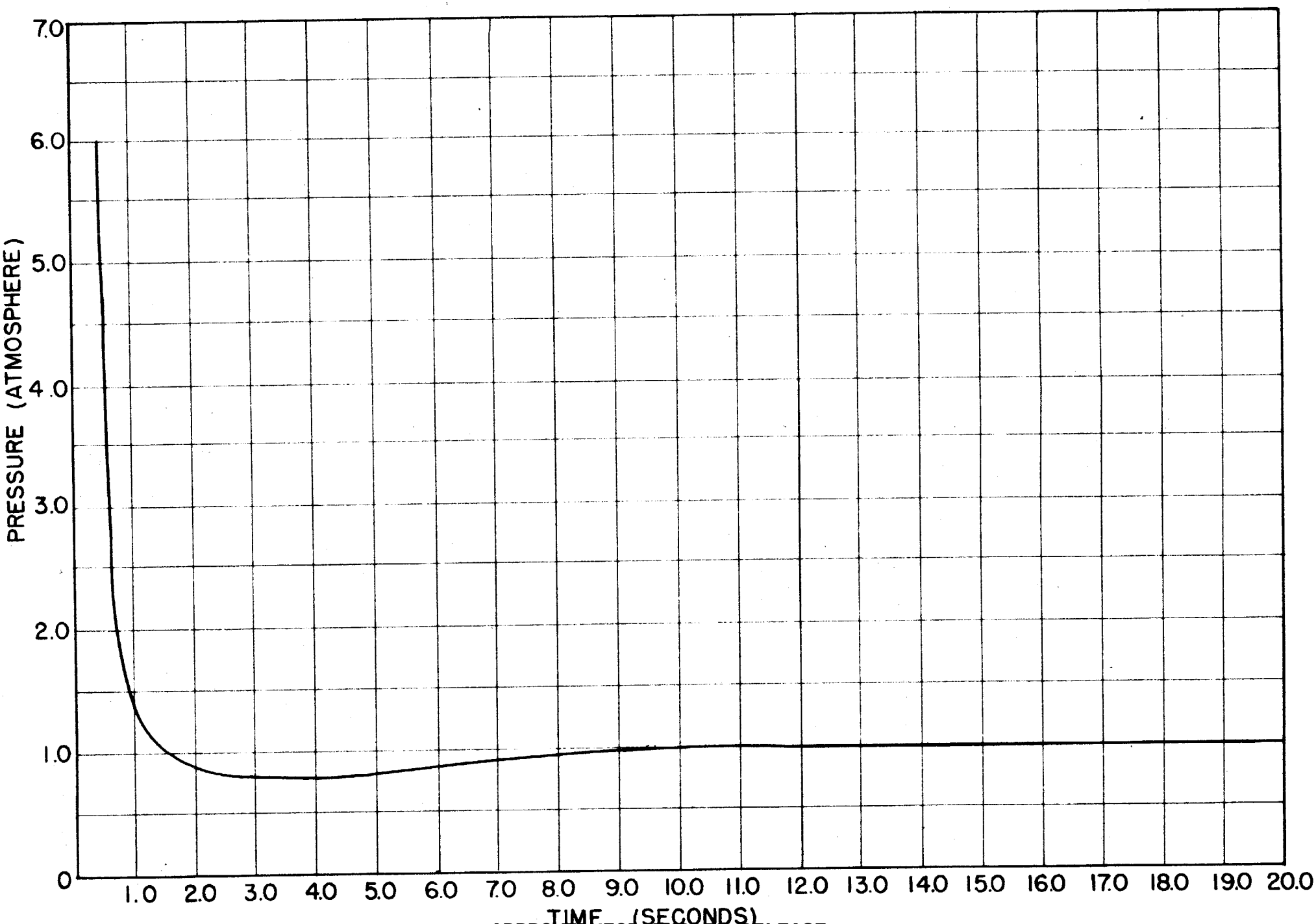

APPROVED FOR PUBLIC RELEASE

Figure 4

Pressure versus Time for Radius 332 meters

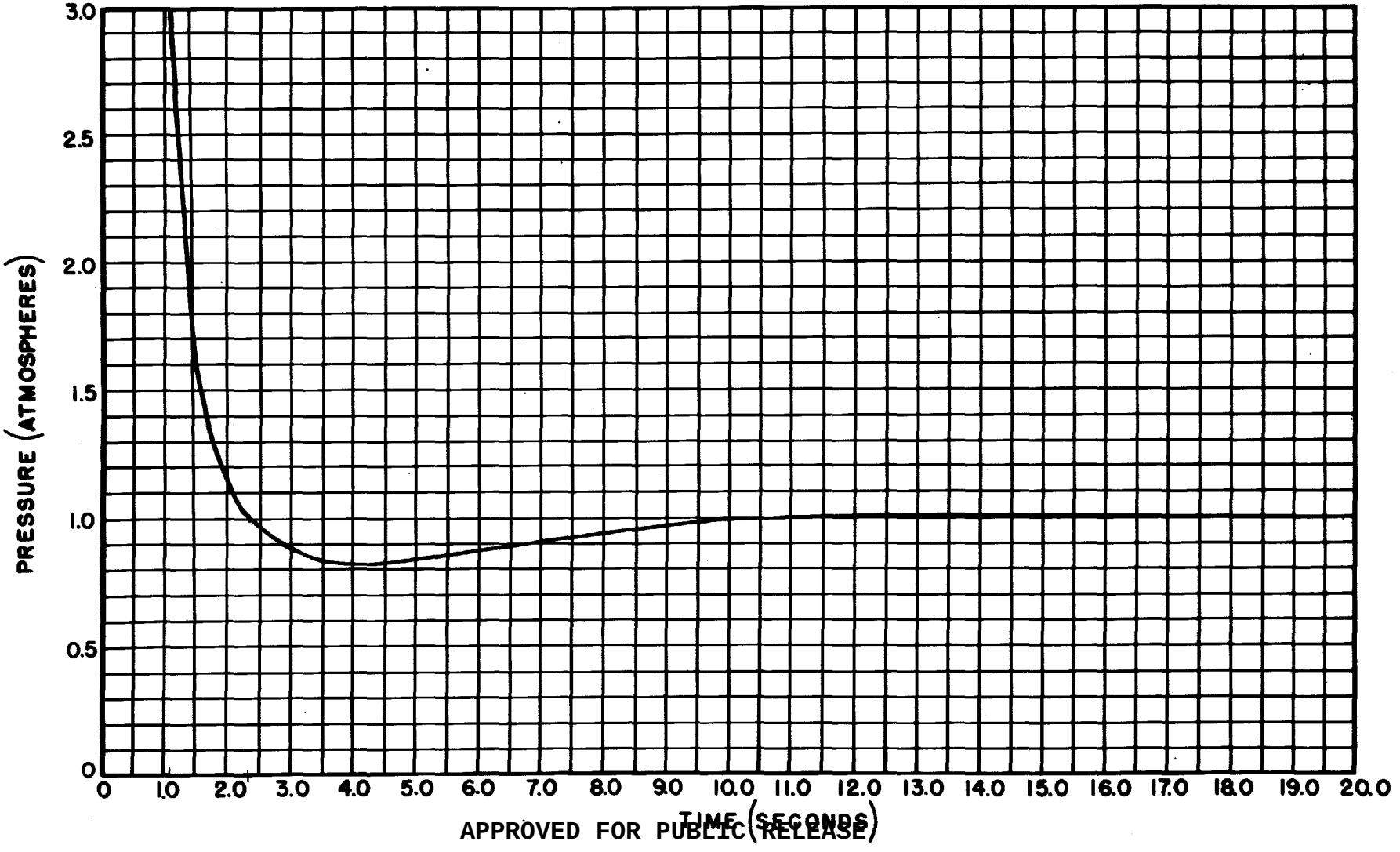

Figure 5

Pressure versus Time for Radius 466.5 meters

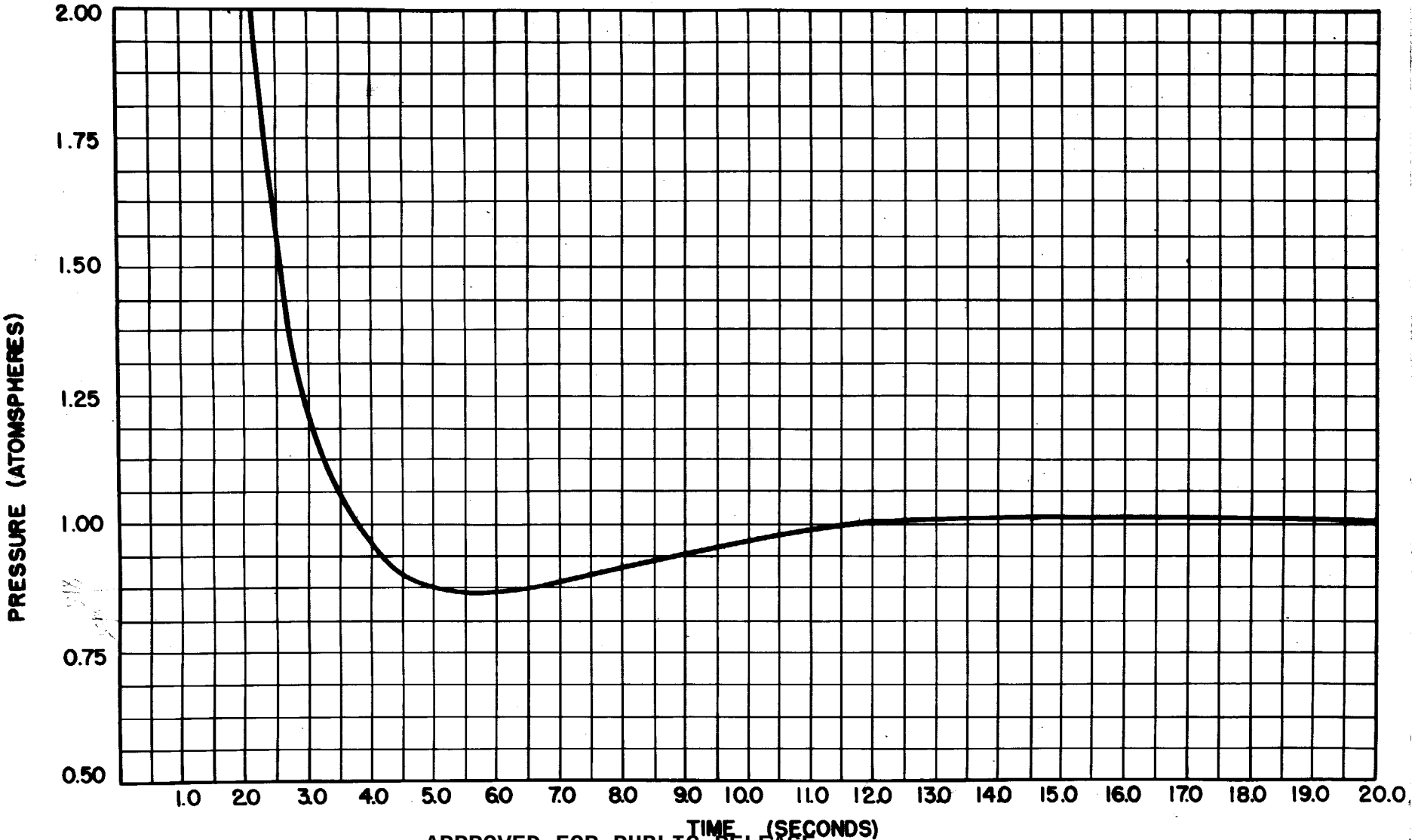

APPROVED FOR PUBLIC RELEASE

Figure 6

Pressure versus Time for Radius 682 meters

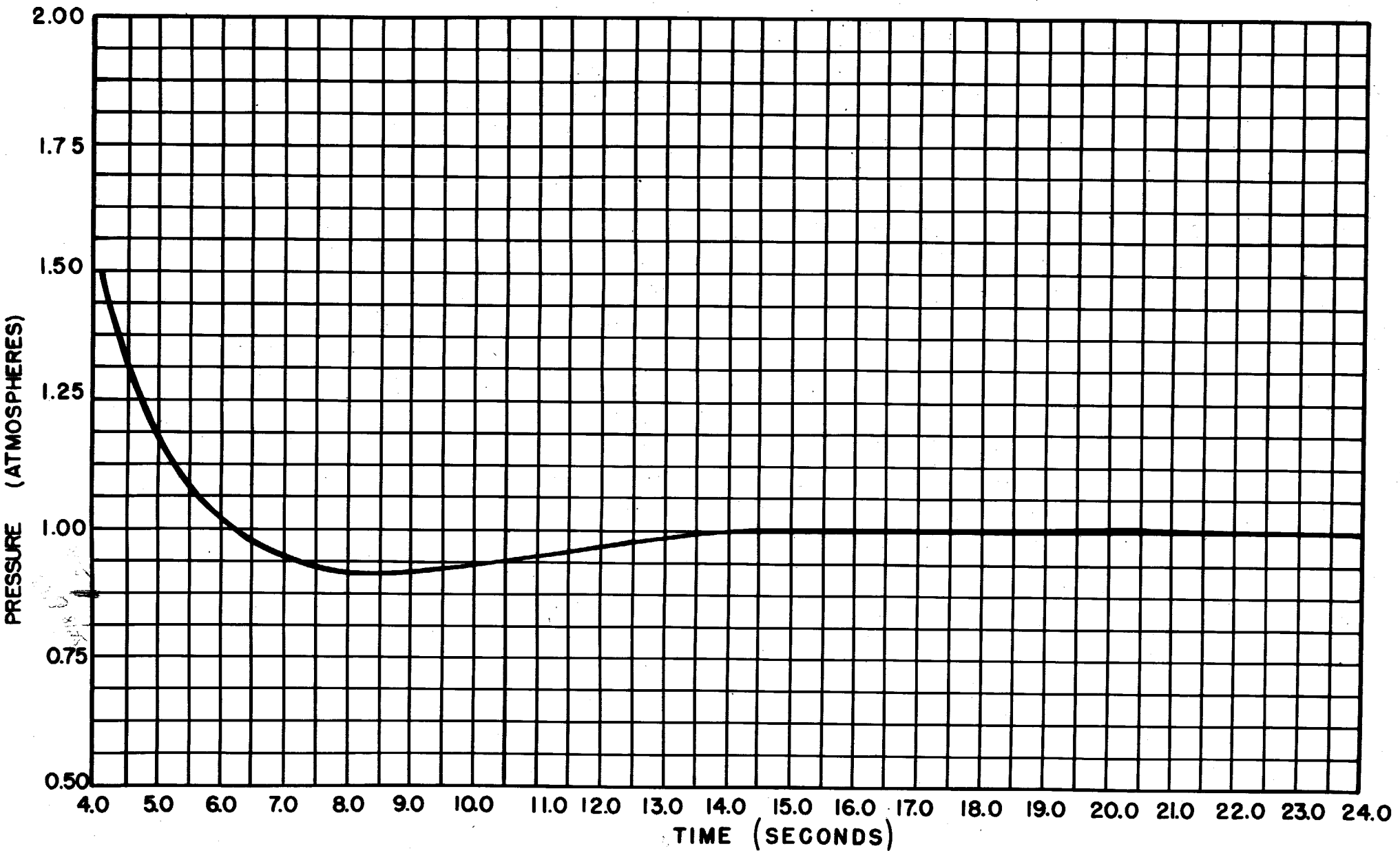

Figure 7

Pressure versus Time for Radius 1224 meters

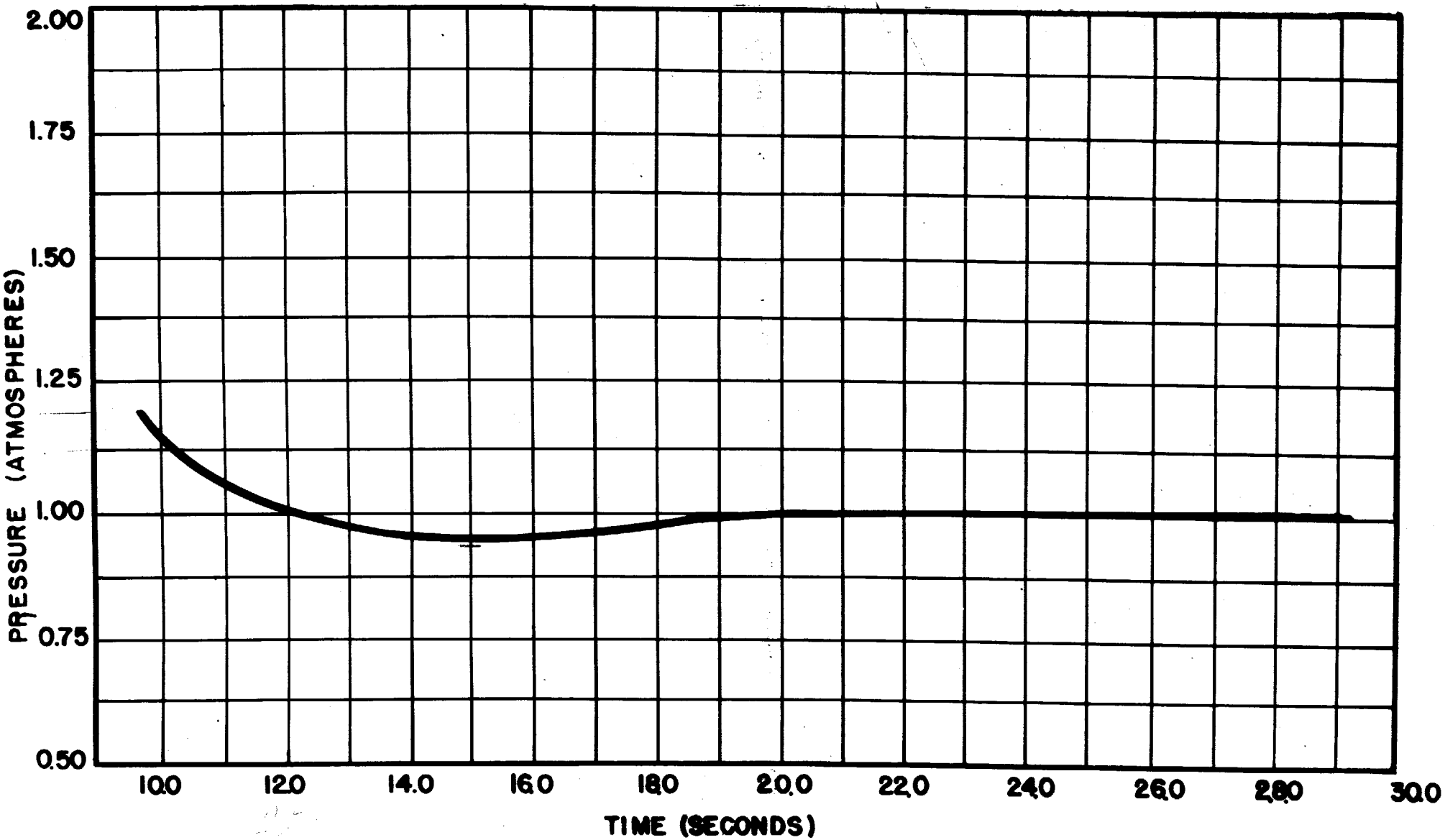

APPROVED FOR PUBLIC RELEASE

Figure 8

Pressure versus Time for Radius 2031 meters

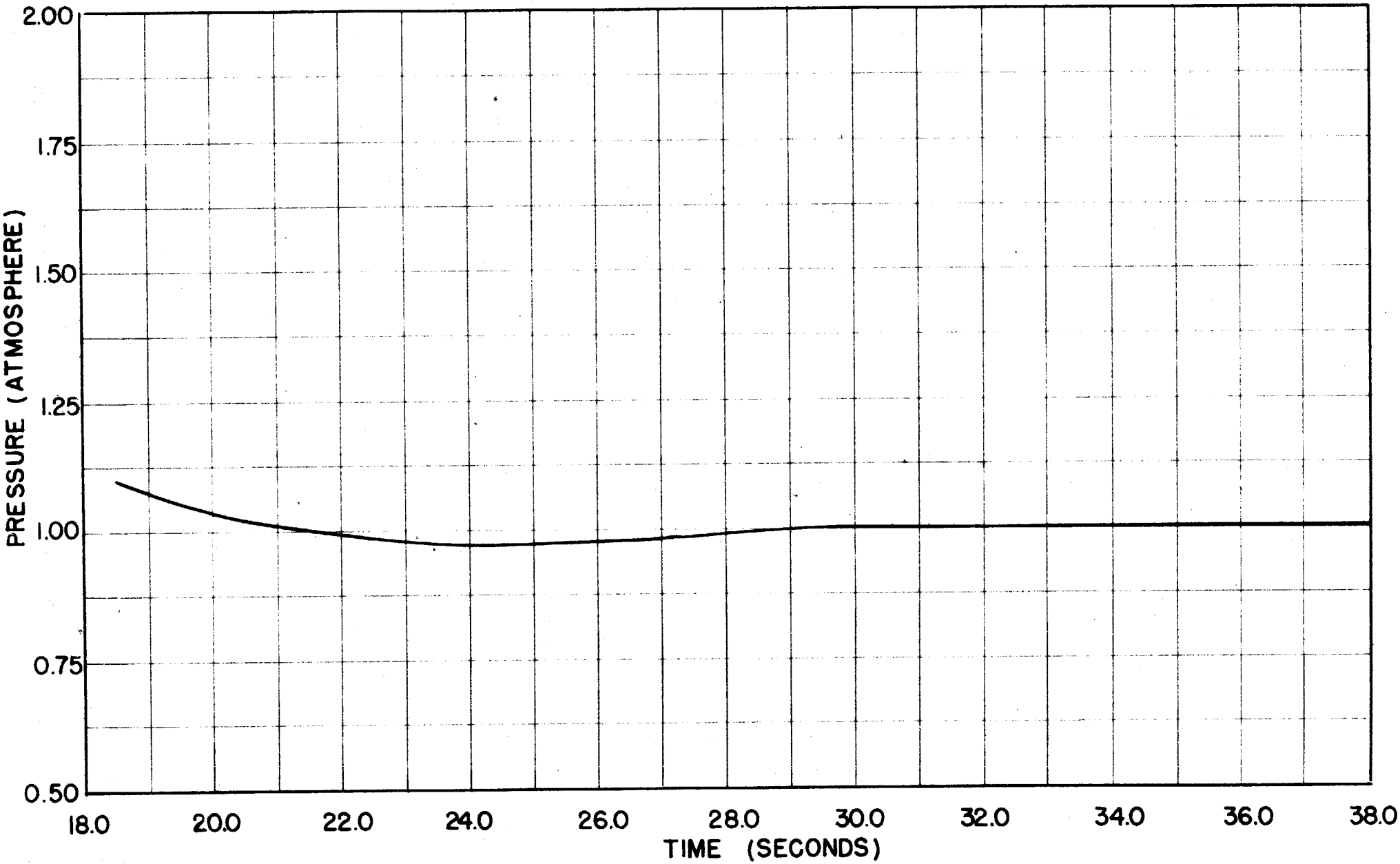

APPROVED FOR PUBLIC RELEASE

Figure 9

Pressure versus Time for Radius 3586 meters

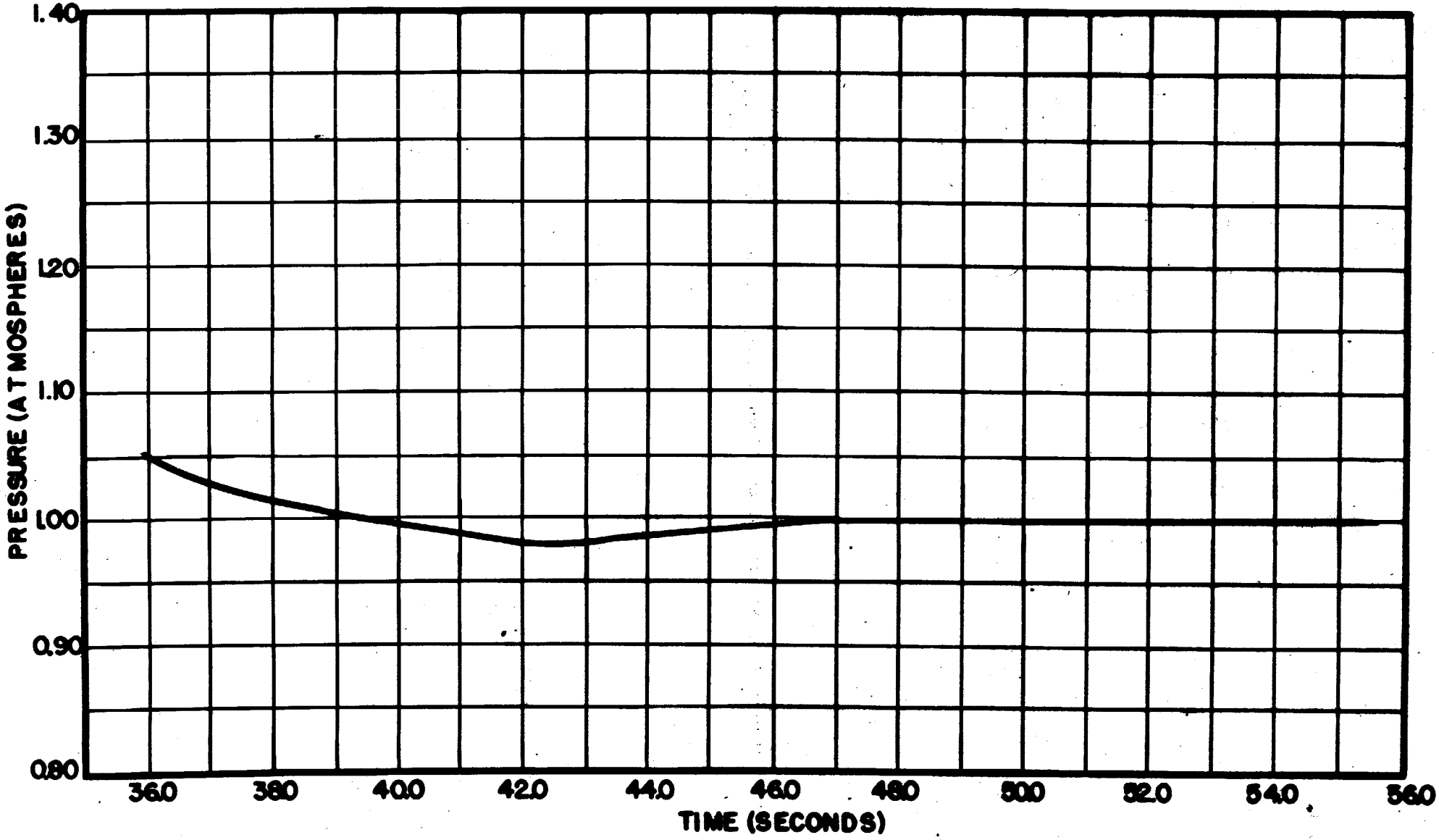

Figure 10

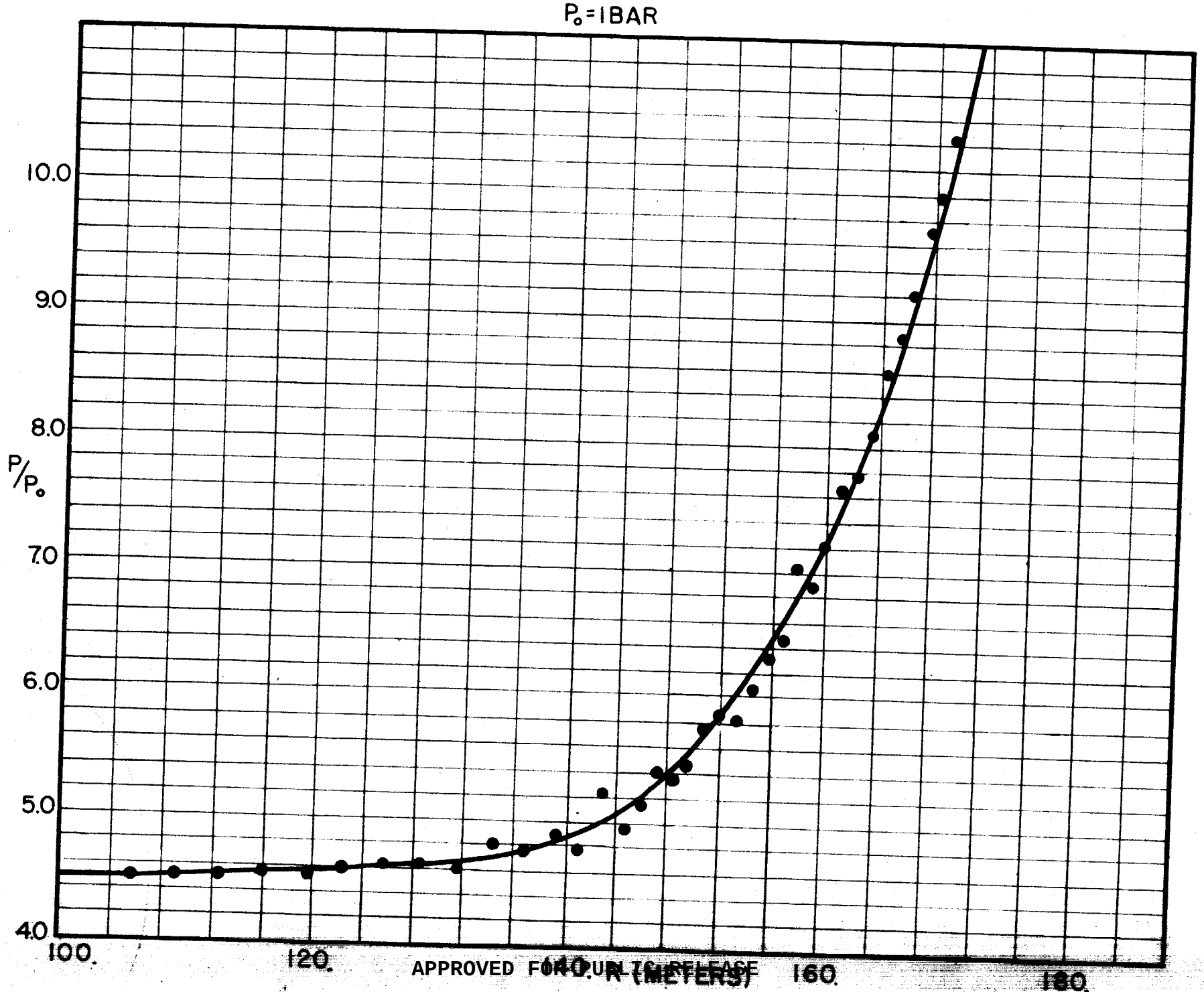

Figure 11

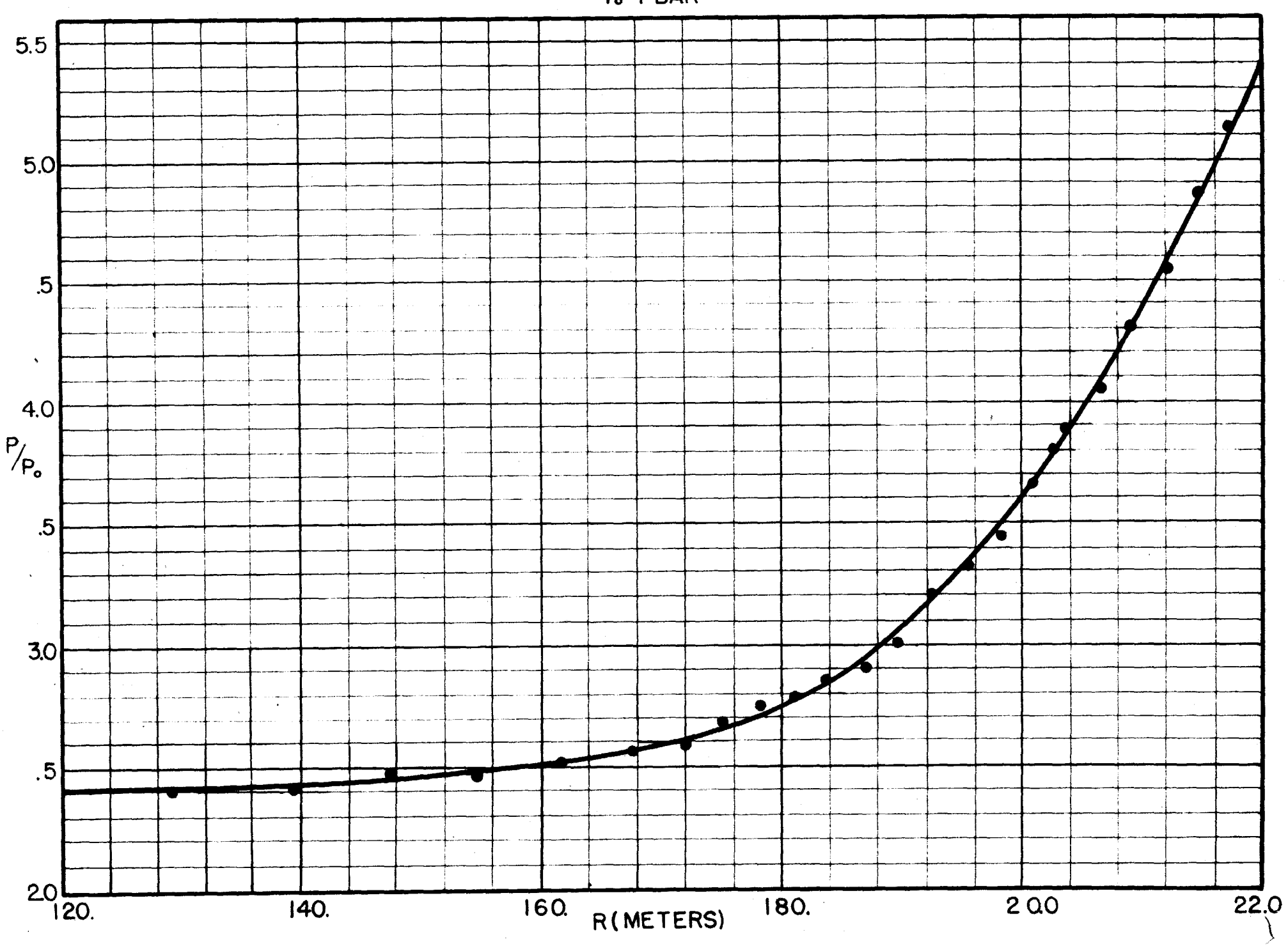

Figure 12

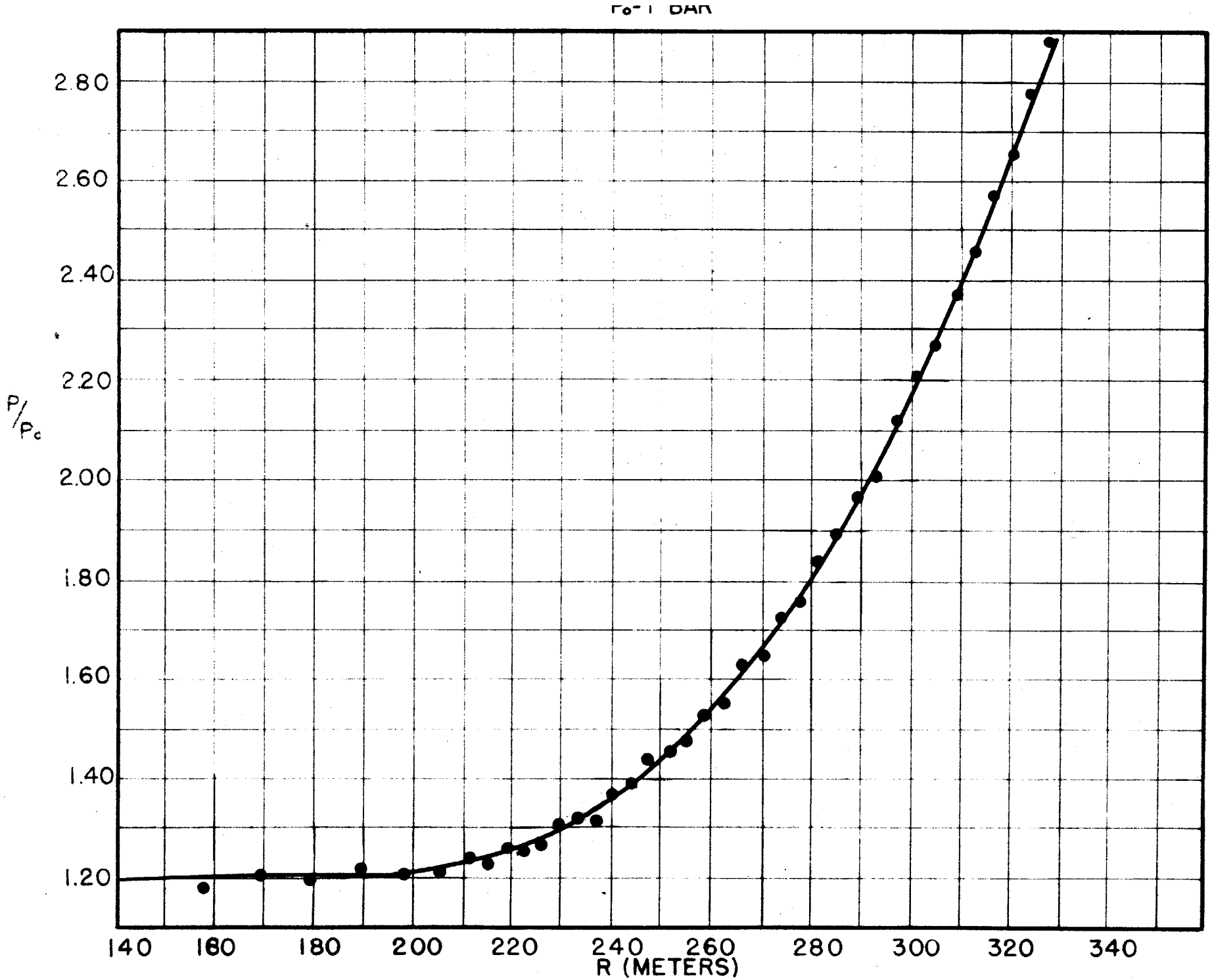

Figure 13

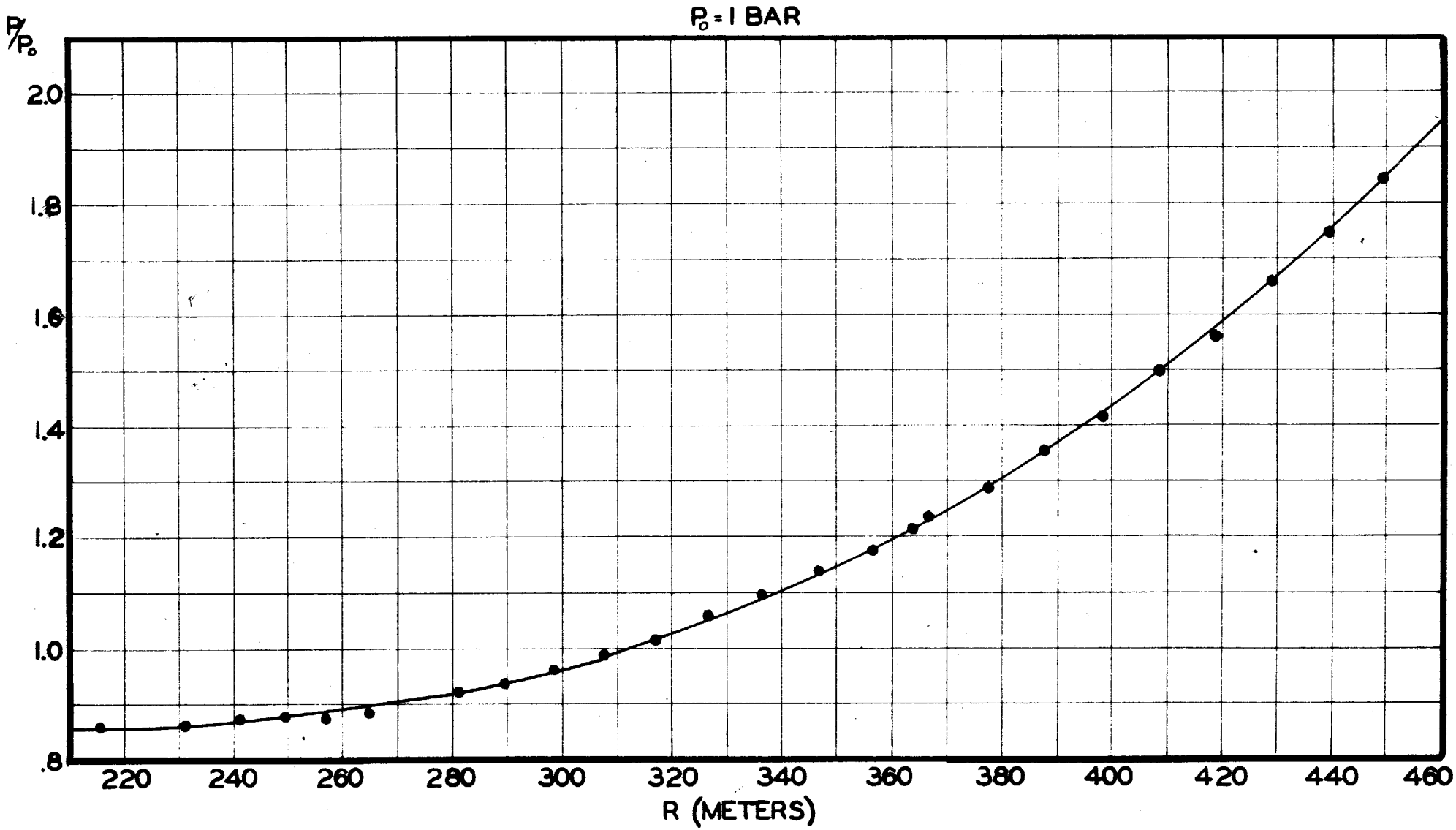

Figure 14

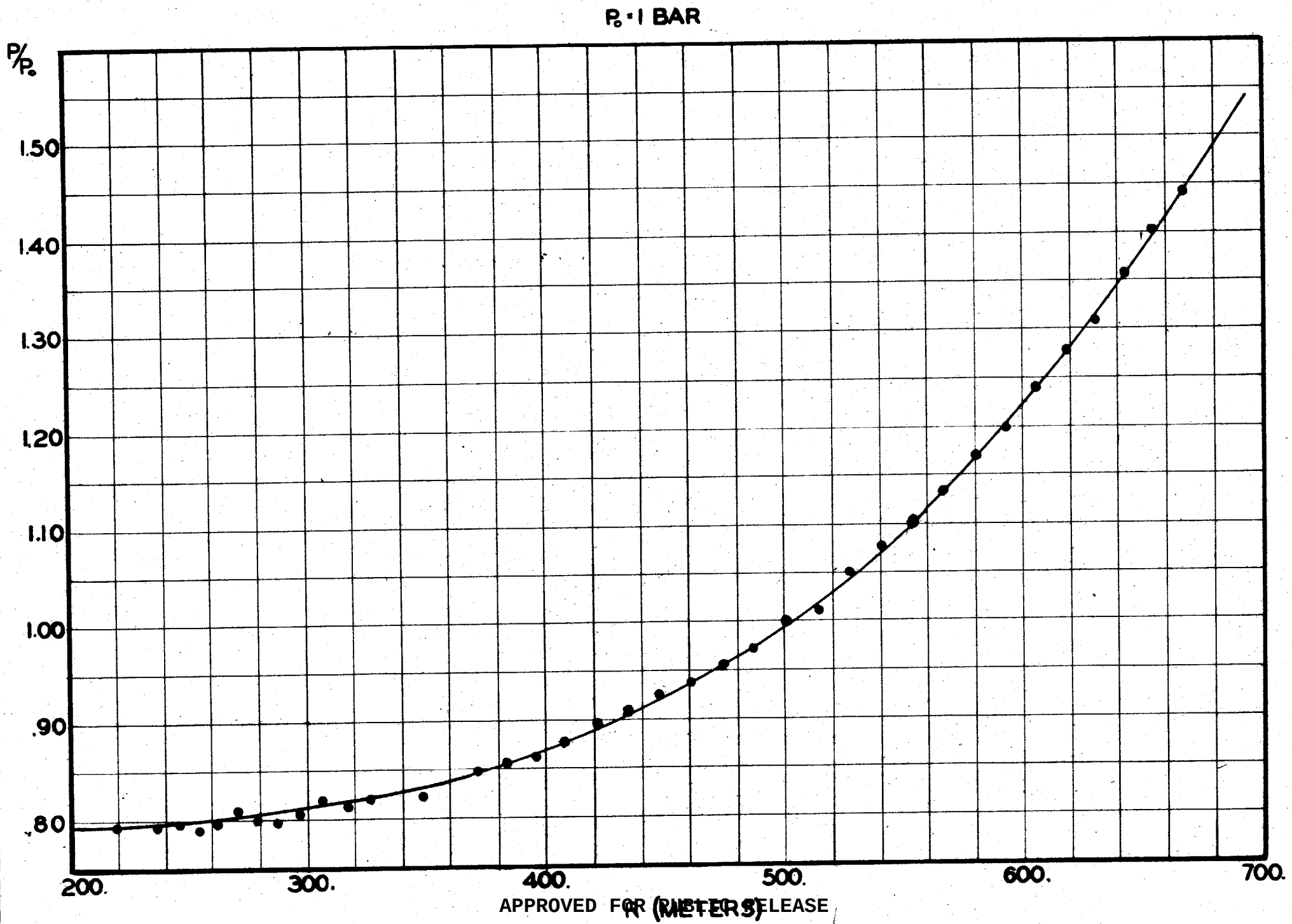

Figure 15

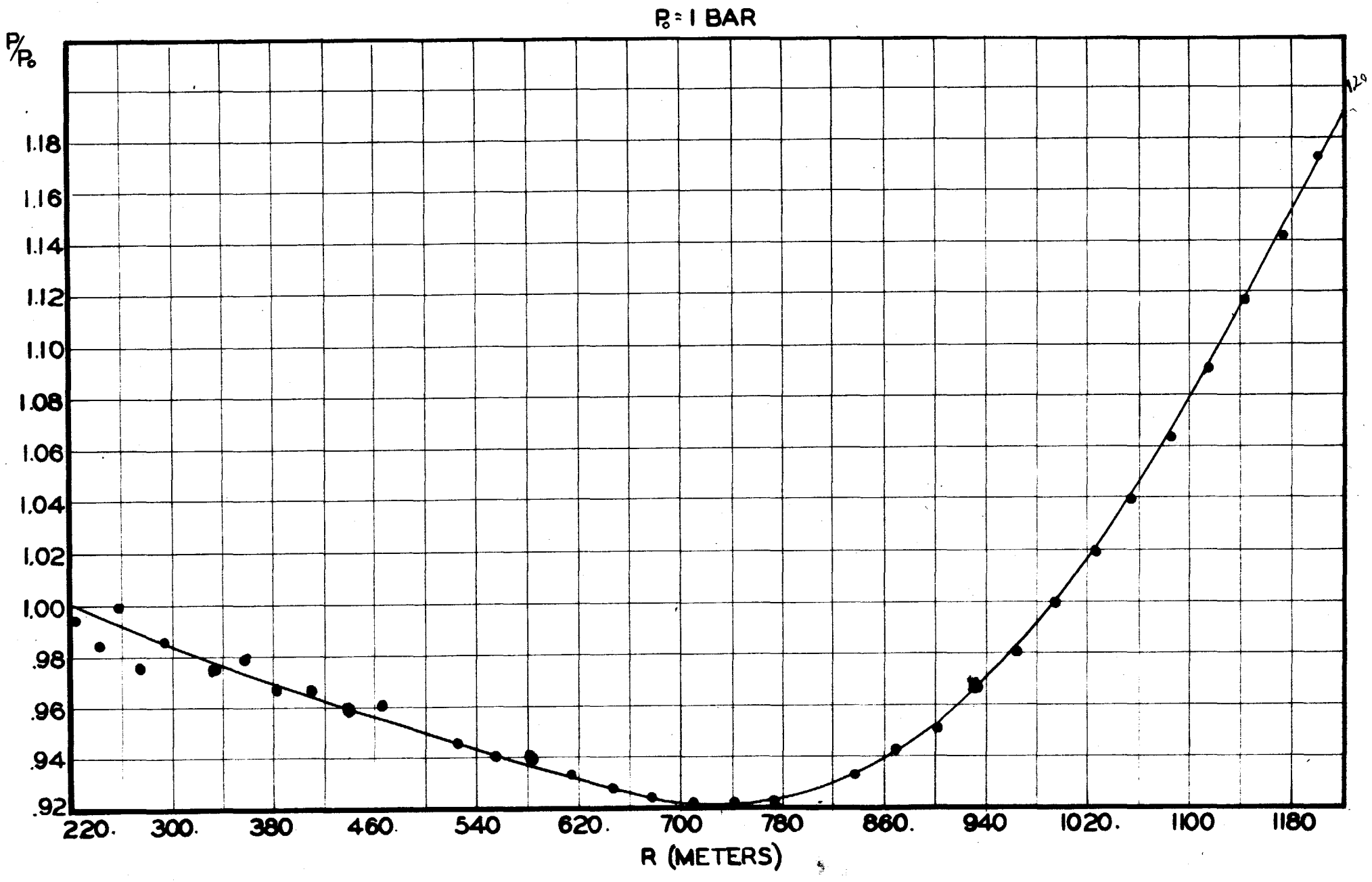

Figure 16

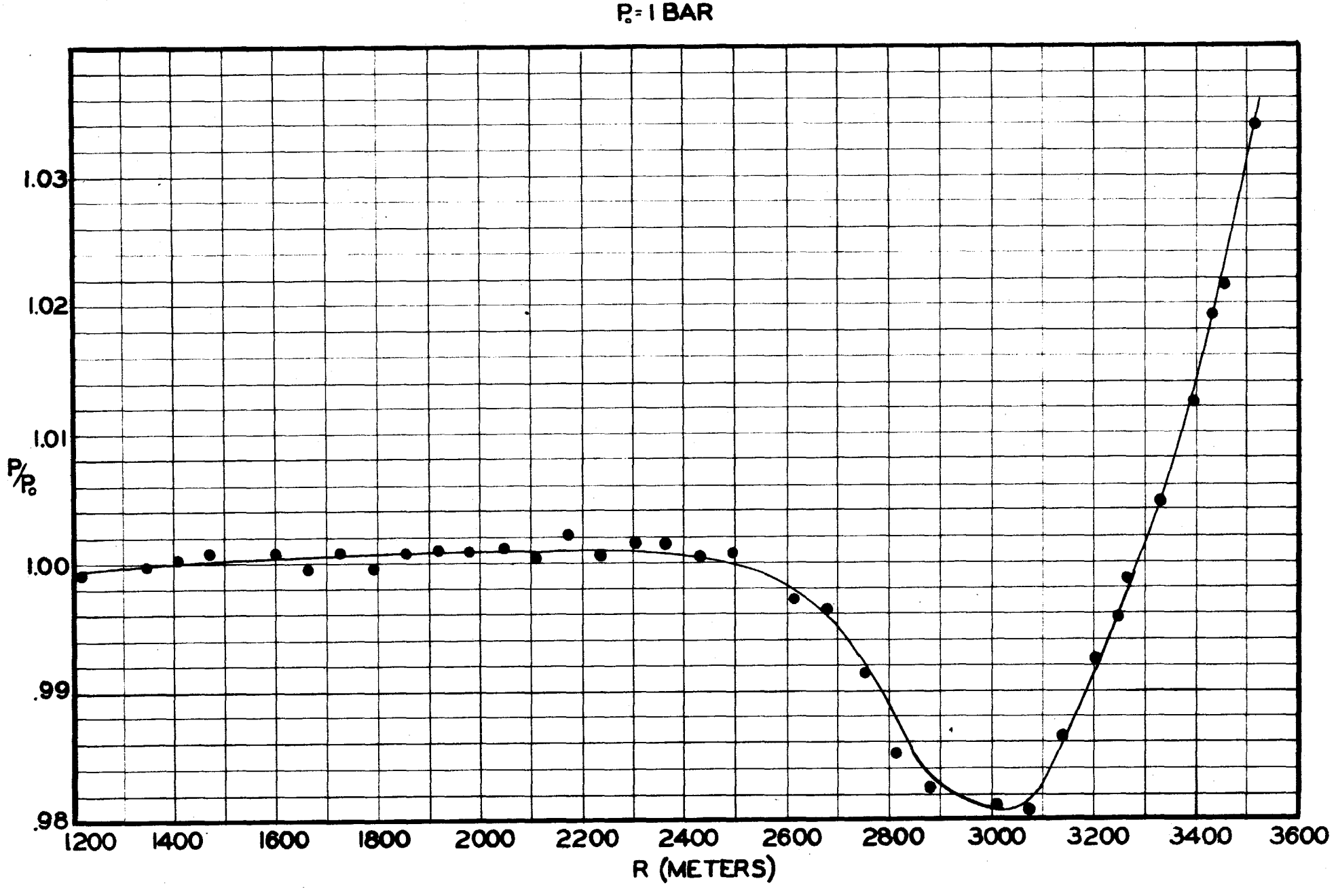

Figure 17

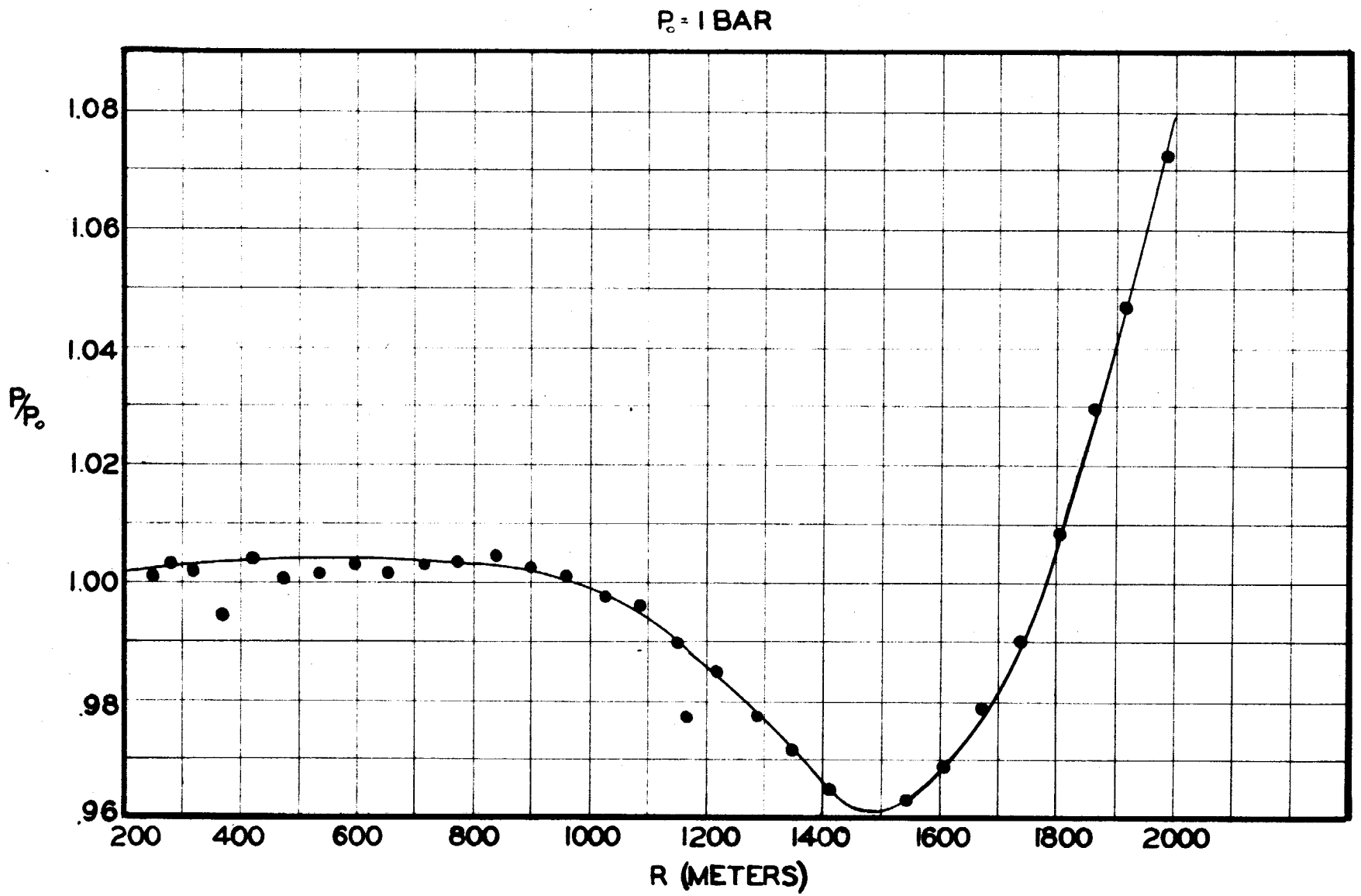

Figure 18

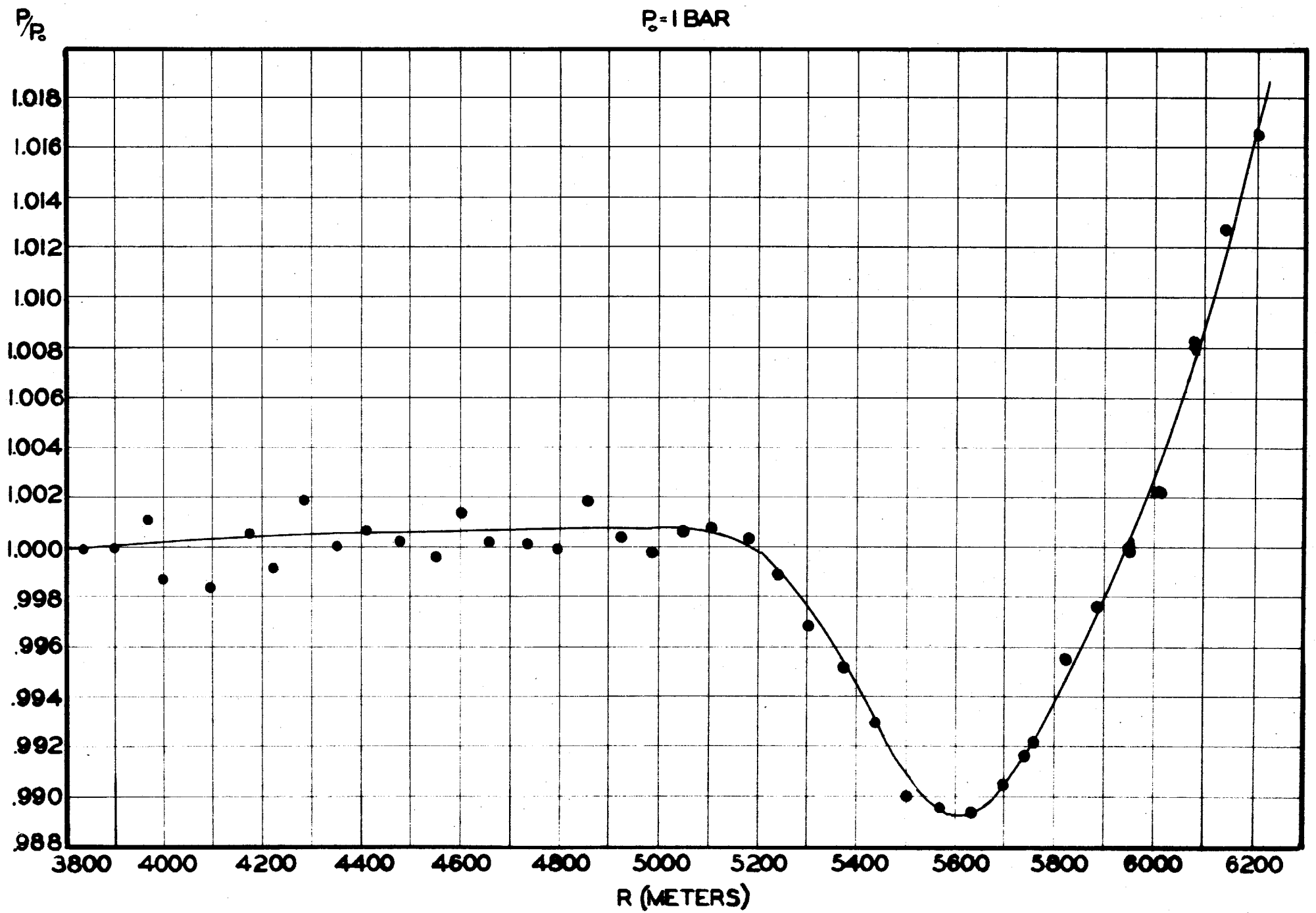

APPROVED FOR PUBLIC RELEASE

Figure 19

Deviation of the positive phase of a pulse at a fixed distance

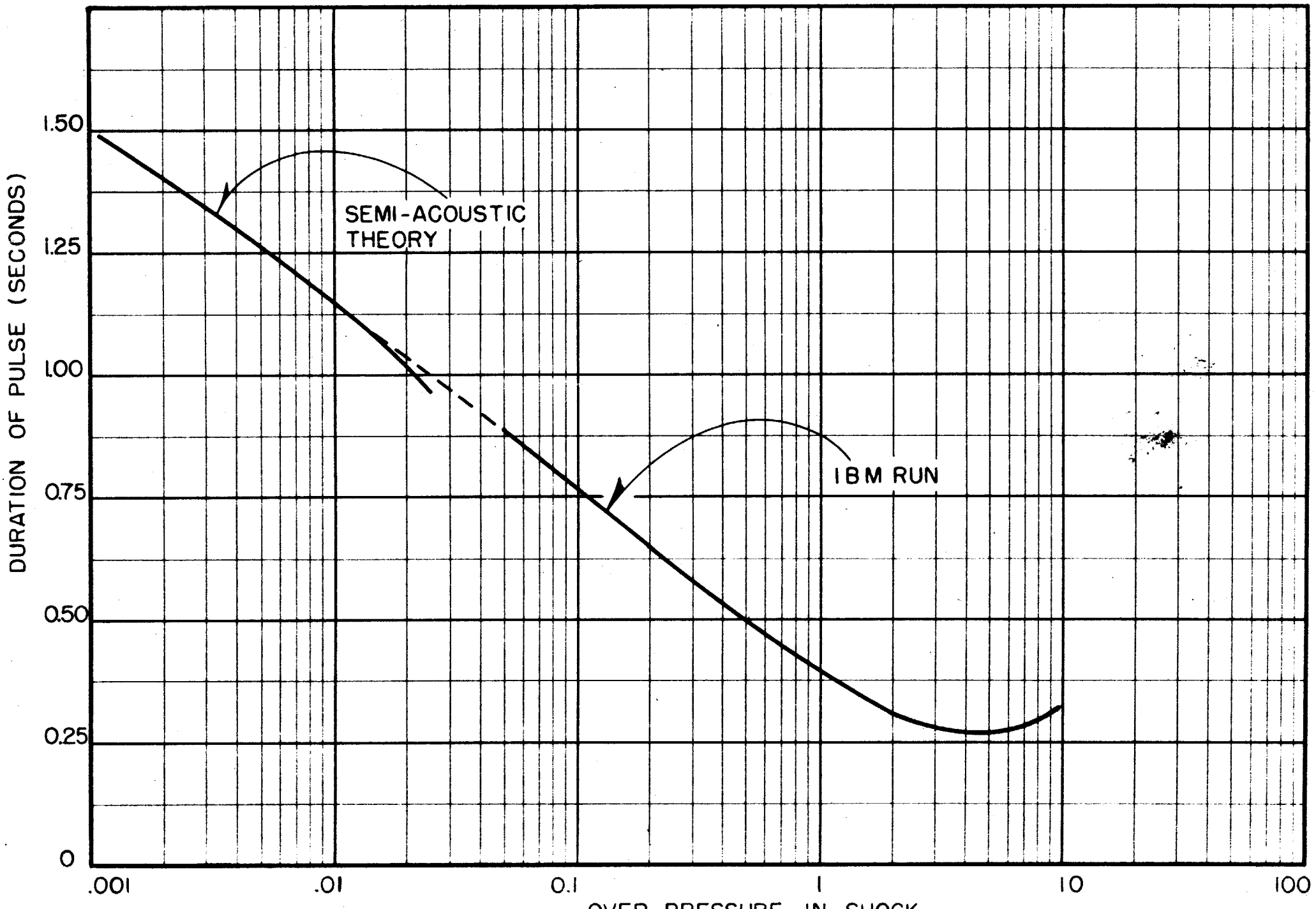

APPROVED FOR PUBLIC RELEASE

Figure 20

The positive impulse and the energy in the blast.

(IBM) run scaled to 40,000 tons.

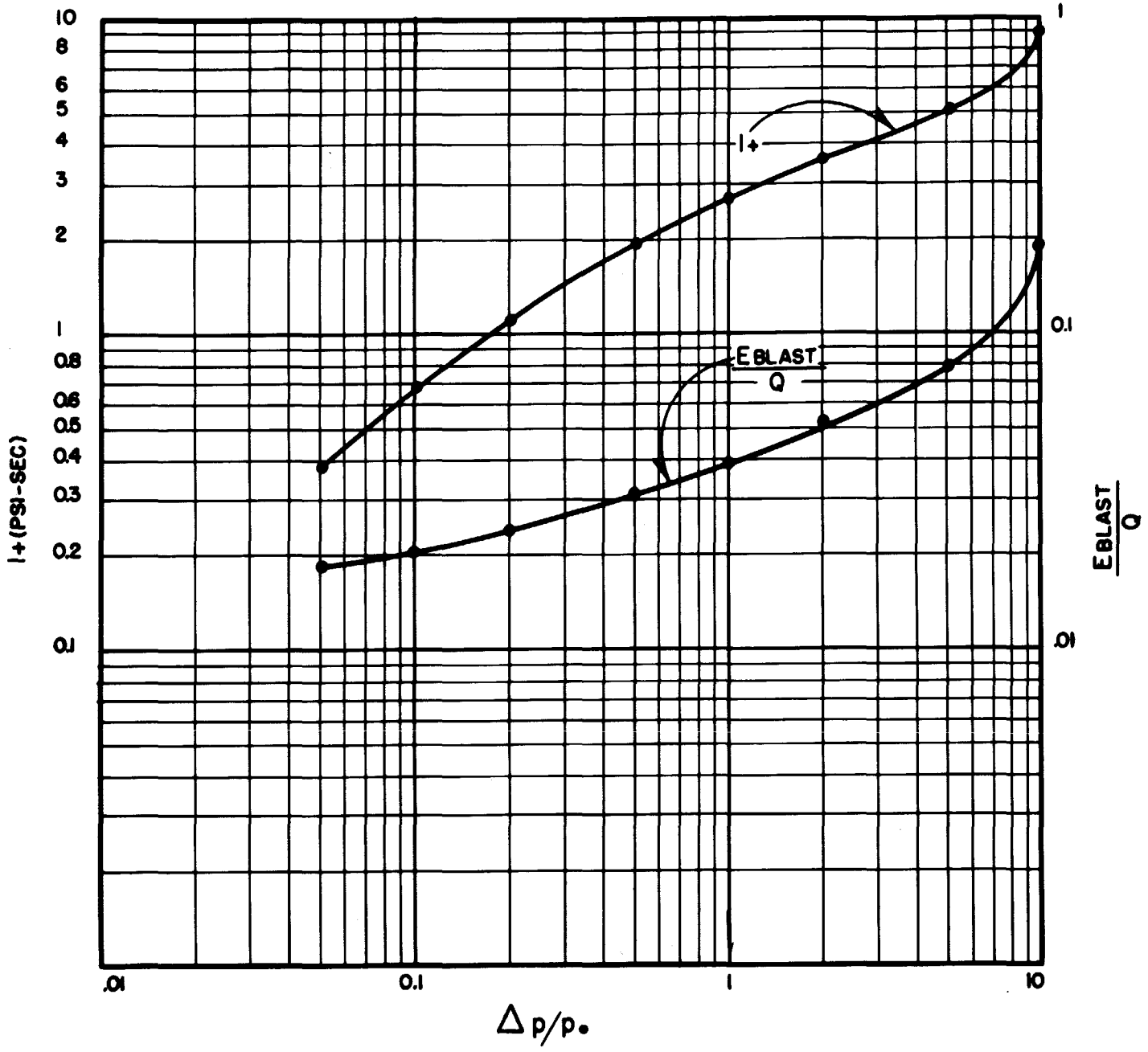

7.6 COMPARISON WITH TNT EXPLOSION. EFFICIENCY OF NUCLEAR BOMB

One purpose of the IBM-run was to find the efficiency of a nuclear bomb compared to an explosion from an equivalent charge of TNT. In the nuclear explosion a greater amount of energy is used for the purpose of heating the air near the center of the explosion to high temperatures. A large fraction of this energy is useless for the propagation of the shock.

Since no comparable IBM-run exists for a TNT explosion, we compared the results for the nuclear explosion with experimental data. For this purpose, the experimental curve prepared by Hirschfelder, Littler and Sheard was used. It is based on experimental data for charges fired on the ground, and for shock pressures in the range from 15 to 2 pounds per square inch. The charges varied from 67 to 550 pounds. The curve is given by the expression

$$\Delta p = \frac{38.5}{x} + \frac{85}{x^2} + \frac{5760}{x^3} \qquad (9)$$

$$x = Y/w^{1/3} \qquad (10)$$

Here Y is the shock radius in feet; w, the weight of the charge in pounds, and Δp the overpressure in psi.

For lower pressures Hirschfelder, Sheard and Littler used the asymptotic formula

$$\Delta p = \frac{35.0}{x\sqrt{\log_{10} x - 0.928}} \qquad (11)$$

The constants were obtained by fitting to the low pressure end of the curve (9). The analytical form of the equation follows from the semi-acoustic theory presented in the next chapter, provided the pressure pulse has reached its asymptotic linear shape.

From these formulae we calculated the weight of the TNT charge required to give the same shock pressure at the same distance as the nuclear explosion. Dividing this charge by the weight of 13,000 tons assumed for the IBM-run, and

multiplying by a factor 2, to take care of the fact that the TNT data apply to an explosion on the ground so that practically all energy is in a half sphere, we obtain the efficiency of the nuclear bomb compared to an equivalent charge of TNT.

The efficiency defined in this way depends on the shock pressure chosen for comparison, and it is not surprising that it should vary with the shock pressure; however, it is surprising that the efficiency should increase with decreasing shock pressure as shown in Figure 21 over the range in which experimental data for TNT exist. However, the individual experimental points scatter appreciably, especially for high shock pressures and, therefore, this variation of efficiency with shock pressure is not necessarily correct. The most reliable data are those at the lower end of the experimental range, which would indicate an efficiency of about 0.6.

The curve has been extended on either side to higher and lower shock pressures. The extension to higher shock pressures by means of formula (9) is quite arbitrary and has been performed only since experimental data for the Trinity test have usually been compared with this formula. The extension to lower pressures depends on the assumption that the asymptotic formula is valid in this range, which is not necessarily correct. Again, the main reason for performing the extension is the fact that experimental data have been analyzed by means of this curve.

A similar comparison has been made by using the experimental curve of A.H. Taub,[1] for half-pound TNT charges in free air. These differ quite

---

(1) Report NDRC-A-4076

---

appreciably from the curve of Hirschfelder, Littler and Sheard, as may be seen from Graph 21. This discrepancy shows the difficulty of assigning any definite value to the efficiency of the nuclear bomb for the purpose of producing blast and makes it desirable to have a comparable IBM-run for TNT.

Figure 21

Efficiency pf nuclear bomb as compared to an equivalent charge of T.N.T.

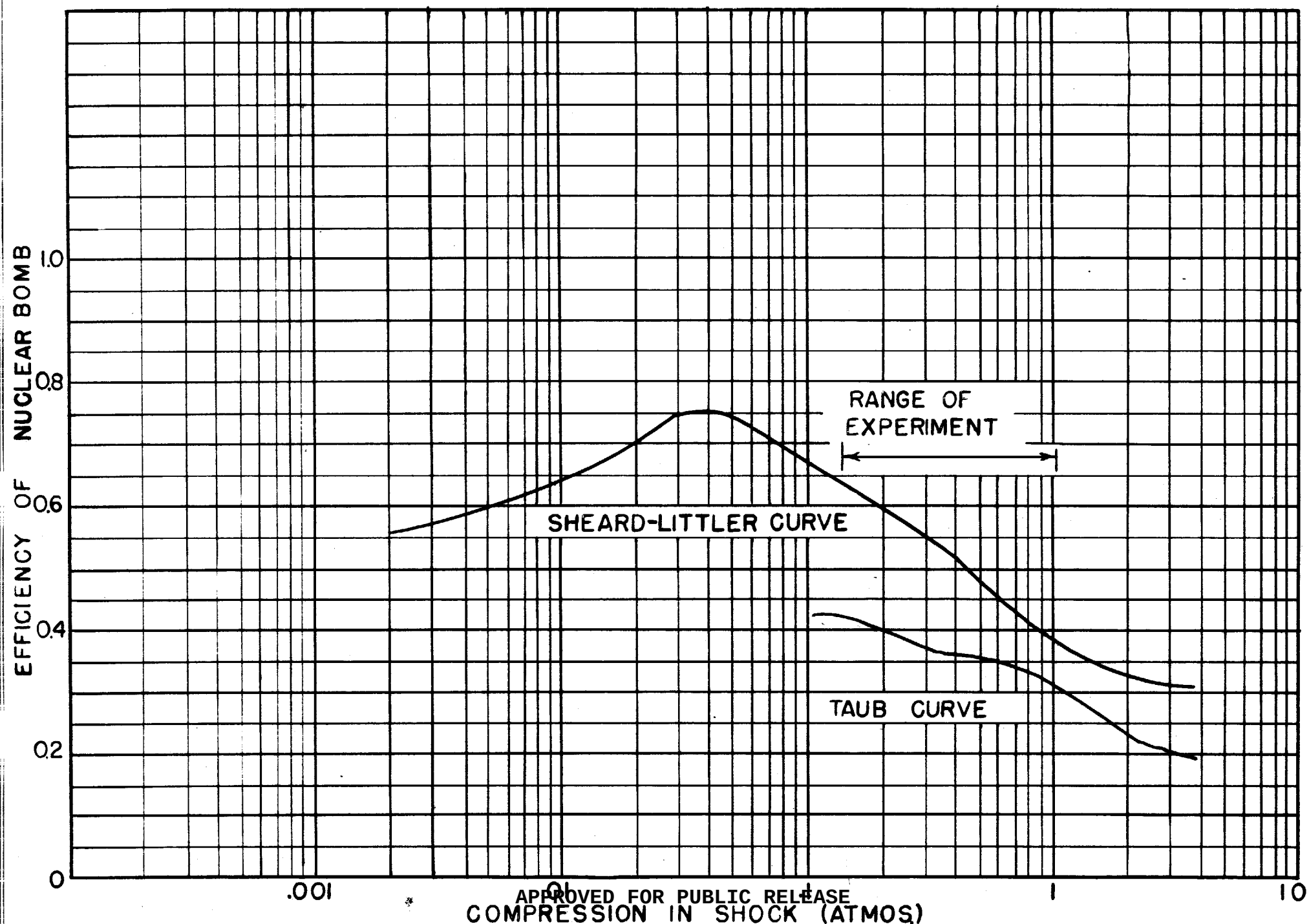

APPROVED FOR PUBLIC RELEASE

It should be noted that two factors, which might be important, have been disregarded in the IBM-calculations. One of these is the radiation transport of energy from the ball of fire into the NO_2 layer, discussed in Chapter 4. This has the effect of equalizing the temperatures in the interior of the shock sphere and it will make the nuclear explosion more similar to a TNT explosion. Consequently, the efficiency of the nuclear bomb is improved. The other effect is the radiation which escapes to large distances. The arguments presented in Chapter 4 show that this radiation occurs at a time and place where it cannot affect the shock pressure in the region of practical interest, i.e. down to about one psi. However, it could reduce the efficiency at very low shock pressures.

7.7 SCALING LAWS

The IBM-run was made assuming a normal density of air $\rho_0 = 1.163$ and a normal pressure $P_0 = 1$ bar (10^6 dyn/cm^2). The sound velocity of normal air is then $c_0 = 347$ centimeters per second. The total energy was $Q = 13{,}000$ tons.

For the change to a different energy release we have exact scaling laws, we keep all pressures and velocities fixed, but change all radii and times in the ratio of the cube root of the energy release.

For the change to different normal densities or pressures no exact scaling laws exist. However, within the accuracy of the primary data which enter the IBM-run, we can use the following scaling laws, which relate the dashed quantities for arbitrary normal conditions to the IBM-quantities:

$$\frac{p'}{p'_0} = \frac{p}{p_0} \qquad R' = \lambda R$$

$$\frac{u'}{c'_0} = \frac{u}{c_0} \qquad t' = \frac{c_\rho}{c'_0}\,\lambda t$$

$$\frac{\rho_1}{\rho'_0} = \frac{\rho}{\rho_0} \qquad Q' = \frac{p'_0}{p_0}\,\lambda^3 Q \qquad (12)$$

i.e. we scale all pressures, velocities and densities in the ratio of their normal values. The linear dimensions are scaled by an arbitrary factor λ, the times by the same factor λ and the inverse ratio of the normal sound velocities, and, finally, the energy release is scaled by λ^3 and the ratio of the normal pressures. The scaling laws for pressure, velocity and density are, of course, not independent of each other, since $\left(\rho_o' c_o'^2 / \rho_o c_o^2 = p_o' / p_o\right)$

These scaling laws are based on the assumption that the equation of state of air can be written in the form

$$\frac{p}{p_o} = \text{function of } \left(\frac{\rho}{\rho_o}\right) \text{and} \left(\frac{E\rho_o}{p_o}\right)$$

which is true for a γ-law, but only approximately correct for the true equation of state of air. (E is the interval energy per unit mass).

For the Trinity test the scaling changes are appreciable, because of the low value of the normal pressure (See Chapter 19).

CHAPTER 8

ASYMPTOTIC THEORY FOR SMALL BLAST PRESSURE

H. A. Bethe K. Fuchs

8.1 INTRODUCTION

It is very desirable to have a theory of shock waves which is valid for small over-pressure. One purpose of such a theory is to provide a natural transition to the well-known acoustic theory, and to set in evidence the limitations of the latter. Another purpose is to give practical results for the pressure up to arbitrarily large distances and to make it possible to stop the numerical calculation with IBM machines (see Chapter 7) at some finite low pressure. This numerical calculation would become increasingly inaccurate and cumbersome with increasing radius of the shock wave; the use of asymptotic formulae therefore improves both the accuracy and the ease of the calculation.

The theory presented in this chapter represents the first terms of an expansion in powers of the ratio L/Y where Y is the radius of the shock wave and L its length, i.e. the distance from the first shock to a point at which the pressure has decreased to a small fraction of the peak pressure. We shall in general retain the first and second power of L/Y and neglect the third. One strong reason for stopping at just this point is that the entropy in the shock is proportional to p^3, where p is the over-pressure at the shock front which in turn is proportional to 1/Y. Therefore, if we neglect terms of order $(L/Y)^3$ we can consider the entire process as adiabatic which involves a great simplification. At one point in our development, however, (Section 7) we shall calculate the actual energy transformed into heat at the shock front and at

this point we shall, of course, carry terms of order $(L/Y)^3$.

Ordinary acoustic theory does not represent the first term in an expansion of the type considered here. We shall find that the length of a spherical shock wave increases gradually as the shock wave moves away from its center, whereas an acoustic wave retains its wave-length all the time. Similarly, the decay of the pressure at the shock front is somewhat faster than that of the pressure in an acoustic wave. However, acoustic theory is very useful to provide some guiding ideas for our theory, and we shall therefore start by a recapitulation of the acoustic theory of an outgoing spherical wave.

8.2 ACOUSTIC THEORY

In the ordinary hydrodynamic equations (see below, Equation (12)) all terms should be neglected which are of second or higher order in pressure p or material velocity u. Then the hydrodynamic equations become

$$\frac{\partial u}{\partial t} = - c \frac{\partial \sigma}{\partial r}$$

$$\frac{\partial \sigma}{\partial t} = - c \left(\frac{\partial u}{\partial r} + \frac{2u}{r} \right) \qquad (1)$$

where σ is Riemann's quantity, (cf. Equation (10)) which for small pressures is given by

$$\sigma = p/\rho_0 \qquad (2)$$

Combining the two equations (1), we get the wave equation

$$D^2 \sigma \equiv \frac{\partial^2 \sigma}{\partial r^2} + \frac{2}{r} \frac{\partial \sigma}{\partial r} = c^2 \frac{\partial^2 \sigma}{\partial t^2} \qquad (3)$$

which has the solution

$$\sigma = \frac{f'(\tau)}{r} \tag{4}$$

where[1]

$$\tau = t - r/c \tag{5}$$

(1) We consider only outgoing spherical waves; for ingoing waves, σ would be a function of $t + r/c$.

and f' is an arbitrary function of τ which is determined by the source which produces the sound. Instead of f', we may also assume $f(\tau)$ as given; $f' = df/d\tau$. Inserting (4) into the first equation (1) and integrating, we get

$$u = \frac{f'(\tau)}{r} + c\,\frac{f(\tau)}{r^2} \tag{6}$$

We see therefore that σ and the pressure p are propagated with sound velocity outwards, and at the same time decay as $1/r$. On the other hand, the material velocity u has one term which behaves in the same way and is actually equal to σ, and a second term which decreases as $1/r^2$. This second term is proportional to

$$f(\tau) = \int f'(\tau)\, d\tau \tag{7}$$

i.e. it depends on the pressure which has existed in the wave at earlier times. For this reason the second term Equation (6) is known as the after-flow term. It is interesting that this term contains a factor c; therefore, it will become very large in the limit of incompressible theory, which corresponds to infinite sound velocity. In this limit the material velocity becomes

$$u = \frac{c\, f(\tau)}{r^2} \tag{8}$$

At any given time, u is inversely proportional to r^2, meaning that the flow through any spherical surface is the same, as would be expected in incompressible theory.

For finite sound velocity the second term in Equation (6) may or may not be important. If the sound signal is of finite duration $T = L/c$, the ratio of the second to the first term in (6) is of the order L/r. With increasing distance r from the source therefore the second term becomes unimportant in comparison with the first.

We shall find that a more accurate theory of pressure waves can be constructed in close analogy to the acoustic theory here outlined.

8.3 GENERAL THEORY

The equations of motion in Eulerian coordinates are

$$\frac{\partial u}{\partial t} + u\,\frac{\partial u}{\partial r} = -\frac{1}{\rho}\,\frac{\partial p}{\partial r} \qquad \rho \frac{d\vec{u}}{dt} = -\nabla p$$

$$\frac{\partial \log \rho}{\partial t} + u\,\frac{\partial \log \rho}{\partial r} = -\frac{\partial u}{\partial r} - 2\,\frac{u}{r} \qquad \frac{d\rho}{dt} = -\rho\,\nabla\cdot\vec{u} \tag{9}$$

The first of these is the equation of motion, the second is the continuity equation. The equation of energy conservation is replaced in our approximation by the condition that the motion is adiabatic (see Section 1).

It is convenient to introduce, instead of the pressure, the quantity

$$\sigma = \int \frac{d\rho}{\rho} = \int \frac{dp}{\rho c^2} \tag{10}$$

in which c is the sound velocity which itself depends on the density. In (10) we have used the definition

$$c^2 = dp/d\rho \tag{11}$$

Inserting (10) into (9) we obtain

$$\frac{\partial u}{\partial t} + u \frac{\partial u}{\partial r} = - c \frac{\partial \sigma}{\partial r}$$

$$\frac{\partial \sigma}{\partial t} + u \frac{\partial \sigma}{\partial r} = - c\left(\frac{\partial u}{\partial r} + \frac{2u}{r}\right) \tag{12}$$

In the acoustic limit the terms containing u as factor can be neglected and (12) reduces to Equation (1).

We know from the acoustic theory that σ and u behave approximately as $1/r$ at large distances. We therefore introduce the abbreviations

$$\Sigma = r\sigma \tag{13}$$

$$U = ru$$

With this notation Equations (12) become

$$\frac{\partial U}{\partial t} + c \frac{\partial \Sigma}{\partial r} + u \frac{\partial U}{\partial r} - c \frac{\Sigma}{r} - \frac{U^2}{r^2} = 0$$

$$\frac{\partial \Sigma}{\partial t} + c \frac{\partial U}{\partial r} + u \frac{\partial \Sigma}{\partial r} + c \frac{U}{r} - \frac{U\Sigma}{r^2} = 0 \tag{14}$$

We know further from acoustic theory that u becomes asymptotically equal to σ for large distances. We therefore further set

$$U = \Sigma + D \tag{15}$$

and we expect that D will become small compared with Σ for large r. Equations (14) now become

$$\frac{\partial \Sigma}{\partial t} + (c+u)\frac{\partial \Sigma}{\partial r} + c\left(\frac{\partial D}{\partial r} + \frac{U}{r}\right) - \frac{U\Sigma}{r^2} = 0$$

$$\frac{\partial D}{\partial t} - (c-u)\frac{\partial D}{\partial r} - c\frac{2\Sigma + D}{r} - U\frac{D}{r^2} = 0 \qquad (16)$$

In the first approximation we may neglect the last three terms in the first equation (16). We should expect that d/dr of any quantity is of the order of that quantity divided by L. Therefore the term U/r, which is approximately equal to Σ/r, is small compared $d\Sigma/dr$, the ratio of the two terms being of the order L/r. The term D/r is small because D is expected to be small compared to Σ as will be proved below. The last term is in turn small compared to the second last term.

In the first approximation, therefore, the first equation (16) reduces to

$$\frac{\partial \Sigma}{\partial t} + (c+u)\frac{\partial \Sigma}{\partial r} = 0 \qquad (17)$$

This equation means that Σ propagates with the velocity $c \pm u$. This is the analogue of acoustic theory in which Σ propagates with velocity c_o. The replacement of the ordinary sound velocity c_o by the effective sound velocity $c - u$ is physically obvious and is analogous to the well-known Riemann method for treating plane problems.

The solution of (17) is

$$\Sigma = \Sigma(\tau) \qquad (18)$$

with

$$\tau = t - \int \frac{dr}{c+u} \qquad (19)$$

The integration in the expression (19) is to be extended over a path along which Σ is constant. The integral therefore depends on Σ and the equation does not give an explicit solution of the Equation (17). The lower limit in the integral may be a function of Σ. If we choose the same lower limit r_o for all Σ, then τ is the time when the value of Σ to which it belongs passes the point r_o. For the present we shall not specify the lower limit. The function $\Sigma(\tau)$ must be determined from the shape of the shock wave at some initial time. This will be discussed in Section 8.10.

8.4 SECOND APPROXIMATION

We shall now try to determine the function D from the second Equation (16) and also to get a better approximation for Σ.

In the second Equation (16) we can certainly neglect the last term. The first two terms can be transformed by introducing instead of t the variable τ defined in (19). We have then

$$\left(\frac{\partial D}{\partial t}\right)_r = \left(\frac{\partial D}{\partial \tau}\right)_r$$

$$\left(\frac{\partial D}{\partial r}\right)_t = \left(\frac{\partial D}{\partial r}\right)_\tau - \left(\frac{\partial D}{\partial \tau}\right)_r \frac{1}{c+u} \qquad (20)$$

and the second Equation (16) becomes

$$\frac{2c}{c+u}\left(\frac{\partial D}{\partial \tau}\right)_r = \frac{2c\Sigma}{r} + c\left(\frac{D}{r} + \left(\frac{\partial D}{\partial r}\right)_\tau\right) + u\left(\frac{D}{r} - \frac{\partial D}{\partial r}\right) \qquad (21)$$

Neglecting all terms of smaller order of magnitude, the right hand side re-

duces to $2c\,\Sigma/r$ and the factor on the left to 2. Then (21) can be integrated and gives

$$D = \frac{c}{r} \int \Sigma \, d\tau \tag{22}$$

This result shows that D is actually of the order $\Sigma L/r$, and is therefore small compared to Σ according to our assumptions. This justifies the first approximation given in the last section, as well as the treatment given in this section. It is, however, of interest to write down the right hand side of Equation (21) to the next approximation. For this purpose we note that according to (22)

$$\left(\frac{\partial D}{\partial r}\right)_\tau = - \frac{D}{r} \tag{23}$$

Therefore (21) becomes

$$\left(\frac{\partial D}{\partial \tau}\right)_r = (c + u)\frac{\Sigma}{r} \tag{24}$$

in which only terms of order uD/r are neglected, but terms of order cD/r and $u\,\Sigma/r$ have been taken into account.

The form of Equation (22) shows that D has the character of an after-flow term and therefore corresponds in all respects to the after-flow term in Section 2.

The integral in (22) must be extended from the shock front to the point at which D is to be calculated. To prove this, it must be shown that D behind the shock front is of smaller order than (22). This can easily be done by using the Hugoniot relations and the definition of σ. We have behind the shock front

$$u^2 = (p - p_0)(V_0 - V) \tag{25}$$

where the subscript $_o$ refers to the undisturbed material, and V is the specific volume. Further, we have generally

$$\sigma = \int_{\rho_o}^{\rho} \sqrt{\frac{dp}{d\rho}}\,\frac{d\rho}{\rho} = \int_{V}^{V_o} \sqrt{-\frac{dp}{dV}}\,dV \tag{26}$$

The value of D behind the shock front is by definition

$$D = r\,(u - \sigma) \tag{27}$$

To evaluate (25) and (26) it is convenient to introduce the quantity

$$x = \frac{V_o - V}{V_o} \tag{28}$$

and to express the pressure in terms of this quantity:

$$p = p_o - V_o \frac{dp}{dV}\,x + \frac{V_o^2}{2}\,\frac{d^2p}{dV^2}\,x^2 - \frac{V_o^3}{6}\,\frac{d^3p}{dV^3}\,x^3 + \cdots \tag{29}$$

Using the definition of the sound velocity we have

$$-\left.\frac{dp}{dV}\right|_o = \frac{c_o^2}{V_o^2} \tag{30}$$

and we write

$$\left.\frac{d^2p}{dV^2}\right|_o = 2\alpha\frac{c_o^2}{V_o^3} = \frac{2\alpha}{V_o}\left(-\frac{dp}{dV}\right)$$

$$-\left.\frac{d^3p}{dV^3}\right|_o = 6\beta\frac{c_o^2}{V_o^4} = \frac{6\beta}{V_o^2}\left(\frac{dp}{dV}\right) \tag{31}$$

where α and β are dimensionless coefficients. If the adiabatic law is of the usual form,

$$p = p_o\,(V/V_o)^{-\gamma} \tag{32}$$

the values of α and β are

$$\alpha = (\gamma + 1)/2$$

$$\beta = \frac{(\gamma+1)(\gamma+2)}{6} \tag{33}$$

With these abbreviations Equation (29) becomes

$$P - P_0 = \frac{c_0^2}{V_0}\left(x + \alpha x^2 + \beta x^3 + \cdots\right) \tag{34}$$

Inserting (34) and (28) into the Hugoniot relation (25) we obtain

$$u' = c_0 x \left(1 + \tfrac{1}{2}\alpha x + \left(\tfrac{1}{3}\beta - \tfrac{1}{8}\alpha^2\right) x^2 + \cdots\right) \tag{35}$$

Further we find,

$$\sqrt{-\frac{dP}{dV}} = \frac{c_0}{V_0}\left(1 + \alpha x + \left(\frac{3\beta}{2} - \frac{\alpha^2}{2}\right) x^2 + \cdots\right) \tag{36}$$

or for the sound velocity

$$c = c_0 \left[1 + (\alpha - 1)\, x + (3\beta/2 - \alpha^2/2 - \alpha)\, x^2 + \cdots\right] \tag{37}$$

Inserting (36) into the expression (26) we find

$$\sigma = c_0 x \left[1 + (\alpha/2)\, x + (\beta/2 - \alpha^2/6)\, x^2 + \cdots\right] \tag{38}$$

and subtracting we get

$$u - \sigma = c_0 \alpha^2 x^3/24 \tag{39}$$

This relation holds generally behind the shock front. It is interesting that it depends on the quantity α, i.e. on d^2p/dV^2 which is also the quantity determining the entropy change at the shock front (see below, Section 8.5). For our present purpose the important point is that $u-\sigma$ is proportional to x^3 and therefore to σ^3, and therefore falls off as $1/Y^3$ where Y is the shock radius. The quantity D just behind the shock front will therefore fall of as $1/Y^2$ which makes it of smaller order of magnitude than the expression (22).

We note in passing that, according to (35) and (37), the velocity of wave propagation is in first approximation

$$c + u = c_0 (1 + \alpha x) \tag{40}$$

We shall now insert our expression for D back into the first Equation (16). We have to calculate the quantity

$$\left(\frac{\partial D}{\partial r}\right)_t \tag{41}$$

Using (20), (23) and (24) and the definition of τ, this becomes

$$-\frac{D}{r} - \frac{\Sigma}{r} = -\frac{U}{r} \tag{42}$$

As was explained above, only quantities of the order $(u/c)(D/r)$ are neglected in this expression.

Inserting (42) into the first Equation (16) we see that the terms U/r cancel. Therefore the first Equation (16) becomes, neglecting the very small term $D\Sigma/r^2$:

$$(c+u)\left(\frac{\partial \Sigma}{\partial r}\right)_\tau = \frac{\partial \Sigma}{\partial t} + (c+u)\left(\frac{\partial \Sigma}{\partial r}\right)_t = \frac{\Sigma^2}{r^2} \tag{43}$$

Neglecting u in $c + u$, this can be integrated to give

$$\frac{1}{\Sigma} = \frac{1}{\Sigma_0} + \frac{1}{cr} \tag{44}$$

In other words, along a line of constant τ, not Σ itself is a constant but the somewhat more complicated quantity

$$\frac{\Sigma}{1-\Sigma/cr} = \Sigma_0 \qquad \Sigma = r\sigma \tag{44a}$$

Σ itself therefore increases as the wave propagates outwards.

8.5 THE MOTION OF THE SHOCK FRONT

Let us assume that the shock front moves from a radius Y to a radius Y + dY. The shock velocity can easily be shown to be in first approximation midway between the effective sound velocities ahead and behind the shock. The former sound velocity is c_0, the latter $c + u$ so that the shock velocity is

$$\dot{Y} = \frac{1}{2}(c_0 + c + u) \tag{45}$$

and the time needed for the shock to travel the distance dY is

$$dt = \frac{2dY}{c_0 + c + u} \tag{46}$$

The shock velocity is smaller than the velocity of sound waves behind the shock, $c + u$. Therefore these sound waves will catch up with the shock wave, and if the shock is followed by a rarefaction as it is in the case of a blast wave, then the rarefaction will gradually cut down the strength of the shock. In our notation, the value of τ at the shock will gradually change; if it has the value τ when the shock is at Y it will have the value $\tau + d\tau$ when the shock has moved to Y + dY.

In order to calculate the variation of τ along the shock front, we have to complete the definition of τ which was left somewhat arbitrary. It is convenient to define the arbitrary constant of integration in (19) as follows

$$\tau = t - \int_{Y}^{R} \frac{dr}{c+u} - \frac{Y}{c_0}$$

where Y is the shock radius at the time when the signal Σ reaches the shock front. Y, therefore, is a function of Σ and this is permissible since the constant of integration was allowed to depend on Σ. If we use the definition above then $\tau + Y/c_0$ is the time when the signal Σ reaches the shock, or τ is the difference in the actual time and the time which would be required for a signal traveling from the origin with normal sound velocity c_0.

The time difference dt between the arrival of the signals τ and $\tau + d\tau$ at the shock front is therefore

$$dt = d\tau + \frac{dY}{c_0} \tag{47}$$

Comparison with (46) yields

$$\frac{d\tau}{dY} = \frac{2}{c_0+c+u} - \frac{1}{c_0} = \frac{c_0-c-u}{c_0(c+c+u)} \cong \frac{c_0-c-u}{2c_0^2} \tag{48}$$

This equation describes the catching up of the rarefaction wave with the shock front.

From (40) and (38) follows

$$c + u = c_0 + \alpha\sigma \tag{49}$$

Hence (48) becomes

$$\frac{d\tau}{dY} = \frac{-\alpha\sigma}{2c_0^2} = -\frac{\alpha\Sigma}{2c_0^2 Y} \tag{50}$$

where we have also used the definition of $\Sigma = \sigma Y$.

8.6 RESULTS FOR VERY LARGE DISTANCES

Up till now we have not made any special assumptions about the function $\Sigma(\tau)$, i.e. about the shape of the shock wave. We can get further results if we assume that initially (at small distances from the origin) the shock wave was of short duration, and that most of the duration at shock radius Y is due to the excess of the shock velocity over the unperturbed sound velocity c_0. This assumption is quite well justified for blast waves at sufficiently large distance. If t_0 is the time at which a given value of Σ exists at a given small radius r_0 then we have for the arrival time of this value of Σ at the distance r (cf. (40)) (49)

$$t = t_0 + \int_{r_0}^{r} \frac{dr}{c+u} \approx t_0 + \int_{r_0}^{r} \frac{dr}{c_0 + \alpha \Sigma / r}$$

$$= \frac{r}{c_0} - \frac{r_0}{c_0} + t_0 - \frac{\sum \alpha}{c_0^2} \log \frac{r}{r_0} \qquad \ln \frac{r + \frac{\alpha \Sigma}{c_0}}{r_0 + \frac{\alpha \Sigma}{c_0}} \tag{51}$$

If we neglect small difference in the values of t_0 and r_0 for different values of Σ it follows that for fixed r, Σ is a linear function of t and therefore also the pressure assumes a linear shape.

We apply the equation (51) in particular at the shock front $r = Y$, $\Sigma = \Sigma_s$. Then t is the time of arrival of the signal Σ_s at the shock radius Y. However, this time was also equal to $\tau_s + Y/c_0$ where τ_s is the value of τ corresponding to Σ_s. Neglecting again r_0 and t_0 as small quantities, we find therefore

$$|\tau_s| = -\frac{\Sigma_s \alpha}{c_0^2} \log \frac{Y}{r_0} \tag{52}$$

In the approximation in which r_0 and t_0 are neglected $|\tau_s|$ is by definition the difference in the arrival time of the shock and of the signal

$\Sigma = 0$, since the latter travels with sound velocity c_0 ; i.e., $|\tau_s|$ is identical with the duration of the positive pressure pulse. This is easily verified from the Equation (51).

In order to obtain τ_s as function of Σ_s , only, we have to express the shock radius Y in terms of Σ_s. For this purpose we substitute (52) into (50). Then we get

$$\frac{d\Sigma_s}{dY} = -\frac{\Sigma_s}{2Y \log (Y/r_0)} \tag{53}$$

which can immediately be integrated to give

$$\Sigma_s = \frac{A}{\sqrt{\log (Y/r_0)}} \tag{54}$$

where A is a constant. In other words, the value of Σ at the shock front is not constant but decreases due to the catching up of the rarefaction. This decrease is very slow; it goes only as the inverse square root of the logarithm of the shock radius.

The derivation given above may give rise to the impression that r_0 may be chosen arbitrarily as long as it is small compared to all values Y for which the formula (54) is applied. This is not so. In fact, it is easily shown that we are led to contradictions if we allow r_0 to vary over any appreciable range.

We shall see later that a detailed analysis will allow us to determine the correct value of r_0 which should be inserted in the equation (54). For the present let it suffice to point out that a pressure pulse of the asymptotic shape, requires two parameters to determine its initial conditions, namely the strength and duration of the pulse. We require, therefore, two constants in the asymptotic law and thus both the constant A and the constant r_0 are determined by the properties of the pulse.

Going back to Equation (51), we find then that the duration of the pressure pulse will increase as the square root of log Y. The product of peak pressure p_ϕ and duration θ, or the so-called impulse of the wave will therefore behave exactly as $1/Y$, namely

$$p_\phi \theta = \text{const.}/Y \qquad (55)$$

We have thus seen that in our approximation a shock wave will spread out gradually, in contrast to the acoustic theory in which the wave retains its shape for all time. The spreading of a shock wave in 3 dimensions is very slow. It would be considerably faster in two and still faster in one dimension. On the other hand, for a space of more than three dimensions this effect will not occur.

Connected with the spreading of the wave there is a decrease of the front pressure which is faster than $1/Y$. Again, in three dimensions this effect is small; in one dimension, elementary acoustic theory would give constant front pressure whereas the actual behavior is as $1/\sqrt{Y}$. The case of two dimensions is again intermediate, and for more than three dimensions, acoustic theory becomes the correct asymptotic limit.

Another interesting phenomenon which is connected with the variation of the sound velocity $c + u$ is the fact that a second shock must be formed in the negative phase of a shock wave. The regions of negative pressure have a particularly small propagation velocity, $c + u$, which is smaller than normal sound velocity c_o. Therefore the very end of the shock wave tends to catch up with the regions of negative pressure and a second shock will result. This will be discussed in more detail in Section 8.9.

Another interesting problem is the motion of the point $\Sigma = 0$, which marks the end of the positive pressure phase ($p > p_o$) and the beginning of the negative phase. In our approximation the propagation velocity of this

point is just the normal sound velocity c_0. Actually, however, μ is somewhat greater than σ by the amount D/r. Therefore the point $\Sigma = 0$ propagates with a velocity slightly greater than normal sound velocity. Since the very tail of the shock wave moves with velocity c_0, the end of the positive phase $\Sigma = 0$ moves with a velocity slightly greater than the end of the negative phase. Consequently the positive phase will tend to become somewhat shorter and the negative phase somewhat longer than the elementary theory indicates. This corresponds to observations.

A very important remark about the shape of shock waves has been made by Penney. It is most easily deduced from the fact that the total mass of air behind the shock must be equal to the original mass of air within the radius Y. This means

$$\int_0^Y \rho r^2 dr = \rho_0 Y^3/3 \qquad (56)$$

There are two regions in which the density is appreciably different from the normal density ρ_0. One is the central region in which the gases have been left at high temperature by the shock and therefore have low density. If the shock wave is far out, these regions have returned to atmospheric pressure and therefore to a definite density. If X denotes a radius small compared to Y, but large compared to the region of the hot gases, we shall have

$$\int_0^X \rho r^2 dr = \rho_0 X^3/3 - M \qquad (57)$$

where M is a constant independent of X and of the time. Subtracting (57) from (56) we get

$$\int_X^Y (\rho - \rho_0) r^2 dr = M \qquad (58)$$

The shock region itself may be assumed to be small in extension compared

to Y. Therefore we can replace, in this region, r by Y. Furthermore the deviation of the density from normal, $\rho - \rho_0$, is proportional to σ. Therefore we obtain from (58):

$$Y^2 \int_{\text{shock}} \sigma \, dr = Y \int_{\text{shock}} \Sigma \, dr = M \tag{59}$$

From this follows that

$$\int \Sigma \, dr \sim 1/Y \tag{60}$$

However, we know that the value of Σ at the front is nearly constant. Therefore the integral in (60) must consist of two contributions which nearly cancel each other. The shock wave must consist of a phase of positive σ (over-pressure) and a phase of negative σ (under-pressure) such that the impulses of the two phases cancel each other in first approximation. This argument is also a proof of the existence of the negative phase; it was first given by Penney using the energy rather than the amount of material.

In particular, in the limit in which the pressure depends linearly on the time, the shape of the shock wave becomes symmetrical, with equal shocks at the beginning and at the end as illustrated in Figure 1.

8.7 THE ENERGY

The energy flux through a given surface consists of two parts, namely (1) the work done by the material on one side, on the material on the other side and (2) the energy transported with the material itself. Since we have proved at the end of the last section that the pressure pulse in a shock wave has a negative phase balancing the positive phase, the final displacement of any point is zero in first approximation

$$\int u \, dt = O(1/Y) \tag{61}$$

Figure 1

Symmetrical, Equal Shock Waves

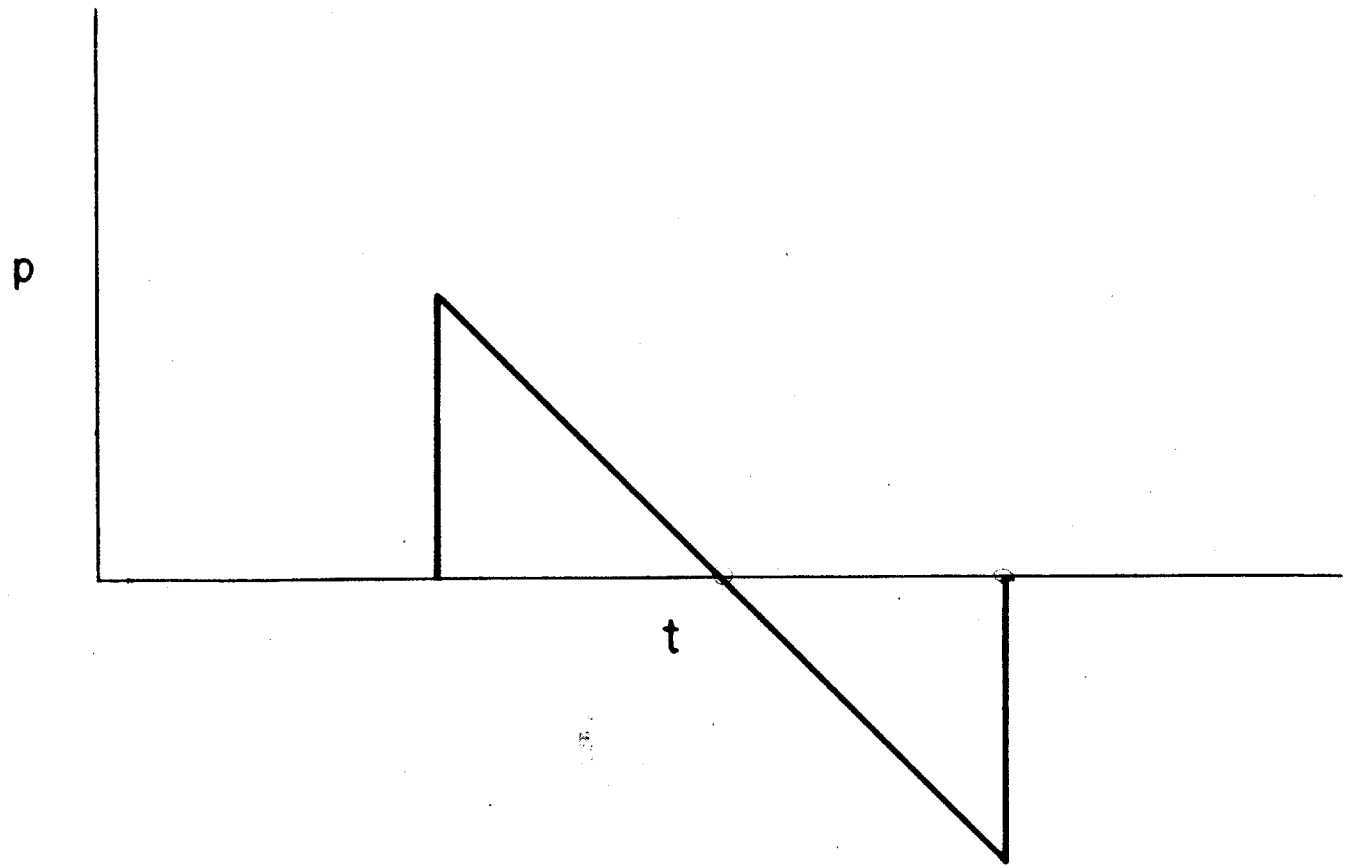

This means that the net transport of energy with the material is zero of higher order than the work term mentioned as (1) above.

Therefore the energy flux in the shock wave through a sphere of radius Y is in sufficient approximation:

$$W = 4\pi Y^2 \int p u \, dt \tag{62}$$

If we set $u = \sigma$ and $p = \rho c \sigma$ and $\sigma = \Sigma/Y$, and if we further assume that the pressure distribution is as indicated in Figure 1, the energy flux becomes

$$W = 4\pi \rho c \int \Sigma^2 dt = 4\pi \rho c \Sigma_f^2 \theta \int_{-1}^{1} x^2 dx \tag{63}$$

where θ is the duration of the positive phase which, according to Equation (52), has the value

$$\theta = \frac{\alpha \Sigma_f}{c_o^2} \log \frac{Y}{r_o} \tag{64}$$

so that

$$W = \frac{8\pi \alpha \rho}{3 c_o} \Sigma_f^3 \log \frac{Y}{r_o} \tag{65}$$

Using the relation (54) for Σ this becomes

$$W = \frac{8\pi \alpha \rho}{3 c_o} \frac{A^3}{\sqrt{\log (Y/r_o)}} \tag{66}$$

Equation (66) shows that the total energy in the shock wave decreases slowly as the shock wave propagates. This fact was first pointed out by Penney and means that it is impossible to define in any general way the energy wasted in the shock wave, but that this waste will depend on the distance to which the shock wave has gone. It is interesting to determine

the decay of the energy in the shock wave also in a different way.

This way is based on the fact that energy is irreversibly converted into heat at the shock front at all times. To determine this wasted energy or increase in entropy, we use the Hugoniot equation for the energy

$$E - E_0 = \tfrac{1}{2}(p+p_0)(V_0 - V) \tag{67}$$

where the quantities without subscript are behind, those with subscript o in front of the shock wave. The energy can be expanded in a Taylor series in the change of volume and of entropy, as follows

$$E - E_0 = \frac{\partial E}{\partial V}(V-V_0) + \frac{1}{2}\frac{\partial^2 E}{\partial V^2}(V-V_0)^2$$

$$+ \frac{1}{6}\frac{\partial^3 E}{\partial V^3}(V-V_0)^3 + \cdots + \frac{\partial E}{\partial S}(S-S_0) + \cdots \tag{68}$$

If we remember that

$$\left(\frac{\partial E}{\partial V}\right)_S = -p_0$$

$$\left(\frac{\partial E}{\partial S}\right)_V = T_0 \tag{69}$$

and introduce the abbreviation (28), (68) becomes

$$E - E_0 = p_0 V_0 \times \textcircled{11} - \frac{1}{2}\frac{\partial p}{\partial V} V_0^2 x^2$$

$$+ \frac{1}{6}\frac{\partial^2 p}{\partial V^2} V_0^3 x^3 + \cdots + T_0(S-S_0) + \cdots \tag{70}$$

Further, we have

$$p = p_0 - \frac{\partial p}{\partial V} V_0 x + \frac{1}{2} \frac{\partial^2 p}{\partial V^2} V_0^2 x^2 \tag{71}$$

Inserting (70) and (71) into (67), we find

$$T_0 (S - S_0) = \frac{1}{12} \frac{\partial^2 p}{\partial V^2} V_0^3 x^3 \tag{72}$$

This is the energy wasted per gram of material swept over by the shock. If we now use (31) and (38) we obtain

$$\frac{dW}{dY} = -4\pi \rho Y^2 T_0 (S - S_0) = -\frac{2\pi}{3} \alpha \rho c_0^2 x^3 Y^2$$

$$= -\frac{2\pi}{3} \frac{\rho \alpha}{c_0} \sigma^3 Y^2 \tag{73}$$

In our shock wave, at very large distances, there are two shocks of equal strength and therefore the energy loss (73) occurs twice. Therefore we find for the decrease of energy in the shock wave itself

$$\frac{dW}{dY} = -\frac{4\pi}{3} \frac{\rho \alpha}{c_0} \frac{\Sigma_f^3}{Y} \tag{74}$$

Comparing this with the expression for the energy itself, (66), we find

$$\frac{dW}{dY} = -\frac{W}{2Y \ln(Y/r_0)} \tag{75}$$

which integrates immediately to

$$W = \frac{\text{const.}}{\sqrt{\ln(Y/r_0)}} \tag{76}$$

This result is exactly the same as deduced above by explicit evaluation of W, Equation (66). We therefore have found the decay of the energy by two entirely independent methods. Both methods are only applicable if the shape

of the pressure pulse remains unchanged.

8.8 THE PROPAGATION OF THE SHOCK AT INTERMEDIATE DISTANCES

The asymptotic form of the pressure pulse behind the shock is usually reached only at very large distances when the shock pressure has become extremely small. There is an intermediate region, in which the shock pressure is quite small, but the pressure distribution behind the shock is not yet linear. We shall now consider this intermediate region. i.e., we make all the assumptions which led to the first approximation considered in the preceding section, but we allow, within certain limitations, an arbitrary shape of the pulse.

Since we are interested to apply the theory to the IBM calculations, we shall slightly change the procedure used in the preceding sections. Instead of introducing as initial condition the shape of the pulse at a fixed point as function of time, we introduce the pulse at a fixed time t_o as function of the radius y . Hence we write the solution of (17) in the form

$$\Sigma = \Sigma(y) \tag{77}$$

$$y = r - \int_{t_o}^{t} (c+u)\, dt \tag{78}$$

Then Σ as function of y is given by the initial pressure distribution at time t_o. Using (49) one finds

$$y = r - c_o (t-t_o) - \int_{t_o}^{t} \alpha \sigma \, dt \tag{79}$$

The remaining integral is a small term and therefore we may replace dt by $d\tau/c_o$. Also $\sigma = \Sigma/r$ and Σ is constant for the purpose of integration.

Thus

$$y = r - c_0 (t - t_0) - \alpha \frac{\Sigma}{c_0} \ln r/y \tag{80}$$

Alternatively we might have replaced r in the integral by $y + c_0 (t - t_0)$ and found

$$y = r - c_0 (t - t_0) - \frac{\alpha \Sigma}{c_0} \ln \frac{y + c_0 (t - t_0)}{y} \tag{81}$$

Since Σ/c_0 must be small compared to y the two equations differ only by terms of the order $(\Sigma/y c_0)^2$.

We introduce the abbreviation

$$g(\Sigma) = \frac{c_0 y}{\alpha} - \Sigma \ln y - k \tag{82}$$

which is a constant. For convenience we define k in such a way that

$$g(0) = 0 \tag{82a}$$

Then equation (80) takes the form

$$r = c_0 (t - t_0) + \frac{\alpha}{c_0} \left[g(\Sigma) + \Sigma \ln r + k \right] \tag{83}$$

In particular, if Σ_s is the value of Σ at the shock front R

$$R = c_0 (t - t_0) + \frac{\alpha}{c_0} \left[g(\Sigma_s) + \Sigma_s \ln R + k \right] \tag{84}$$

Differentiation yields

$$\frac{dR}{dt} \left[1 - \frac{\alpha \Sigma}{c_0 R} \right] = c_0 + \frac{d\Sigma_s}{dt} \frac{\alpha}{c_0} \left[\frac{dg}{d\Sigma_s} + \ln R \right] \tag{85}$$

The shock velocity is also equal to the average value of $c + u$ in front and behind the shock, i.e.

$$\frac{dR}{dt} = \frac{1}{2} \left[c_0 + c + u \right] = c_0 \left[1 + \frac{\alpha \Sigma_s}{2 c_0 R} \right] \tag{86}$$

Here we have made use of the Equation (49). Comparing the two equations for dR/dt and observing that $\Sigma/c_0 R$ is a small quantity, one finds

$$\frac{\Sigma_s}{2R} + \frac{1}{c_0}\frac{d\Sigma_s}{dt}\left[\frac{dq}{d\Sigma_s} + \ln R\right] = 0 \tag{87}$$

or

$$\frac{\Sigma_s}{2R}\frac{dR}{d\Sigma_s} + \frac{dq}{d\Sigma_s} + \ln R = 0 \tag{88}$$

This is an inhomogeneous linear equation in $\ln R$ and can therefore be solved with the result

$$\ln R = +\frac{2}{\Sigma_s^2}\int_{\Sigma_s}^{\Sigma_0} \Sigma\,\frac{dq}{d\Sigma}\,d\Sigma + \frac{\Sigma_0^2}{\Sigma_s^2}\ln R_0 \tag{89}$$

Here Σ_0 is the value of Σ_s at time $t = t_0$, when $R = R_0$.

Partial integration yields

$$\ln R = 2\left[\frac{q_0}{\Sigma_0} - \frac{q_s}{\Sigma_s} - \frac{1}{\Sigma_s^2}\int_{\Sigma_s}^{\Sigma_0} g(\Sigma)\,d\Sigma\right] + \frac{\Sigma_0^2}{\Sigma_s^2}\ln R_0 \tag{90}$$

This form of the equation is more convenient if g is given as function of Σ in numerical form, since it avoids numerical differentiation.

Either of the two equations gives the shock radius R as function of $\Sigma = R\sigma$. Now from (10)

$$\Delta p = \rho_0 c_0 \sigma \tag{91}$$

and, since

$$c_0^2 = \gamma\frac{p_0}{\rho_0} \tag{92}$$

it follows that

$$\frac{\Delta p}{p_0} = \gamma\frac{\sigma}{c_0} = \gamma\frac{\Sigma}{Rc_0} \tag{93}$$

Thus we obtain the shock pressure Δp_s as function of the shock radius.

Since $q(\Sigma)$ and Σ are finite the right hand side of (90) is finite except for $\Sigma_s = 0$. Hence Σ_s tends to zero as R tends to infinity.

Let us write (89) in the form

$$\ln R = \frac{1}{\Sigma_s^2}\int_0^{\Sigma_0} \Sigma \frac{dq}{d\Sigma}\, d\Sigma + \frac{\Sigma_0^2}{\Sigma_s^2}\ln R_0 - \frac{2}{\Sigma_s^2}\int_0^{\Sigma_s} \Sigma \left\{\frac{dq}{d\Sigma} - \left(\frac{dq}{d\Sigma}\right)_{\Sigma=0}\right\} d\Sigma - \frac{2}{\Sigma_s^2}\int_0^{\Sigma_s} \Sigma \frac{dq}{d\Sigma}\, d\Sigma \tag{89a}$$

Then the last term tends to 0 if Σ_s tends to zero and we have asymptotically

$$\Sigma_s = \frac{A}{\sqrt{\ln(R/R^*)}} \tag{94}$$

where

$$\left.\begin{aligned} A^2 &= 2\int_0^{\Sigma_0} \Sigma \frac{dq}{d\Sigma}\, d\Sigma + \Sigma_0^2 \ln R_0 \\ \ln R^* &= -\left(\frac{dq}{d\Sigma}\right)_{\Sigma=0} \end{aligned}\right\} \tag{95}$$

This is essentially the equation derived previously for very large distances. However, we have obtained here the constant A in terms of the initial conditions and furthermore we have now a definite radius R^* in terms of which the radius R should be measured. The contradictions which arose previously are therefore avoided.

It will be observed that the asymptotic law (94) is obtained only if Σ is sufficiently small; if we plot Σ against y, it will have some shape of the form shown in Figure 2, approximating roughly the initial pressure

Figure 2

Initial Pressure Pulse

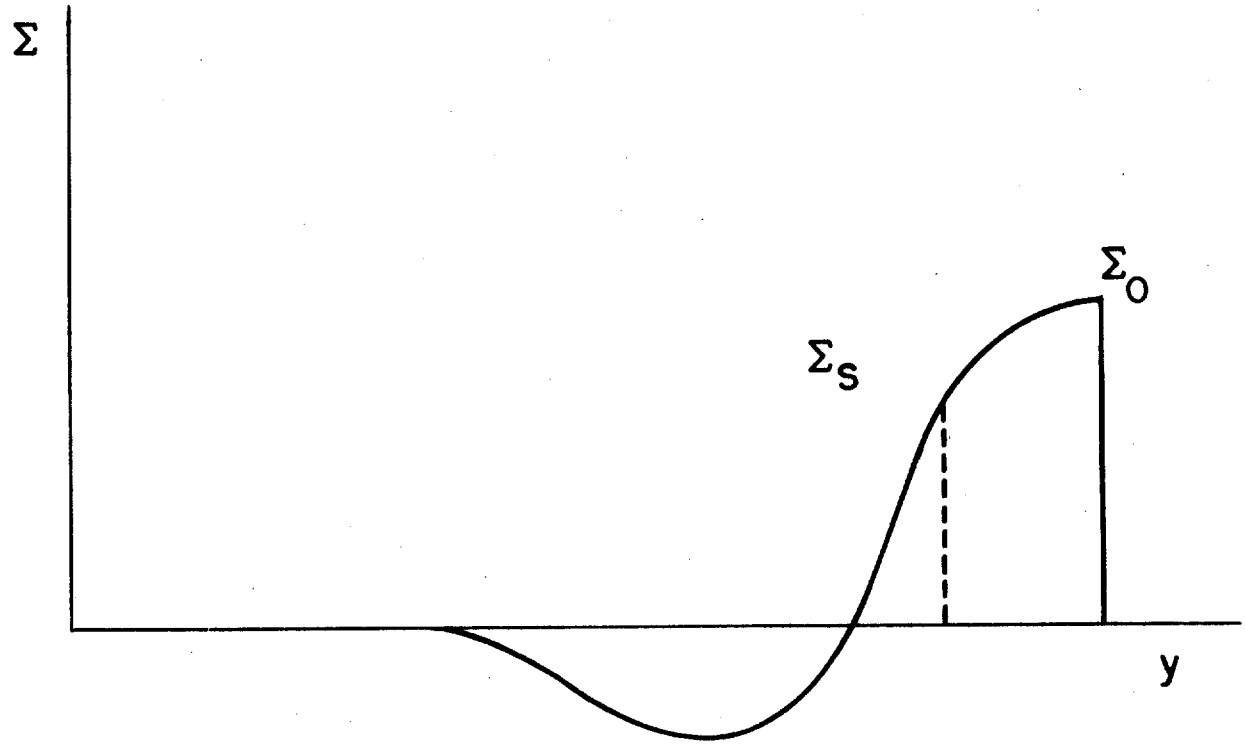

pulse. As time goes on various Σ values catch up with the shock front and the range of values which initially extended to Σ_0 contracts and extends only to Σ_s. The asymptotic law holds only if Σ_s has become small compared to Σ_0 or more precisely if Σ_s is so small that Σ may be considered a linear function of y between $\Sigma = 0$ and $\Sigma = \Sigma_s$. The smaller Σ the longer it takes for this Σ to catch up with the shock front, and therefore it may take an appreciable time before the asymptotic law is established, unless the initial pulse is already close to a linear function.

The pressure distribution behind the shock in space is most easily obtained from the Equation (81)

$$r = y + c_0 (t-t_0) + \frac{\alpha \Sigma}{c_0} \ln \frac{y + c_0(t-t_0)}{y} \tag{96}$$

Asymptotically Σ tends to zero. (We have proved this only for the positive phase, but previous considerations have shown that asymptotically the positive and negative phase become symmetric. We shall consider the negative phase in some detail below). At the same time y tends to a fixed value y_0. Hence Σ and, therefore, also the pressure, becomes linear in r. The length of the positive phase is obtained from (96) by subtracting r for $\Sigma = 0$ from R for $\Sigma = \Sigma_s$; i.e.

$$L_+ = y_s - y_c + \frac{\alpha \Sigma_s}{c_0} \ln \frac{y_s + c_0 (t-t_0)}{y_s} \tag{97}$$

Asymptotically we have $y_s \longrightarrow y_0$ and

$$y_0 + c_0 (t-t_0) = R - L_+ \cong R \tag{98}$$

Inserting this expression into the $\ln$ of (97) and using (94) one finds

$$L_+ \longrightarrow \frac{\alpha A}{c_0} \frac{\ln (R/y_0)}{\sqrt{\ln (R/R^*)}} \tag{99}$$

If we wish to obtain the pressure as function of time at a fixed point, it is more convenient to use the Equation (80) instead of (81)

$$c_o (t-t_o) = r - y - \frac{\alpha \Sigma}{c_o} \ln r/y \tag{80}$$

Following the same arguments as above one finds that the pulse is asymptotically linear. The duration of the positive pulse if given by

$$T_+ = \frac{1}{c_o}\left[y_s - y_o + \frac{\alpha \Sigma_s}{c_o} \ln R/y_s \right] \tag{100}$$

or asymptotically

$$T_+ \rightarrow \frac{\alpha A}{c_o^2} \frac{\ln (R/y_o)}{\sqrt{\ln (R/R^*)}} = \frac{1}{c_o} L_+ \tag{101}$$

as it should be. Alternatively we may use Equation (83) to determine the length of the pulse; with (82a) we find

$$L_+ = \frac{\alpha}{c_o}\left[g(\Sigma_s) + \Sigma_s \ln R \right] \tag{99a}$$

and for the duration

$$T_+ = \frac{\alpha}{c_o^2}\left[g(\Sigma_s) + \Sigma_s \ln R \right] \tag{100a}$$

The shape of the pulse is obtained from (83). If Δt is the time interval between the arrival of the shock and the arrival of the signal Σ at the point r, one finds

$$\Delta t = \frac{\alpha}{c_o^2}\left[g(\Sigma_s) - g(\Sigma) + (\Sigma_s - \Sigma) \ln r \right] \tag{102}$$

8.9 THE NEGATIVE PHASE. DEVELOPMENT OF THE BACK SHOCK.

We assume that the initial conditions are as indicated in Figure 2, so that the negative phase gradually returns to normal pressure. The value

$\Sigma = 0$ travels with normal sound velocity, whereas all other Σ values in the negative phase travel more slowly. In fact, throughout the whole region in which $d\Sigma/dy$ is negative, the Σ - values have a tendency of catching up with each other. At some stage a Σ - value in this region will overtake another and then a shock starts.

As long as r increases with increasing y the Σ - values are in the correct initial order. If r as function of y has an extremum, some Σ - values have already overtaken others. A shock starts at the boundary between the two cases, when r as function of y has a point where both the first and second derivatives vanish.

From (83) follows for fixed t

$$\frac{dr}{dy}\left[1 - \frac{\alpha \Sigma}{c_o r}\right] = \frac{\alpha}{c_o}\left[\frac{dg}{dy} + \frac{d\Sigma}{dy} \ln r\right] \tag{103}$$

The condition that $dr/dy = 0$ gives

$$\frac{dg}{dy} + \frac{d\Sigma}{dy} \ln r = 0 \tag{104}$$

Now from (82)

$$\frac{dg}{dy} = \frac{c_o}{\alpha}\left[1 - \frac{\alpha \Sigma}{c_o y}\right] - \frac{d\Sigma}{dy} \ln y \tag{105}$$

and (since $\alpha\Sigma/c_o y$ is small), dg/dy and $d\Sigma/dy$ cannot vanish simultaneously. Hence they must both be finite in (104) and we may write

$$\frac{dg}{d\Sigma} + \ln r = 0 \tag{106}$$

If we differentiate (103) once more and put $dr/dy = d^2r/dy^2 = 0$, we find

$$\frac{d}{dy}\frac{dg}{d\Sigma} = 0 \quad \text{or} \quad \frac{d^2 g}{d\Sigma^2} = 0 \tag{107}$$

If we neglect small terms of the order $\Sigma/c_o y$ and L/y, this condition can easily be reduced to

$$d^2\Sigma/dy^2 = 0 \tag{107a}$$

and similarly (106) yields with (105)

$$\ln r/y = \frac{c_o}{\alpha}\Big/\frac{d\Sigma}{dy} \tag{106a}$$

The Equation (107) determines the value $\Sigma = \Sigma_1$, at which the back shock starts. Substitution into (106) gives the radius $r = r_1$ and finally (83) gives the time $t = t_1$.

The back shock starts somewhere inside the negative phase and for some time at least the pressure in the rear and in front of the back shock differs from normal. If Σ_f, Σ_r are the corresponding Σ values, we have for the shock velocity in analogy to (86)

$$\frac{dY}{dt} = c_o\left[1 + \alpha\,\frac{\Sigma_f + \Sigma_r}{2 c_o Y}\right] \tag{108}$$

where Y is the position of the back shock. In addition we have two equations similar to (84)

$$\frac{c_o}{\alpha}\left[Y - c_o(t - t_o)\right] = g(\Sigma_f) + \Sigma_f \ln Y + k = g(\Sigma_r) + \Sigma_r \ln Y + k \tag{109}$$

Following the procedure used for the first shock, we find equations similar to (88)

$$\frac{\Sigma_f - \Sigma_r}{2Y}\,\frac{dY}{d\Sigma_f} + \frac{dg}{d\Sigma_f} + \ln Y = 0$$

$$\frac{\Sigma_r - \Sigma_f}{2Y}\,\frac{dY}{d\Sigma_r} + \frac{dg}{d\Sigma_r} + \ln Y = 0 \tag{110}$$

Combining the two equations we find

$$\frac{d\Sigma_r}{d\Sigma_f} + \frac{\ln Y + dg/d\Sigma_f}{\ln Y + dg/d\Sigma_r} = 0 \tag{111}$$

Eliminating Y by means of (109) one finds

$$\frac{d\Sigma_r}{d\Sigma_f} + \frac{g(\Sigma_r) - g(\Sigma_f) + (\Sigma_f - \Sigma_r)\, dg/d\Sigma_f}{g(\Sigma_r) - g(\Sigma_f) + (\Sigma_f - \Sigma_r)\, dg/d\Sigma_r} = 0 \tag{112}$$

This equation requires in general numerical integration.

Since both Σ_r and Σ_f are negative the shock travels with a velocity below the velocity of sound. Hence the value $\Sigma = 0$ will eventually catch up with the back shock, and then the back shock leaves the material behind at normal pressure. Then the equations for the propagation of the back shock take a form similar to those for the first shock

$$\frac{\Sigma_f}{2Y}\frac{dY}{d\Sigma_f} + \frac{dg}{d\Sigma_f} + \ln Y = 0, \quad \Sigma_r = 0 \tag{113}$$

with the solution

$$\ln Y = \frac{2}{\Sigma_f^2}\int_{\Sigma_f}^{\Sigma_2} \Sigma \frac{dg}{d\Sigma}\, d\Sigma + \frac{\Sigma_2^2}{\Sigma_f^2} \ln Y_2 \tag{114}$$

Here Σ_2, Y_2 are the values of Σ_f and Y at the time when Σ_r reaches 0.

Just as for the first shock it follows that Σ_f approaches zero for large Y and one has asymptotically

$$\Sigma_f = \frac{-B}{\sqrt{\ln Y/Y^*}} \tag{115}$$

$$B^2 = 2\int_0^{\Sigma_2} \Sigma \frac{dg}{d\Sigma}\, d\Sigma + \Sigma_2^2 \ln Y_2 \tag{116}$$

$$\ln Y^* = \left(\frac{dg}{d\Sigma}\right)_{\Sigma=0} = \ln R^* \tag{117}$$

We have seen previously that asymptotically the strength of the back shock must be the same as that of the first shock. Hence A should be equal to B. I.e.

$$2\int_{\Sigma_2}^{\Sigma_0} \Sigma \frac{dg}{d\Sigma}\, d\Sigma + \Sigma_0^2 \ln R_0 - \Sigma_2^2 \ln Y_2 = 0 \tag{118}$$

Using the expression (82) for g we find by means of partial integration

$$2\int^{\Sigma} \Sigma \frac{dg}{d\Sigma}\, d\Sigma = -\Sigma^2 \ln Y + \int \frac{c_0}{\alpha} \Sigma \left\{2 - \frac{\alpha \Sigma}{c_0 y}\right\} dy \tag{119}$$

The last term in the integral is small and we require therefore

$$\int_{\Sigma_2}^{\Sigma_0} \Sigma\, dy = \frac{\alpha}{2c_0} \Sigma_2^2 \ln Y_2/y_2 \tag{120}$$

Here y_2 is the value of y corresponding to Σ_2 and we have made use of the fact that $y = R_0$ for $\Sigma = \Sigma_0$. If we choose our initial conditions at the time when Σ just vanishes behind the back shock, they $y_2 = Y_2$ and the integral of Σ taken over the whole pulse vanishes. The same is true if we choose the initial conditions at any later time.

For later application we shall finally write down the equations which result if the initial pulse has linear shape. I.e., we assume

$$\Sigma = \Sigma_0 \frac{y + L_0 - R_0}{L_0}, \quad \text{for } t = t_0,\ R_0 - 2L_0 < y < R_0 \tag{121}$$

where R_0 is the shock radius and L_0 the length of the positive pulse at time $t = t_0$. Σ_0 is the value of Σ at the shock front, which is related

to the shock pressure by the Equation (93)

$$\Sigma_0 = \frac{R_0 c_0}{\alpha} \frac{\Delta p_s}{p_0} \tag{122}$$

Differentiating the function $g(\Sigma)$ defined by (82) one finds with the help of (121)

$$\frac{dg}{d\Sigma} = \frac{c_0}{\alpha} \frac{L_0}{\Sigma_0} - \left(1 - \frac{\alpha \Sigma}{c_0 y}\right) - \ln y \tag{123}$$

Neglecting the second term in the bracket, which is small and observing that y is for practical purposes constant and equal to R_0, we find that $dg/d\Sigma$ is constant.

$$\frac{dg}{d\Sigma} = \frac{c_0}{\alpha} \frac{L_0}{\Sigma_0} - \ln R_0 = -\ln R^* \tag{124}$$

Here we have used the definition (95) for R^*.

For the constant A^2 defined by (95) we find

$$A^2 = \Sigma_0^2 \left(\frac{dg}{d\Sigma} + \ln R_0\right) = \frac{c_0}{\alpha} L_0 \Sigma_0 = \Sigma_0^2 \ln (R_0/R^*) \tag{125}$$

The pulse is characterized by the two constants R^* and A^2; A^2 is essentially the product of the duration $\theta = L_0/c_0$ and the shock pressure Δp_s, multiplied by the radius R. More precisely

$$A^2 = \frac{c_0^3}{\alpha \gamma} \theta \frac{\Delta p_s}{p_0} R \tag{125a}$$

The radius R^* is similarly given by

$$R^* = R\, e^{-\frac{\gamma}{\alpha}\left\{c_0 \theta / R\left(\frac{\Delta p_s}{p_0}\right)\right\}} \tag{124a}$$

Here the subscripts o have been dropped, since these quantities are constants and apply therefore at any time.

8.10 TWO PRESSURE PULSES CATCHING UP WITH EACH OTHER

If the explosion of the gadget takes place at some considerable height and the pressure pulse is measured by airborne instruments, the problem arises whether the reflected shock from the ground catches up with the first shock, and what happens if it does.

We assume for simplicity that both pressure pulses have reached the asymptotic form. As long as the front of the second pulse has not reached the rear of the first pulse the two pulses behave independently and the calculations of the preceding sections apply. The mid-point of either pulse travels with sound velocity c_o and they keep, therefore, at a constant distant (apart from geometrical factors arising from the fact that the reflected shock has a center different from that of the first shock; these are neglected in the following considerations). However, the length of each pulse increases indefinitely and therefore the reflected shock will some time catch up with the rear of the first pulse. We then have three shocks as shown in Figure 3.

The equation for the first shock, of course, remains unaltered; i.e.

$$\Sigma_1 = \Sigma_{10} \sqrt{\frac{\ln R_o/R^*}{\ln R/R^*}} \tag{126}$$

where the suffix 1 refers to the first shock, and the suffix o to some specified time, e.g. to the time when the second shock just catches up with the first pulse. R^* is given by (124). Observing that the length of the positive pulse at time t_o is equal to $1/2\ (R_o - Y_o)$, we find

$$\ln R^* = \ln R_o - \tfrac{1}{2}\, \frac{c_o}{\alpha}\, \frac{R_o - Y_o}{\Sigma_{10}} \tag{127}$$

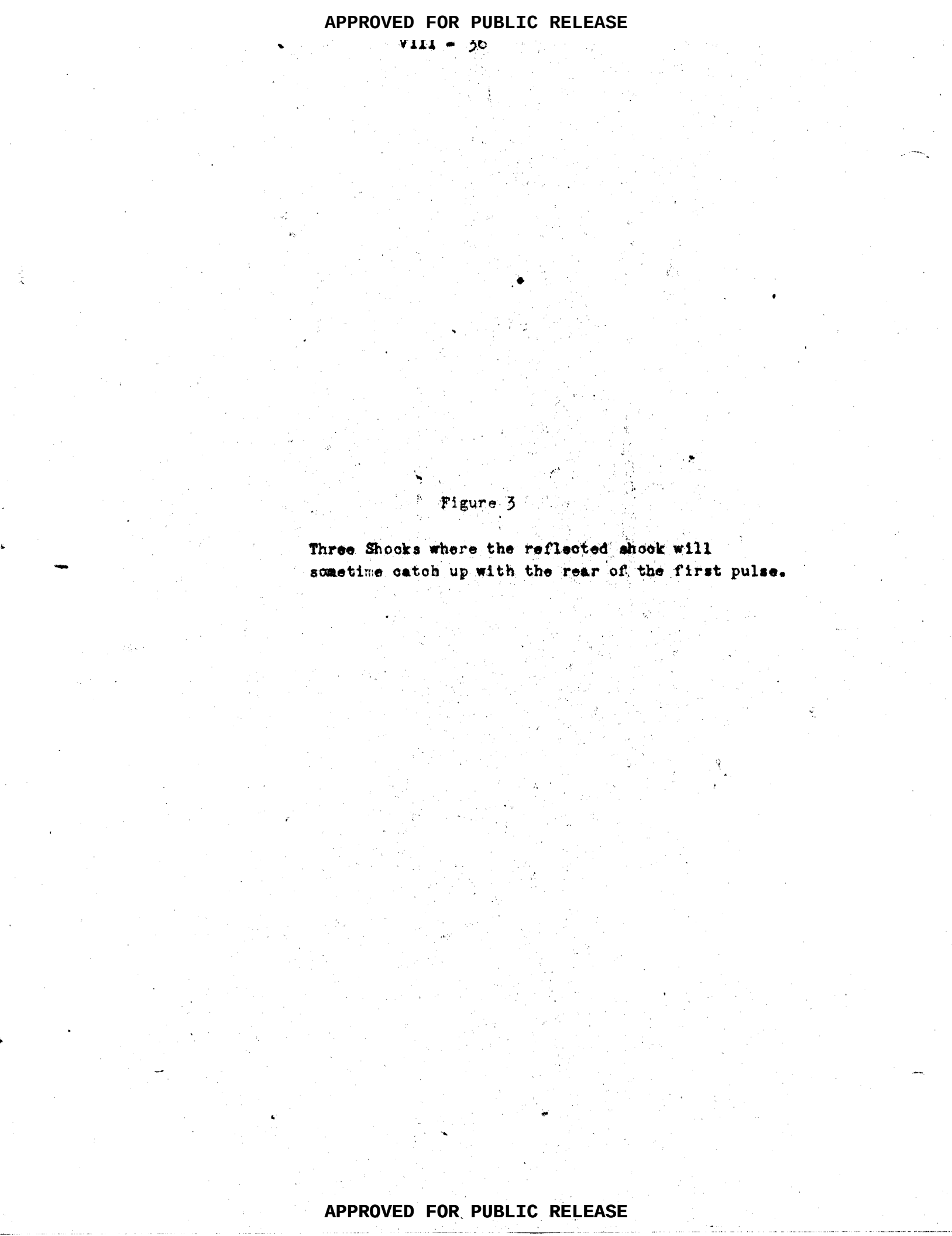

Figure 3

Three Shocks where the reflected shock will sometime catch up with the rear of the first pulse.

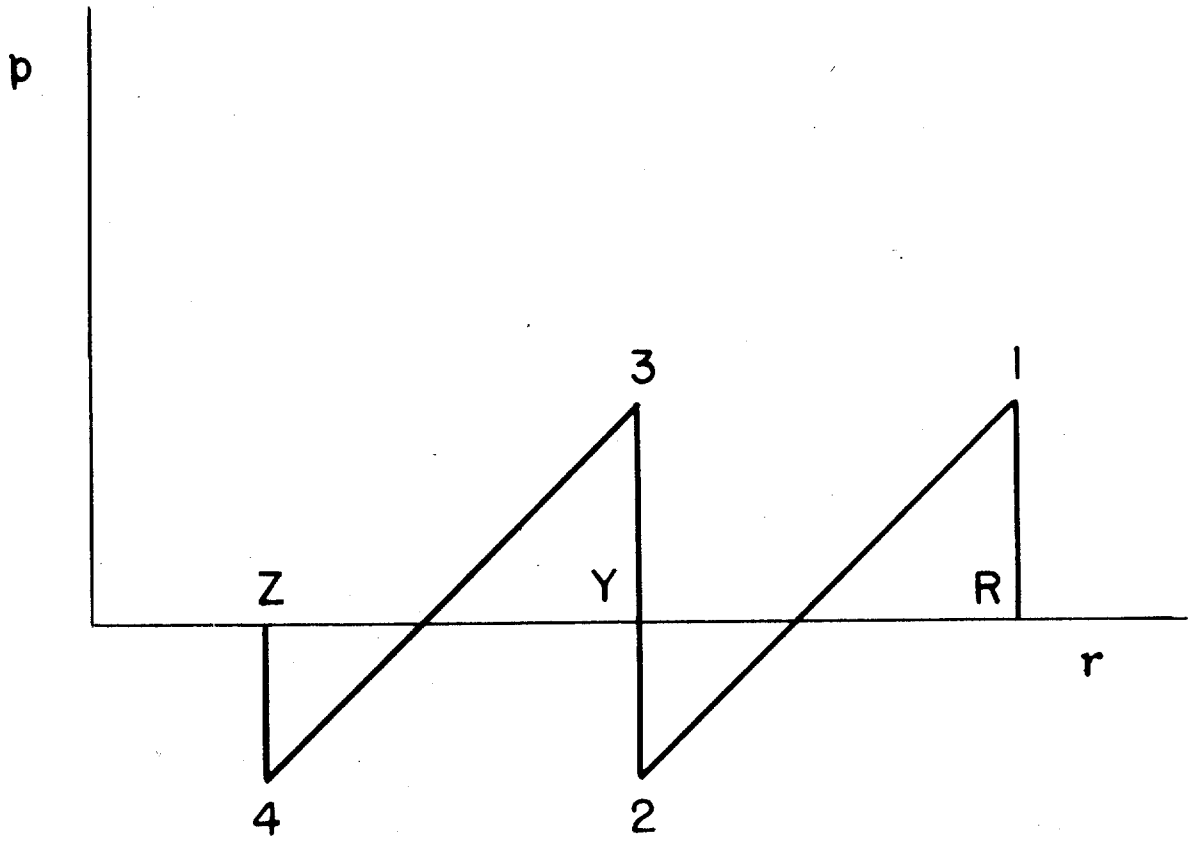

Similarly we have for the back shock of the second pulse

$$\Sigma_+ = -\Sigma_{30}\sqrt{\frac{\ln Z_0/Z^*}{\ln Z/Z^*}} \tag{128}$$

$$\ln Z^* = \ln Z_0 - \frac{1}{2}\frac{c_0}{\alpha}\frac{Y_0 - Z_0}{\Sigma_{30}} \tag{129}$$

For the central shock we have to use the equations devised for the case when both the air in front and in rear of the shock deviate from normal. These occurred previously in the treatment of the back shock and are given by (110)

$$\frac{\Sigma_2 - \Sigma_3}{2Y}\frac{dY}{d\Sigma_2} + \frac{dg}{d\Sigma_2} + \ln Y = 0$$

$$\frac{\Sigma_3 - \Sigma_2}{2Y}\frac{dY}{d\Sigma_3} + \frac{dg}{d\Sigma_3} + \ln Y = 0 \tag{130}$$

in the first of these equations $dg/d\Sigma_2$ is to be taken from the g-function of the first pulse; i.e. it is equal to $-\ln R^*$ (see Equation (124)). Similarly, in the second equation $dg/d\Sigma = -\ln Z^*$. Thus

$$\frac{\Sigma_2 - \Sigma_3}{2Y}\frac{dY}{d\Sigma_2} + \ln Y - \ln R^* = 0$$

$$\frac{\Sigma_3 - \Sigma_2}{2Y}\frac{dY}{d\Sigma_3} + \ln Y - \ln Z^* = 0 \tag{131}$$

These equations may be combined to give

$$\frac{2Y}{\Sigma_3 - \Sigma_2}\frac{d(\Sigma_3 - \Sigma_2)}{dY} + \frac{1}{\ln Y/R^*} + \frac{1}{\ln Y/Z^*} = 0 \tag{132}$$

Integration yields

$$\Sigma_3 - \Sigma_2 = (\Sigma_{30} - \Sigma_{20})\sqrt{\frac{\ln(Y_0/R^*)\ln(Y_0/Z^*)}{\ln(Y/R^*)\ln(Y/Z^*)}} \tag{133}$$

If we substitute this expression into one of the Equations (13) and integrate, we obtain Σ_2 and Σ_3 separately. The result is

$$\left.\begin{aligned} \Sigma_2 &= -A\,\frac{\sqrt{\ln(Y/Z^*)}-\sqrt{\ln(Y/R^*)}}{\sqrt{\ln(Y/R^*)}} + B \\ \Sigma_3 &= A\,\frac{\sqrt{\ln(Y/Z^*)}-\sqrt{\ln(Y/R^*)}}{\sqrt{\ln(Y/Z^*)}} + B \end{aligned}\right\} \tag{134}$$

where

$$\left.\begin{aligned} A &= (\Sigma_{30}-\Sigma_{20})\sqrt{\frac{\ln(Y_0/Z^*)\ln(Y_0/R^*)}{\ln(R^*/Z^*)}} \\ B &= \frac{\Sigma_{20}\sqrt{\ln(Y_0/R^*)}+\Sigma_{30}\sqrt{\ln(Y_0/Z^*)}}{\sqrt{\ln(Y_0/R^*)}+\sqrt{\ln(Y_0/Z^*)}} \end{aligned}\right\} \tag{135}$$

If $\ln(Y/R^*) >> |\ln(R^*/Z^*)$, the equations can be simplified

$$\Sigma_2 = -\tfrac{1}{2}(\Sigma_{30}-\Sigma_{20})\sqrt{\frac{\ln(Y_0/R^*)\ln(Y_0/Z^*)}{\ln(Y/R^*)}} + B$$

$$\Sigma_3 = \tfrac{1}{2}(\Sigma_{30}-\Sigma_{20})\sqrt{\frac{\ln(Y_0/R^*)\ln(Y_0/Z^*)}{\ln(Y/Z^*)}} + B \tag{136}$$

The shock strength of the central shock is related to $\Sigma_3 - \Sigma_2$. According to (133) it drops much faster than either the rear shock or the front shock. However, the pressure level at which this shock occurs tends, according to (136), to a finite Σ value. This implies that the central shock must either catch the first shock (if $B > 0$) or the rear shock must catch the central shock (if $B < 0$).

Let us consider first the exceptional case $B = 0$. Since $\Sigma_{20} = -\Sigma_{10}$

B = 0 implies that

$$\Sigma_{10}\sqrt{\ln(Y_0/R^*)} = \Sigma_{30}\sqrt{\ln(Y_0/Z^*)} \qquad (137)$$

Neglecting the small difference between Y_0 and R_0, these quantities are identical with the quantity A defined by (125), which in turn is related to the "impulse" of the pulse $\theta \Delta p_s$ multiplied with the shock radius (see Equation (126a)). We conclude that B = 0, if the impulse of the two pulses is the same at the same radius. It will be noticed that R^* and Z^* may nevertheless differ. Thus, one pulse may have long duration and low shock pressure; the other short duration and comparatively large shock pressure.

If B = 0, then both Σ_2 and Σ_3 tend to 0 more rapidly than either Σ_1 or Σ_4. Thus the positive phase of the second pulse and the negative phase of the first pulse are eventually eliminated and there remains the positive phase of the first pulse, which combines with the negative phase of the second pulse. All this, of course, takes some time, until $\ln(Y/R^*) >> \ln(Y_0/R)$. If R^* and Z^* differ from each other the pressure gradients in the positive and negative phase will also differ, only the product of shock pressure and duration will be the same. If the two pulses were completely identical, the remaining pulse would be indistinguishable from either, so that the reflected shock has simply disappeared.

If B is positive, we require that the impulse in the second pulse is greater than the impulse in the first and in this case the central shock catches up with the first shock. Eventually the first pulse has disappeared and only the second pulse remains. Similarly, if B is negative, the second pulse will eventually disappear and only the first pulse remain.

Asymptotically the energy in the blast wave is therefore not equal to the sum of the energy in the two pulses but equal to the energy in either

the first or the second pulse, whichever is the greater. The remainder of the energy has been dissipated at the central shock. This increased energy dissipation is due to the fact that the shock front of the second pulse must go through the negative phase of the first pulse. E.g. the energy dissipation just before the second pulse catches up with the first is proportional to $4(\Delta p_s)^3$, assuming for simplicity equal shock strengths in both pulses. The factor 4 arises from the 4 shocks. Just after the second pulse caught up with the first, there are two shocks of strength Δp_s and one of strength $2\Delta p_s$ and the energy dissipation is proportional to

$$2(\Delta p_s)^3 + (2\Delta p_s)^3 = 10(\Delta p_s)^3$$

and has, therefore, increased by a factor 2.5.

If $B > 0$, the radius at which the central shock catches up with the first shock is given by the condition $\Sigma_2 = \Sigma_1$. After some manipulation one finds as consequence that $\Sigma_3 + \Sigma_4 = 0$, i.e. the front shock, which is now Σ_3 has the same value it would have had if there had been no first pulse. Also one finds for the radius R the condition

$$\sqrt{\ln(R/R^*)} = \sqrt{\ln(R_0/R^*)}\;\frac{\Sigma_{10}^2 \ln(R_0/R^*) + 2\Sigma_{10}\Sigma_{30}\ln(R_0/Z^*) + \Sigma_{30}^2 \ln(Z_0/Z^*)}{\Sigma_{30}^2 \ln(Z/Z^*) - \Sigma_{10}^2 \ln(R/R^*)} \qquad (138)$$

8.11 THE CONTINUATION OF THE IBM-RUN

The methods developed in the preceding sections have been used to continue the IBM results of Chapter 7. The IBM machines give us the pressure Δp as function of the radius at a fixed time. From these data we obtain immediately the function $\Sigma(y)$ and we can deduce the function $g(\Xi)$ defined by (82). This function should, of course, be independent of the time. It is shown in Figure 4. The circles refer to the last IBM cycle when the

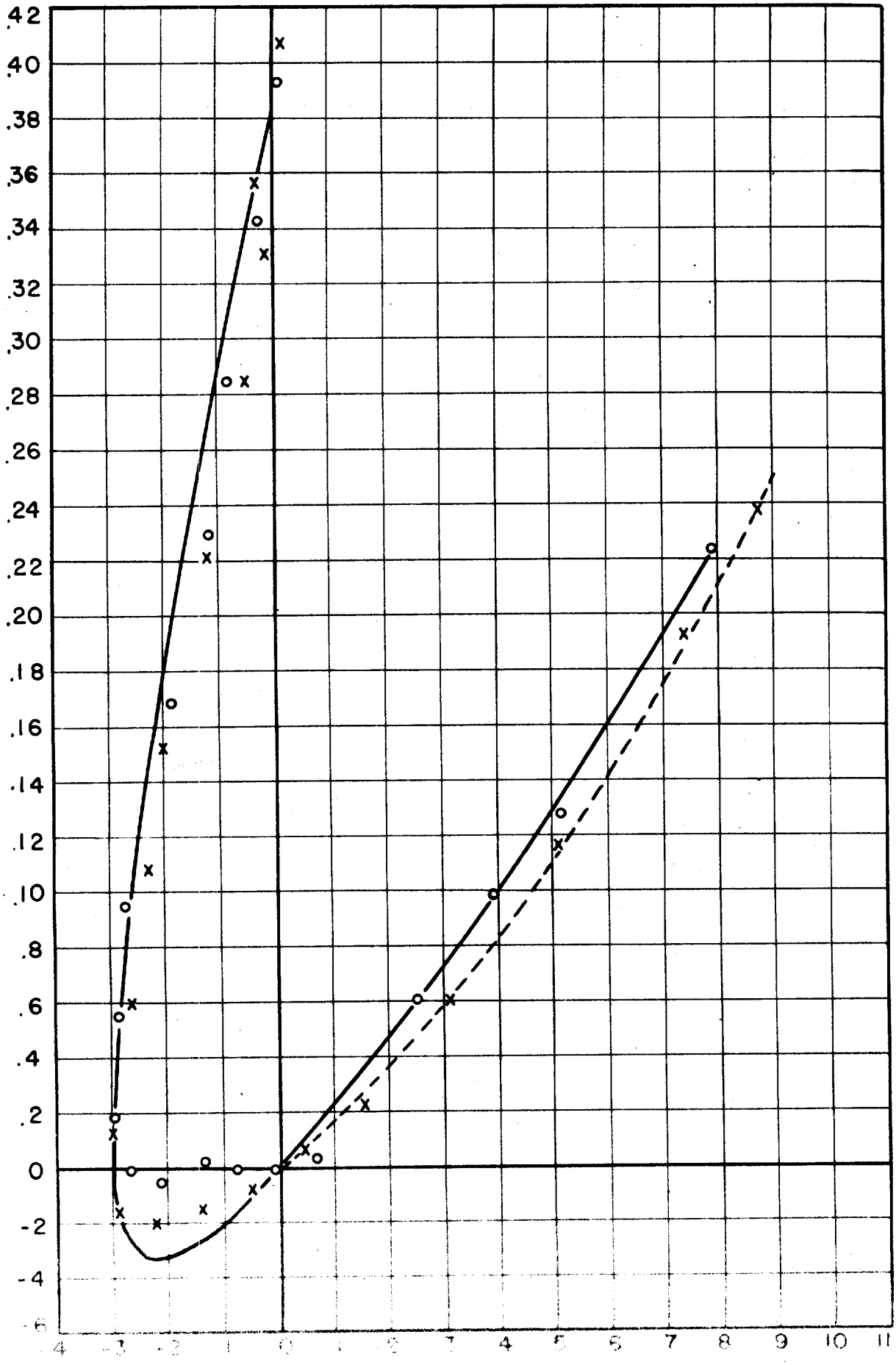

Figure 4

shock radius is 314.7 (we use here the "IBM-unit" for the radius which is 19.97 meters). The crosses refer to an early cycle, when the shock radius is only 200.2.

For the numerical evaluation it was convenient to introduce, instead of Σ the quantity,

$$s = \frac{\gamma \Sigma}{c_o} = \frac{R \Delta p}{p_o} \tag{139}$$

and instead of g

$$g(s) = -\frac{\alpha q(x)}{c_o} \tag{140}$$

then the positive phase can be represented in the form

$$g = 2.2\, s + .075\, s^2 \tag{141}$$

Substitution into (89) yields

$$\ln R = \frac{170.4}{s_F^2} + \frac{\gamma}{\alpha}\left[2.2 + .05\, s_F\right] ; \quad \frac{\Delta p_s}{p_o} = \frac{s_F}{R} \tag{142}$$

where s_F is the value of s at the shock front. Here we have used the boundary condition that at $R = 314.7$, $\Delta p_s = .0251\, p_o$.

As s_F becomes small, we have approximately

$$\frac{\Delta p_s}{p_o} = \frac{\sqrt{170.4}}{R\sqrt{\ln (R/R^*)}} ; \quad \ln R^* = \frac{2.2\,\gamma}{\alpha} ; \quad R^* = 13.03 \tag{143}$$

(R in IBM units)

Introducing the meter as unit, one finds

$$\frac{\Delta p_s}{p_o} = \frac{260.7}{R\sqrt{\ln(R/260.1)}} \tag{144}$$

(R in meter)

The data from the earlier cycle are better represented by the formula

$$g = 1.6\, s + 0.13\, s^2 \tag{141a}$$

which leads to

$$\ln R = \frac{194.6}{s_f^2} + \frac{\gamma}{\alpha}\left[1.6 + .0867\, s_f\right] \tag{142a}$$

and asymptotically,

$$\frac{\Delta p_s}{p_o} = \frac{278.6}{R\sqrt{\ln (R/129.1)}} \qquad (R \text{ in meter}) \tag{144a}$$

which differs by about 6 per cent from the previous formula. This is the error to be expected, since at the smaller radius the over-pressure is 4.4 per cent. The data from the larger radius should be more reliable and have been used for all calculations.

For the negative phase, we get a good approximation by the formula

$$g = (11 + 0.38\, s)\left\{\sqrt{3} \pm \sqrt{3 + s}\right\} + 5.38\, s \qquad (s < 0) \tag{145}$$

The constants in this representation have been chosen in such a way that we get not only a good representation of the numerical data, but that also the slope of the function g is continuous at $s = o$ and that the integral of the pressure taken over the pulse vanishes. In actual fact, the data from the last IBM-cycle are somewhat erratic in the neighborhood of $s = o$. This must be due to an error in the IBM-run, since the data from the earlier cycle are quite smooth. For this reason no attention has been paid to this erratic behavior and the condition that dg/ds be continuous at $s = o$ has been used instead, in order to get a reasonable

function g.

We have seen before (see Equation (107)) that the back shock will start at a value of s for which

$$d^2g/ds^2 = 0 \tag{146}$$

If we use the presentation (145) we find that this condition cannot be satisfied for any negative s. However, this is due to the analytic representation; if we go back to the numerical data, we find that the curvature changes sign. The exact value of s where the change of sign occurs is not easily determined; however the minimum slope can be determined fairly accurately and is 8.2. The slope determines the radius at which the back shock starts (see Equation (106))

$$\ln r = \frac{\gamma}{\alpha}\left(\frac{dg}{ds}\right)_{\text{minimum}} = \frac{1.4}{1.2}\ 8.2 \tag{147}$$

$$r = 1.4 \times 10^4 \text{ IBM units} = 2.8 \times 10^5 \text{ meters}$$

We shall not be interested in such large distances.

For the duration of the positive pulse we find from (100a)

$$\theta = \frac{1}{c_0}\left[\frac{\alpha}{\gamma} s_F \ln R - g(s_F)\right] \tag{148}$$

or with (142) and (141)

$$\theta = \frac{1}{c_0}\left[\frac{\alpha}{\gamma}\frac{170.4}{s_F} - .025\, s_F^2\right] \tag{148a}$$

The shape of the pulse at a fixed distance as function of time is similarly given by the formula (see Equation (102))

$$T\ \theta = \frac{1}{c_0}\left[\frac{\alpha}{\gamma} s \ln R - g(s)\right] \tag{149}$$

$$\frac{\Delta p}{p_0} = \frac{s}{R}$$

where s varies from its value s_f at the shock front to -3 at the pressure minimum and back to zero. In order to obtain the time in seconds, we should use for c_o the "IBM-value" $c_o = 17.38$.

The peak pressure versus shock radius curve is shown in Figure 5, using "IBM-units". For comparison some points obtained, if we stop the IBM-run at an earlier instent, are also shown.

The duration versus peak pressure is shown in Figure 19 of Chapter 7. The equations for the shape of the pressure pulse are used in the next chapter, to obtain data for the two combat bombs.

Figure 5

Peak Pressure versus Shock Radius

------- Semi-Accoustic theory plotted at R 314.7

X Semi-Accoustic theory plotted at R 200.2

------ IBM Results

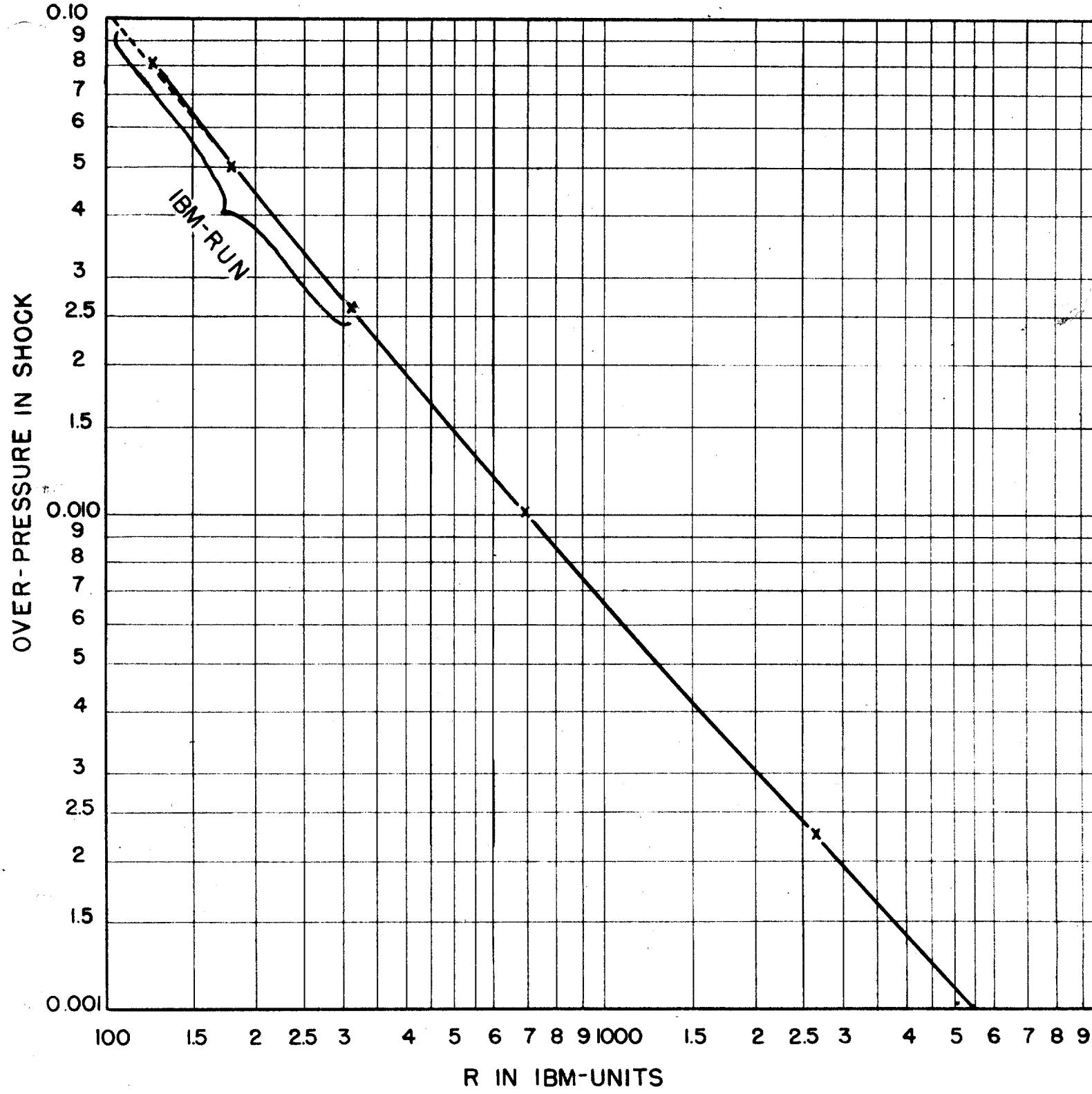

CHAPTER 9

THE EFFECT OF ALTITUDE

K. Fuchs

9.1 INTRODUCTION

One of the easiest measurements of the effect of a nuclear bomb in combat conditions is a measurement of the pressure pulse by means of airborne gauges. The instruments used for this purpose are described in Chapter 18. Safety considerations for the planes from which these gauges are released make it impossible to get close to the bomb. Furthermore, since these gauges are released at great height at about the same time the bomb is released, but are attached to parachutes, they will still be at a considerable height when the blast reaches them.

The information received from the airborne gauges was in fact the only quantitative information on the bombs dropped over Hiroshima and Nagasaki, until scientific teams could enter these towns after the cessation of hostilities. The instruments recorded at a height of about 30,000 feet, where the atmospheric pressure is considerably reduced. They were at a distance of 36,000 to 40,000 feet from the bomb.

Such large distances can be covered by the semi-acoustic theory developed in the preceding chapter. However, we have to estimate also the effect of the change of pressure and temperature with altitude in order to interpret the records.

We shall make the assumption that the energy is emitted uniformly in all directions. This assumption appears eminently reasonable, since the altitude effect will become pronounced only after the shock wave has decayed

into a pressure pulse of length small compared to the distance from the bomb.

If in addition we assume the acoustic treatment, we obtain the Rayleigh correction factor for the over-pressure

$$\frac{\Delta p}{\Delta p_0} = \sqrt{\frac{\rho c}{\rho_0 c_0}} \qquad (1)$$

where ρ, c, Δp are density, sound velocity and over-pressure at a given height, and ρ_0, c_0, Δp_0 are the same quantities for a uniform atmosphere. The duration of the pulse and the energy in the pulse are unchanged. The latter follows immediately from the fact that in the acoustic theory the energy in the pulse is constant.

We have seen in Chapter 8 that the energy-dissipation in the pressure pulse is important. Clearly, if the energy dissipation is taken into account, the pressure pulse at a given altitude will depend not only on the conditions at that altitude, but also on the past history of the pulse. For a linear pulse we shall find that the correction factor is composed of two factors. The first is identical with (1). The second factor represents a change in the form of the energy dissipation term, which in a uniform atmosphere is $(\log (R/r_0))^{-1/2}$. The log is replaced by the integral dR/R, weighted with a function which depends on the variation of the atmospheric conditions. The result is

$$\frac{\Delta p}{\Delta p_0} = \sqrt{\frac{\rho c}{\rho_0 c_0}} \left\{ \log (R/r_0) \Big/ \int_{r_0}^{R} \frac{c_0^2}{c^2} \sqrt{\frac{\rho_0 c_0}{\rho c}} \, \frac{dR}{R} \right\}^{1/2} \qquad (2)$$

Clearly

$$\frac{c}{c_0} \left(\frac{\rho c}{\rho_0 c_0}\right)^{3/4} < \frac{\Delta p}{\Delta p_0} < \left(\frac{\rho c}{\rho_0 c_0}\right)^{1/2} \qquad (3)$$

The duration of the pulse, which in the acoustic theory is unchanged, also undergoes a change, if dissipation of energy is taken into account.

We shall find for a linear pulse

$$\frac{\theta}{\theta_0} = \left\{ \int_{r_0}^{R} \frac{c_0^2}{c^2} \sqrt{\frac{\rho_0 c_0}{\rho c}} \cdot \frac{dR}{R} \Big/ \log (R/r_0) \right\}^{1/2} \tag{4}$$

so that

$$1 < \frac{\theta}{\theta_0} < \frac{c_0}{c} \left(\frac{\rho_0 c_0}{\rho c} \right)^{1/4} . \tag{5}$$

The duration of the pulse therefore increases with altitude.

In Section 9.4 these formulae are generalized for an arbitrary shape of the pulse.

Compared to the acoustic theory the pulse is therefore less strong, but longer. In principle it is therefore easy to check the theory by considering the distortion of the pulse shape, which is approximately independent of the energy release.

However, if we try to do so, we are confronted with the embarrassing situation that the Hiroshima record and Nagasaki record contradict each other. This is the more mysterious, since they were taken at exactly the same altitude and approximately the same distance from the explosion. Hence, we should expect the shape of the pulse to be approximately the same in either case. In actual fact the Nagasaki record gave a higher peak pressure but exactly the same duration as the Hiroshima record.

If this result is real, it cannot be explained as an altitude effect, unless the variation of temperature and pressure with altitude differed completely in the two cases. Neither could it be explained on the basis of any effect which obeys the usual scaling laws.

If we trust the peak pressure measurements, the Nagasaki bomb was about 5 times as powerful as the Hiroshima bomb, in moderate agreement with the factor 4 deduced by Penney from the blast damage. If the duration of the

pulse is used, the two bombs were equally powerful.

The Hiroshima record gives a shape of the pressure pulse in fairly close agreement with the theory; the Nagasaki pulse, however, is much steeper than expected.

The values of the nuclear energy release derived from either theory, using the peak pressure or the duration of the pulse as criterion are given in the following table:

Table 9.1

Energy release of combat bombs in tons of TNT

	obtained from peak pressure	obtained from duration
	Nagasaki	
Acoustic theory	35,000	20,000
Theory with energy dissipation	51,000	11,700
	Hiroshima	
Acoustic Theory	7,700	19,500
Theory with energy dissipation	10,600	11,400

9.2 ACOUSTIC THEORY

We make the following assumptions:

(1) The pulse is weak; more precisely $\Delta p << \rho c^2$

(2) The length of the pulse is small compared to the radius to which it has penetrated.

(3) The length of the pulse is small compared to a distance over which the atmosphere changes appreciably.

(4) The energy is emitted uniformly in all directions.

An important consequence of the assumption (3) is that the distortion of the pulse is confined to a change of scale only. In particular the ratio

of the mean square of the pulse to the square of the shock pressure is unchanged. This is not true if energy dissipation is taken into account, unless the pulse has the asymptotic linear form.

$$\frac{\overline{(\Delta p)^2}}{(\Delta p_s)^2} = \frac{\overline{(\Delta p_o)^2}}{(\Delta p_{so})^2} \tag{6}$$

Here the suffix o refers to the same quantities in a uniform atmosphere.

In the acoustic theory all signals travel with the velocity of sound. If at time $t = o$, the end of the positive phase was at $r = r_o$, then at time t it will have reached the radius r, where

$$t = \int_{r_o}^{r} \frac{d\tilde{r}}{c(\tilde{r})}$$

Similarly for the head of the pulse

$$t = \int_{r_o + L_o}^{r + L} \frac{d\tilde{r}}{c(\tilde{r})}$$

where L_o, L is the length of the pulse at time $t = o$, and at time t. Subtracting the two equations we find

$$\int_{r_o}^{r_o + L_o} \frac{d\tilde{r}}{c(\tilde{r})} = \int_{r}^{r+L} \frac{d\tilde{r}}{c(\tilde{r})} \tag{7}$$

These integrals, however, are identical with the duration of the pulse. Hence we find that the duration of the pulse is constant.

$$\theta = \theta_o \tag{8}$$

The energy per unit solid angle in the pulse is given by

$$w = R^2 \int \Delta p\, u\, dt \tag{9}$$

to be integrated over the path of a volume element. For a weak pulse, we can integrate keeping the position in space fixed. Also $\Delta p = \rho c u$. Hence

$$w = 2R^2 \overline{(\Delta p)^2}\, \theta/\rho c \tag{10}$$

The factor 2 arises from the negative phase.

Since in the acoustic theory the energy per unit solid angle is constant, it follows with (6) and (8) that

$$\frac{\Delta p_s}{\Delta p_{so}} = \sqrt{\frac{\rho c}{\rho_o c_o}} \tag{11}$$

This is the Rayleigh correction for the pressure.

9.3 THEORY INCLUDING ENERGY DISSIPATION

In order to include the effect of energy dissipation, we shall make one additional assumption to those mentioned in Section 2. That is

(5) The pulse has linear shape.

This assumption is at least approximately true for the positive phase in the region in which we are interested. Since the positive and negative phases do not interfere with each other, the assumption is therefore approximately correct.

One of the shock conditions is

$$\Delta p_s = \rho c u_s \tag{12}$$

in view of assumption (3), we can treat the history of any given volume element on the basis of a theory in a uniform atmosphere. Then the equation (12) is satisfied throughout the pulse

$$\Delta p = \rho c u \tag{13}$$

The energy per unit solid angle is again given by (9); for a linear pulse we find

$$w = R^2 \int \Delta p\, u\, dt = \frac{2}{3} R^2 (\Delta p_s)^2 \theta / \rho c \tag{14}$$

The energy dissipation in the shock and back shock can be expressed in the form (compare Equation (74) Chapter 8)

$$\frac{dw}{dR} = -\frac{1}{3}\,\frac{\alpha R^2 (\Delta p_s)^3}{\rho^2 c^4} \qquad \alpha = \frac{\gamma+1}{2} \tag{15}$$

Combining the two equations we find

$$2\frac{d}{dR}\left[R^2(\Delta p_s)^2\,\theta/\rho c\right] + \alpha R^2 (\Delta p_s)^3/\rho^2 c^4 = 0 \tag{16}$$

The shock velocity is given by the Hugoniot condition

$$\frac{dR}{dt} = c + \frac{\alpha \Delta p_s}{2\rho c} \tag{17}$$

So far we have been concerned only with the local conditions at the point where the pulse happens to be. We require one more equation, in which the variation of atmospheric conditions appears.

For this purpose we observe that the average velocity of the pulse is given by the sound velocity. This follows from the fact that the velocity of the back shock lags as much below sound velocity as the velocity of the front shock is above sound velocity, and that the pulse is symmetric. The latter was shown in Chapter 8 by means of the general argument that the total displacement of any volume element decreases as $1/R^2$ and therefore asymptotically

$$\int u\,dt = \frac{1}{\rho c}\int \Delta p\,dt = 0$$

Thus the midpoint of the pulse, which is also the end of the positive phase, travels with sound velocity. If θ is the duration of the pulse at radius R, we have therefore

$$t = \int^R \frac{dr}{c} - \theta \tag{18}$$

where t is the time when the shock front reaches the radius R.

We now have all necessary equations and proceed to solve them. Differentiation of (18) yields

$$\frac{dt}{dR} = \frac{1}{c} - \frac{d\theta}{dR} \tag{19}$$

Observing that the second term is small, we find

$$\frac{dR}{dt} = c + c^2 \frac{d\theta}{dR} \tag{20}$$

Comparison with (17) yields

$$\frac{d\theta}{dR} = \frac{\alpha \Delta p_s}{2\rho c^3} \tag{21}$$

This equation can be used to eliminate Δp_s from (16), with the result

$$\frac{d}{dR}\left[R^2 \rho c^5 \theta \left(\frac{d\theta}{dR}\right)^2\right] + R^2 \rho c^5 \left(\frac{d\theta}{dR}\right)^3 = 0 \tag{22}$$

Integration of this equation gives

$$R^2 \rho c^5 \theta^2 \left(\frac{d\theta}{dR}\right)^2 = \text{const} = \frac{1}{4} B^4 \tag{23}$$

A second integration yields

$$\theta^2 = B^2 \int_{r_0}^{R} \frac{1}{\sqrt{\rho c}\, c^2} \frac{dR}{R} \tag{24}$$

where r_0 is another constant of integration.

Substitution into (21) gives the shock pressure

$$\Delta p_s = \frac{B\sqrt{\rho c}}{\alpha R} \Big/ \left[\int_{r_0}^{R} \frac{1}{c^2 \sqrt{\rho c}} \frac{dR}{R}\right]^{1/2} \tag{25}$$

In a uniform atmosphere of density ρ_0 and sound velocity c_0, we find the asymptotic law of Chapter 8

$$(\Delta p_s)_0 = \frac{B(\rho_0 c_0)^{3/4} c_0}{\alpha R \sqrt{\ln (R/r_0)}} \tag{26}$$

thus r_0 should be identified with the radius R^* in the asymptotic law

cf (124a)

for a uniform atmosphere. The altitude correction factor is the ratio of (25) and (26)

$$\frac{\Delta p_s}{(\Delta p_s)_0} = \sqrt{\frac{\rho c}{\rho_0 c_0}} \quad \frac{\theta_0}{\theta} \tag{27}$$

where θ/θ_0 is the altitude correction factor for the duration, which is given by

$$\frac{\theta}{\theta_0} = \left[\int_{R^*}^{R} \frac{c_0^2}{c^2} \sqrt{\frac{\rho_0 c_0}{\rho c}} \quad \frac{dR}{R} \Big/ \ln (R/R^*) \right]^{1/2} \tag{28}$$

9.4 ALTERNATIVE DERIVATION

We shall now give an alternative derivation of the formulae given above. This derivation follows closely that given in Chapter 8 for a uniform atmosphere.

In this derivation we use the concept of Σ - signals. In a uniform atmosphere Σ remains constant along a characteristic. If atmospheric conditions change, this is no longer true. We shall make the assumption that all Σ - values change with the distance from the center of the explosion, by a common factor K, the same for all Σ. This would seem to be a reasonable assumption as long as the length of the pulse is small compared to the distance over which the atmosphere changes appreciably. However, the complete equivalence of the assumption about the behaviour of the Σ- signals with the approximation of a small pulse, is only demonstrated by the fact that we shall obtain the same results as in Section 9.3. For this reason we preferred the previous derivation, quite apart from its simplicity.

The derivation which we shall give below has on the other hand the advantage that it applies to an arbitrary shape of the pulse and allows us to make a prediction about the shape of the pulse. The pulse is distorted by the change in the Σ - values by the factor k. The shock pressure, however,

is changed in addition by another factor, expressing the fact that the energy dissipation has changed and, therefore, the Σ- value at the shock front is no longer the same as before. This second factor has no influence on the shape of the pulse, except insofar as it cuts off the pulse at a different Σ - value. The derivation of Section 9.3 gave us only the product of these two factors. Now we shall obtain each factor separately.

Furthermore, in the derivation of Section 9.3, we had an arbitrary constant of integration r_0, which represented the radius at which the atmospheric conditions could still be considered uniform. We should have expected that we should take $r_0 = 0$. However, in order to get correct results we found that r_0 should be identified with the radius R^* in the asymptotic law for a uniform atmosphere. The treatment given below will resolve this difficulty.

Our assumption can be stated in the form

$$\Sigma = \Sigma^\circ k \tag{29}$$

where Σ° is the value of Σ at the radius $r = r_0$ and k is a function of the radius. Equation (29) holds along the path of a characteristic, which goes with velocity $c + u$. The excess velocity of the characteristic above the local sound velocity is given by $\alpha \Sigma / r$. If at time $t = t^\circ$, the characteristic is at $r = r_0$, the equation of the characteristic is

$$t - t^\circ = \int_{r_0}^{r} \frac{dr}{c + \alpha \Sigma / r} = \int_{r_0}^{r} \frac{dr}{c} - \frac{\alpha \Sigma^\circ}{c_0^2} K(r) \tag{30}$$

$$K = \int_{r_0}^{r} \frac{c_0^2 k}{c^2 r}\, dr \tag{31}$$

Here r_o is assumed a fixed radius and t° is then evidently a function of Σ°. K appears only in a small term and instead of integrating over the path of a characteristic, we can integrate over the path of the shock front. Then the integral is independent of Σ°.

At the shock front we have

$$t - t^\circ = \int_{r_o}^{R} \frac{dr}{c} - \frac{\alpha \Sigma_s^\circ}{c_o^2} K(R) \tag{32}$$

Differentiation yields

$$\frac{dt}{dR} = \frac{1}{c} - \left(\frac{\alpha K}{c_o^2} - \frac{dt^\circ}{d\Sigma^\circ} \right) \frac{d\Sigma_s^\circ}{dR} - \frac{\alpha \Sigma_s^\circ}{c_o^2} \frac{dK}{dR} \tag{33}$$

The shock velocity is given by

$$\frac{dR}{dt} = c + \frac{\alpha \Sigma_s}{2R} = c + \frac{\alpha \Sigma_s^\circ k}{2R} = c + \frac{\alpha c^2}{2 c_o^2} \frac{dK}{dR} \Sigma_s^\circ \tag{34}$$

Comparison yields

$$\left(K - \frac{c_o^2}{\alpha} \frac{dt^\circ}{d\Sigma^\circ} \right) \frac{d\Sigma_s^\circ}{dR} + \frac{1}{2} \Sigma_s^\circ \frac{dK}{dR} = 0 \tag{35}$$

Let us introduce instead of R the variable Z defined by

$$\frac{dZ}{Z} = \frac{c_o^2 k}{c^2} \frac{dr}{r} \qquad Z_o = r_o \tag{36}$$

then

$$K = \ln (Z/Z_o) \tag{37}$$

and

$$\left(\ln Z/Z_o - \frac{c_o^2}{\alpha} \frac{dt^\circ}{d\Sigma^\circ} \right) \frac{d\Sigma_s^\circ}{dZ} + \frac{1}{2} \frac{\Sigma_s^\circ}{Z} = 0 \tag{38}$$

In this form, the variation of the atmosphere has been eliminated. Hence Σ_s° is the same function of Z, as Σ for a uniform atmosphere is of R.

i.e.

$$\Sigma_s^\circ = \Sigma_{os}(Z) \tag{39}$$

where $\Sigma_{os}(R)$ is the Σ_s for a uniform atmosphere. In order to calculate k we use again the energy dissipation. The work done by the pulse per unit solid angle is

$$w = r^2 \int p u \, dt = k^2 \rho c \int (\Sigma^\circ)^2 \, dt \tag{40}$$

However, for fixed r we have from (30)

$$dt = -\left(\alpha \frac{K}{c_o^2} - \frac{dt^\circ}{d\Sigma^\circ}\right) d\Sigma^\circ \tag{41}$$

Hence

$$w = k^2 \rho c \int^{\Sigma_s^\circ} (\Sigma^\circ)^2 \left(\frac{\alpha K}{c_o^2} - \frac{dt^\circ}{d\Sigma^\circ}\right) d\Sigma^\circ \tag{42}$$

We assume that the back shock has not yet started; then the integral extends to the minimum value of Σ° in the negative phase and then back to $\Sigma^\circ = 0$. Differentiation of (42) yields

$$\frac{dw}{dR} = \frac{d(k^2\rho c)}{dR} \frac{w}{k^2 \rho c} + \frac{\alpha k^2 \rho c}{c_o^2} \left\{ \frac{dK}{dR} \int^{\Sigma_s^\circ} (\Sigma^\circ)^2 \, d\Sigma_\circ + (\Sigma_s^\circ)^2 \left(K - \frac{c_o^2 \, dt^\circ}{\alpha \, d\Sigma^\circ}\right) \frac{d\Sigma_s^\circ}{dR} \right\} \tag{43}$$

In the first integral the negative phase does not contribute and the positive phase gives $(\Sigma_s^\circ)^3/3$. Utilizing (35) we find

$$\frac{dw}{dR} = \frac{d(k^2\rho c)}{dR} \frac{w}{k^2 \rho c} - \frac{\alpha k^2 \rho c}{6 c_o^2} (\Sigma_s^\circ)^3 \frac{dK}{dR} \tag{44}$$

The energy dissipation occurs at the shock front and can be expressed in the form (see Chapter 8, Equation (73))

$$\frac{dw}{dR} = -\frac{1}{6}\,\frac{\rho\alpha\,\Sigma_s^3}{cR} = -\frac{1}{6}\,\frac{\rho\alpha(\Sigma_s^\circ)^3 k^3}{cR} \tag{45}$$

Using the definition (31) of K it is found that this is identical with the last term in (44). Hence the first term in (45) vanishes. This requires

$$k = \sqrt{\frac{\rho_0 c_0}{\rho c}} \tag{46}$$

and

$$K = \ln(Z/Z_0) = \int_{r_0}^{r} \frac{c_0^2}{c^2}\sqrt{\frac{\rho_0 c_0}{\rho c}}\,\frac{dr}{r} \tag{47}$$

The shock pressure is given by

$$\Delta p_s = \rho c\, k\, \Sigma_s^\circ / R \tag{48}$$

With (46), (47) and (39) we find

$$\Delta p_s = \frac{\rho_0 c_0}{R}\sqrt{\frac{\rho c}{\rho_0 c_0}}\,\Sigma_{os}(Z) \tag{49}$$

and the altitude correction factor is

$$\frac{\Delta p_s}{(\Delta p_s)_0} = \sqrt{\frac{\rho c}{\rho_0 c_0}}\,\frac{\Sigma_{os}(Z)}{\Sigma_{os}(R)} \tag{50}$$

The equation (49) can clearly also be written in the form

$$\Delta p_s = \frac{Z}{R}\sqrt{\frac{\rho c}{\rho_0 c_0}}\,\Delta p_{so}(Z) \tag{49a}$$

where $\Delta p_{so}(R)$ is the shock pressure in a uniform atmosphere.

From (30) follows that the arrival of the signal Σ° at the radius r is delayed with respect to the shock by the time interval

$$\Delta t = t^\circ(\Sigma^\circ) - t^\circ(\Sigma_s^\circ) + \frac{\alpha}{c_0^2}K(r)\left[\Sigma_s^\circ - \Sigma^\circ\right] \tag{51}$$

$$= t^\circ(\Sigma^\circ) - t^\circ(\Sigma_s^\circ) + \frac{\alpha}{c_0^2}\ln(Z/Z_0)\left[\Sigma_s^\circ - \Sigma^\circ\right] \tag{52}$$

For a uniform atmosphere, we can replace Σ° by Σ and Z by R. Comparison with Equation (102) of Chapter 8 shows that

$$\frac{c_o^2}{\alpha} t^\circ(\Sigma) + \Sigma \ln r_o = g(\Sigma) \tag{53}$$

where $g(\Sigma)$ is the function introduced in Chapter 8. Hence

$$\Delta t = \frac{\alpha}{c_o^2}\left[g(\Sigma_s^\circ) - g(\Sigma^\circ) + (\Sigma_s^\circ - \Sigma^\circ)\ln Z\right] \tag{54}$$

In view of (39) this can also be written in the form

$$\Delta t = \Delta t_o(\Sigma_i^\circ ; \Sigma_s^\circ) \tag{54a}$$

where Δt_o is the corresponding function for a uniform atmosphere. The duration θ is obtained by putting $\Sigma^\circ = 0$. Then

$$\theta = \frac{\alpha}{c_o^2}\left[g(\Sigma_s^\circ) + \Sigma_s^\circ \ln Z\right] = \theta_o(\Sigma_s^\circ) \tag{55}$$

The equations we have derived no longer contain the radius r_o except in Z. It is clear that the equations should be independent of r_o provided we can find a value of r_o sufficiently large that the semi-acoustic theory applies and at the same time sufficiently small, so that up to the radius r_o the atmosphere can be considered uniform. With that assumption we proceed to get rid of r_o in the expression for Z. We write (43) in the form

$$\ln Z = \ln r_o + \int_{r_o}^{R} \frac{c_o^2}{c^2}\sqrt{\frac{\rho_o c_o}{\rho c}}\,\frac{dr}{r} = \ln R + \int_{r_o}^{R}\left\{\frac{c_o^2}{c^2}\sqrt{\frac{\rho_o c_o}{\rho c}} - 1\right\}\frac{dr}{r} \tag{56}$$

Since the atmosphere is assumed uniform for $r < r_o$, the integrand vanishes

in this region and we can extend the integral to $r = 0$

$$\ln Z = \ln R + \int_0^R \left\{ \frac{c_0^2}{c^2} \sqrt{\frac{\rho_0 c_0}{\rho c}} - 1 \right\} \frac{dr}{r} \tag{57}$$

It remains to show that our equations coincide with those derived in Section 9.3 for a linear pulse. For this case (see Chapter 8, Equation (94))

$$\Sigma_{os} = \frac{A}{\sqrt{\log (R/R^*)}} \tag{58}$$

It should be noted that the R^* here has nothing to do with the r_0 which we had before, but is determined by the properties of the pulse as shown in Chapter 8.

From (57) follows

$$\ln (Z/R^*) = \ln R + \int_0^R \left\{ \frac{c_0^2}{c^2} \sqrt{\frac{\rho_0 c_0}{\rho c}} - 1 \right\} \frac{dr}{r} - \ln R^* \tag{59}$$

If the atmosphere can be considered uniform up to the radius R^* this can be written in the form

$$\ln (Z/R^*) = \int_{R^*}^R \frac{c_0^2}{c^2} \sqrt{\frac{\rho_0 c_0}{\rho c}} \frac{dr}{r} \tag{60}$$

Substituting (58) and (60) into (50), we obtain the formula (27), (28), with the correct radius R^*. It is now clear that the necessity which arose previously of identifying r_0 with R^* was artificial, introduced by the limitations of a theory which assumes the pulse to be linear throughout. The results which we have obtained can be expressed in terms of simple scale changes. Define

$$\lambda = \exp \int_0^R \left\{ \frac{c_0^2}{c^2} \sqrt{\frac{\rho_0 c_0}{\rho c}} - 1 \right\} \frac{dr}{r} \tag{61}$$

since R is proportional to the altitude h, it can also be written as

$$\lambda = \exp \int_0^h \left\{ \frac{c_0^2}{c^2} \sqrt{\frac{\rho_0 c_0}{\rho c}} - 1 \right\} \frac{dh}{h} \tag{62}$$

and depends clearly only on the altitude, but not on the properties of the pulse. Then the altitude correction is taken care of by changing the radius scale by λ, the pressure scale by $\lambda\sqrt{\rho c/\rho_0 c_0}$ and the time scale remains unchanged. The factor λ appears in the pressure scale because $\rho c\,\Sigma = R\Delta p$ and the Σ-scale is changed by the factor $k = \sqrt{\rho_0 c_0/\rho c}$. Hence the scale factor for $R\Delta p$ is the acoustic correction factor $\sqrt{\rho c/\rho_0 c_0}$, but the scale factor for Δp itself contains the length scale factor λ (see also Equation (49_a)).

9.5 EVALUATION OF ALTITUDE CORRECTION FACTORS

The temperature T is a linear function of the altitude up to about 10,000 - 12,000 meters. It is given by

$$\frac{T}{T_0} = 1 - a\,h \tag{63}$$

$$a = 2.26 \times 10^{-5}/\text{meters} \tag{64}$$

It follows that the density ρ is given by (See for example Durand, Aerodynamic Theory, Volume I, pp 219-223).

$$\frac{\rho}{\rho_0} = (1 - a\,h)^{2k} \tag{65}$$

$$k = 2.128 \tag{66}$$

The sound velocity is proportional to the square root of the temperature

$$\frac{c}{c_0} = (1 - a\,h)^{1/2} \tag{67}$$

Substitution into (62) yields

$$\ln\lambda = \int_0^{ah} \left\{ \frac{1}{(1-\xi)^{k+\frac{3}{4}}} - 1 \right\} \frac{d\xi}{\xi} \tag{68}$$

Usually ah will be sufficiently small so that an expansion of the integral can be used

$$\ln\lambda = (K+\tfrac{5}{4})\ ah + \frac{(K+\frac{5}{4})(K+\frac{9}{4})}{2\,!\,2}\ (ah)^2 + \frac{(K+\frac{5}{4})(K+\frac{9}{4})(K+\frac{13}{4})}{3\,!\,3}\ (ah)^3 + \cdots \tag{69}$$

Also

$$k = \sqrt{\frac{\rho_a c_o}{\rho c}} = (\,1-ah\,)^{-(k+\frac{1}{4})} \tag{70}$$

9.6 APPLICATION TO HIROSHIMA AND NAGASAKI

The experimental data for Hiroshima and Nagasaki are given in Chapter 18. Using the semi-acoustic continuation of the IBM-run and the formulae for the altitude effect, we can determine the nuclear energy release required to give the observed peak pressure or the observed duration of the pulse. The energies obtained in this way have been recorded and discussed in the introduction.

The altitude correction is quite appreciable. The scale factor λ for the length is 2.527 and that for the pressures is 1.442; i.e., the pulse at that altitude was the same as that expected in a uniform atmosphere at 2.527 times the distance, except that the pressures have to be increased by the factor 1.442.

The predicted pulse shape is shown in Chapter 19, Figures 5 and 6, assuming 11,000 tons energy release for Hiroshima and 30,000 tons for Nagasaki. The Hiroshima record agrees quite well with the theory. The experimental Nagasaki record, on the other hand, looks quite different from the expected curve. This, of course, is not surprising, in view of the large discrepancy in the energy release estimated either from the peak pressure

or from the duration.

A strange feature of the Nagasaki record is the fact that the shape of the negative phase agrees very well with the prediction, as is shown by the dotted curve, which is identical with the predicted curve except that it is displaced by 0.4 seconds.

At present we have no explanation for the shape of the Nagasaki pulse.

CHAPTER 10

THE MACH EFFECT AND THE HEIGHT OF BURST

J. von Neumann and F. Reines

10.1 GENERAL CONSIDERATIONS ON THE PRODUCTION OF BLAST DAMAGE

Bomb damage to structures is largely caused by reflection on the structures of the shock wave generated by the bomb, and in the case of long blasts such as caused by an atomic bomb, by the ensuing blast wind. In this article we will consider the pressure criteria which determine the height at which the bomb should be burst so as to maximize the area of blast damage. The problem of maximizing the incendiary effect of the atomic bomb is treated elsewhere in this volume.

The first conclusion one reaches in studying the problem of blast damage is that the problem is extremely complex and can only be solved in a statistical or average manner. This is so for two reasons; first, the detailed description of a military target can never be completely given, and second, the complete analytical solution of even such a relatively simple problem as the behavior of a blast wave incident on a wall at an oblique angle has never been obtained for all angles. As we shall see later, a solution of the basic problem of shock reflection from a rigid wall can be obtained by a combination of theory and experiment. This solution is, however, not readily adapted to yielding the effect of blast in better than an average sense in a more complicated situation. As to the detailed description of the target, not only are the structures of odd shape, but they have the additional complicating property of not being rigid. This means that they do not merely deflect the blast wave without absorbing

energy from it, but take a tariff on the blast at each reflection.

In addition to being weakened by destroying structures, the blast may, of course, also be weakened by imparting kinetic energy to the debris. The removal of energy from the blast as it does its job decreases the blast pressure at any given distance from the point of detonation to a value somewhat below that which it would have in the absence of dissipative objects such as buildings. The presence of such dissipation makes it necessary to consider somewhat higher values of the pressure than would be required if there were only one structure set by itself on a rigid plane. The ideal would be to determine for a given explosion and given target configuration the required pressures by treating these diffractional and other losses theoretically and from first principles. Even this, however, would probably be too difficult in any well defined but realistic special case, and, furthermore, the necessary statistical theory to derive valid average results for the actual irregular and variable target configuration is not known. The next best procedure would be to derive from theory or from experiment the lethal pressures for a given isolated structure, to average this properly over various actual structures, and then to compare this with the average pressure level at which the damage under consideration has been empirically found to occur. The ratio of these two pressure levels would then express the losses in question. This procedure is not practical either, mainly because the first mentioned pressure criterion is not sufficiently well known or sufficiently reproducibly defined. These influences must therefore be accounted for in qualitative ways, not on an absolute basis, but rather in the sense of comparing them in two situations - one, the situation of actual interest, and the other one, a standard where the pressure level corresponding to the observed damage radius is empirically known.

The pressures which are actually inflicted upon a given structure will have been amplified by reflections from its own or nearby surfaces and decreased

by diffractions around openings and corners. The latter forms part of the losses referred to above. The former may cause local increases in pressure which will, under suitable conditions, be quite considerable. For overpressures of less than, say, 10 pounds per square inch, the acoustic theory applies in the main satisfactorily, except for rather glancing reflections. According to it any reflection, head-on or oblique, doubles the overpressure at the surface. (Concerning the limitations of this assertion - cf. Section 10.3.) It is not difficult to find geometrical arrangements where as many as three such reflections superpose their amplifications without any losses, e.g. the phenomenon of a shock running into a 90° corner. (Figures 1a, 1b, and 1c.) Thus, in such a case there is a local increase in pressure of four times the initial overpressure in the shock, even in acoustic theory. (The exact shock theory gives even higher increases, cf. below.) The case cited is a special example of the more general problem of the pressure increase which may be obtained when an acoustic shock runs into a corner having an angular opening θ at an angle of incidence α. In this general case it can be shown that the pressure increase to be expected is np where p is the overpressure in the shock wave, n is the number of shocks that have traversed the region; n is determined by the angle of the wedge θ and the angle of incidence α. Reasoning from the fact that infinite pressures are expected in a convergent cylindrical shock as:

$$\theta \longrightarrow 0 \text{ for } \alpha = \theta/2,\ n \longrightarrow \infty$$

The actual pressure amplifications that can be attained are limited by the rarefaction wave from the edges of the necessarily finite wedge.

These local increases are real and well-known: indeed the blast is notoriously erratic, and frequently affects some parts of a structure much more than other closely adjacent ones. In spite of its reality, it is clearly

Figure 1, a, b, c.

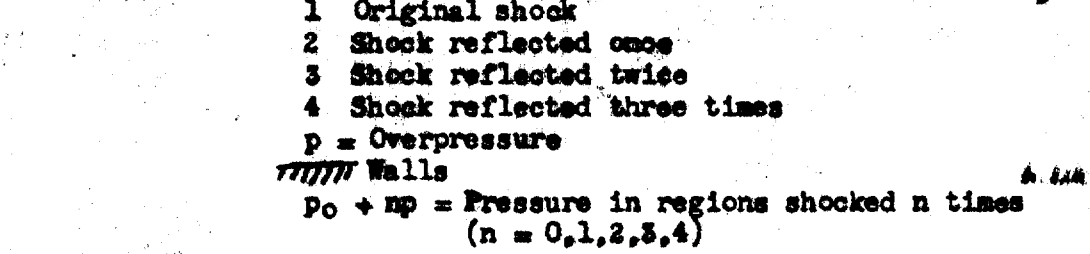

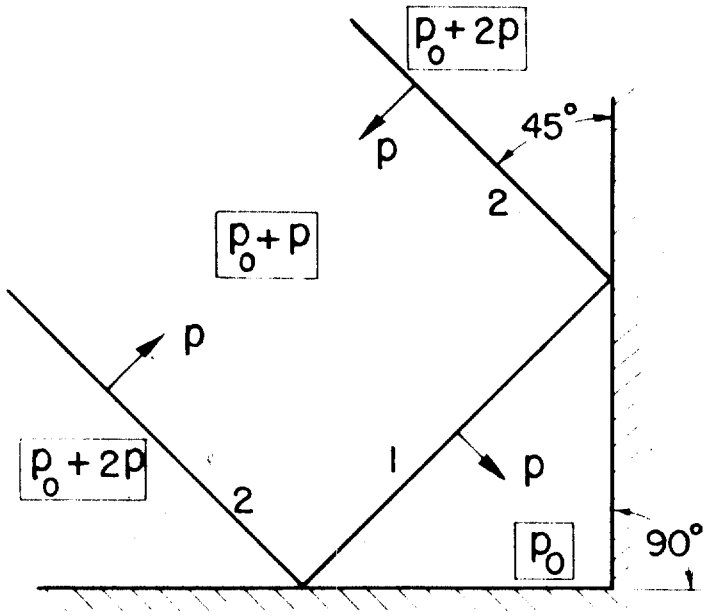
p_o+2p
p
45°
2
p_o+p
p
p_o+2p
2
1
p
p_o
90°

1a

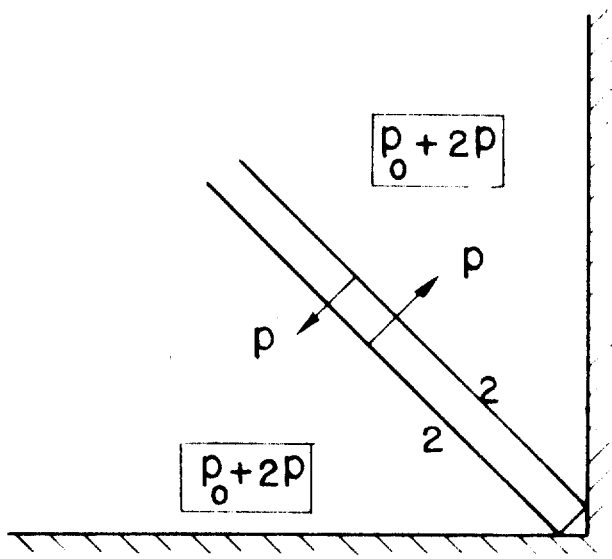
p_o+2p
p
p
2
2
p_o+2p

1b

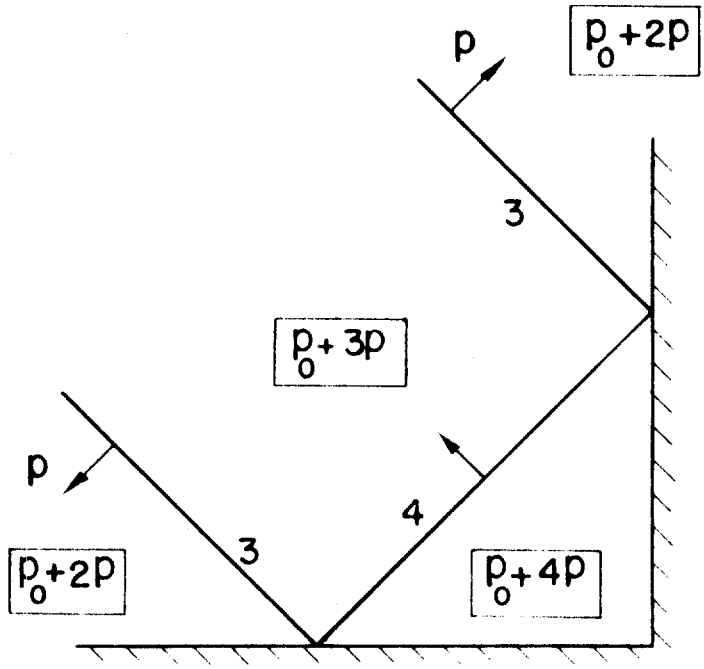
p
p_o+2p
3
p_o+3p
p
4
3
p_o+2p
p_o+4p

1c

hopeless to attempt to follow this effect into all its ramifications. On the other hand this is not absolutely necessary, since what is really needed, is an average statistical theory. Now these local reflection amplifications and the opposite diffraction shielding effects which necessarily accompany them in neighboring areas, are clearly all perturbations of the main blast phenomenon, caused by the irregularities represented by the target and other structures. Consequently what must be estimated is this: Which formations can be disregarded as local irregularities not materially affecting the main, average evolution of the blast wave?

We do not possess an exact theory of this phenomenon. There exist, however, good guiding analogies with acoustics and optics - that is, with linear wave theory. It is well-known (cf., e.g. Wood, Physical Optics) that irregularities with dimensions of less than 1/16 of a wave length leave reflection "perfect" from the "optical" point of view. Probably a good deal less than this, as much as 1/4 wave length, will not affect average intensities significantly, i.e. they are negligible in the sense outlined above. The linear dimensions of typical houses are of the order of 30 feet to 50 feet, they may conceivably go up to the order of 100 feet. Hence they are negligible for wave lengths of 120 feet to 200 feet or over, and even in extreme cases for wave lengths of 400 feet or over. In the case of a blast wave, a certain difficulty is caused by the absence of a well-defined wave length in combination with departures from linearity for higher shock strengths. It is clear, however, that Fourier analysis, as well as any other possibly preferable decomposition procedure, will have to assign to the length of the main blast the essential role of a wave length. This main part of the blast wave is the so-called positive phase of the blast. Hence, it is felt to be justified in treating houses as statistically irrelevant perturbations, if the positive phase has a spatial tension of at least 120 feet to 200 feet, or perhaps at least 400 feet. It is clear that

these arguments are loose and rather qualitative, but they probably do justice to the main features of the situation.

The length of the positive phase of the blast due to an explosion caused by W tons of TNT - or any other explosive of equivalent blast energy - varies slowly with the shock pressure level at which it is taken, and is proportional to $W^{1/3}$. In the significant region, which will turn out to be at 5 to 10 pounds per square inch, the duration of the positive phase is about 0.025 seconds for W = 1 ton.

The shock velocity in this range averages about 20 per cent higher than sound velocity, i.e. it is about 1.2 x 1100 feet per second = 1320 feet per second. Hence the length of the positive phase is 0.025 x 1320 feet = 33 feet. For a nuclear explosion, say 20×10^3 tons TNT blast equivalent this becomes $(20 \times 10^3)^{1/3} \times 33$ feet = 900 feet.

To sum up: For the nuclear explosions under consideration (and actually even for much smaller explosions) houses and other obstructions of comparable dimensions may be treated as small perturbations which do not appreciably affect the main evolution of the blast. For a later application it is useful to point out, that houses, quite apart from their established "small" size, are also a feeble overall influence because they cover only a small part of the ground. Even in "built-in areas" they hardly ever cover more than 25 per cent of the ground, and therefore, the progress of a blast wave along the ground takes place in the main over a smooth surface.

This being understood, the one obstruction which cannot be disregarded on these counts will now be considered since its dimensions are more properly described as infinite. This is the ground itself. In other words: In following the main evolution of the blast, the reflections and diffraction of a blast from everything else but the ground can be neglected, but its reflection from the ground must be taken into account. According to these principles,

the ground can be treated as a plane reflecting surface as long as its formation is plane from an average topographical point of view. (Focussing, shielding, and other gross effects of hills, valleys, etc. are well-known, but we do not propose to consider them here.) Also, since its density is 1,000 times that of the air, the transfer of energy through the air into the ground is negligible and it may therefore be treated as a rigid reflector.

There is a great deal of direct experimental evidence confirming these views (cf., e.g. data obtained at Woods Hole and Princeton on high burst).

Thus we have reached a standpoint where the reflection of the blast from the ground, idealized as a rigid, reflecting plane, is taken fully into account, and all target structures are then viewed as immersed into the average pressure field thus produced. Two situations (in two different explosions, at two different positions) for two targets will be viewed as equivalent, if the surrounding pressure fields obtained in this manner appear to be equivalent.

Thus far nothing has been said about the characteristics of a pressure field which determine damage. A static pressure, i.e. one which lasts forever, will damage a given structure in a given way, if it exceeds a certain minimum value p_∞, which is easily determined experimentally. A pressure which lasts only a shorter time, say t, will clearly have to exceed a higher minimum value p_t, in order to cause comparable effects. Clearly p_t will not differ significantly from p_∞, if t exceeds some time τ characteristic of the structure in question, being essentially the elastic half period of an elastic structure, or the time in which irreversible basic deformation occurs in the case of an inelastic structure. For ordinary houses, etc. this τ is of the order of 15 milliseconds.* For the 900-foot long nuclear explosion blast (cf. above), which therefore lasts about 3/4 second, this limit is clearly far exceeded.

In actual blasts p varies with time: $p = p(t)$. When the duration $\leq \tau$, experience shows that the significant damage criterion is the impulse $\int p\,dt$.

For a duration which is $\geq \tau$, the beginning of the peak pressure curve up to τ is in the main p(o), and it is known that the significant quantity from the point of view of damage is the peak pressure. Thus for nuclear explosions (cf. above), the damage criterion is the peak pressure viewed statically and the situation boils down to something fairly simple: reflection from the ground and then only the peak pressure to consider.

10.2 THE HEIGHT OF DETONATION AND A QUALITATIVE DISCUSSION OF THE MACH EFFECT

A bomb detonated on the ground is certainly closer to the target than an air burst. For an air burst bomb, the height of burst has no profound effect on the blast received at a point which is several times the height of burst from the bomb. At distances which are small or of the same order as the height of burst, the fact that the bomb is air burst has a profound effect on the blast characteristic. In the immediate neighborhood of a ground burst a target suffers extremely high pressures which it could not receive if the bomb were air burst. For big charges this is, however, not an advantage because it means that the immediate neighborhood would be destroyed more radically than is necessary, and the energy so wasted would not be available elsewhere. In other words, the immediate neighborhood would be overpulverized.

It is actually practice when using smaller bombs to try to make a full hit and detonate it exactly on the target. When using larger bombs, however, one does not try to make a full hit, but rather to wreck an entire area. In this case there is some point in trying not to detonate it on the ground, but at a certain altitude. In this way the area nearest the bomb is not overdestroyed, more energy is not used on it than is required, and the air burst does not permit nearby structures to shield those which are remote.

For nuclear bombs there is a further reason for detonation at an altitude.

It is not desirable to let the enormous temperatures (about 10^5 to 10^6 degrees) immediately around the explosion get in contact with matter in bulk, in particular with the ground. Such contact would allow the wastage of much energy in evaporating the earth.

An example of the loss of energy from the explosion by evaporation of matter in bulk can be found in the disappearance of the tower which carried the atomic bomb at Trinity. Figure 2 indicates the asymmetric shock-ball, as actually shown in several Fastax photographs of the explosion. It shows that the progress of the shock wave has been visibly retarded where it intersects the tower, presumably because of the loss of energy incurred in evaporating the steelwork.

There is a further advantage in air burst, a discussion of which constitutes the bulk of this report. An air burst is accompanied by certain forms of blast reflection which would not occur in the case of a surface burst.

As an orientation let us first consider the case of a bomb detonated on the ground. It might at first be thought that because the shock has a hemispherical shape and always touches the ground at right angles there would be no reflection from the ground. Actually, this is not true. If the ground were an absolutely rigid reflecting surface, then the energy normally transmitted to the lower hemisphere will not disappear but will be sent into the upper hemisphere in coincidence with the energy normally sent there in the absence of the ground. In other words, a bomb detonated on the ground is equivalent to two bombs insofar as the blast in the region above the ground is concerned. Now twice the charge weight means, if one considers peak pressure, that all pressures are the same for the ground burst charge as for the same charge burst in free air if all distances from the charges are in the ratio of the similarity[1] factor $2^{1/3}$.

---

(1) The similarity factor comes from the fundamental hydrodynamical equations in which the distance, R, always occurs in the combination $R/W^{1/3}$ with the blast energy W; i.e. the unit of length is determined by the blast tonnage. The time scale is similarly extended.

Figure 2

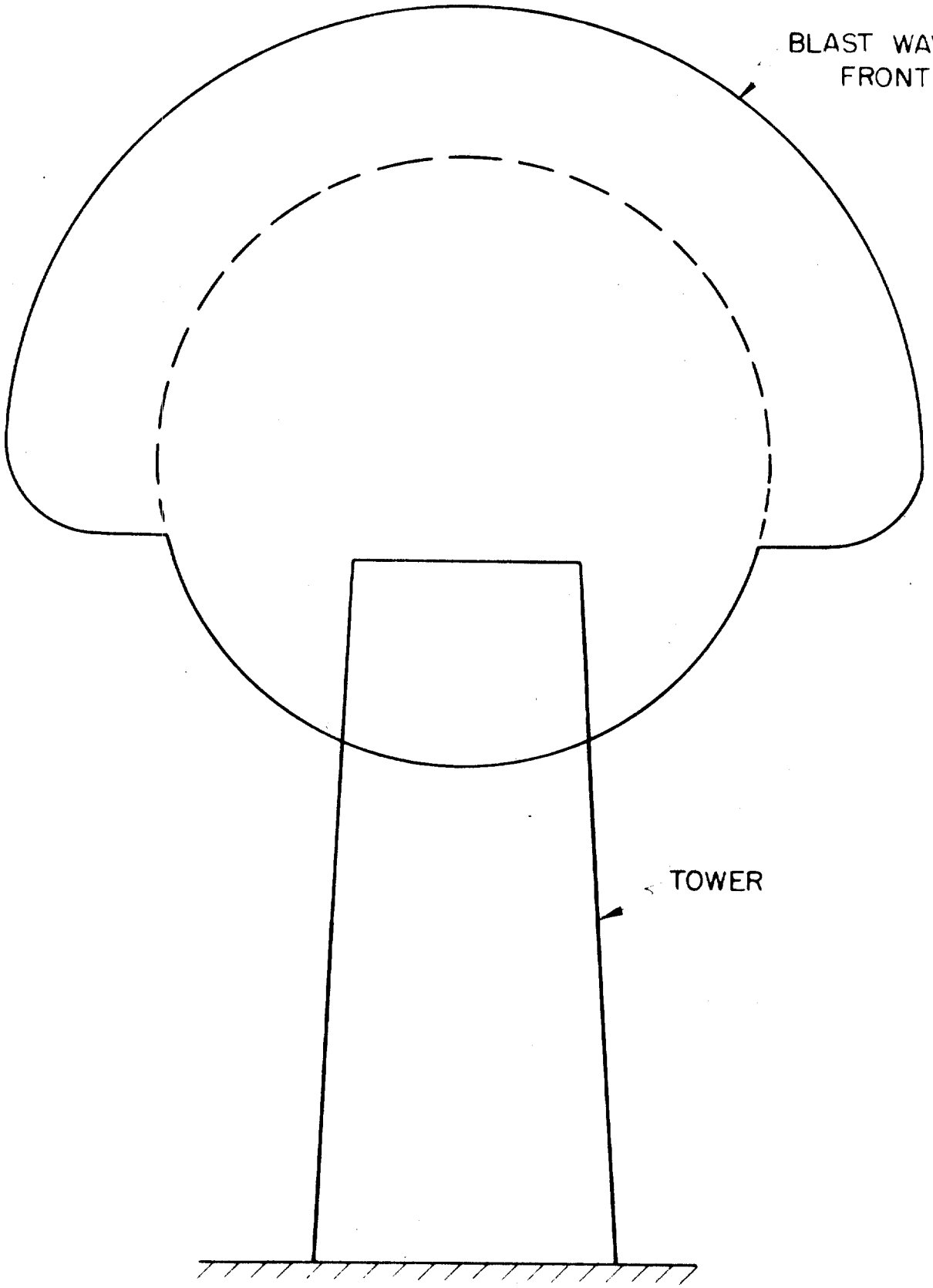

Comparing pressures at the same point, in the region in which pressure decreases as $1/R$ or $1/R^{3/2}$ (R = distance from the bomb) peak pressures are obtained in the presence of the ground which are $2^{1/3}$ to $2^{1/2}$ higher because of reflection. The $1/R$ law holds roughly at large distances, i.e. low pressures, but the variation is like $1/R^{3/2}$ in the region of interest, at 5 to 10 pounds per square inch.

It is clear that one would not get the indicated pressure increase if there were cratering because cratering means that some energy does go into the lower hemisphere. In other words: If the bomb is burst on the ground the peak pressure is increased to anything from 1.26, ($2^{1/3}$) to 1.41, ($2^{1/2}$) times its original value provided that no cratering occurs, and less than this if there is cratering.

Let us now consider the effects of air burst, at distances which are great compared to the height of burst. It is common sense to expect that at such distances this height itself, and all phenomena caused by it, ought to have a small influence, and as the distance increases become entirely negligible. Hence one should expect, that for air burst at distances which are very large compared to the height of burst (as for ground burst at all distances) the pressure is amplified by 1.41 at most if there is no cratering and by appropriately less if there is.

Now one must observe that this picture is in disagreement with the acoustic theory. This is of importance since the above picture is plausible and will turn out to be the correct one.

10.2-1 Acoustic Picture of Air Burst

We will now describe the action of an air burst charge in the acoustic approximation.

Independently of this approximation, the shock which emerges from the bomb bursting above the ground, will be spherical and remain so until it makes contact with the ground. Indeed, up to that time it is effectively in free space and

behaves accordingly.

When the shock sphere hits the ground, it produces a reflected shock. In the acoustic approximation this reflected shock is a part of another, which is congruent to the first one, and behaves as if it were the blast wave coming from a "virtual bomb", which is situated at the image point of the real bomb, reflected with respect to the ground (Figure 3). When the shock first hits the ground, it does so at normal incidence, and hence, by acoustic theory doubles the overpressure, i.e. the pressure increases over atmosphere in this region. Even later, when the shock sphere intersects the ground at oblique angles, the laws of acoustics also call for a doubling of overpressure or pressure increase above atmosphere in the twice shocked region at the reflecting surface (Figures 4 and 5). In other words: At all angles $\alpha \geq 0°, < 90°$, the reflected overpressure is independently of α equal to 2p (p = the incident overpressure). For $\alpha = 90°$ the incidence is glancing and no reflection in the sense of acoustics occurs (cf. however, the discussion of ground burst above; cf. also the non-acoustic discussion of nearly glancing incidence in the succeeding pages).

Let us now try to give a complete chronological account of the sequence of events as the blast wave expands, gets reflected, etc. Figure 6 shows the appearance, in the acoustic approximation, of the blast pattern as it travels outward from the air burst bomb.

The essential features of the reflection phenomenon are:

(1) Incident and reflected waves make equal angles with the ground.

(2) The pressure increases in the incident and reflected waves are equal.

(3) The total pressure increases exerted by the blast at any point on the surface is twice the pressure increase to be expected at the same distance in the absence of the ground.

Figure 3

——— Real blast wave
– – – -Spherical continuation of real blast waves

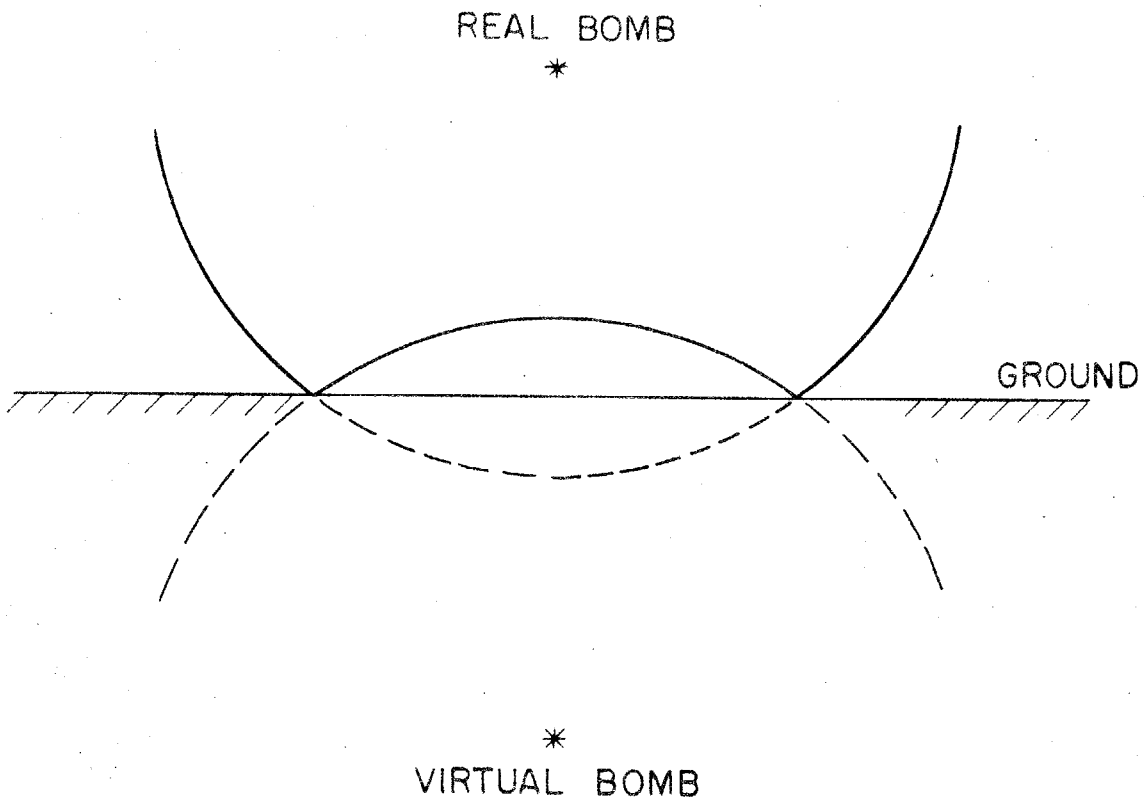

APPROVED FOR PUBLIC RELEASE

Figure 4

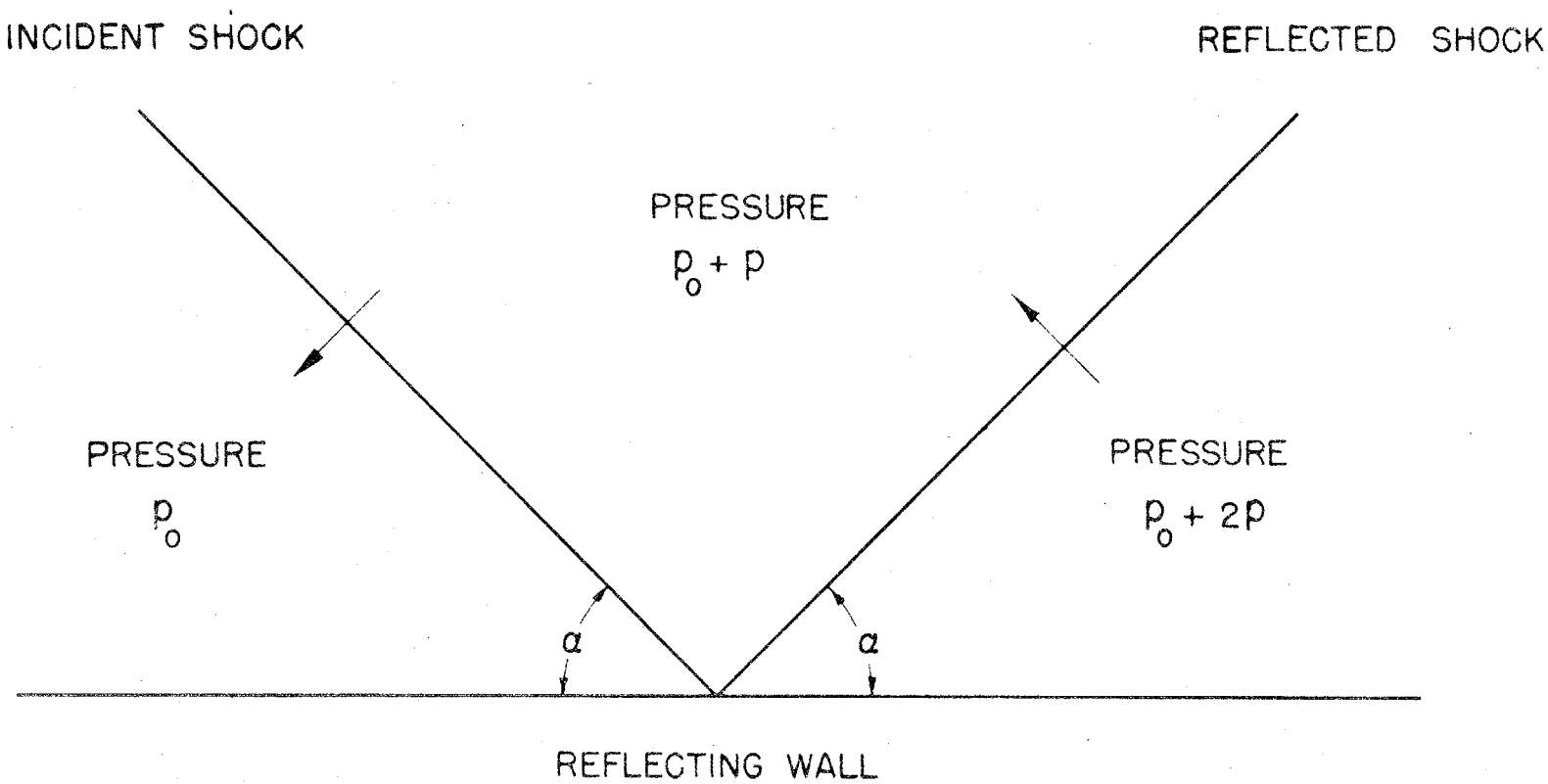

Figure 5

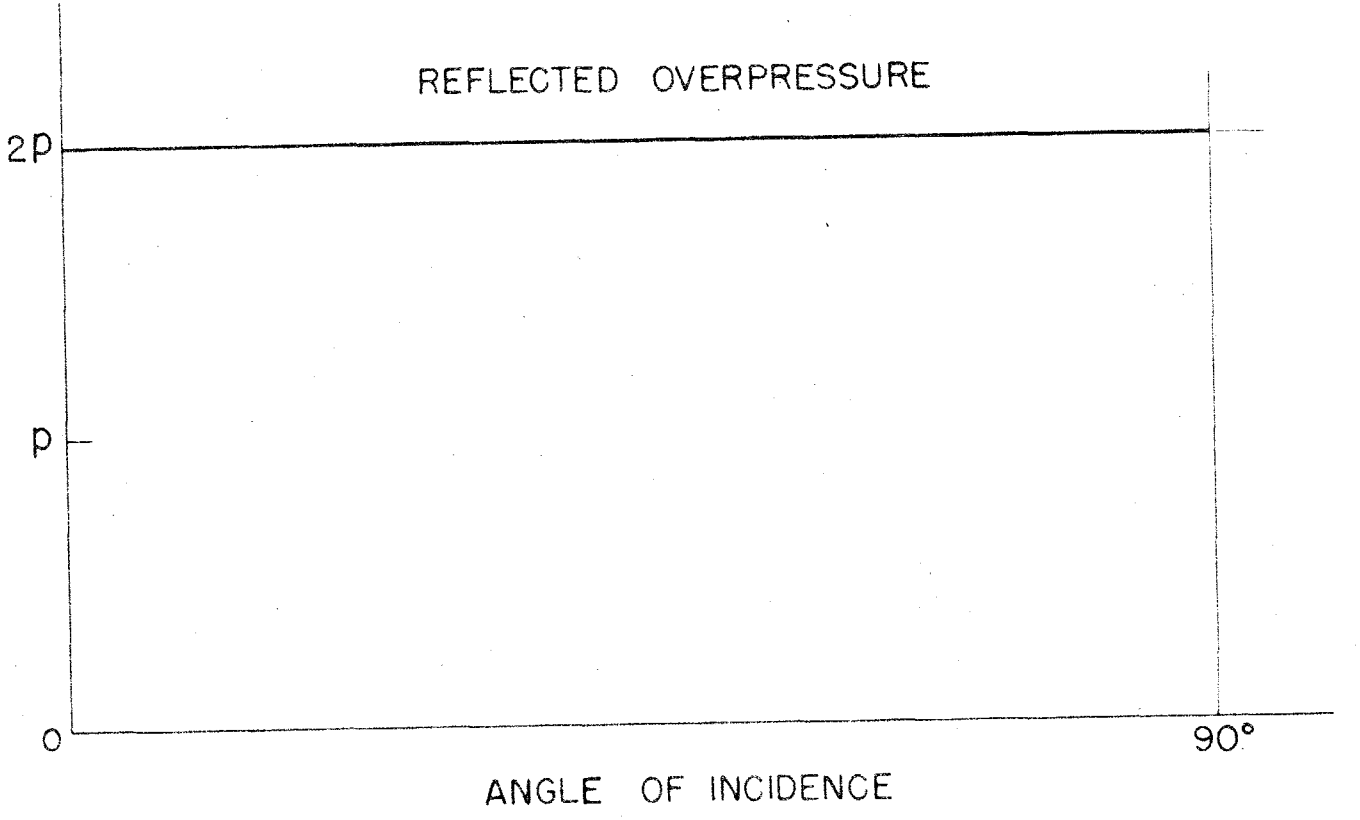

Figure 6

Reflection of a blast wave in the acoustic limit

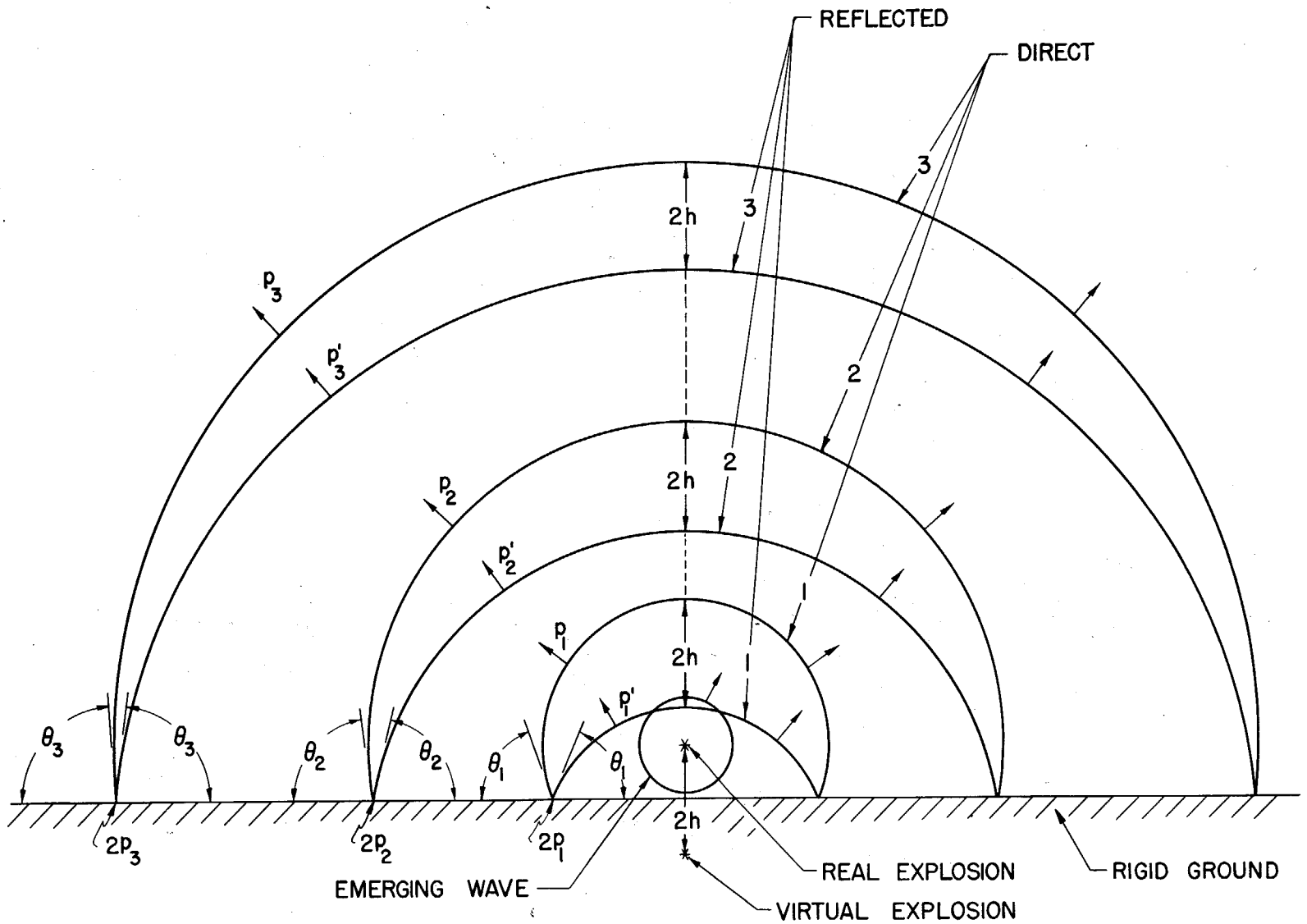

APPROVED FOR PUBLIC RELEASE

(4) The incident and reflected waves have a constant separation, equal to 2h; i.e. twice the height of burst at the zenith. At an angle φ from the zenith the separation is smaller; it tends to 2h cos φ as the wave expands out from the bomb (real and virtual). For $\varphi = 90^\circ$; i.e. on the ground, the separation is of course 0, since the incident and reflected waves are necessarily in contact there. Correspondingly, the separation tends to 0 as $\varphi \longrightarrow 90^\circ$; i.e. as the ground is being approached.

(5) As the wave expands, θ, the angle of incidence (and reflection) starts at 0° and approaches 90° in the limit of large distances.

Figures 7 to 10 indicate the p, t dependence (overpressure versus time dependence) at selected positions in the blast pattern: Figure 7 shows the single rise to 2p everywhere on the ground; Figures 8a, b and c, the double rise to p and to p + p' at a fixed height above the ground for increasing projected distances from the bomb; Figures 9a, b and c, the corresponding double rise at a fixed zenith angle and increasing distances from the bomb; Figure 10, the double rise anywhere at the zenith. p is the free air overpressure at the point under consideration; p' is the additional reflected blast overpressure which is describable as originating from the "virtual bomb" - since any point above the ground is closer to the real than the "virtual bomb" p>p', but this difference tends to zero (even relatively to p) as the distance from the bomb increases.

In Figures 8a, b and c, the time interval $\triangle$ t between the two shock (pressure rises) tends to zero. In Figures 9a, b and c, $\triangle$t tends to $\frac{2 \cos \varphi \cdot h}{C}$ where C is the velocity of sound. In Figure 10 $\triangle$t is $\frac{2h}{C}$.

All these sketches are strictly valid for shocks with overpressures of infinite duration only (Figure 11a). Actually a decay of the overpressure occurs behind the shock because of the finite duration of the explosion (Figure 11b). Consequently Figure 7 is changed in the manner indicated in Figure 12, and

Figure 7

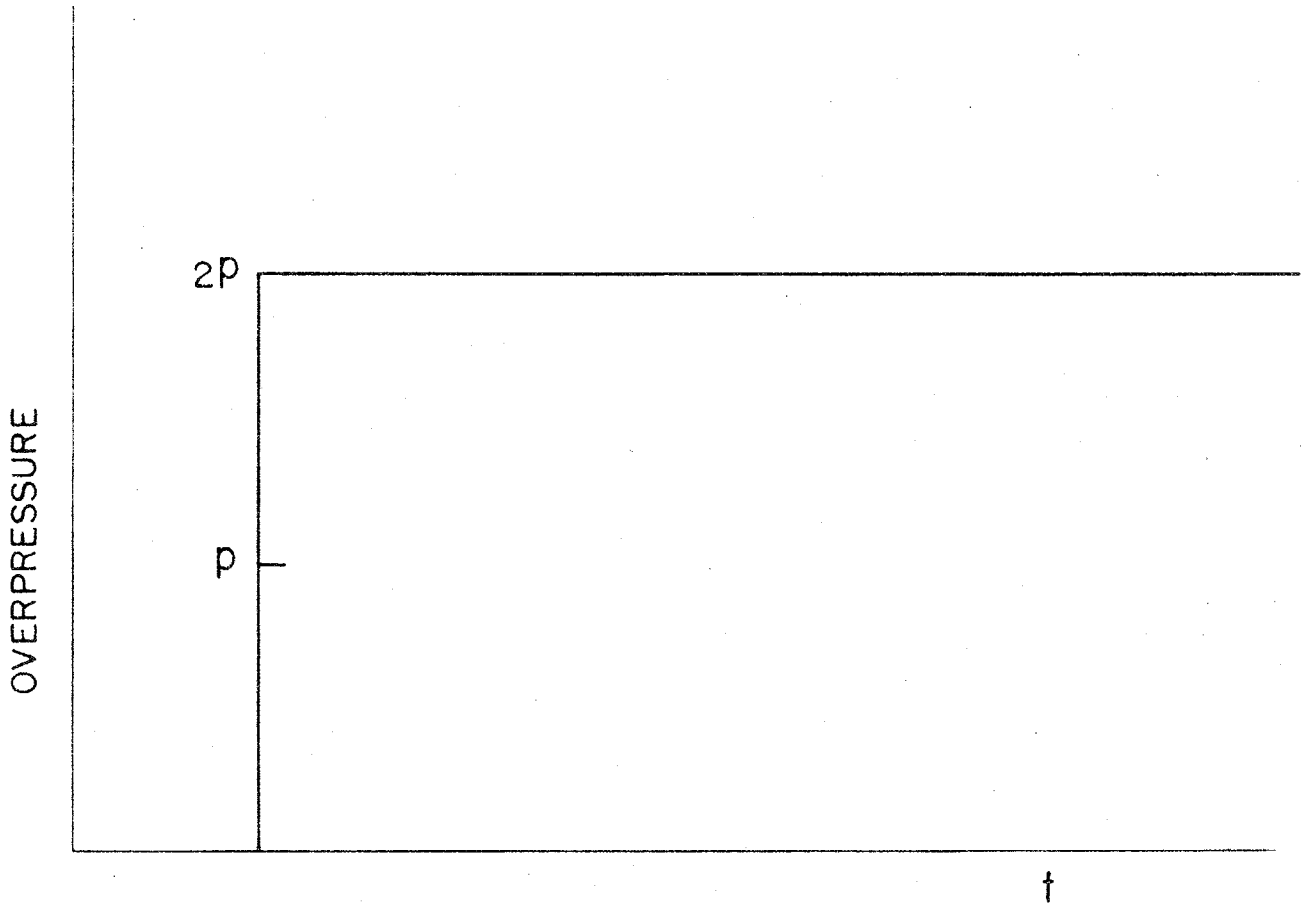

Figure 8
a,b,c

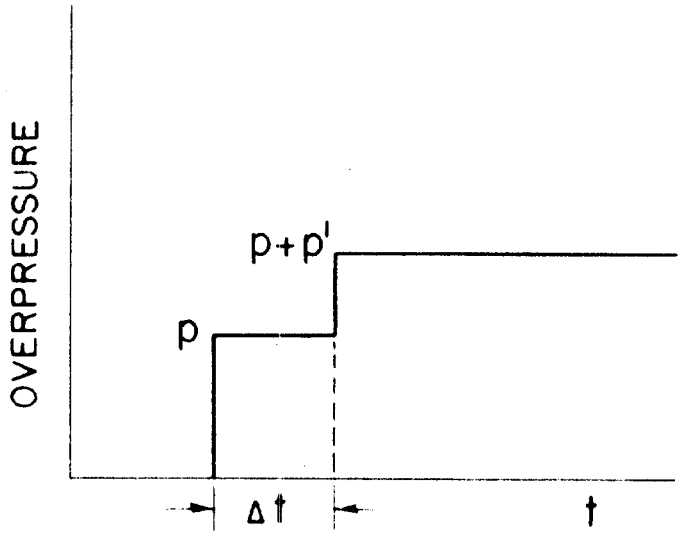
OVERPRESSURE
p+p'
p
Δt
t

8a

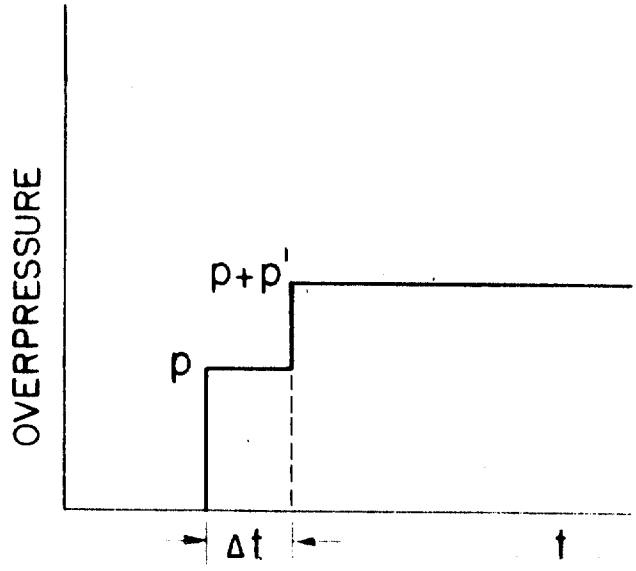
OVERPRESSURE
p+p'
p
Δt
t

8b

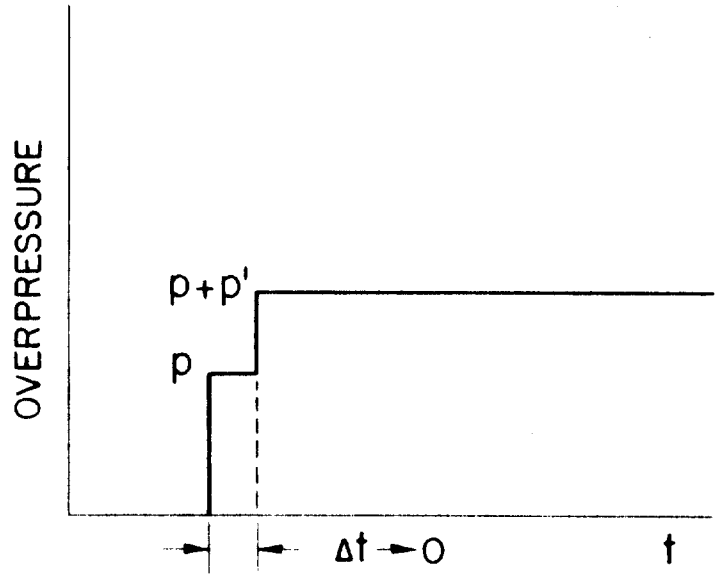
OVERPRESSURE
p+p'
p
Δt→0
t

8c

Figure 9
a,b,c

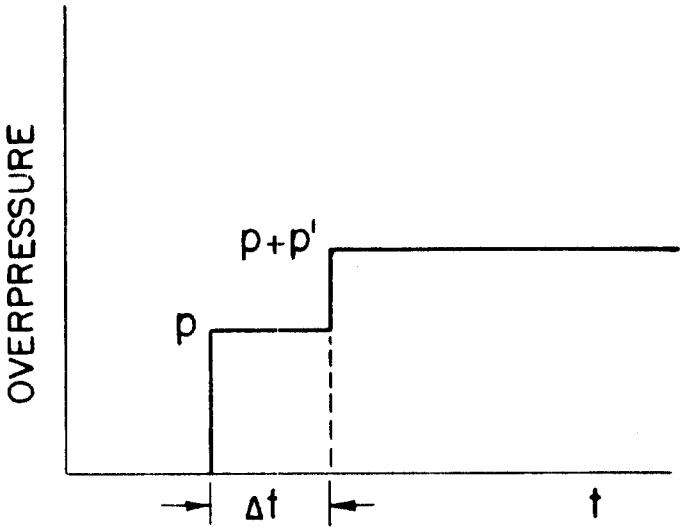
OVERPRESSURE
p+p'
p
Δt
t

9a

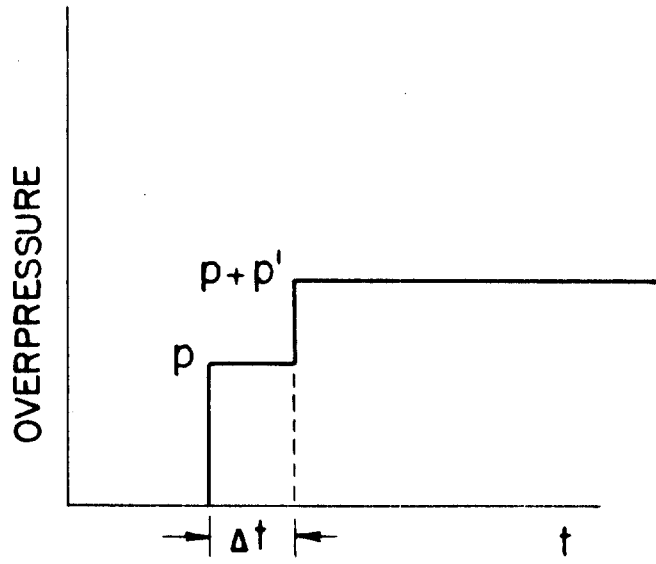
OVERPRESSURE
p+p'
p
Δt
t

9b

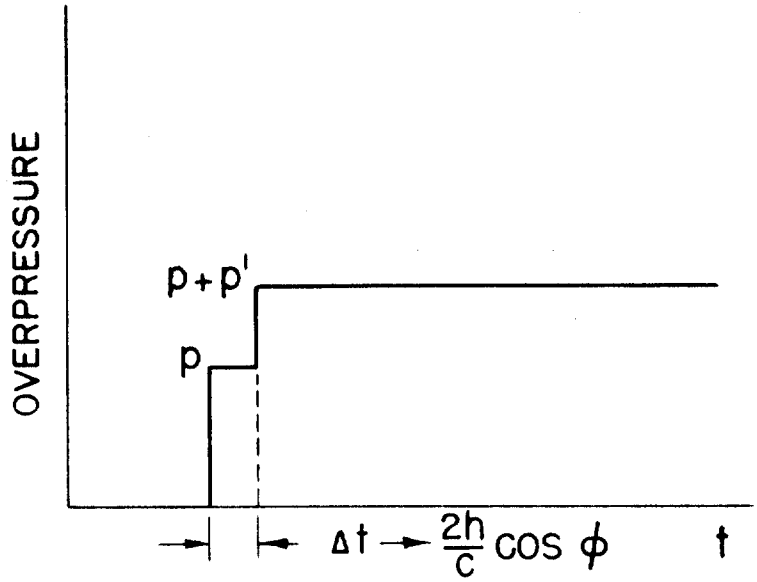
OVERPRESSURE
p+p'
p
Δt → 2h/c cos φ
t

9c

Figure 10

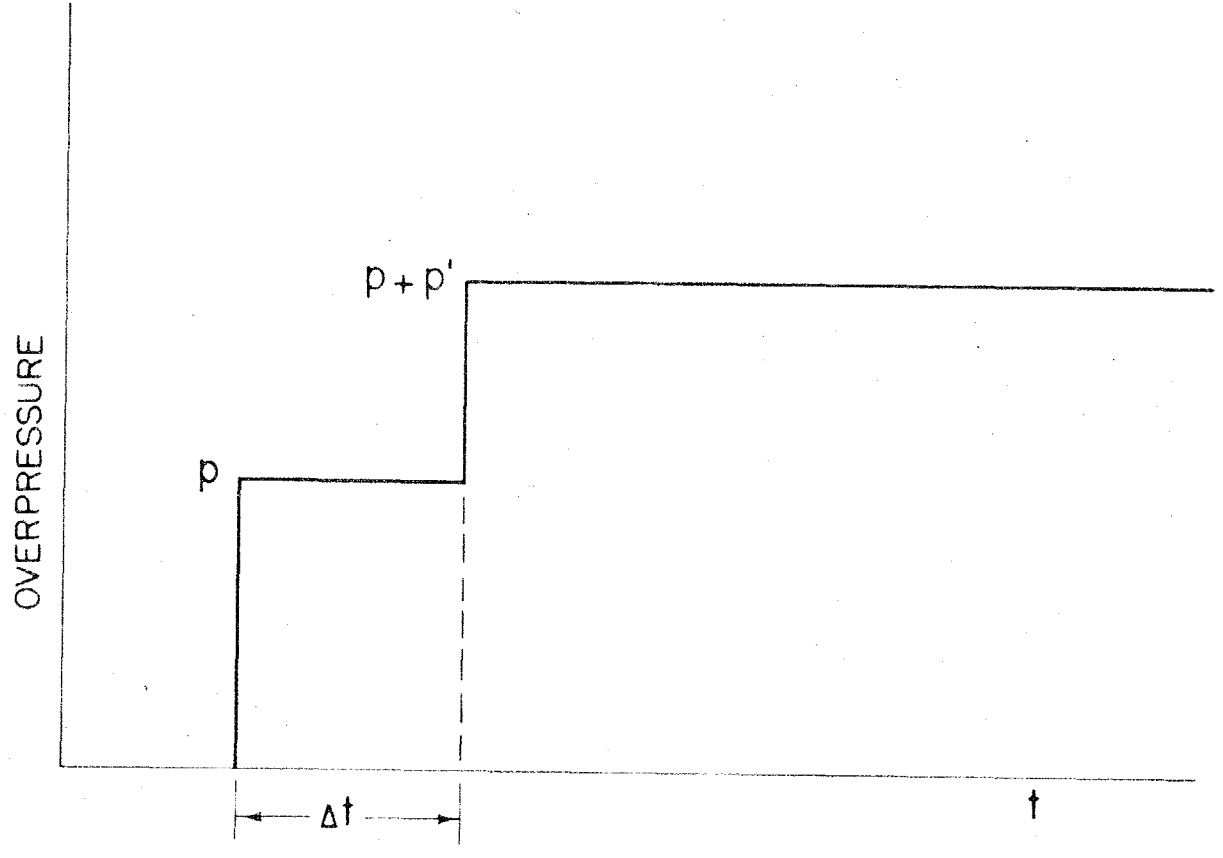

Figure 11
a,b

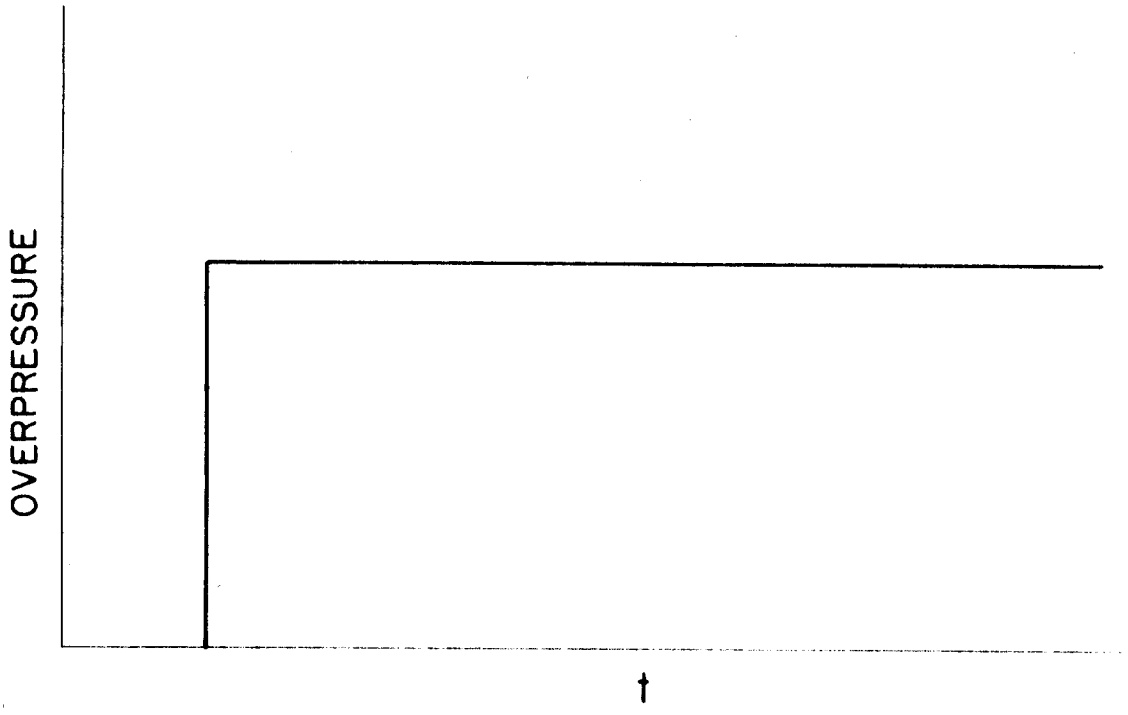

11a

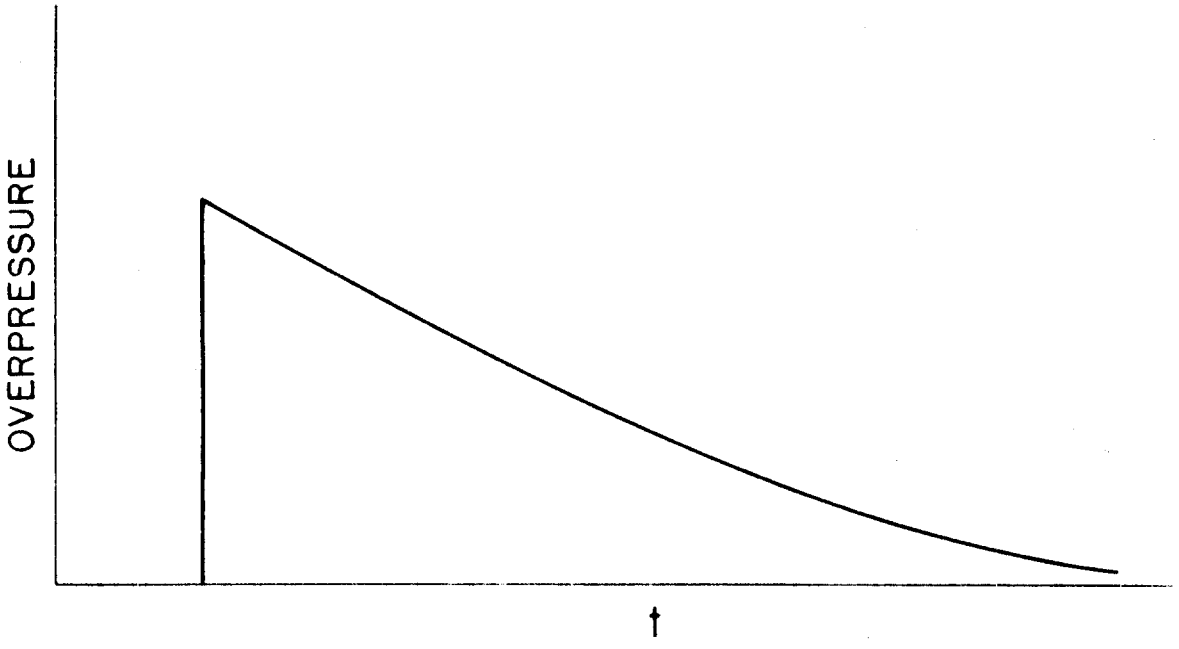

11 b

Figure 12

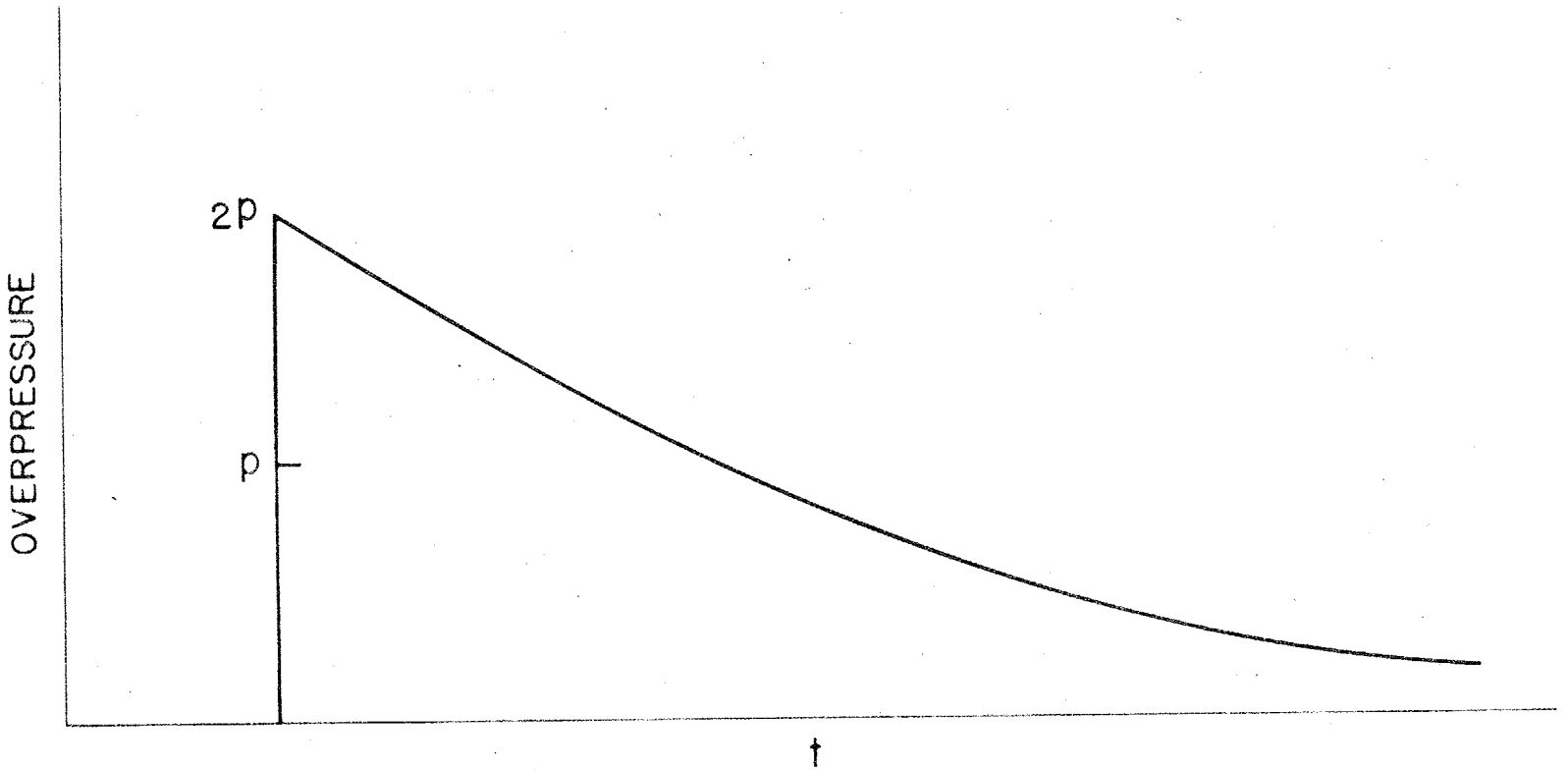

Figures 8 to 10 are affected as shown in Figure 13.

The situation depicted in Figure 13 is of sufficient importance, as a consequence of the finite duration of the shock overpressure, to deserve one more comment. Depending on the height of burst it is quite possible that no amplification of the original (free space) pressure by the reflected shock occurs everywhere.

The drop shown in Figure 13 between the pressure rises p and p' may well exceed the second pressure rise p'. However, at or near the reflecting surface, because of the (exactly or approximately) simultaneous arrival of the two shocks in that region, amplification must certainly occur.

10.2-2 Criticism of Acoustic Picture - Formation of a Mach Stem

Certain parts of the above acoustic description of the blast pattern from a charge burst above a rigid ground are in disagreement, first of all with our intuition and, secondly, with the facts.

As to the first point, we have already spoken of replacing the source, wall system by a real and virtual source - an explosive dipole. Now one would expect that from large distances, such an explosive dipole having the combined mass would look like a single charge. This conclusion is analogous to the result in electrostatics, according to which the field produced by two equal electric charges of the same sign is essentially the field of the total charge when the distance to the point of observation is great compared with the separation between the charges. As to the second point, in reality for shocks of finite strength, the situation is like the one expected intuitively in the preceding section, for the following reason. The permanent separation of the original and the reflected shocks in acoustic theory (cf. above) is clearly due to their having the same velocity; i.e. sound velocity. Actually shocks of finite strength are faster than sound. Furthermore, the reflected shock is faster than the original one because it travels through air heated by the former, and hence,

Figure 13

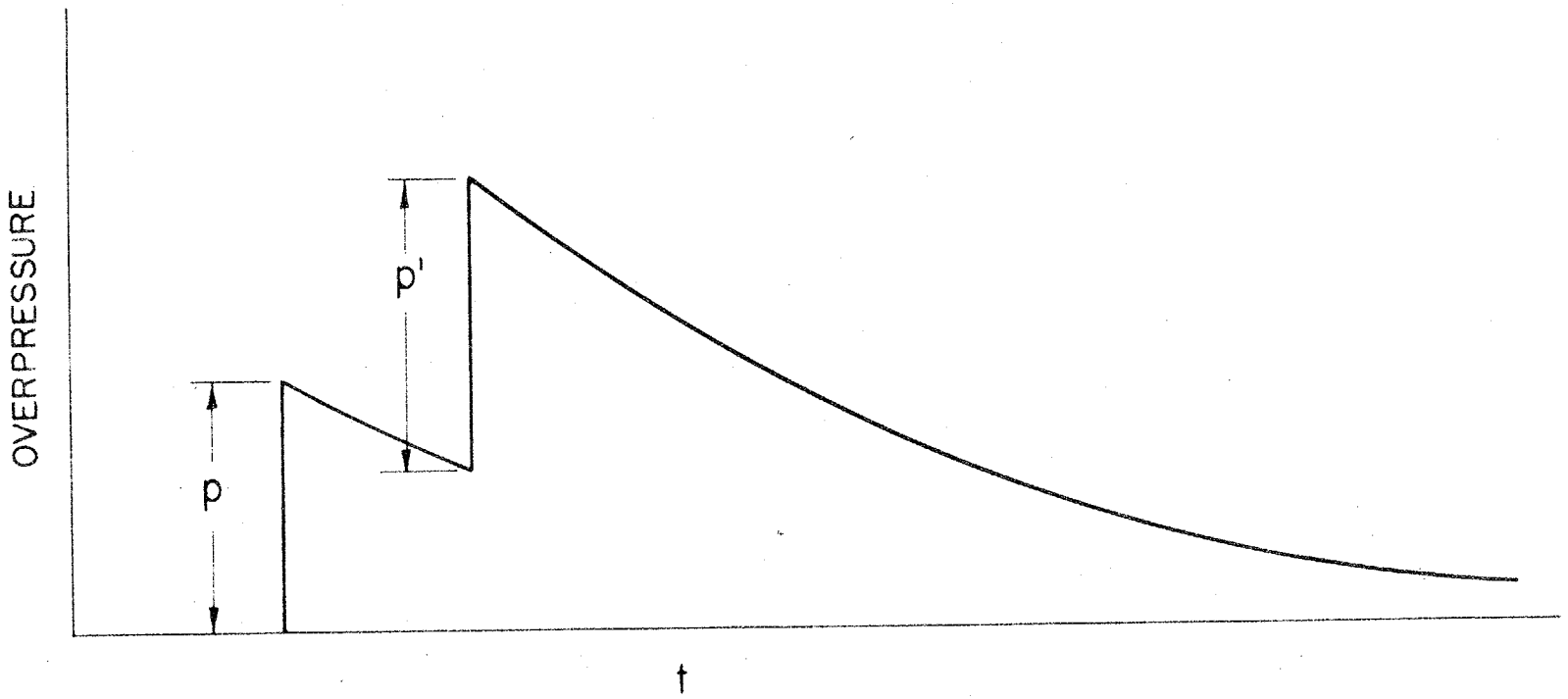

has its speed increased relative to it. In fact, we know from hydrodynamics (cf. Section 10.3) that if one shock follows another, and is in the region of positive overpressures behind that shock, i.e. in the positive phase, then it travels faster than the first shock. Consequently, while acoustically the reflected shock is not able to catch up with the incident shock, if the shock has a finite size it will in reality catch up in regions where the positive phases overlap. Since the two shocks are close together near the ground and in contact at the ground, the positive phases certainly overlap in this region. The reflected shock is therefore faster than the direct shock and since they are getting more and more parallel as time goes on, a merger should sooner or later take place here.

We know in fact from the theory of oblique reflection and from experiment that the above is the case and that the overpressure at the fusion shock is about twice that at either of the two original shocks. As the spherical shock expands conditions become suitable for fusion further and further from the ground. Consequently, the fused portion gradually rises and covers more and more of the shock sphere and it is possible to show that eventually the merger is complete and the two shocks are finally everywhere fused and form a single shock front. In other words, the shock due to the virtual bomb will have everywhere overtaken the shock of the true bomb; the two shocks will have merged over the sphere[2] which corresponds to the double charge. Figures 14 and 15 show the appearance for a wave of finite amplitude, of the blast pattern as it travels outward from the air burst bomb. The essential features of the

---

(2) If the charge is burst at such a height that the merger occurs at great altitude, say 30,000 feet, because of the variation in density of the pre-shocked air neither the original nor the fused shocked front will be spherical. (See Chapter on Altitude Effect.) Since we are here primarily concerned with the merger near the ground we will not discuss this point.

Figure 14

Reflection of a spherical blast wave of finite amplitude

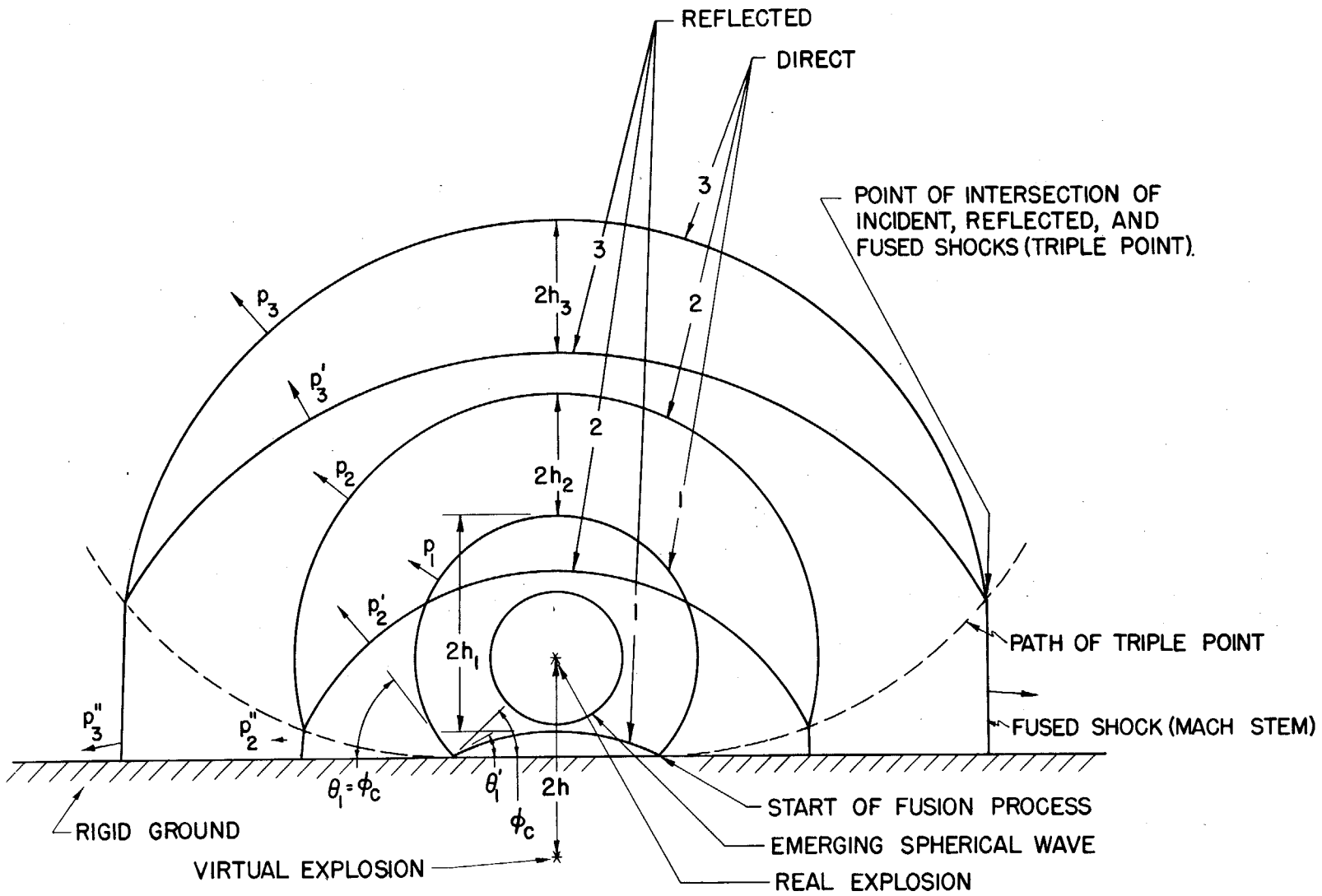

APPROVED FOR PUBLIC RELEASE

Figure 15

Growth of Mach stem

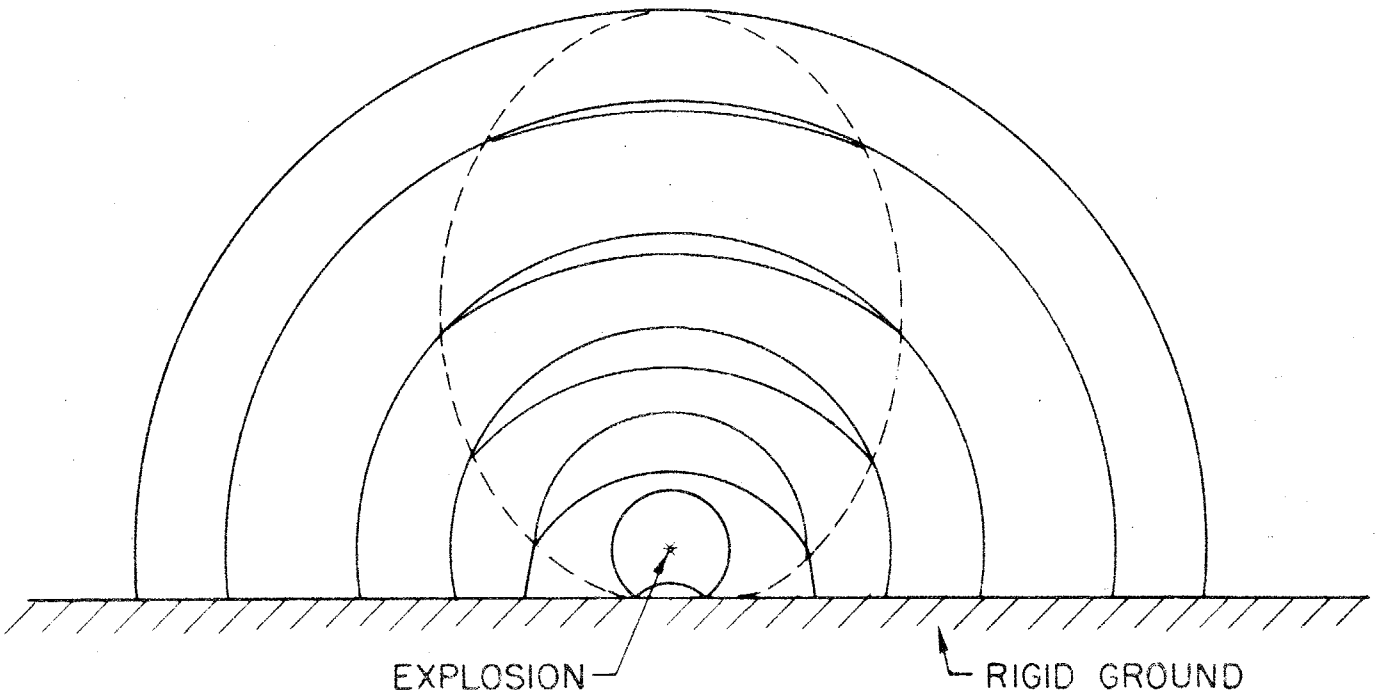

APPROVED FOR PUBLIC RELEASE

reflection phenomenon are:

(1) Incident and reflected waves do not intersect on the ground for all angles of incidence greater than a critical angle φ_c. When incident and reflected waves intersect on the ground they do not make equal angles with the ground.

(2) The overpressure in the incident and reflected waves are unequal.

(3) The total overpressure exerted by the blast at any point on the surface varies with the height of burst, the projected distance from the bomb, and the blast energy released by the bomb. It is not obtained as in the acoustic approximation, by multiplying the free air pressure at the point in question by a factor of two.

(4) The incident and reflected waves have a separation at the zenith which, as the waves expand, at first varies little from the value 2h and then decreases to zero as the fusion process proceeds. At an angle from the zenith the separation in the early stages of the expansion is smaller and becomes zero as the two waves fuse, forming the Mach stem.

At distances which are large compared to the height of burst, the direct and reflected waves from an air burst bomb have fused and proceed outward as a single shock. From complete fusion on, the shock wave appears to have come from double the charge detonated on the ground.

(5) As the wave expands, θ, the angle of incidence starts at 0° and the stem becomes perpendicular to the ground in the limit of large distances.

Figures 16 and 17 indicate the p, t, dependence (overpressure versus time dependence) at selected positions in the blast pattern. Figure 16a shows the

Figure 16, a,b,c,

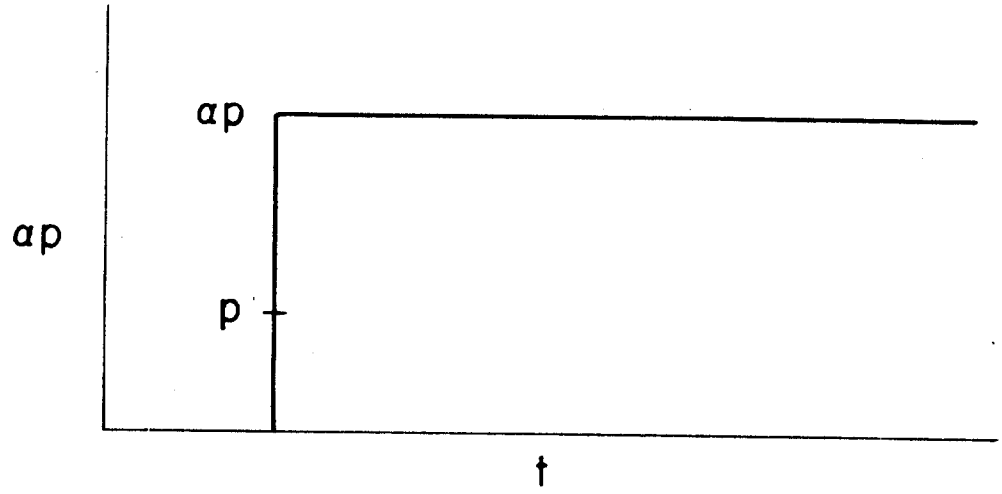

16a

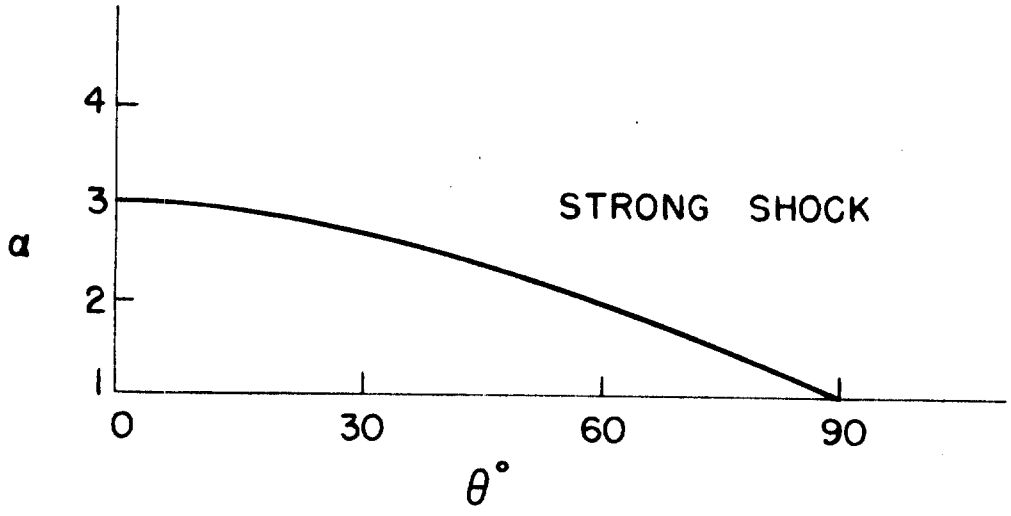

16b

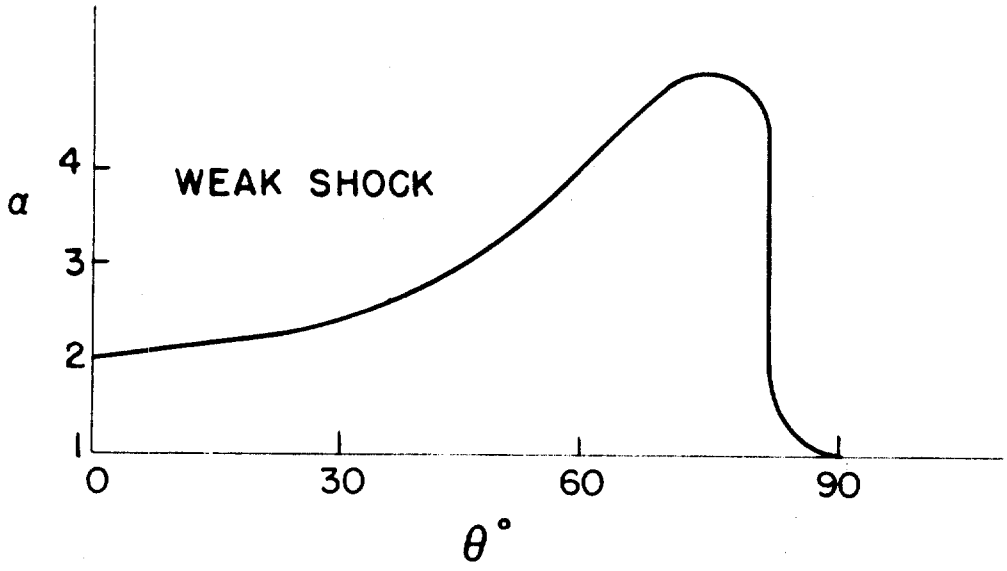

16c

Figure 17 a,b,c

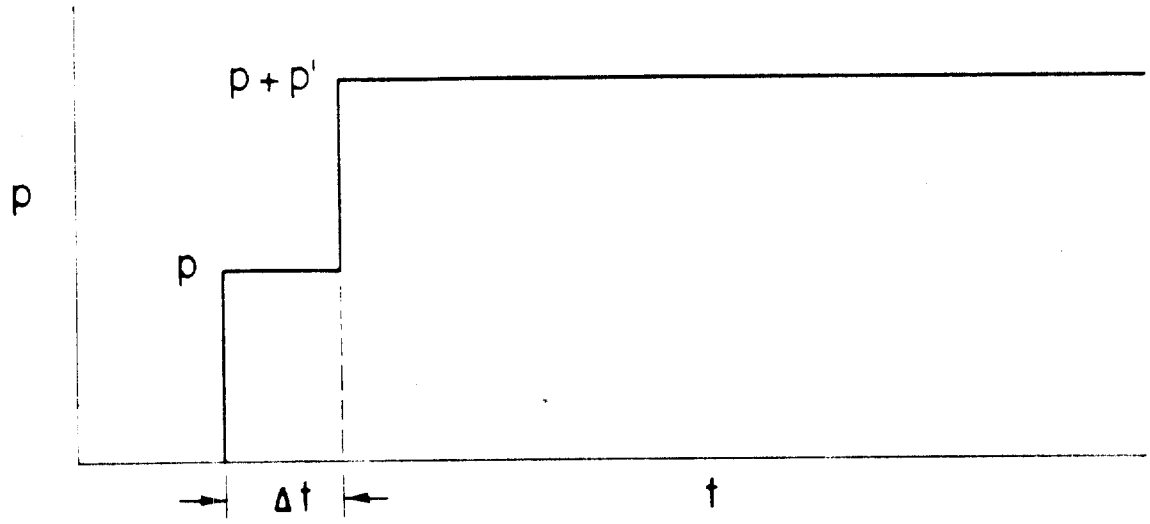

17a

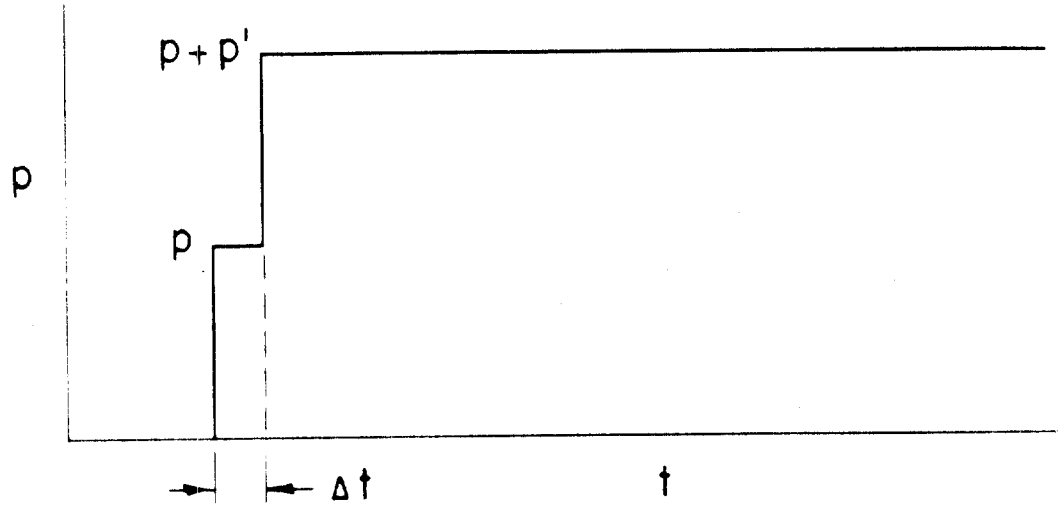

17 b

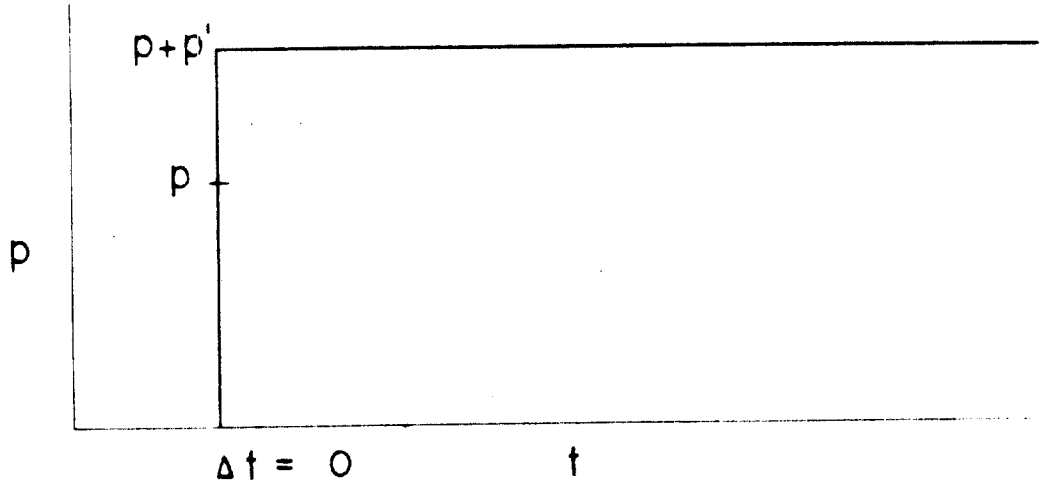

17 c

single rise to α p everywhere on the ground. Figures 16b, c, show the dependence of α on the angle of incidence for strong and weak shocks respectively. Figures 17a, b, and c show the double rise to p and then to p + p' at a fixed height above the ground for increasing projected distances from the bomb. Figure 17a, b, and c also apply to the corresponding double rise at a fixed zenith angle and increasing distances from the bomb. All these sketches are valid only for shocks of infinite duration. If the pressure has a finite duration, Figures 16 and 17 should be modified in a manner similar to the modifications (Figures 11 to 13) of Figures 7 to 10.

10.2-3 Oblique Reflection - Deviation from Acoustic Behavior

A detailed theoretical discussion of the shock wave pattern produced by the reflection of an expanding spherical shock wave from a rigid plane surface must start with a description of what happens exactly on the ground where the incident and reflected shocks always intersect each other, and where the reflected shock was originally produced. It will be recalled that according to the acoustic theory a reflection always produces the same increase in overpressure as the incident shock.

This result is independent of the angle of incidence up to, but not including 90°, at which it ceases to be valid. If the shock is of finite strength, there will be deviations from the acoustic result. Since the acoustic behavior is discontinuous at 90°, one would expect deviations from acousticity to set in earlier than 90° for the true shock must exhibit some kind of continuous behavior in the neighborhood of 90°. There are, then, two factors which perturb the acoustic behavior: the finite strength of the shock and the obliquity, especially in the neighborhood of 90°.

10.2-4 Head-on Collision

Let us first consider the true behavior of a finite shock for a head-on reflection. (See Section 10.3 for detailed calculations.) The result is usually stated as follows: A shock which hits on absolutely rigid wall will be strengthened more than the acoustic theory predicts. The acoustic theory

predicts a doubling of overpressure at the rigid wall. This is an incomplete description because there are two different ways to measure the strength of a shock. One measure is the absolute overpressure in the shock; i.e., the difference in pressure immediately before and immediately behind the shock front. The other measure of shock strength is given by the relative overpressure; i.e., the ratios of the pressures immediately before and behind the shock front minus 1. Now, in the limit of small overpressures, it does not matter which criterion is adopted because the reflected shock is equal in strength to the incident shock if measured either by the pressure difference or by the pressure ratio minus 1. For finite shocks, however, the reflected shock is stronger than the incident shock if measured by the pressure difference and weaker if measured by the pressure ratio minus 1.

The clearest example of this is the case of a very strong shock. Here it is well-known (cf. Section 10.3) that for air the reflected shock has an overpressure eight times greater than the original one. On a relative scale although the reflected pressure is eight times as great as the incident pressure, the incident pressure is very great compared with the initial pressure of the unshocked air and therefore the strength of the reflected shock as determined by the second criterion is very much less than the strength of the incident shock. To summarize, the absolute overpressure is greater and the relative overpressure is smaller. We will measure the shock strength by the absolute overpressure and on this basis the reflected shock is stronger than the incident shock.

10.2-5 Simple Oblique Reflection

In the acoustic limit the incident and reflected shocks form a stable configuration regardless of the angle of incidence regardless of the shock strength. Since the two shocks have the same velocity component parallel to the ground as their point of intersection, O, the angles of incidence and

reflection will also be equal. This is, of course, just the application of Snell's principle in a very simple case (Figure 18).

Let us now consider the case of a finite shock, where the reflected and incident shocks may be of unequal strengths and hence have unequal velocities relative to the air and ground. If the intersection of the two shocks is to remain on the ground this difference of velocities requires that the reflected and incident shocks make unequal angles with the ground. If we set up the equations of motion (cf. Section 10.3) we find that there are as many equations as there are variables and, in general, there are solutions.

We must qualify this last statement. In the first place, when there exists a solution, there exists, in general, another one as well. Thus there are two solutions; i.e., given an incident shock the reflected shock can be in two positions, one less and one more inclined to the surface (Figure 19). The reflected shock which is steeper, turns out to be faster. This is easy to see both qualitatively and mathematically. One, therefore, has to ask which of these two shocks exists in reality. It is relatively easy to see that under these conditions it is the less strong shock which exists because if we continue to decrease the strength of the incident shock and go over to the acoustic case we find that the less steep shock goes over asymptotically to the same strength as the incident shock at the same angle, whereas the steeper shock goes over into a finite non-acoustic shock and becomes vertical; i.e., as p incident $\longrightarrow 0$, $\theta_3 \longrightarrow \theta_1$, $\theta_2 \longrightarrow \frac{\pi}{2}$. Now since this latter does not happen, and is energetically impossible without an external source of energy, we assume at least in the case of a weak shock that it is the less steep, weak solution which exists. One might assume by continuity, although this argument is not quite safe, that the strong reflected shock is forbidden for all incident shock strengths. The experimental observations of all who have worked on this subject, in particular the very detailed observations of L. G. Smith, support this

Figure 18

$\theta_1 = \theta_2$ acoustic case
$\theta_1 \neq \theta_2$ non-acoustic case

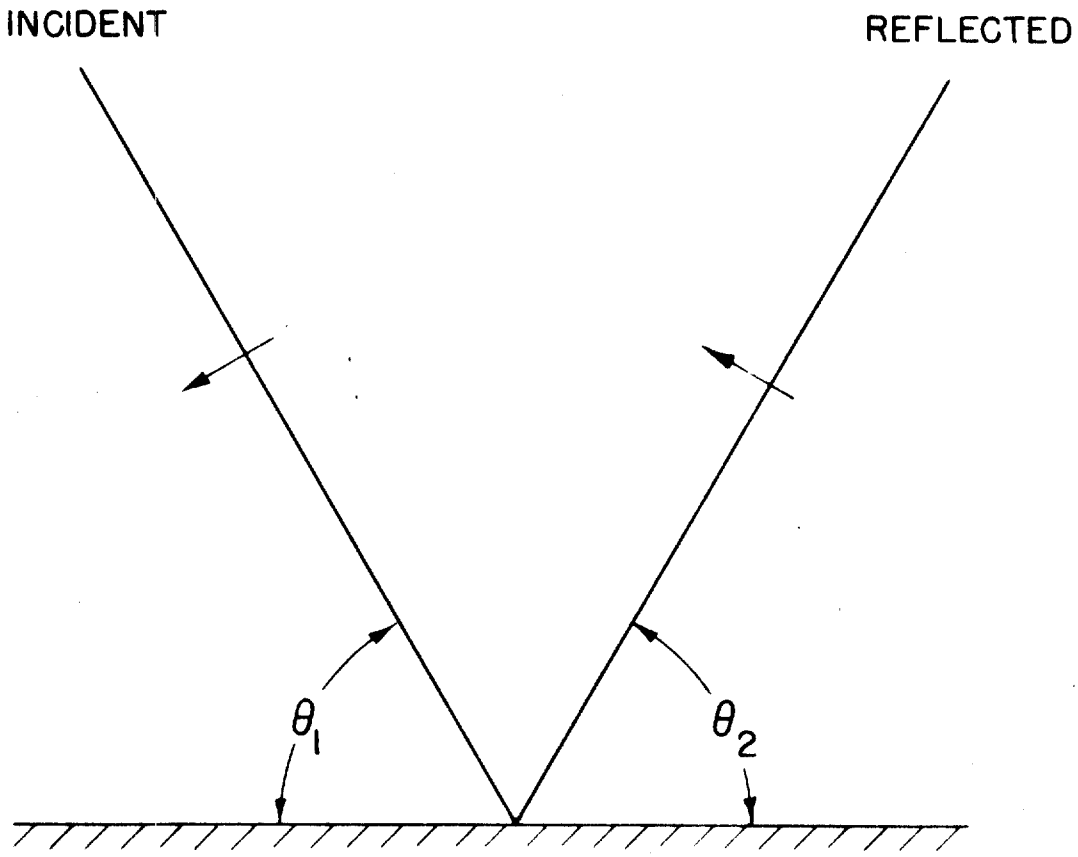

Figure 19

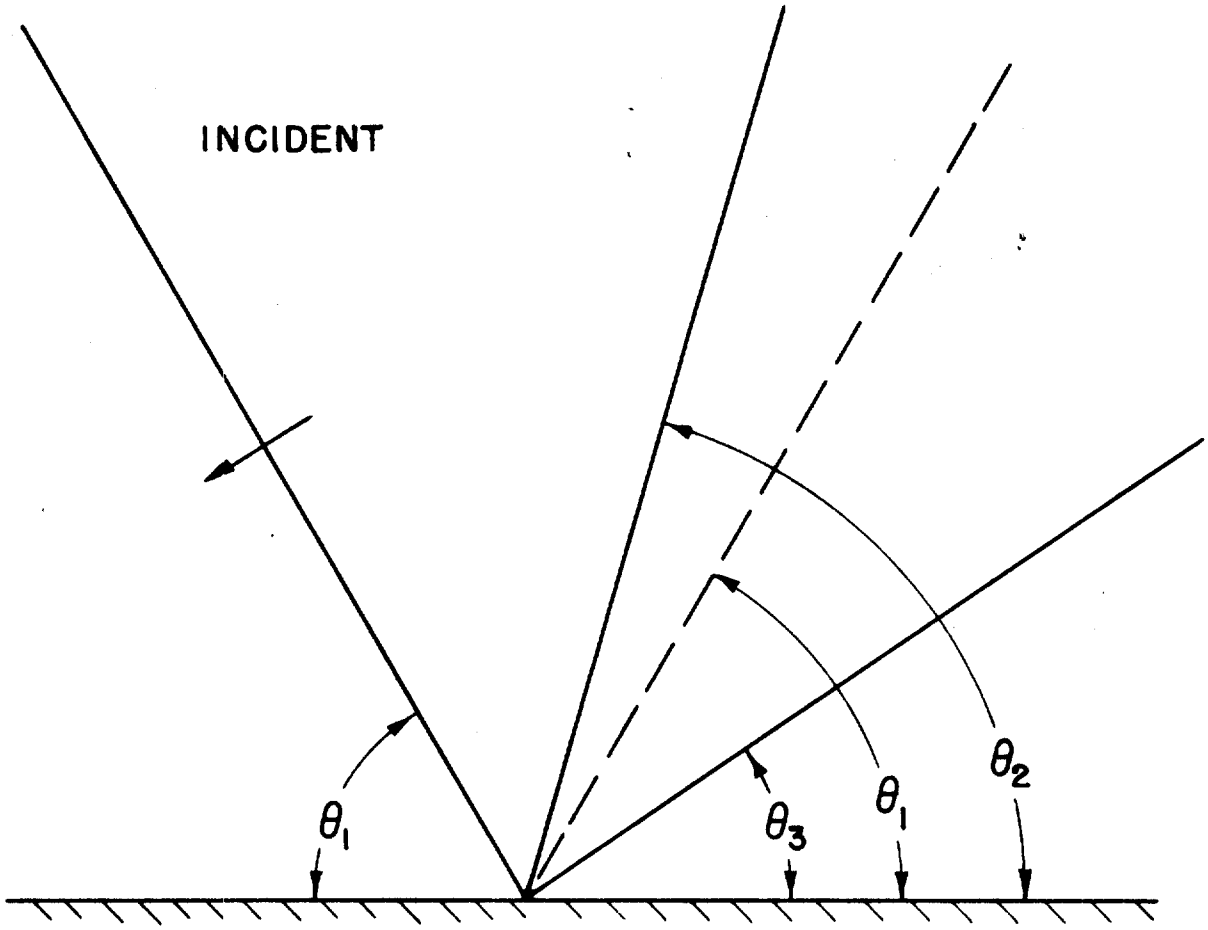

conclusion. If we consider this oblique shock theoretically and let the angle at which the incident shock strikes the wall increase from 0° towards 90°, the glancing value, we find that as this happens, the less steep of the two reflected possibilities gets steeper and steeper, the initially steeper solution becomes less steep. In other words, the two solutions for the reflected shock move toward each other. We are satisfied that it is the less steep solution which is real. However, when the incident shock has reached a sufficient obliquity the two solutions for the reflected shocks merge; i.e., become identical, and beyond this there is no solution;(3) so there is an

(3) For shocks of any reasonable strength this obliquity is far from 90° (cf. Chapter 3) e.g., for a shock strength of about an atmosphere this angle of incidence is about 50° and even for a shock strength of 0.1 atmosphere this extreme angle is around 80°.

extreme angle below which there exist two solutions for the reflected shock, an angle at which there is just one solution and beyond which there is no solution.

10.2-6 The Critical Angle - Irregular Reflection

There is then, an extreme angle below which there are two solutions. We choose the lower solution for tolerably good theoretical reasons which are very well confirmed by experiment, but beyond this extreme angle there simply is no reflection of this type. There must, however, be a reflection of some kind. We call the reflection of the first kind, the reflection which really is the extrapolation of the acoustic case, regular reflection, and all kinds of other reflection, irregular. From the above, one can see that the region of regular reflection is limited to angles of incidence below a certain critical angle.

Now the variations with shock pressure of the limiting angle for regular reflection are of some interest (Figure 20). It is quite clear that as the shock strength is decreased, the acoustic limit is approached and, therefore, the limiting angle must be nearer and nearer to 90°. For reasons previously

Figure 20

Critical angle at which regular reflection ceases to be possible, as a function of the overpressure in the incident shock

Ideal gas $\gamma = 1.40$,
Normal pressure = 14.7 psi

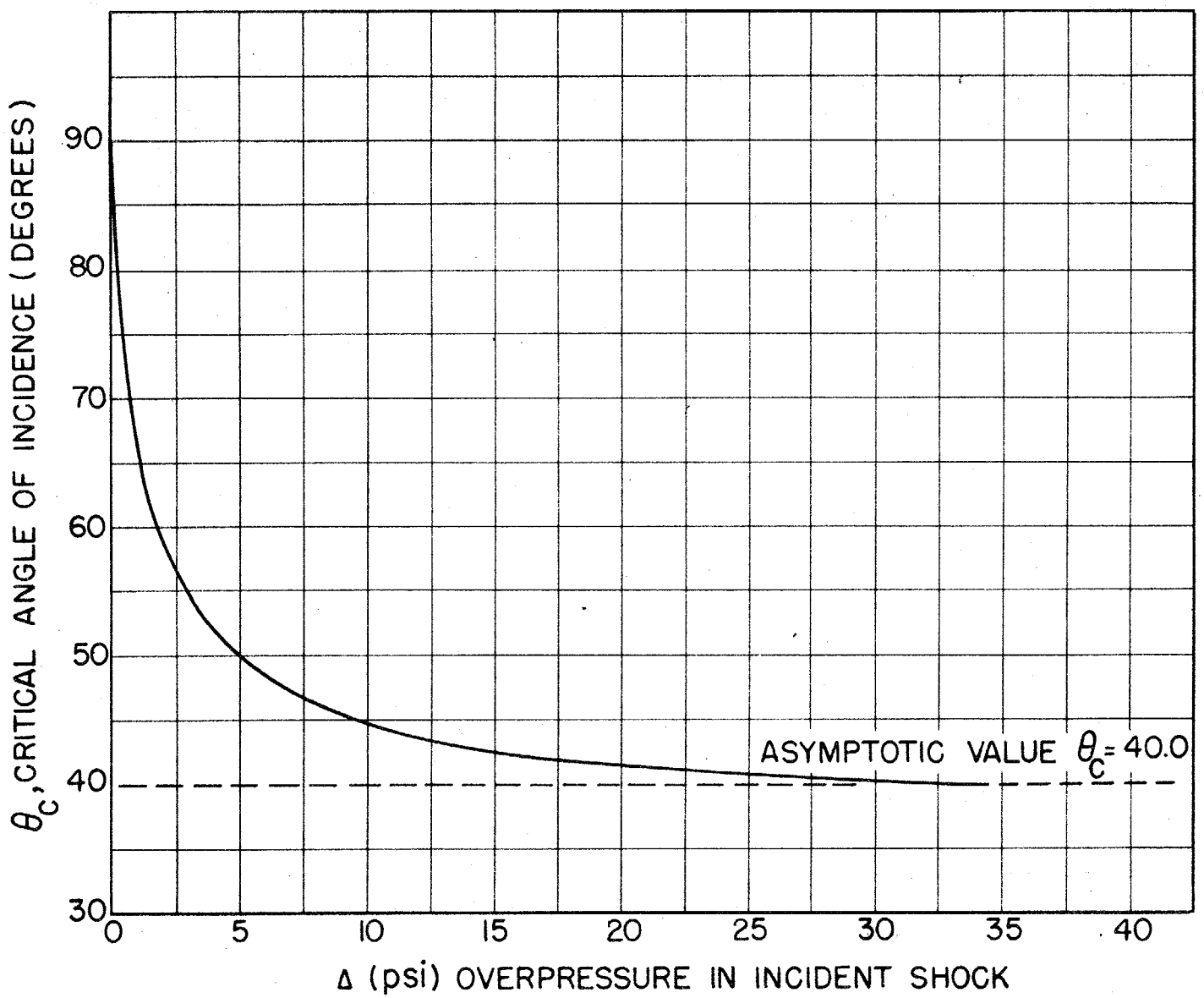

mentioned, as the angle of incidence becomes close to 90°, deviations from acoustic behavior should be expected no matter how weak the incident shock is. Theory as well as experiment show that such deviations do occur. As will be shown later (cf. Section 10.3) the critical angle converges to 90° rather slowly, as the square root of a shock strength. More interesting is the fact that as the shock strength increases, the critical angle decreases from 90°. For a few atmospheres overpressure it gets into the neighborhood of 40°. For one and one-half atmospheres overpressure it reaches 40°. After this it does a peculiar thing. It drops a little below 40° to something like 39° which it reaches at 6 atmospheres overpressure and then it rises again to 40°, which value it retains for infinitely strong shocks. This means that for shocks of 1.5 atmospheres or greater, the critical angle has already practically reached its limiting value of 40°. For half an atmosphere overpressure, it is 50° or 60°. Since most blast damage by large bombs is based on controlled pressure criteria and likely to occur between 3 and 6 pounds per square inch overpressure, that is, between a quarter and one-half atmosphere, we must expect regular reflection to become impossible in the neighborhood of 50° to 60°.

Another interesting characteristic of regular reflection is the variation of the absolute overpressure on the surface as a function of the angle of incidence and the strength of the incident shock. Figure 21 gives the relative overpressure as a function of the angle of incidence for acoustic, weak and strong shocks.

10.2-7 Mach Reflection

Now we must ask what will happen if we go past the extreme angle of regular reflection. There is a very simple argument which uses the analogy of this phenomenon with the collision of a blast with a wedge.

10.2-8 Collision of a Supersonic Flow with a Wedge

A plane supersonic flow is incident on a wedge of semi-angle θ_w . As the

Figure 21a

Relative overpressure on surface due to reflection versus angle of incidence

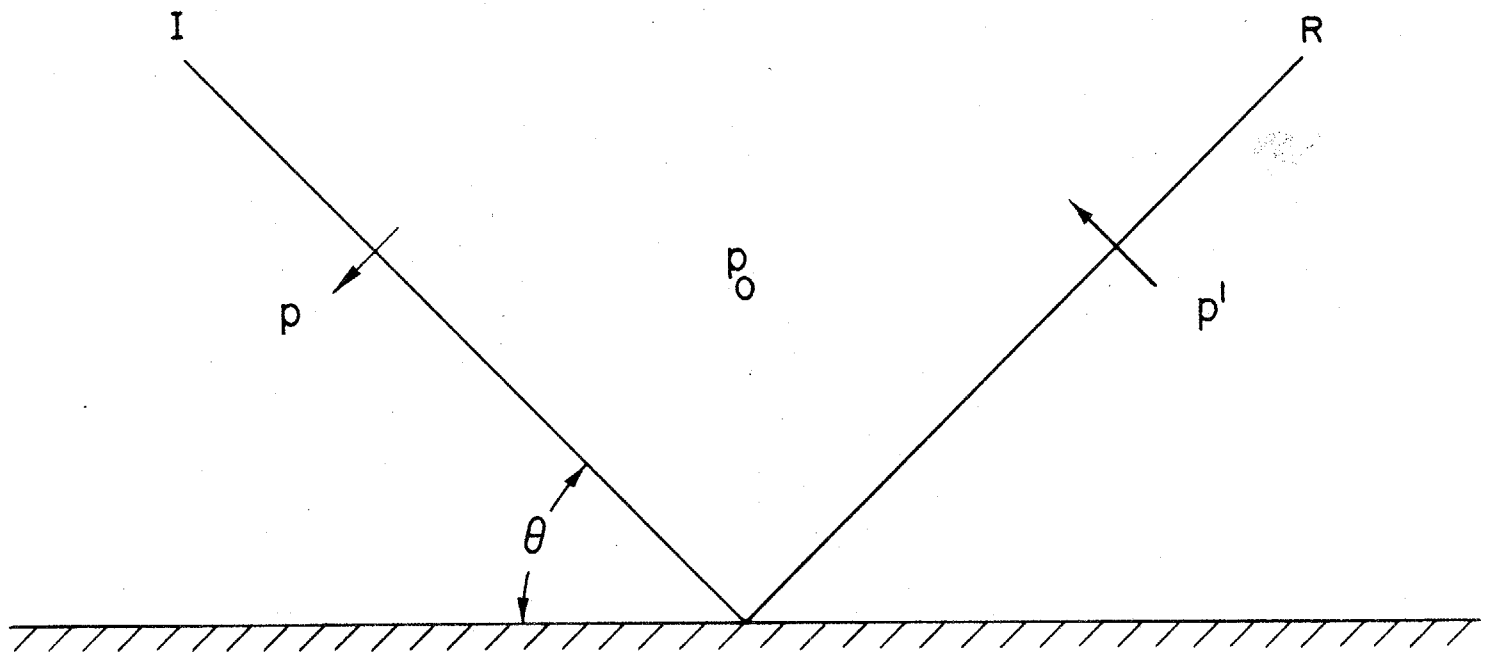

Figure 21b

Relative overpressure on surface due to reflection versus angle of incidence

Ideal gas $\gamma = 1.40$

$$\xi' = \frac{p'}{p_o}, \quad \xi = \frac{p}{p_o}$$

where p = pressure in front of incident shock
p_o = pressure behind incident shock
p' = pressure in front of reflected shock

For acoustic case $\xi' \cong \xi \cong 1$

$$\xi' = \frac{p+2\Delta}{p+\Delta} \cong 1 + \frac{\Delta}{p}, \quad \xi = \frac{p}{p+\Delta} = 1 - \frac{\Delta}{p}$$

$$\Delta p' = p' - 1 = p\left[\frac{1+\frac{\Delta}{p}}{1-\frac{\Delta}{p}} - 1\right] = 2\Delta$$

Δ = overpressure in incident shock

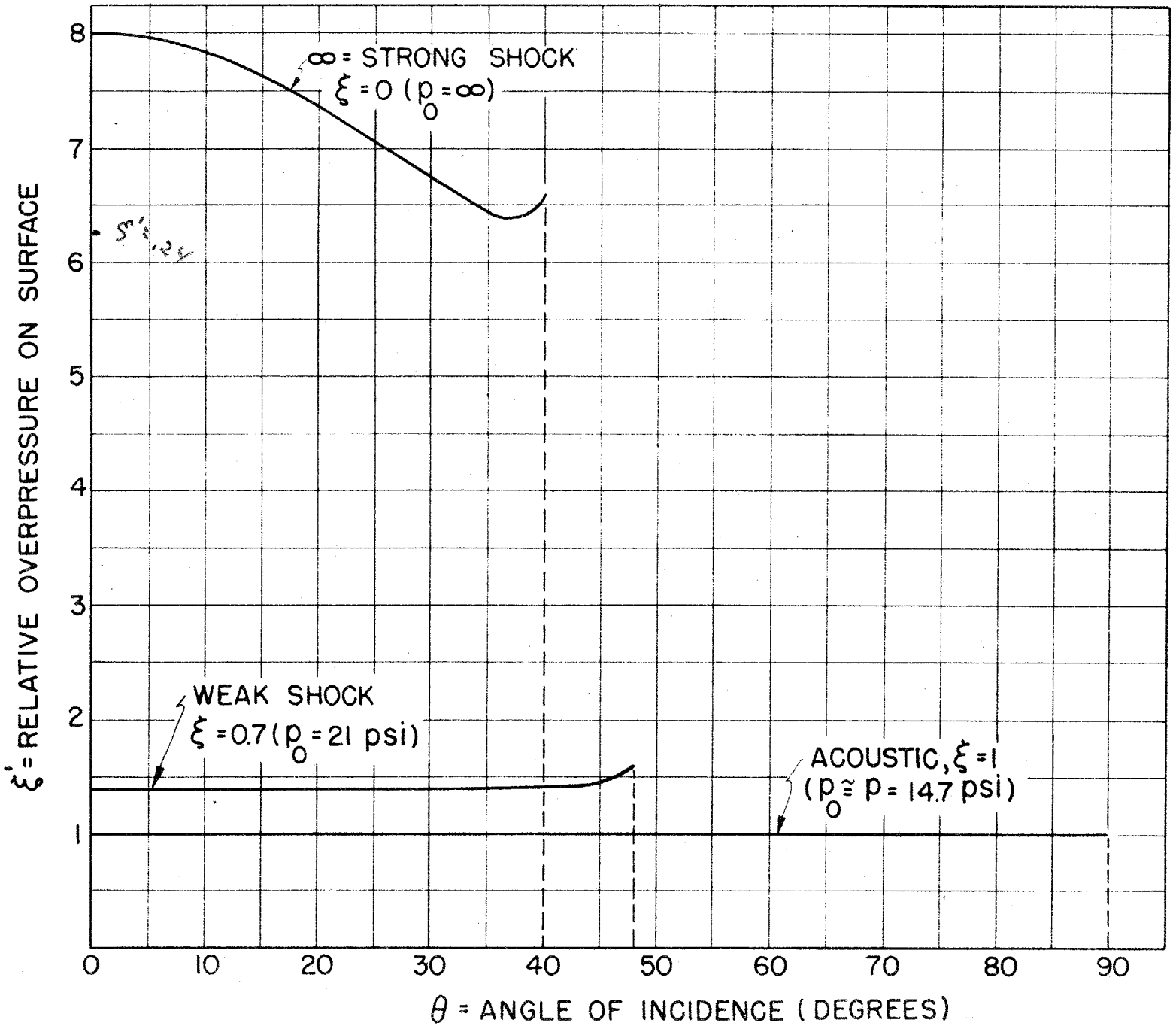

flow collides with the wedge it is deflected through an angle ($\theta_R + \theta_\omega$) by a shock SOS becoming parallel to the plane side of the wedge. The conditions are constant throughout the regions A and B which are separated by the shock discontinuity SOS. It is found experimentally, and could be shown by theoretical consideration of an oblique shock,(4) that depending on the wedge angle θ_ω

(4) Taylor and MacColl, "The Mechanics of Compressible Fluids" in W. F. Durand "Aerodynamic Theory", Guggenheim Fund, 1934, Vol. III, Section H.

there is a critical value of the supersonic material velocity for which no shock exists which is capable of deflecting the stream so that it becomes parallel to the wedge wall. Above this critical value of material velocity there are in general two theoretical solutions(4) for each wedge angle. Only the solution with the smaller value of θ_R actually occurs. At the critical value there is just one solution and below it there are no solutions of the type pictured in Figure 22. Instead, experiment shows a detachment of the shock wave from the top of the wedge such as pictured in Figure 23. This is the so-called "detached headwave". This means that there is no solution of the type pictured in Figure 22, that considering a given value of supersonicity, there exists an upper limit on the angle of incidence ($\theta_R - \theta_\omega$) for which the flow can be rendered parallel to the wedge face immediately behind the shock. Beyond this angle a new type of phenomenon is in evidence. This is the detachment of the shock. It is of particular interest because it means that signals are sent back from the tip at O into the region bounded by a now curved shock: there is a propagation of signals back against the impinging stream.

The connection between this phenomenon and the reflection of a blast wave from a plane surface can be shown in a simple way. In Figure 24, the incident shock impinges on the wall giving rise to a reflected shock. If we adopt the frame of reference which reduces the motion of the point P and the two shocks

Figure 22

Flow past wedge

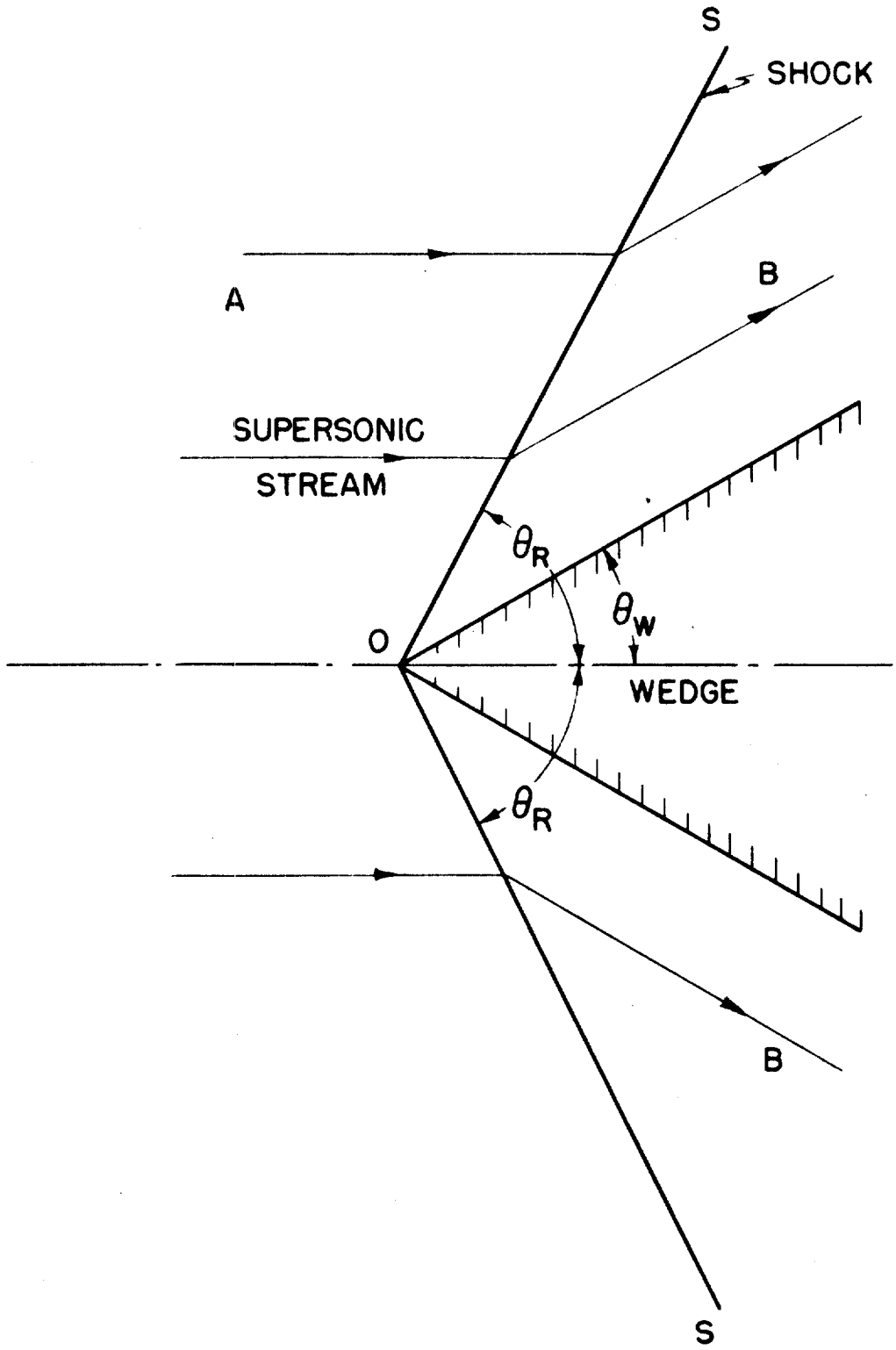

Figure 22'

Supersonic flow past wedge

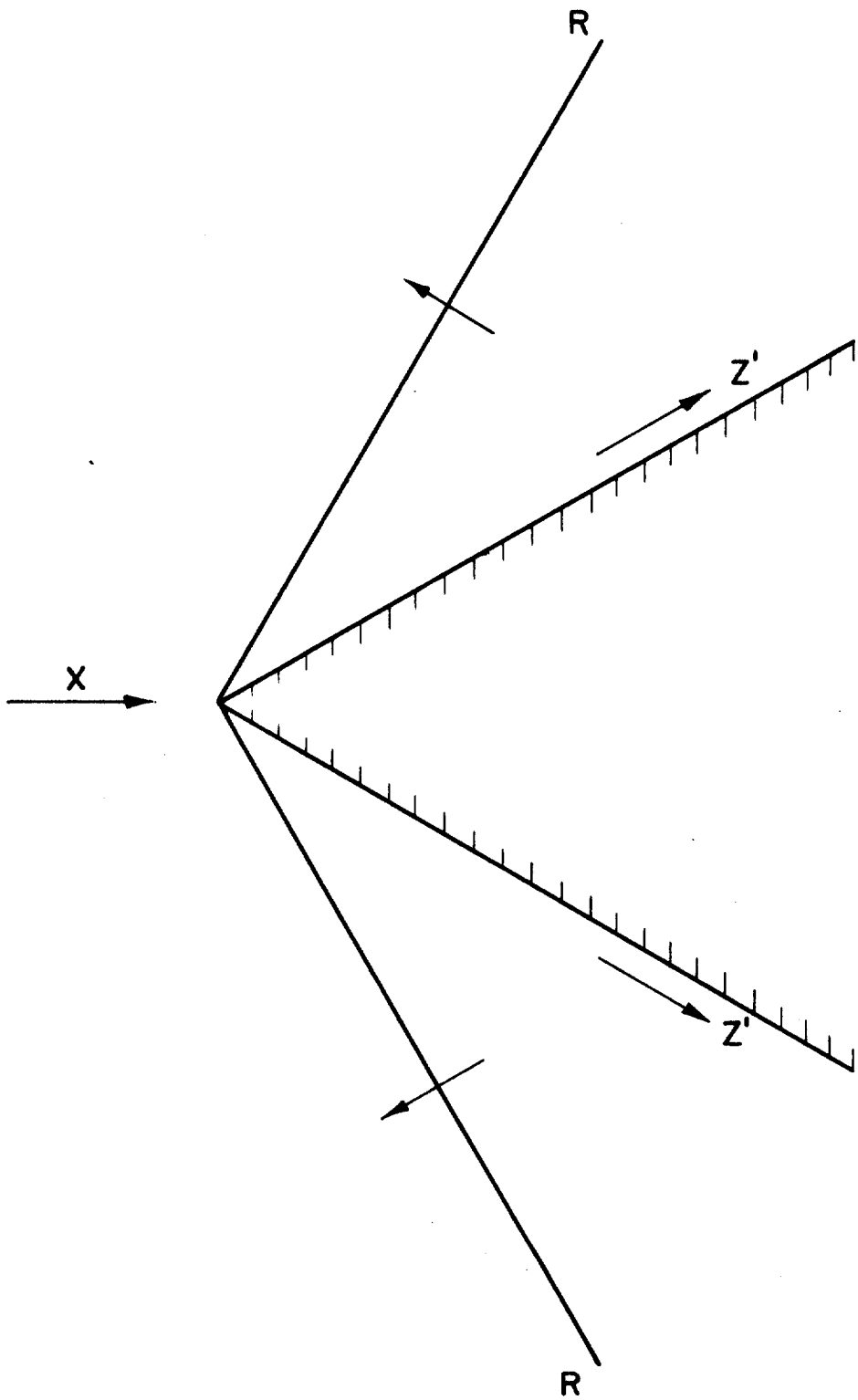

Figure 23

Detached headwave

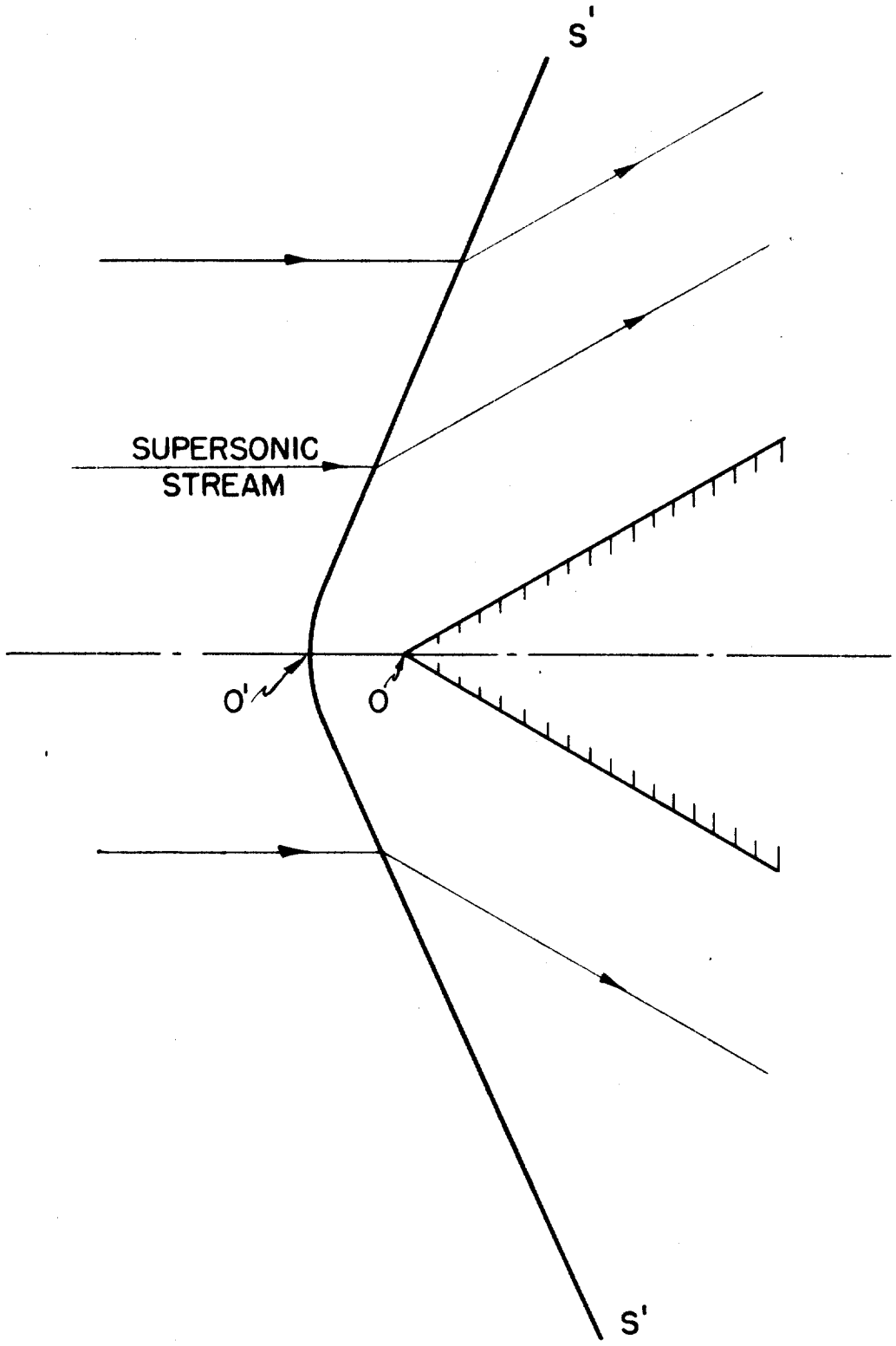

Figure 24

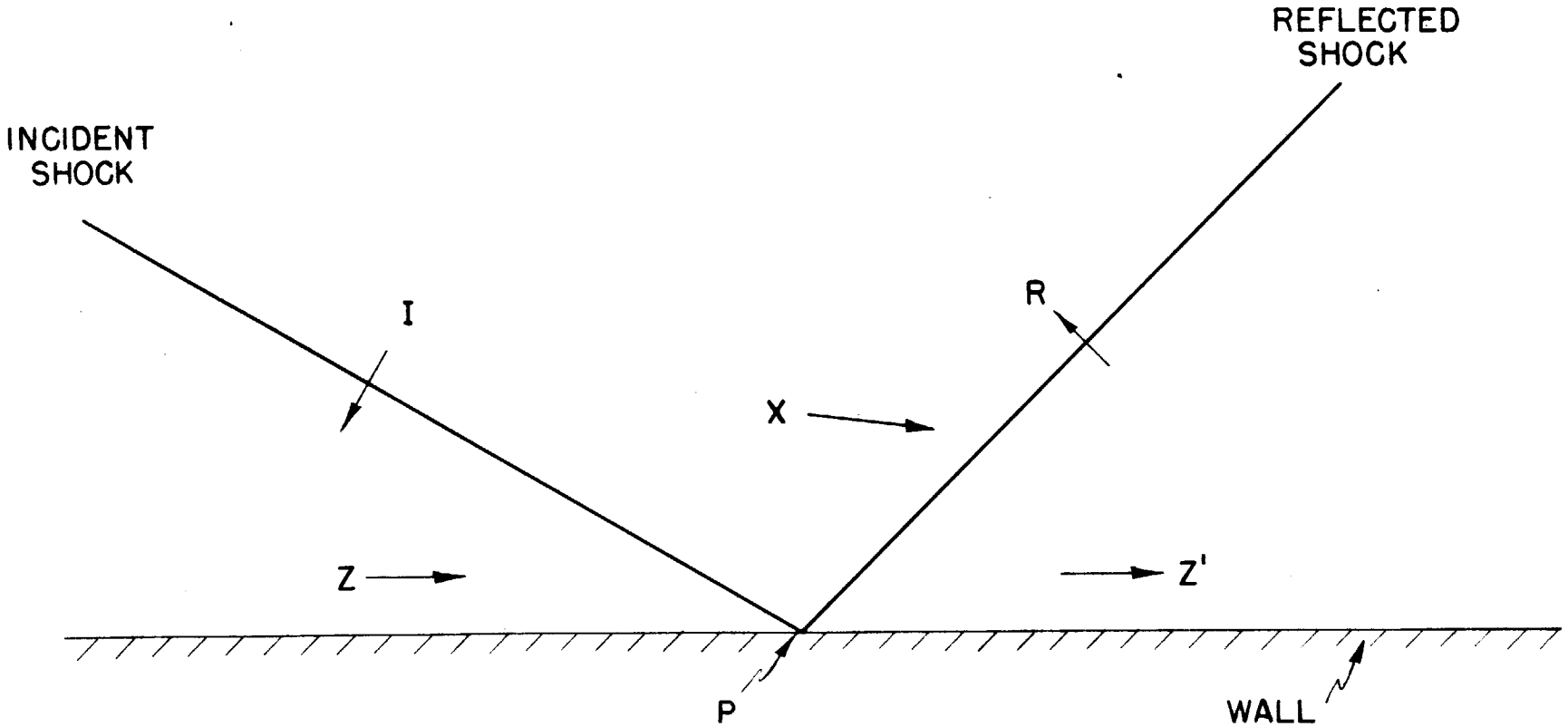

to rest then the material will appear to flow through the shocks from left to right as shown. The incident shock causes the material originally flowing parallel to the wall to be deflected toward the wall in the direction of I. The reflected shock renders the flow again parallel to the wall. If we identify the flow in the region between the two shocks with the supersonic stream of Figure 22, the reflected shock with SO and the wall to the right of P with the wedge wall in the same figure, the analogy is complete (Figure 22'). The unapplicability of Figure 22 under the certain conditions discussed above is reflected in the failure of Figure 24 under corresponding conditions; i.e., there exists a critical angle of reflection (and hence of incidence) for a given strength shock. Beyond these critical conditions we expect from the analogy that a signal propagates back from the reflected shock into the region between the shocks and causes a fusion of the incident and reflected shocks starting in the neighborhood of P.

This analogy therefore, shows that the reflected shock must be expected to overtake the incident shock whenever $\theta > \theta_c$. This process of overtaking originates at the wall and gradually spreads into the volume of the gas. As it spreads the two shocks merge and form a single shock for a certain distance from the wall, beyond which they are separate. In the case of irregular reflection, then the two shocks will no longer look like a V but like a Y standing on the wall. (See Figures 25a and b.)

In Mach reflection it is as if reflection were no longer caused directly by the wall but rather by a cushion of air resting on the wall. Now that this species of irregular reflection really occurs, it is a seventy year old experimental observation of Ernst Mach[5], after whom it was named. It has been

(5) Paper of E. Mach with various collaborators appeared in the Vienna Academy "Sitzungsberichte" Vol. 72 to 92 (1875-1889), cf. in particular Vol. 78 (1878) page 819.

Figure 25,a,b.

25a Regular reflection
25b Mach reflection

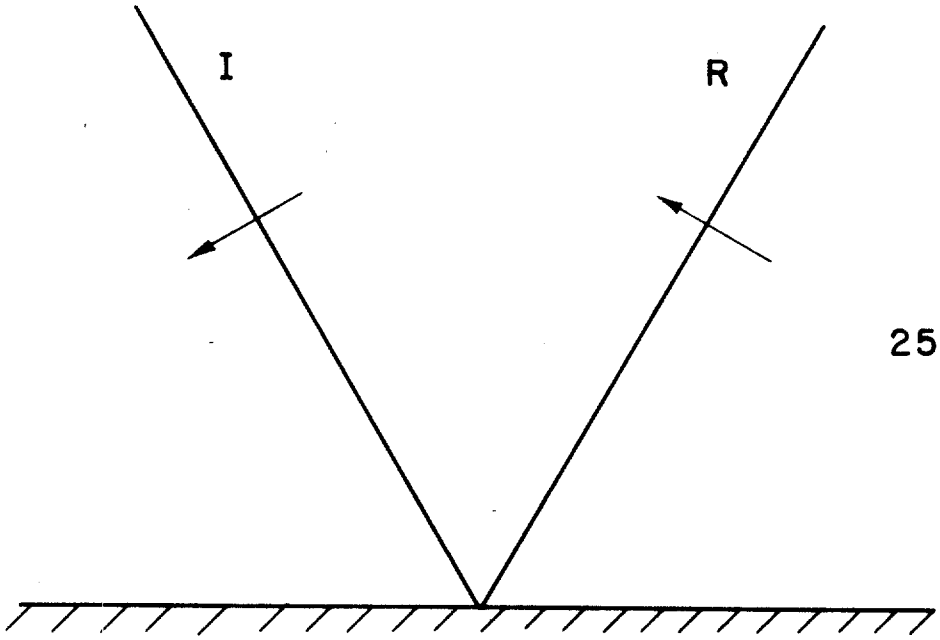

25 a

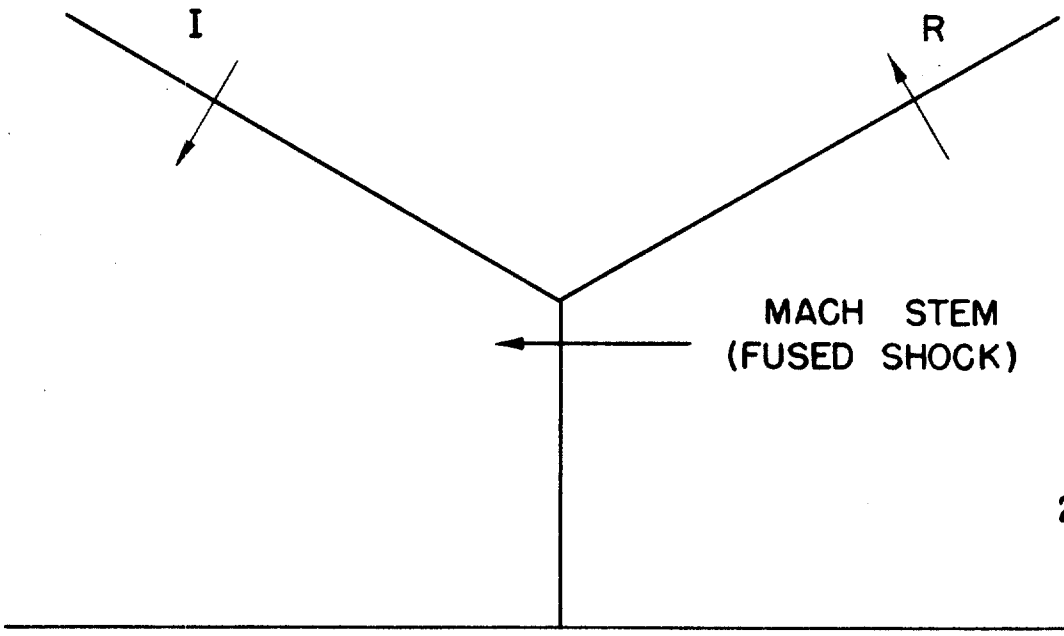

25 b

explored in great detail by hydrodynamical research done during this war.(6)

---

(6) J. von Neumann, "Oblique Reflection of Shocks", Bureau of Ordnance E.R.R. No. 12 (1943).

H. Polachek and R. J. Seeger, "Interaction of Shock Waves in Waterlike Substances", Bureau of Ordnance E.R.R. No. 14 (1944).

P. C. Keenan and R. J. Seeger, "Analysis of Data on Shock Intersections, Progress Report No. 1", Bureau of Ordnance E.R.R. No. 15 (1944).

H. Polachek and R. J. Seeger, NavOrd No. 88-46, "Analysis of Data on Shock Intersections, Progress Report No. 2" (1946).

NavOrd Report No. 74-46, "Technical Conference on Optical Phenomena in Supersonic Flow" (1945) (Confidential).

Lincoln G. Smith, "Photographic Investigation of the Reflection of Plain Shocks in Air" (1945) (Final Report) OSRD Report No. 6271.

The qualitative picture of Mach reflection is quite simple for the case of a plane shock incident on a wall. Here the incident shock makes a constant angle with the wall. The situation is more complicated in the case of blast produced by a bomb. First of all, the angle of incidence changes as the blast wave proceeds outward from the bomb. In addition, the sphericity of the blast wave makes a quantitative difference where Mach reflection occurs, while it introduces no additional features in the case of regular reflection. This is so because regular reflection takes place entirely in the neighborhood of a single point of the wall and, therefore, only local conditions at that point enter. The definable size Y type reflection, on the other hand, extends over a finite area and grows up on the shock. Therefore, the properties of the shock in the large area now become relevant. As indicated earlier, the reflected shock merges with a continuously increasing fraction of the incident shock, and eventually the incident and reflected shock may even coincide completely. Most

of the theoretical and experimental work on the phenomenon, but not all of it, was done in the case which is somewhat simpler; i.e., a plane wave incident on a plane wall. It is found that, in general, the dimensions of the Y in this case are not constant, but that they grow with time. In other words, while the regular reflection, which produces a V, is stationary, that is, the V never changes, this new kind of reflection is not stationary, i.e., the Y grows as time goes on. Of course one must admit that the Y contains a length, and hence a size can be attributed to it, in a manner which is not possible for the V. The length associated with the Y is the length of the stem; the V has no stem and definable size. Since all experimentation, as well as theoretical considerations, show that in the plane case the stem of the Y grows proportionally in time, the Mach effect must have a well defined beginning. The length of the Y stem at any moment defines the duration which the phenomenon must have had from the time of its inception to the time of observation.

10.2-9 Difficulties with Irregular Reflection

As was shown at a certain obliquity θ_c, regular reflection ceases. All forms of reflection occurring after this, i.e. for $\theta > \theta_c$, are by definition, irregular. It is believed that irregular reflection at its very inception, i.e. for the θ immediately following θ_c, belongs to the type described above as Mach reflection, although if one goes into the minutiae, there is an interval of a few degrees where one might conceivably have doubts. These doubts as to the nature of early irregular reflection are based on experiments by L. G. Smith.(7)

(7) Lincoln G. Smith, "Photographic Investigation of the Reflection of Plain Shocks in Air" (1945) (Final Report) OSRD Report No. 6271.

We would expect that the small angle between the trajectory of the triple point and the wall should be zero exactly where regular reflection ceases. According to Smith's experiments the triple point is not visible for about 2° after

regular reflection ceases. If the angle between the triple point trajectory and the wall is measured in the region of 2° to 15° past the critical angle of incidence and then extrapolate back to zero, it hits zero at about 1° from the extreme angle. Whether this effect is real we cannot be certain as yet. It may be that a higher resolution will settle this point.

A further complication is caused by the fact that the reflection phenomena must necessarily have a beginning at a definite point, where the shock first meets the oblique wall. This point is clearly a corner which can belong to any one of several types. Figures 26a, b, and c are some examples of such corners. (It will be noted that 26b and c represent alternatives, which are equivalent since viscosity and wall friction are disregarded.) Both theory and experiment show that this corner must be the source of a disturbance behind the reflected shock R. Smith's schlieren photographs indicated that this disturbance is always a rarefaction wave. This rarefaction's edge shows up as a curved wave R' terminating (on the back side) the homogeneous region between R and the wall. It makes contact with R at S and beyond S it has "eaten into" R, and thereby replaced the straight shock R by a weaker curved shock R*. It will be noted that R' does not catch up with R along the wall. This is so because the above mentioned homogeneous flow immediately behind R is supersonic, and R' is a rarefaction, and hence precisely sonic. See Figure 27.

As the obliquity of I, Θ, increases, the flow behind R becomes increasingly nearly sonic, and correspondingly R' moves close to R, and S' close to the wall. Consequently the straight piece R shortens. At a certain angle Θ_{cu} the flow becomes exactly sonic, S reaches the wall and the entire reflected shock becomes curved, i.e. R* replaces R in its entirety. Thus Θ_{cu} has been computed, it lies very close to Θ_c but it is definitely less. ($\Theta_c - \Theta_{cu}$ varies with the shock strength, in air it is never more than about .6°.) From the point of view of the empirical evidence one cannot even be quite certain, whether the

Figure 26,a,b,c

26b Obtuse angle obstacle
26c Acute angle obstacle

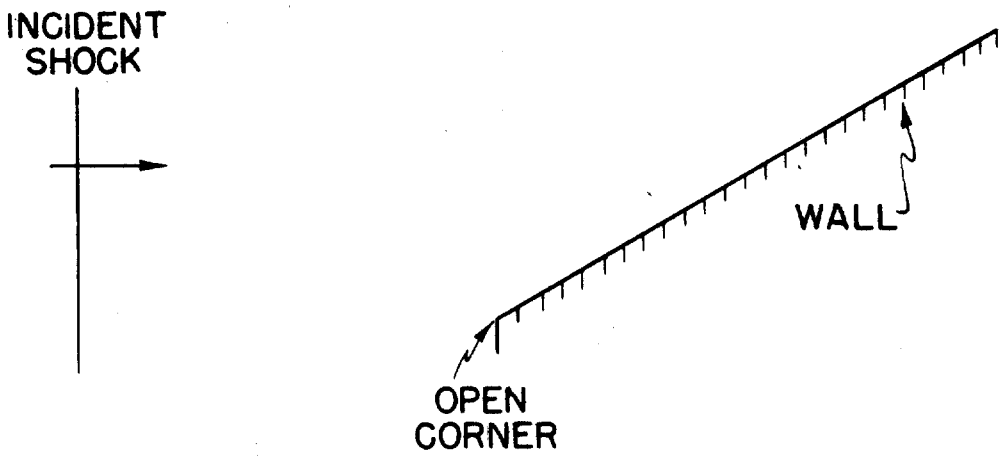
INCIDENT
SHOCK
WALL
OPEN
CORNER

26 a

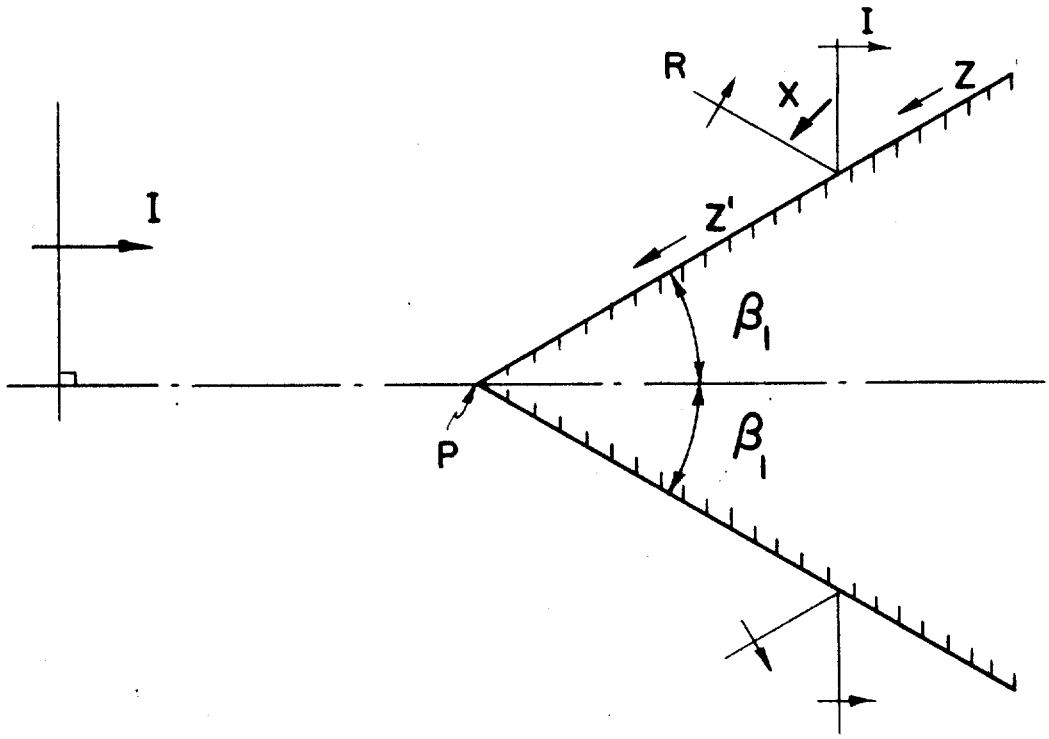
I
R
X
Z
Z'
I
β_1
β_1
P

26 b

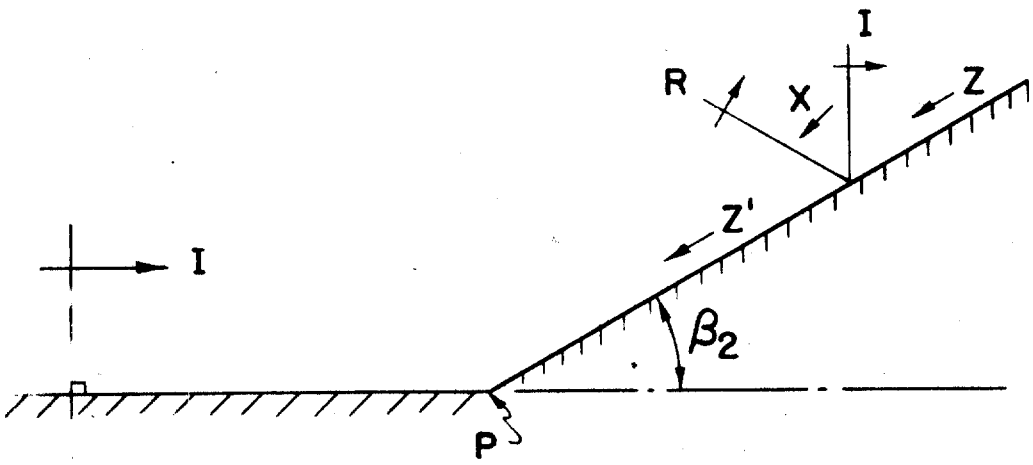
I
R
X
Z
Z'
I
β_2
P

26 c

Figure 27

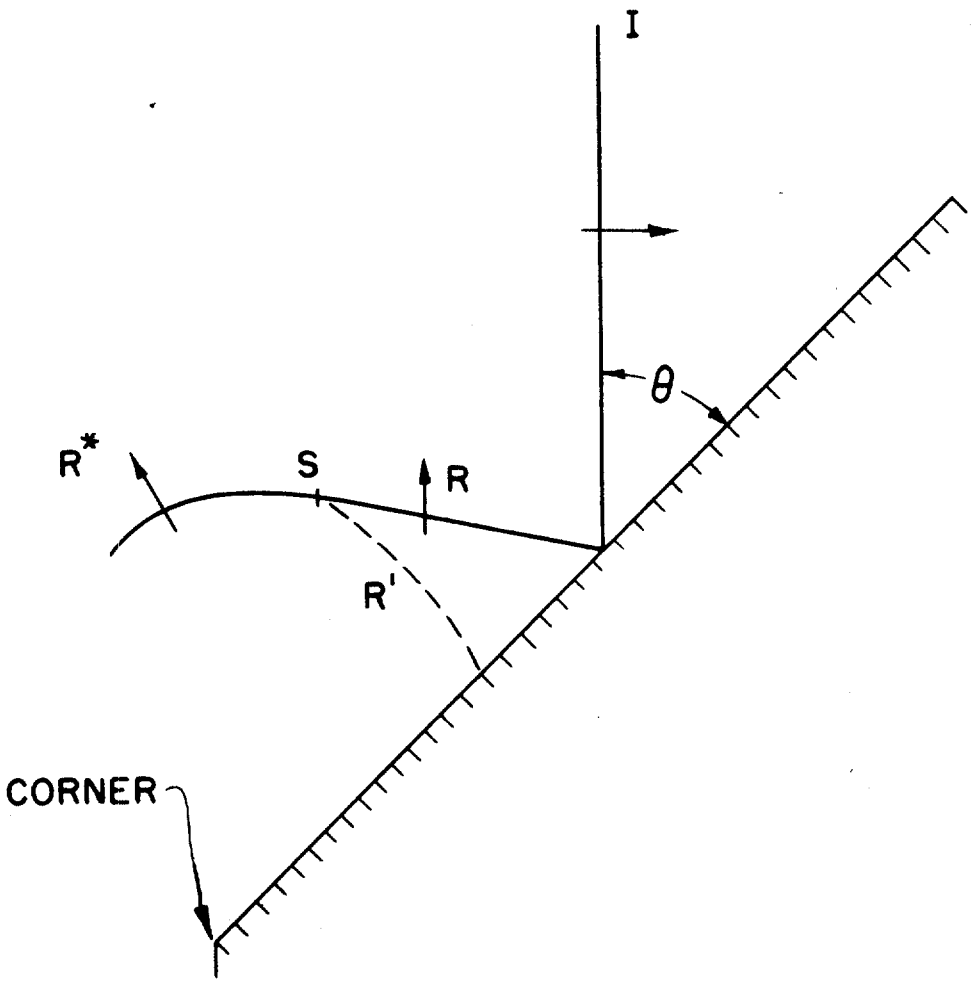

mts. 8/6

regular reflection still exists beyond θ_{cu} , i.e. whether it ceases at θ_c or at θ_{cu} .

In the plane cases studied, it was found both theoretically and experimentally that the shock configuration remains similar to itself in time, i.e. it can be described in terms of two variables, r/t, and θ , where r and θ are polar coordinates with the origin at the corner, and t is the time of travel of the incident shock from the corner to the position given by r , θ . We repeat, the configuration remains similar to itself as it proceeds, the triple point travelling a linear path (Figure 28).

In the region of regular reflection it is clear that the angle of the triple point trajectory is 0°. We know from Smith's results that with the onset of irregular reflection the angle φ made by the trajectory with the plane surface (Figure 29) is small but becomes greater as the critical angle is exceeded by larger amounts. Actually, it is very small for a considerable angular interval. For overpressures of about 1/4 atmosphere, the range in which the most detailed observations are available, the Mach effect begins when the angle between shock and wall is 56°. Even at 66° incidence the angle of the triple point trajectory with the wall is only 1 or 2°.

10.2-10 Spherical Mach Effect

In the case of a spherical wave, there is no question of edge effects but additional complications arise from the fact that the angle of incidence changes and the shock weakens as it proceeds outward from the center. The increase in the angle of incidence of the expanding spherical shock is, therefore, expected to be accompanied by an increase in the rate of rise of the triple point, as already indicated in Figure 14. The rise of the stem of the Y takes place in a manner for which there is a good qualitative description. Halverson and Taub have made extensive studies of the experimental data on the Mach effect for spherical waves. Despite the lack of a satisfactory theory, the use of available

Figure 28

Linear travel of triple point

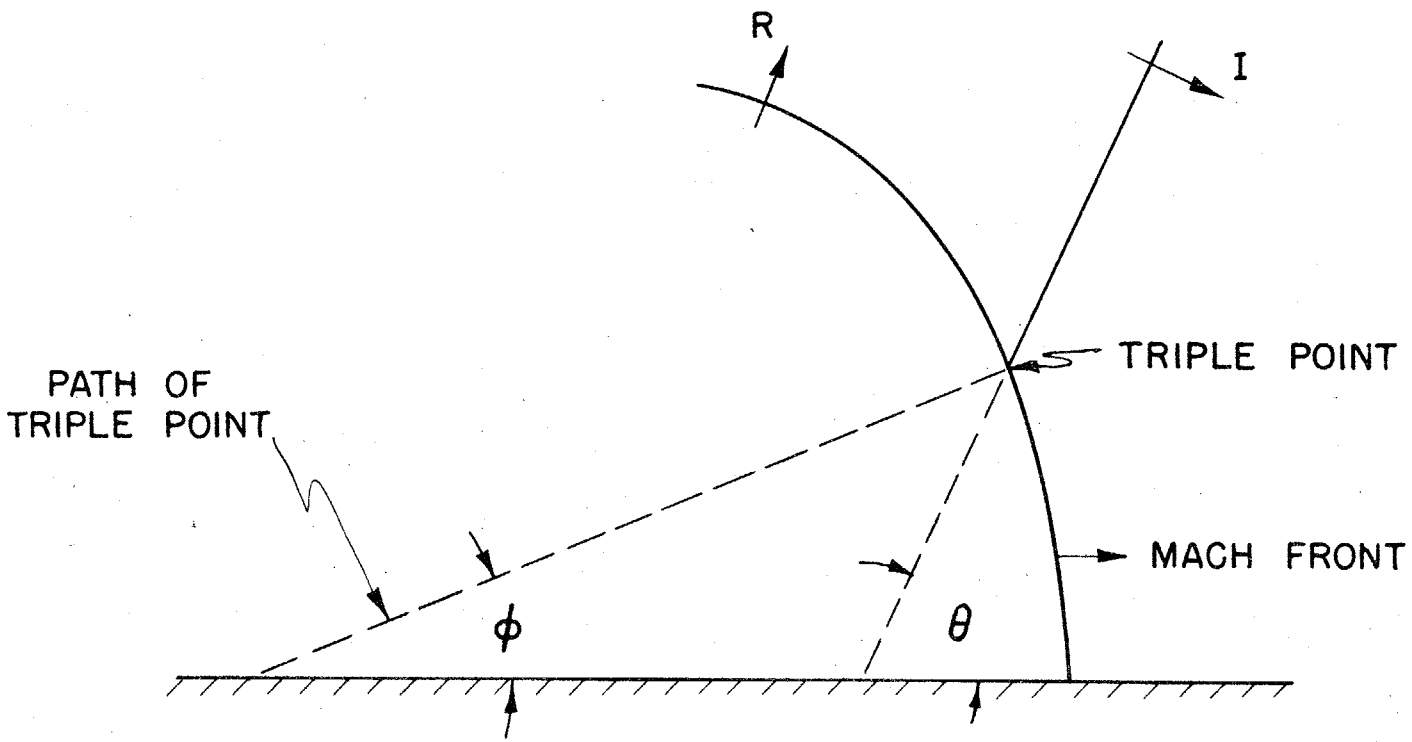

Figure 29

Angle made by triple point trajectory with plane surface (ϕ) versus angle of incidence (θ) of plane shock

(Data from L.G. Smith NDRC A-350)

Overpressure in incident shock = 1/4 atmosphere

" = 3.7 psi

$$\xi_0 = \frac{14.7}{14.7+3.7} = 0.8$$

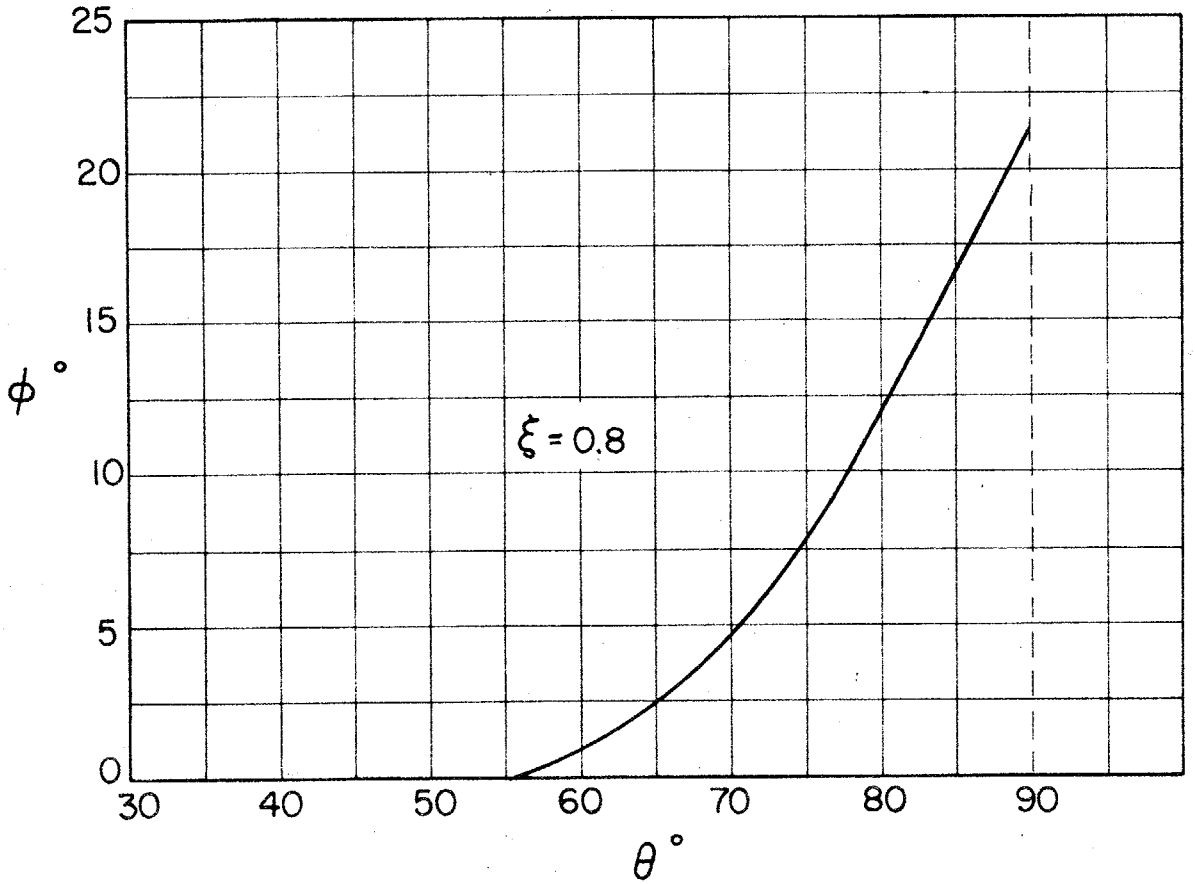

experimental data together with the $W^{1/3}$ scaling law enables us to predict the main features of the behaviour of a reflected spherical blast wave.

10.2-11 Other Difficulties with Plane Mach Effect

Returning again to the case of a plane wave, we note that certain difficulties appear in the study of irregular reflection as the angle of incidence approaches 90°. As the angle of incidence gets close to 90° the appearance of the reflection changes considerably. Specifically, the contribution of the reflected shock begins to become less and less, and in the neighborhood of the triple point, the back branch of the Y, i.e. the reflected shock, gets weaker and weaker. In other words, a situation develops where it gets progressively more difficult to tell the forward branch of the upper part of the Y from its stem and to observe the backward branch of the upper part of the Y.

If one is completely phenomenological, if one talks only about what one sees and not what one expects theoretically, then one must admit that in the Mach effect, after 80° the back side of a Y has not been observed. It looks as though the incident shock simply makes a turn and gets deflected away from the wall without the benefit of the reflected shock. Further, from the triple point the reflected shock is observable but it does not reach the other shocks to form a Y. This may be so, not because it is absent in this region, but because it gets too weak to be observed with the experimental technique employed. However, we really do not know whether late reflection is of the Mach type or has some other form.

In any case, this late form of irregular reflection is the one which corresponds for the spherical wave produced by the bomb to the double point charge, and which, in the end, yields a pressure increase by a factor of $2^{1/3}$ or $2^{1/2}$, depending on the pressure distance curve in the region of interest.

This concludes our qualitative description of the reflection of plane and spherical shock waves from a rigid plane surface.

We now proceed to a more detailed discussion of the present status of the theory of regular and Mach reflection. We will refer frequently to experimental results.

10.3 THEORY OF REFLECTION

In this section we treat in some analytical detail certain relevant topics in the theory of reflection, some of which have been mentioned in the general discussion of Section 10.2. We assume step shocks in non-viscous gases throughout, although such stringent restrictions are not necessary to all ensuing discussion. First, we discuss the one dimensional case: a step shock normally incident on a wall, and the phenomenon of "catchup" which occurs when the positive pressure region of two shocks overlap. Next, we consider questions related to the regular reflection of a plane shock such as the pressure multiplication as a function of the angle of incidence and shock strength, and the critical angle beyond which a two-shock solution no longer exists. Finally, there is a discussion of the irregular reflection of a plane wave and attendant difficulties.

10.3-1 Shocks in One Dimension

We will first consider a single plane shock, starting with the classical Rankine-Hugoniot formulae.[8] Consider such a shock S (Figure 30). It separates

---

(8) For a derivation of these formulae, see Vol. XIII, Chapter 3 on Shock Waves, by K. Fuchs.

---

two domains M_o and M, in which the physical characteristics of the substance pressure and specific volume have the values p_o, v_o, and p, v, respectively. The corresponding sound velocities are c_o and c, respectively. It is helpful to tie the frame of reference to the shock front S. Then the substance of M_o flows into the shock with the shock velocity V_o, while the substance M flows

Figure 30

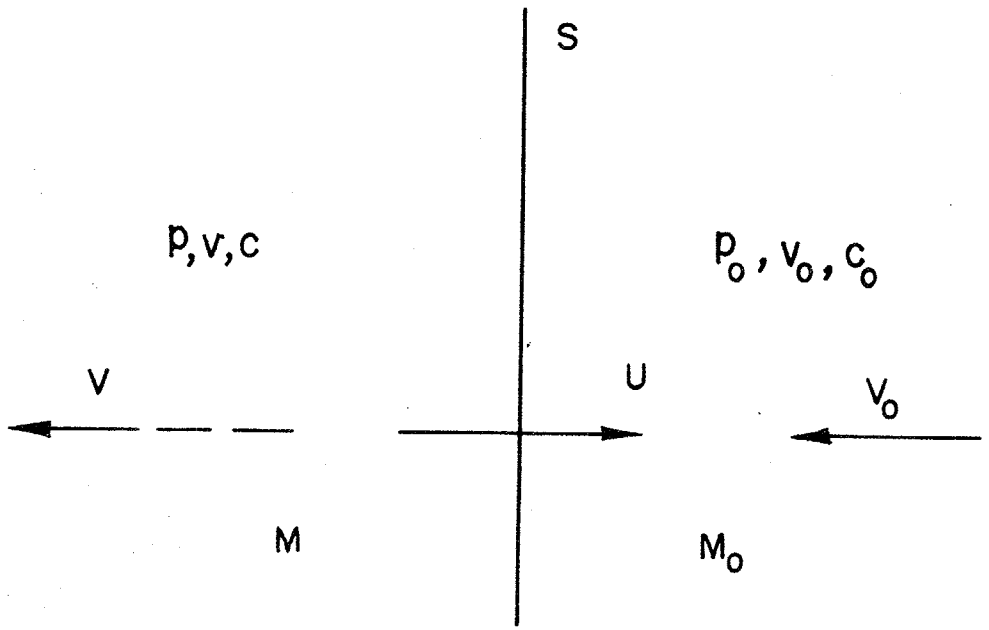

out of it with the velocity V. The shock S thus causes a decrease in velocity.

$$U = V_0 - V$$

and its compression ratio is $\xi = p/p_0$

The formulae of Rankine and Hugoniot express the conservation of mass, momentum and energy. The first part of this system correlates the inner properties of the substance on both sides of the shock, i.e. p_0, v_0 and p, v:

$$E - E_0 = \frac{1}{2}(p + p_0)(v_0 - v) \tag{1}$$

Where E is the energy density of the substance in the state M, and E_0 is the energy density in the state M_0:

$$E = E(p, v) \quad , \quad E_0 = E_0(p_0, v_0) \tag{2}$$

The second part of the system expresses the velocities V_0, V, U in terms of p_0, v_0 and p, v:

$$V/v = V_0/v_0 = \pm\sqrt{\frac{p - p_0}{v_0 - v}} \qquad (\pm \text{ is the sign of } v_0 - v) \tag{3}$$

and hence the difference in material velocity, relative to the shock front is

$$U = V_0 - V = +\sqrt{(v_0 - v)(p - p_0)} \tag{4}$$

Equations (1), (3) and (4) imply that

$$\left(\begin{array}{l}\xi > 1 \text{; i.e. } p > p_0 \text{ implies } v < v_0 \text{ and } \because V_0 > V > 0 \\ \text{In Figure 25 this implies a shock "facing" right}\end{array}\right) \tag{5}$$

$$\left(\begin{array}{l}\xi < 1 \text{; i.e. } p < p_0 \text{ implies } v > v_0 \text{ and } V < V_0 < 0 \\ \text{In Figure 25 this implies a shock "facing" left}\end{array}\right) \tag{6}$$

For $p \longrightarrow p_0$ the shock becomes a sound wave. (1) shows that in this limit

$p \sim -\frac{dE}{dv}$. On the other hand since $p = \frac{\partial E}{\partial v}$ (identically) at constant entropy, an infinitesimal shock leaves the entropy asymptotically constant. Now (3) gives $V_o \sim V \sim v\sqrt{-\frac{dp}{dv}} = \sqrt{\frac{\partial p}{\partial 1/v}}$, with constant entropy, i.e. adiabatically the shock velocity becomes sound velocity. Therefore, with respect to an infinitesimally weak shock the flow on both sides becomes asymptotically sonic.

For a shock of finite strength the following rule is generally valid:

(A) The shock velocity is supersonic with respect to the lower pressure side and subsonic with respect to the high pressure side.

For (5) these two sides are M_o, M, respectively. For (6) they are M, M_o, respectively. So we have:

$$\xi > 1 \quad \text{implies} \quad |V_o| > c_o \ , \ |V_o| < C \tag{7}$$

$$\xi < 1 \quad \text{implies} \quad |V_o| < c_o \ , \ |V_o| > C \tag{8}$$

This rule can be demonstrated quite readily for an ideal gas but it is also generally valid for any substance with a p, v characteristic that is concave upward.(9)

---

(9) H. A. Bethe, "The Theory of Shock Waves for an Arbitrary Equation of State," OSRD Report No. 545.

Consider a shock moving to the right. Restating (3) and (5)

$$V_o/v_o = +\sqrt{\frac{p - p_o}{v_o - v}}$$

But

$$C = \sqrt{\frac{\partial p}{\partial 1/v}}_{\substack{\text{constant} \\ \text{entropy}}} \ , \qquad C_o = \sqrt{\frac{\partial p_o}{\partial 1/v}}_{\substack{\text{constant} \\ \text{entropy}}}$$

For an ideal gas the adiabatic law and the equation of state, and the internal energy density are respectively

$$\text{(a)} \quad p v^{\gamma} = \text{constant} \ , \quad \text{(b)} \quad pv = RT \ , \quad \text{(c)} \ E = \frac{pv}{\gamma - 1} \tag{9}$$

So $c = \sqrt{\gamma p v}$, $c_0 = \sqrt{\gamma p_0 v_0}$

What we wish to prove is that

$$c > V_0 > c_0 \tag{10}$$

Substituting the expressions for V_0, c, c_0 , this inequality becomes

$$\sqrt{\gamma p v} > v_0 \sqrt{\frac{p - p_0}{v_0 - v}} > \sqrt{\gamma p_0 v_0}$$

or

$$\gamma \xi \frac{v}{v_0} > \frac{\xi - 1}{1 - v/v_0} > \gamma \qquad \text{where} \quad \xi = p/p_0 \tag{11}$$

An additional relation between v/v_0 , ξ and γ is required so that the correctness of this inequality can be demonstrated. Substituting (9c) into (1) we obtain

$$\frac{v}{v_0} = \frac{(\gamma-1)\xi + (\gamma+1)}{(\gamma+1)\xi + (\gamma-1)} \tag{12}$$

Combining (11) and (12) and simplifying we get in each case the same inequality, namely

$$\xi > 1 \tag{13}$$

This condition $\xi > 1$ was already required by the energy density condition (9c). This proves the statement (A) for an ideal gas.

10.3-2 Shock Catchup

Having demonstrated (10) we are now in a position to show under what conditions two successive shocks will merge. Consider two step shocks (Figure 31). By (10) shock I is supersonic with respect to undisturbed medium ⊙ , and is subsonic with respect to the once-shocked medium (1), i.e. $c_1 > V_0 > c_0$ Similarly, shock II is supersonic with respect to once-shocked medium (1) and subsonic with respect to twice-shocked medium (2) i.e. $c_2 > V_0' > c_1$ Combining these two statements $V_0' > c_1 > V_0$ or $V_0' > V_0$

Figure 31

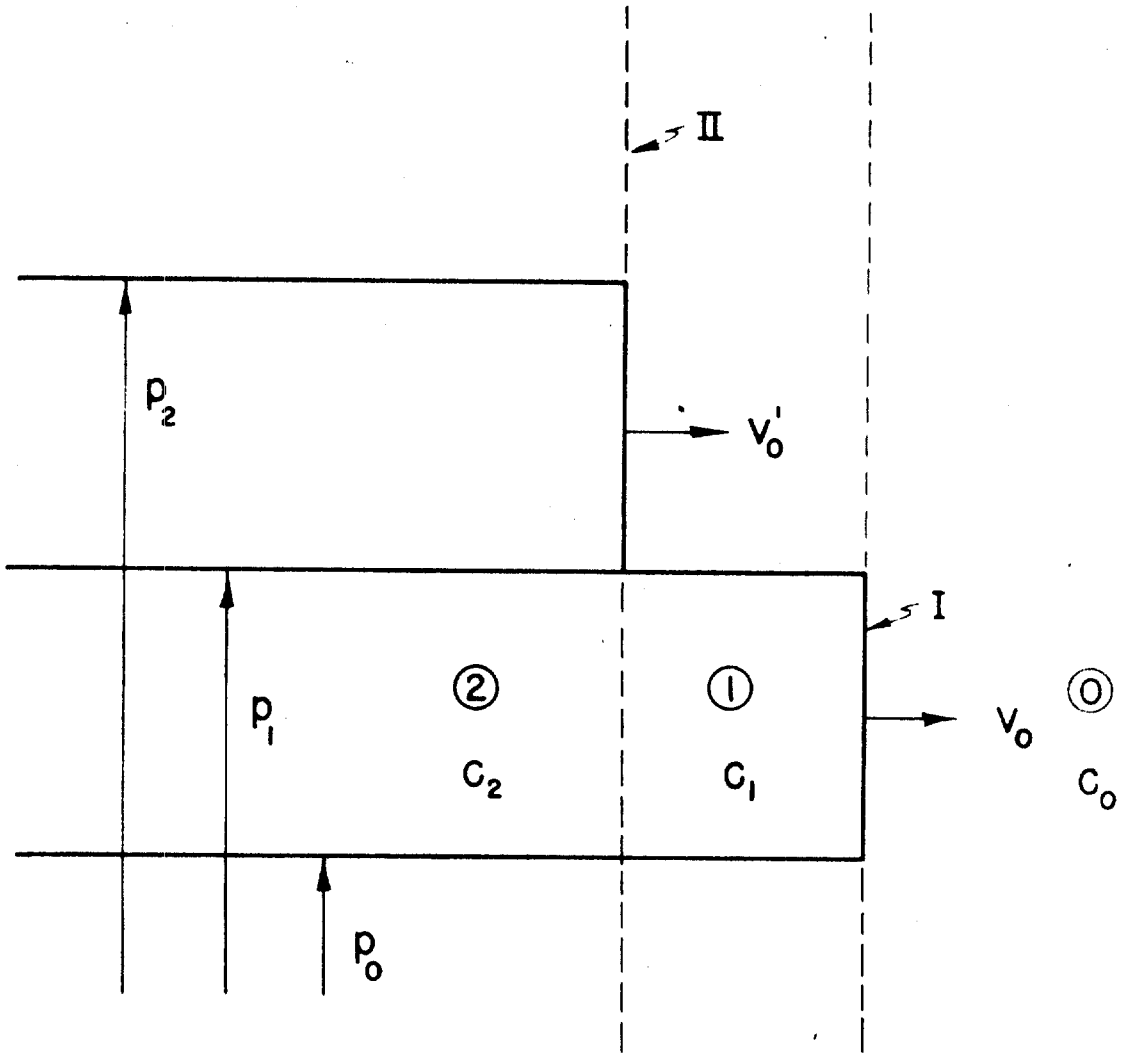

and Shock II will overtake Shock I. This is true as long as $\frac{p_2}{p_1} > 1$ and hence catchup will certainly occur whenever the positive phases of two shock waves overlap (Figure 32).

A more detailed investigation would show that catchup would occur even if the second shock were in the early part of the rarefaction region of the first shock, but we will not go into this question here.

10.3-3 Normal Reflection by a Rigid Wall (Ideal gas)

The Figures 33 have three domains A, B, and C which are defined in terms of the number of times that a shock has passed through them. The pressure, specific volume and sound velocity in these regions are p, v, c; p_0, v_0, c_0; p', v', c', respectively.

Since reflection increases the overpressure

$$p < p_0 < p'$$

or
$$\xi < 1 < \xi' \tag{14}$$

where $\xi = p/p_0$, $\xi' = p'/p_0$

In the present setup there occur no movements parallel to the rigid wall. Hence the substance of the domains A and C which cannot move normally to the wall either is necessarily at rest. The substance of the domain B has therefore the velocity U from Figure 33a and the velocity U' from Figure 33b. The condition relating the strengths of Shocks I and R is therefore

$$U = U' \tag{14'}$$

Now for an ideal gas characterized by (9a, b, c) we recall that

$$v/v_0 = \frac{(\gamma-1)\xi + (\gamma+1)}{(\gamma+1)\xi + (\gamma-1)} \tag{12}$$

Solving for U, U' from (2) and (4) we find that

$$\frac{U}{c_0} = + \frac{2(\xi-1)}{\sqrt{2\gamma[(\gamma+1)\xi + (\gamma-1)]}} \tag{15a}$$

Figure 32

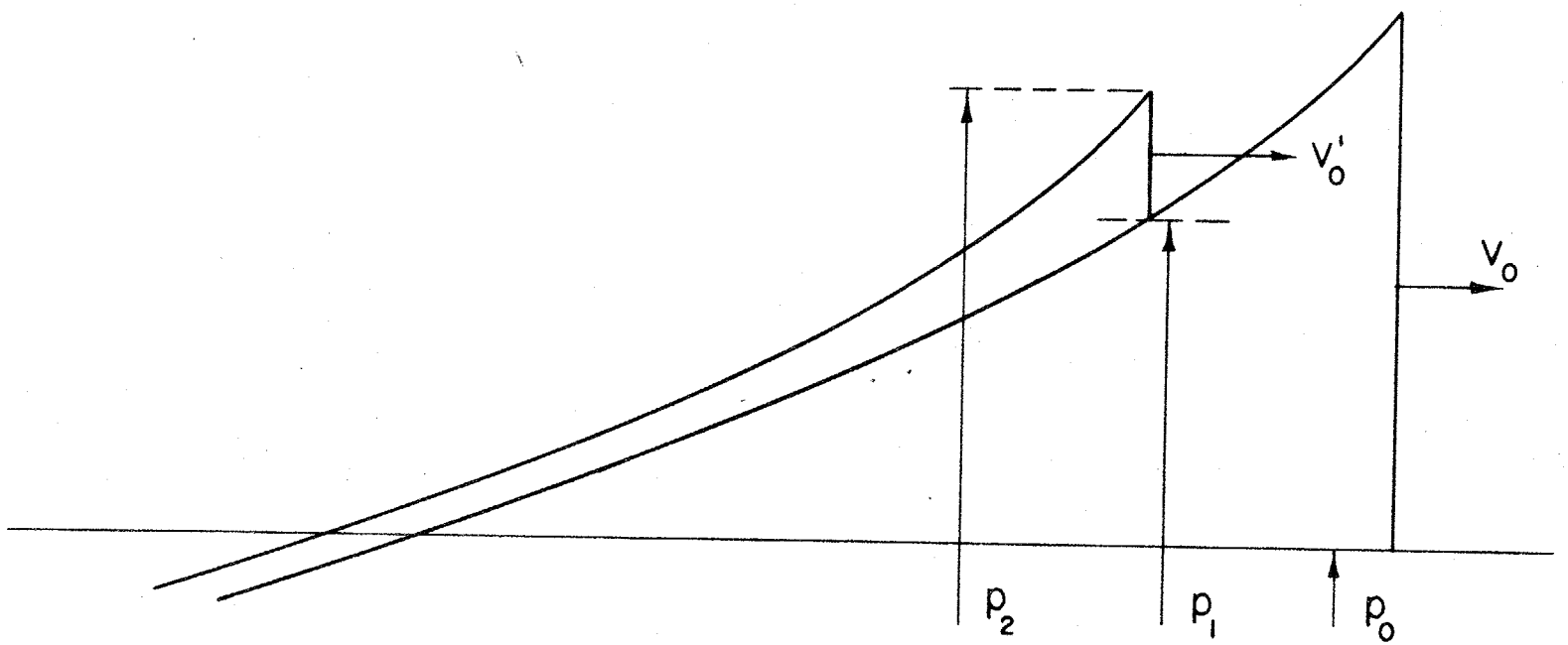

Figure 33 a,b

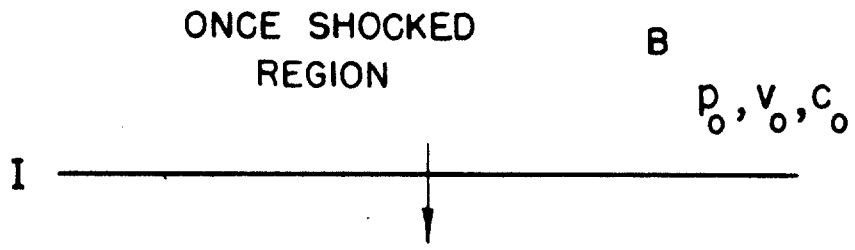

33a

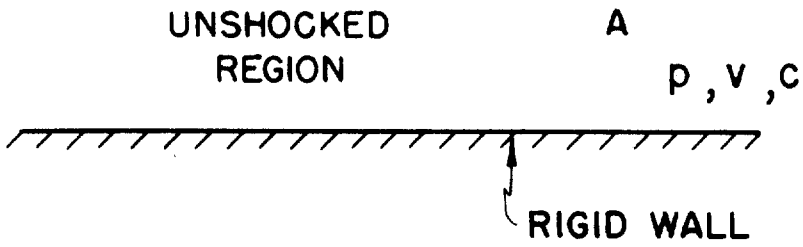

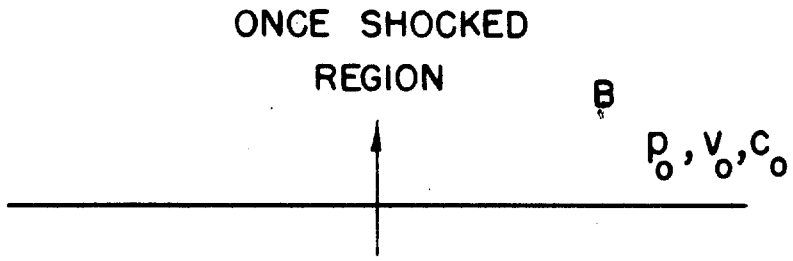

33 b

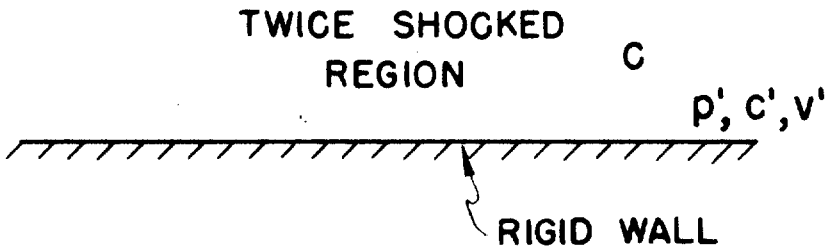

$$\frac{U'}{c_0} = -\frac{2(\xi'-1)}{\sqrt{2\gamma[(\gamma+1)\xi+(\gamma-1)]}} \qquad (15b)$$

The minus sign in (15b) appears because of the opposite directions of travel of the incident and reflected shocks. Equating (15a) and (15b) as required by (14) and solving for ξ' in terms of ξ

$$\xi' = \frac{(3\gamma-1)-(\gamma-1)\xi}{(\gamma+1)\xi+(\gamma-1)} \quad , \quad \xi' = p'/p_0 \quad , \quad \xi = p/p_0 \qquad (16)$$

consequently $0<\xi<1$ corresponds to $1<\xi'<\frac{3\gamma-1}{\gamma+1}$

For air (at moderate temperatures and densities) $\gamma = 1.4$ and $\frac{3\gamma-1}{\gamma-1} = 8$. These results deserve a brief discussion because they contain the first quantitative indications about the "unacoustic" effects in shock reflection: that is, the deviations which shocks of finite strength present from "acoustic" laws, which hold asymptotically for shocks of infinitesimal strength.

From (16) we infer easily that

$$1-\xi < \xi'-1 \quad , \quad \frac{1}{\xi}-1 > \xi'-1 \qquad (17)$$

This means (as was stated without proof in a previous part of this chapter) that

$$p_0-p < p'-p_0 \quad , \quad p_0/p > p'/p_0 \qquad (18)$$

The reflected shock is stronger than the incident shock if strength is measured by the absolute compression (pressure difference), but it is weaker if the strength is measured by the relative compression (pressure ratio).

In the limit of infinitesimal shocks, the acoustic limit (16) can be manipulated to show that $p_0-p \sim p'-p_0$, $p_0/p \sim p'/p_0$, i.e. that both absolute and relative criteria give the same result in the acoustic limit.

Thus the "unacoustic" theory is so far just a plausible extension of the acoustic theory with little individuality of its own. We shall see how radically this changes when oblique reflection is considered.

10.3-4 Regular Oblique Reflection

We will now consider the case of the oblique reflection of a shock of finite strength (Figure 34).

A single plane shock wave, I, is incident on the wall, the included angle being α. It produces a secondary shock wave, the reflected wave, R, which includes the angle α' with the wall. We will derive relationships between the strength of I (measured by its compression ratio), the value of α, the strength of R and the value of α'.

The shock waves I and R and the wall define three domains in the substance: the unshocked material ahead of I; the once shocked material between I and R; the twice shocked material behind R. We denote these domains by A, B, C, respectively.

The ordinary frame of reference has the unshocked material A at rest, while the waves I and R move with shock velocities U and U' respectively normal to themselves. A more advantageous frame of reference is one which is tied to the reflection point, P, where I, R and the wall meet. Here the substance A comes in with a velocity $\vec{z}$, parallel to the wall, while the substance B, leaves with a velocity $\vec{z}'$, parallel to the wall. From this point of view, the first shock causes flow which is initially parallel to the wall to be deflected toward the wall and the second shock renders this oblique flow again parallel. In this frame of reference, the shocks I and R and the reflection point P are at rest.

Clearly the pressures in the three regions increase with the number of times the regions received a compressive shock, so that $p < p_0 < p'$ where p, p_0, p' are the pressures in regions A, B, and C respectively. Or:

$$\xi < 1 < \xi' \qquad (19)$$

Figure 34

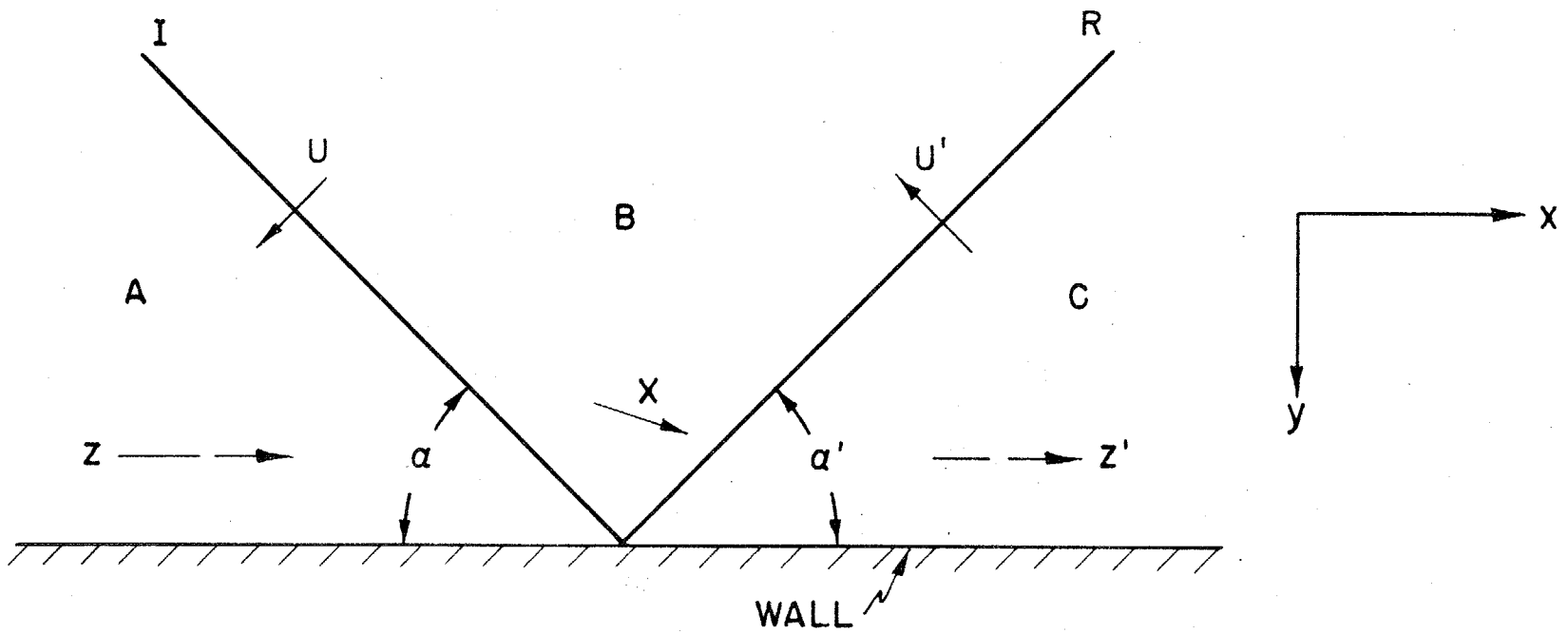

The velocity components in A & C in units of the sound velocity in B, normal to I and R are $|\vec{z}| \sin\alpha = \tau$, $|\vec{z}'| \sin\alpha' = \tau'$ i.e.

$$|\vec{z}| = \frac{\tau}{\sin\alpha} \quad , \quad |\vec{z}'| = \frac{\tau'}{\sin\alpha'} \tag{20}$$

In our present units I, R modify the velocities of the substance which crosses them by the amounts

$$\omega = \frac{|U|}{c_0} \quad \text{and} \quad \omega' = \frac{|U'|}{c_0}$$

respectively.

If we denote the components of the velocity $\vec{X}$ in B by x and y and then calculate these components by passing into B through I and then through R, we obtain:

Through I: $x = \frac{\tau}{\sin\alpha} + \omega \sin\alpha$, $y = -\omega \cos\alpha$

Through R: $x = \frac{\tau'}{\sin\alpha'} + \omega' \sin\alpha'$, $y = +\omega' \cos\alpha'$

Combining these relations

$$\frac{\tau + \omega \sin^2\alpha}{\sin\alpha} = \frac{\tau' + \omega' \sin^2\alpha'}{\sin\alpha'} \tag{21}$$

$$-\omega \cos\alpha = \omega' \cos\alpha' \tag{22}$$

where by (15) for an ideal gas

$$\omega = \frac{U}{c_0} = \frac{2(\xi - 1)}{\sqrt{2\gamma[(\gamma+1)\xi + (\gamma-1)]}} \quad , \quad \omega' = \frac{U'}{c_0} = \frac{2(\xi' - 1)}{\sqrt{2\gamma[(\gamma+1)\xi' + (\gamma-1)]}} \tag{23}$$

and from (3) and (12) for an ideal gas

$$\tau = \frac{V}{c_0} = \frac{(\gamma-1)\xi + (\gamma+1)}{\sqrt{2\gamma[(\gamma+1)\xi + (\gamma-1)]}}$$

$$\tau' = \frac{V'}{c_0} = \frac{(\gamma-1)\xi' + (\gamma+1)}{\sqrt{2\gamma[(\gamma+1)\xi' + (\gamma-1)]}} \tag{24}$$

A more convenient form of (21) is obtained if we introduce a new variable σ

where $\sigma = \omega + \tau$ i.e. by the definitions and by (3) $\sigma = \frac{v_0}{v}\tau$.

$$\frac{\sigma - \omega \cos^2\alpha}{\sin\alpha} = \frac{\sigma' - \omega' \cos^2\alpha'}{\sin\alpha'} \tag{21'}$$

where for an ideal gas

$$\sigma = \sqrt{\frac{(\gamma+1)\xi + (\gamma-1)}{2\gamma}} \quad , \quad \sigma' = \sqrt{\frac{(\gamma+1)\xi' + (\gamma-1)}{2\gamma}} \tag{25}$$

Equations (21') and (22) in conjunction with (23) and (24) relate the shock strengths ξ , ξ' , to the angles of incidence and reflection α , α' so that given ξ , α , the quantities ξ' , α' can be obtained.

Eliminating α' from (21') and (22), using (23) we find an expression for σ' in terms of σ and α .

$$(\gamma+1)\sigma^4 \cdot \sigma'^4 - \left\{ 2(\gamma+1)^2\sigma^4 + 4\gamma\sigma^2(\sigma^2-1)\cos^2\alpha + \sigma^2\left[(\gamma-1)\sigma^2+2\right]^2 \operatorname{ctn}^2\alpha \right\} \sigma'^2$$
$$+ \left\{ (\gamma+1)^2\sigma^4 - 4(\sigma^2-1)^2\cos^2\alpha + \left[(\gamma-1)\sigma^2+2\right]^2 \operatorname{ctn}^2\alpha \right\} = 0 \tag{26}$$

The condition (22) in conjunction with (25) yields the relation for α' in terms of σ', σ and α .

$$\cos\alpha' = \frac{1/\sigma - \sigma}{1/\sigma' - \sigma'} \cos\alpha \tag{27}$$

There are, in general, two solutions for ξ', α' given ξ , α : one has greater values for ξ', α', the other lower values for ξ', α'. For each value of the shock strength ξ , however, there is a maximum value of α (i.e. $\alpha_{ext.}$) at which these two solutions coalesce and beyond which there is no two shock solutions of the type predicated. For reasons cited in Section 10.2, the less steep solution is the one considered physically admissible.

We will now discuss briefly the question of the existence of two solutions and the coalescence of these two solutions as the critical angle of incidence $\alpha_{ext.}$ is approached. Rewriting (26)

$$x^2 - Bx + C = 0 \tag{28}$$

where: $\sigma'^2 = \dfrac{(\gamma+1)\xi' + (\gamma-1)}{2\gamma} > 1 \quad , \sigma' > 1$

$$B = 1 + \frac{4\gamma(\sigma^2-1)^2}{(\gamma+1)^2\sigma^2}\cos^2\alpha + \frac{1}{\sigma^2}\left[\frac{(\gamma-1)\sigma^2+2}{(\gamma+1)}\right]^2 \operatorname{ctn}^2\alpha$$

$$C = 1 - 4\frac{(\sigma^2-1)^2}{(\gamma+1)\sigma^4}\cos^2\alpha + \frac{1}{\sigma^4}\left[\frac{(\gamma-1)\sigma^2+2}{(\gamma+1)}\right]^2 \operatorname{ctn}^2\alpha$$

$$\sigma^2 = \frac{(\gamma+1)\xi + (\gamma-1)}{2\gamma} \quad , \quad 1 > \sigma > \sqrt{\frac{\gamma-1}{2\gamma}}$$

$$\chi = \sigma'^2 = \frac{B}{2}\left\{1 \pm \left(1 - \frac{4C}{B^2}\right)^{1/2}\right\} \tag{29}$$

Now if $\dfrac{4C}{B^2} \lessgtr 1$; $<$ two solutions exist (corresponds to regular reflection).

$=$ one solution exists (corresponds to critical angle).

$>$ no real solution exists (30)

These three conditions can be met. To see this, since C and B are continuous functions, we need only show that the $\gtrless$ conditions are met at least at two points.

At $\alpha = 90^\circ$, $B = 1$, $C = 1$, so that $\dfrac{4C}{B^2} > 1$ and for

$$\alpha << 90^\circ, \; B \cong \frac{1}{\sigma^2}\left[\frac{(\gamma-1)\sigma^2+2}{(\gamma+1)}\right]^2 \operatorname{ctn}^2\alpha, \quad C = \left[\frac{(\gamma-1)\sigma^2+2}{(\gamma+1)}\right]^2 \operatorname{ctn}^2\alpha$$

so that $\dfrac{4C}{B^2} \cong \dfrac{4}{\left(\frac{(\gamma-1)\sigma^2+2}{(\gamma+1)}\right)^2 \operatorname{ctn}^2\alpha} < 1$

and the three criteria (30) can be met.

Using the values of σ' and the assumed value of σ and α we can find the corresponding values of α' by means of (27).

$\alpha_{ext.}$ obtained from $=$ in (30) is given by the following equation

$$\begin{aligned} &16\gamma^2(\sigma^2-1)^4 y^3 - \left\{16(\gamma+1)^2(\gamma\sigma^2+1)(\sigma^2-1)^2 + 16\gamma^2(\sigma^2-1)^4 - 8\gamma(\sigma^2-1)^2\left[(\gamma-1)\sigma^2+2\right]\right\} y^2 \\ &- \left\{4(\gamma+1)^2(\sigma^2-1)\left[(\gamma-1)\sigma^2+2\right]^2 - \left[(\gamma-1)\sigma^2+2\right]^4 + 8\gamma(\sigma^2-1)^2\left[(\gamma-1)\sigma^2+2\right]\right\} y \\ &- \left[(\gamma-1)\sigma^2+2\right]^4 = 0 \end{aligned} \tag{31}$$

where $y = \sin^2 \alpha_{ext}$

These equations have been investigated in numerical detail by H. Polachek and R. J. Seeger.[10] Some of their results are embodied in Section 10.2,

(10) Regular Reflection of Shocks in Ideal Gases (AM-524) Feb. 12, 1944.

Figures 20 and 21.

It is of interest to see how the critical angle approaches 90° as the shock becomes sonic.

$$\xi = p/p_0 = \frac{p}{p+p\Delta} = 1-\Delta \ , \ \Delta << 1$$

and by (25) $\sigma^2 - 1 = -\frac{\gamma+1}{2\gamma}\Delta$. Inserting in (31) and neglecting terms in Δ^2

$$y = \sin^2 \alpha_{ext.} = 1 - \frac{2\Delta}{\gamma} \quad \text{or}$$

$$90 - \alpha_{ext.} = \sqrt{\frac{2\Delta}{\gamma}}$$

The critical angle converges to 90° as the shock overpressure approaches zero, the approach to 90° varying as the square root of the shock overpressure.

10.3-5 Mach Reflection

Let us now turn to the case in which regular reflection ceases to be possible.

When α increases beyond $\alpha_{ext.}$ We wish to investigate the case in which regular reflection continues as long as it is possible, i.e., up to $\alpha = \alpha_{ext.}$, and we shall try to determine what happens beyond this point.

That regular reflection is impossible, means that the oblique flow in region B (Figure 34) cannot be deflected by a standing oblique shock R so that it becomes parallel to the wall. This corresponds to the propagation of signals from the shock R, back against the flow X into the region B, a fact well substantiated by the experimentally observed fusion of the incident and reflected

shocks I and R (cf. Section 10.2). Another way of describing the critical angle is to say that it is the greatest angle at which the components of U' and U orthogonally to the wall can be made equal, i.e.

$$U' \cos \alpha' = U \cos \alpha \qquad (32)$$

Beyond this angle, the compensation of the normal components of the flow velocity is no longer possible by such a simple, stationary process. The phenomenon of irregular reflection which is thus produced will not be stationary - even in the frame of reference in which P (and I) is at rest. The wave of impact of X on the wall will propagate from P in all directions and thus change in "size" at all times and never reach a final equilibrium state. However, while the shock configuration shows a continuous change in size, its shape will be permanent (cf. the comments connected with Figure 28 in Section 10.2). Its size is proportional to the time t that has lapsed since its formation: For $t = 0$ it begins concentrated into a single point.

Since the shocks R and M are advancing into two different media A and B, a discontinuous change of direction of the RM front must be expected at T, (Figure 35). That is, T is really the contact point for three different shocks - I, R, M. The point p_0 is the so-called "center of similitude" from which the phenomenon originates (the "corner" in the sense of the discussion in Section 10.2).

Now consider a frame of reference in which I and T are at rest (Figure 36). The flow $\geq$ * of the substance in A crosses the shock system I, R, M, to finally reach the domain C. However, this process operates in two different ways even in the immediate neighborhood of T: the substance in A above the line ll crosses into C through two shocks I and R; while the substance in A below ll crosses into C through one shock M. Since we assume no shocks beyond R, M (in C), both processes must compress the substance to the same pressure. But this compression occurs in the "upper" half in two stages (I, R) and in the "lower" half in one (M). The former process is less irreversible than the latter - essentially because it is less abrupt. Hence the substance which

Figure 35

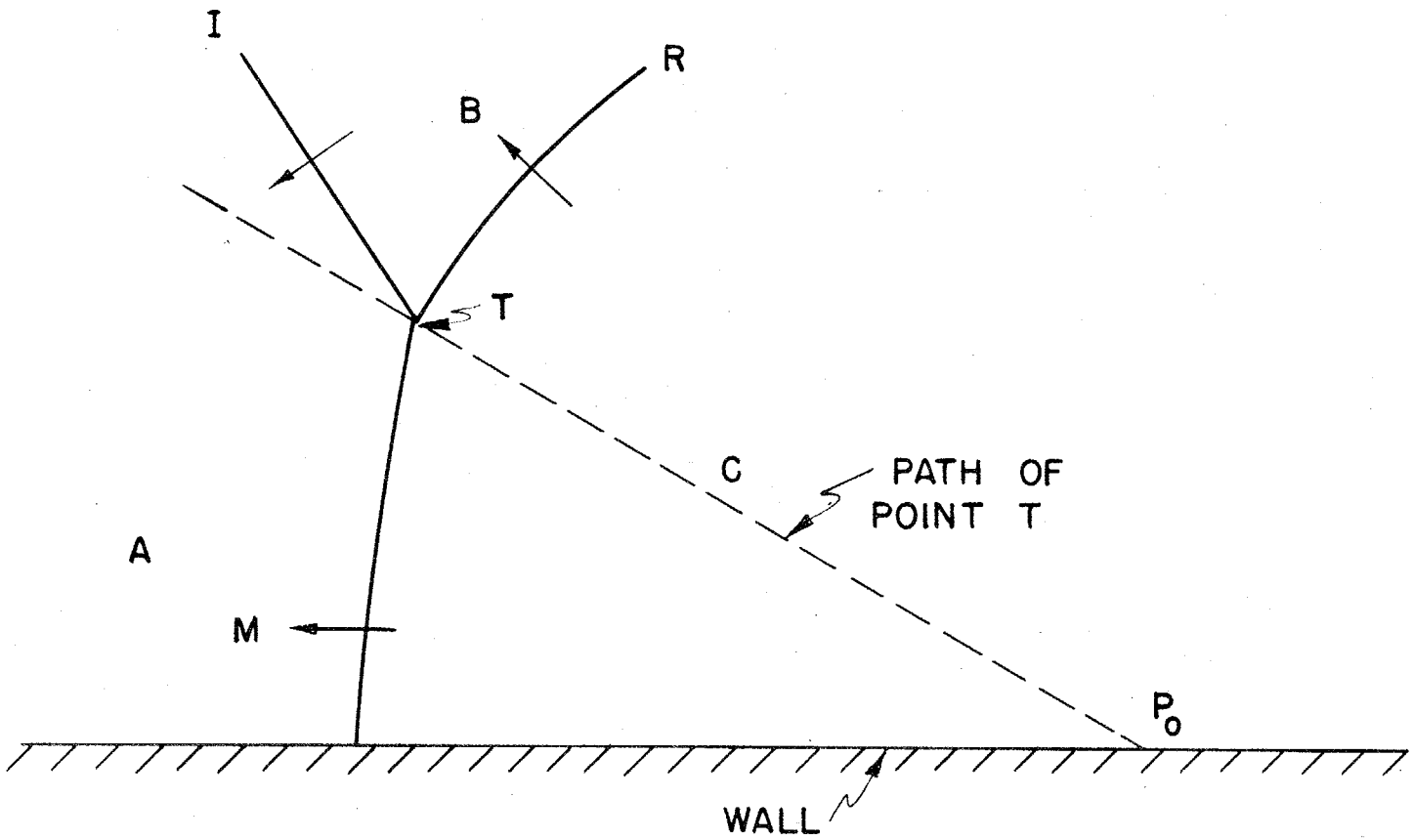

Figure 36

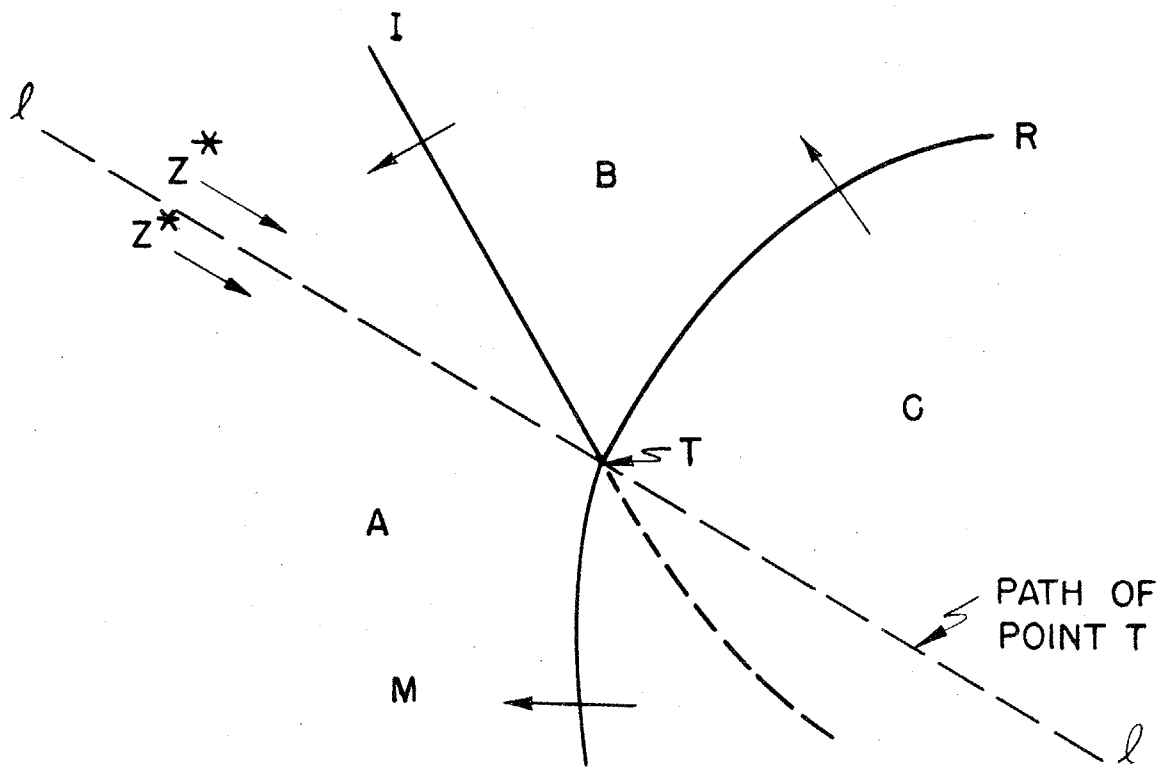

crossed "above" T may be expected to have a lower entropy than that which crossed "below" T. Thus we have in C near T two flows: both with same pressure, but the "upper" flow has lower entropy. Since the two flows have the same pressure, but the "upper" flow has the lower entropy, therefore it must also have the lower temperature, i.e. inner energy, and the higher density. Again, since it has the lower inner energy, it follows from Bernouilli's principle that it must have (in this frame of reference) higher kinetic energy, i.e. velocity. Therefore these two flows must be gliding past each other along a dividing line D issuing from T. So D is a slipstream, and also a discontinuity-line for entropy, temperature and density, but not for pressure. We therefore have a pattern consisting of four discontinuity lines I, R, M, D, all confluent in T: the three shocks I, R, M, and the slipstream D (Figure 37).

That D is a slipstream and not a shock is indicated by the experimentally observed large angles between M and D and the requirement that the flow into a shock be supersonic with respect to the medium into which the shock travels (cf. rule A). The flow is subsonic behind M and it is inconceivable that it can become rapid enough before reaching D that its component across D should be supersonic.

Since the existence of the extra shock, M, and the irregular reflection its presence implied was first recognised by Mach, it seems appropriate to give his name to this type reflection. We shall therefore designate irregular reflection according to the scheme of Figure 37 as Mach reflection.

10.3-6 Three Shock Solutions

On the basis of the above it would seem indicated that a theoretical investigation of Mach reflection should be undertaken. For regular reflection Figure 34 provided the basis for theoretical discussion. For Mach reflection Figure 37 may seem to provide the basis in the same sense, and therefore we have to see what possibilities of a theoretical treatment it offers.

Figure 37

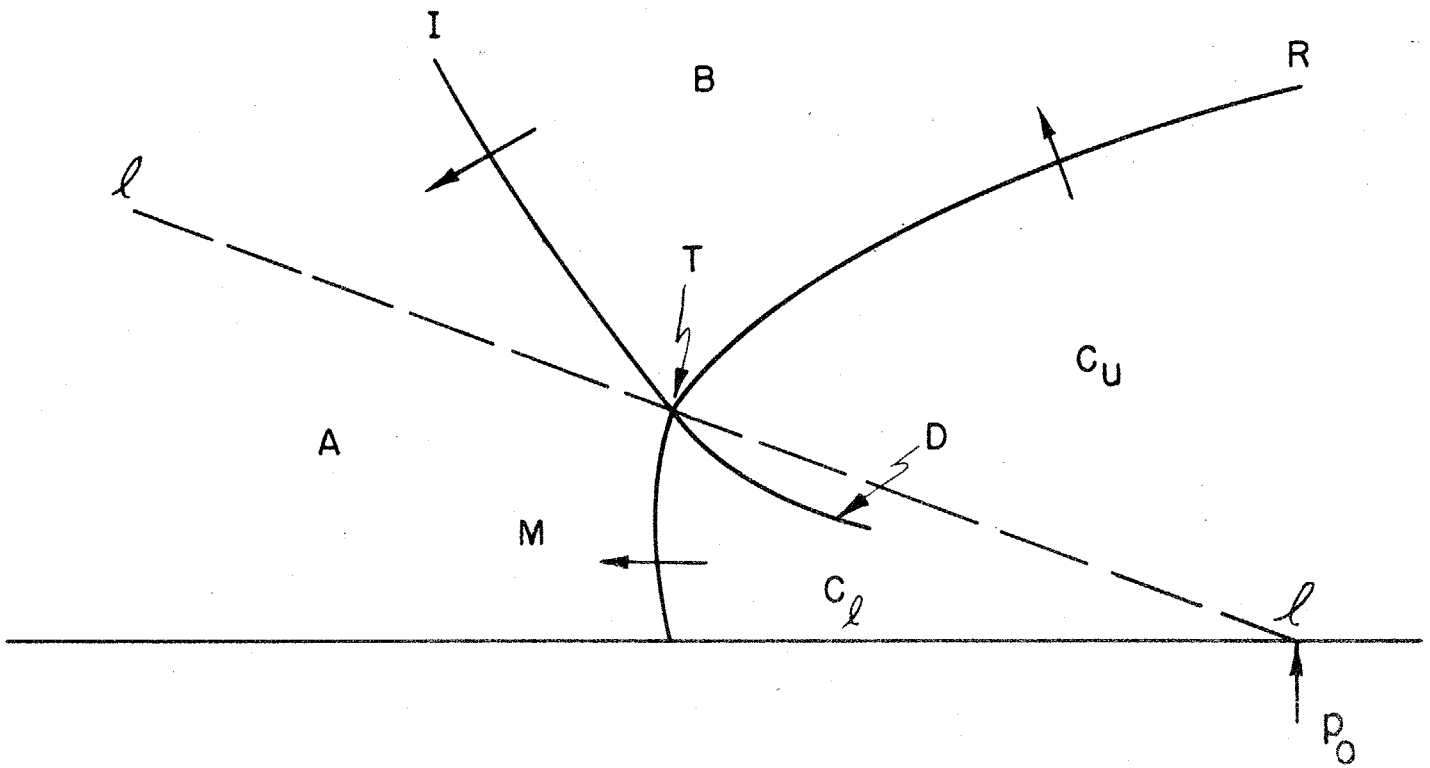

The theoretical treatment of regular reflection was greatly simplified by the fact that conditions in each one of the three domains A, B, C of Figure 34 were constant. We needed only to discuss the purely algebraical connections between them by applying the Rankine-Hugoniot conditions to the straight shocks I,R, which separate them.

In Figure 37, conditions in the domain C_u are certainly not constant and the shock R is certainly curved.

Probably the same is true for the domain C_ℓ, the shock M and the slip-stream D. Thus we must resort to the differential equations of compressible fluid dynamics, aggravated by the appearance of curved shocks, which introduce varying amounts of irreversibility.

It would, however, be pointless to attack these difficult partial differential equations, without having first ascertained the nature of the conditions at the boundaries of the areas in which they apply. These areas are C_u and C_ℓ. The boundaries are the lines R, M, D, and the point T at which they all meet is one of particular interest.

The Rankine-Hugoniot conditions take care of the situation along R and M. For the slipstream D we must require that it be a streamline in C_u as well as in C_ℓ and that at each point the pressure on its C_u side be the same as on its C_ℓ side, but we must also reconcile all these requirements at the point T, where R, M, D meet. Therefore a discussion of the conditions at T is a necessary preliminary of any theoretical treatment of Figure 37.

The discussion of conditions in the immediate neighborhood of T is best done in the frame of reference where T (and I) is at rest. This is the scheme of Figure 37 except that we may replace the lines I, R, M, D by their tangents at T - i.e. we may assume them to be straight.(Figure 38).

The following remarks are now in order:

(1) The velocity vector Z* of the incoming flow in A is determined by the strength of the incident shock I and the orientations of I and the wall.

Figure 38

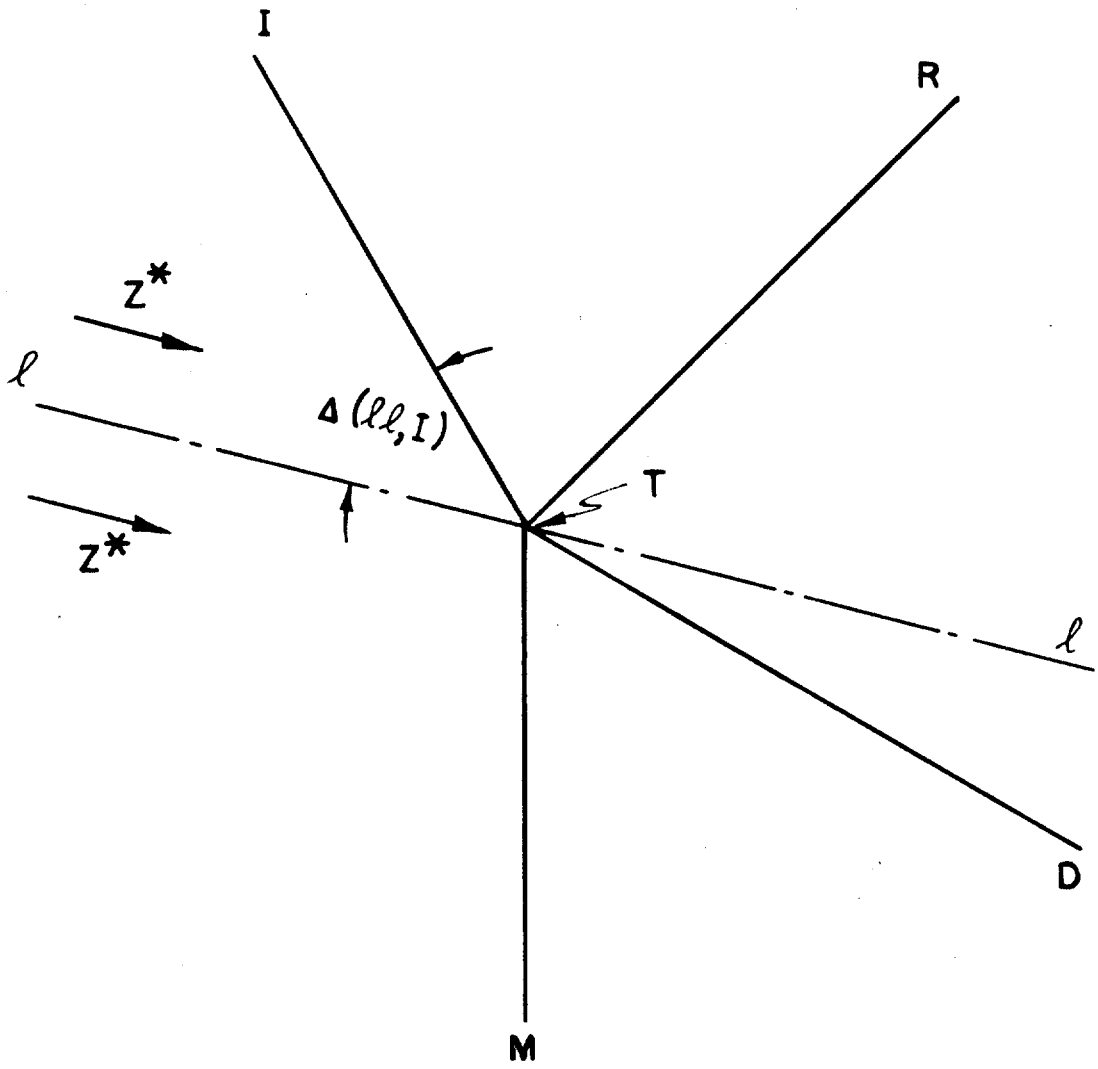

Indeed, the former determines the velocity of the flow normal to I on the A side. We know that Z* has the direction of $\ell\ell$, and so the statement about the normal component amounts to $|Z^*| \sin(\Delta[\ell\ell, I])$: V completing the determination of Z*.

(2) The four discontinuity lines I, R, M, D divide the field into four sectors A, B, C_u, C_ℓ. Assuming continuity within each one of these sections, we may even treat them as domains of constant conditions, since we are investigating an immediate (infinitesimal) neighborhood of T only. Thus we have a situation in which straight shocks delimit domains of constant conditions. The resulting problem is therefore again only one of applying the Rankine-Hugoniot conditions (and those of a slipstream), involving no differential equations.

Considering the importance of this conclusion, it is essential to re-emphasize the assumption on which it is based; continuity in each section A, B, C_u, C_ℓ at T. Let us see what the basis of this assumption is.

The main reason is the experimentally established aspect of Figure 37 which shows the lines I, R, M, D, and no others. Hence there are certainly no lines of discontinuity across either sector A, B, C_u, C_ℓ. However, this is not the only possible type of discontinuity. Thus a supersonic flow around a convex corner "turns" in a manner, where the state at each point is a function of the direction from the corner to that point. In this way there is a discontinuity at the corner, but nowhere else. This Meyer discontinuity or angular discontinuity was discovered by Prandtl[11] and Meyer[12].

---

(11) Phys. Zeitschrift, Bd. 8, p. 23 (1907).

(12) Forschungsarbeiten auf dem Gebiete des Ingenieurwesens, V.D.I. Heft 62 (1908).

There are reasons which make the appearance of an angular discontinuity under the conditions prevailing at T not at all improbable. Without discussing them, we point out this: the angular discontinuity is unlikely in the sector C_ℓ because the flow there is in many cases subsonic[13]. It is unlikely in A,

(13) cf. discussion of Prandtl-Meyer angular discontinuity in article by Taylor and MacColl, previously cited (footnote 4).

because A is ahead of the incident shock I, which is the "signal" of the approaching disturbance, and therefore A ought to be entirely undisturbed. It is unlikely in B, because B (while behind I) is ahead of the reflected shock R, which is the "signal" of I having run into an obstacle, and therefore B ought to be unaffected by any reflection phenomena. Hence the angular discontinuity, if there is one at all, should be in C_u.

We shall point out that the assumption of continuity at T is in many cases untenable, because the conclusion conflicts with experience. We shall point out further that an angular rarefaction in C_u does not appear to be able to resolve the difficulty. It may be, that there is one in B, i.e. that R is not the "first signal" of reflection. (In some, but not in all cases even A and C_ℓ may be questioned.) Alternatively, existing theory does not allow us to rule out entirely the possibility of point-discontinuities at T which are not angular discontinuities. The situation is obscure. However, in order to understand the situation and its difficulties, we must first follow up the assumption of continuity at T, following the scheme pictured in Figure 38.

The general procedure to be followed would be this: Knowing the strength of the incident shock I and the orientations of all five lines I, R, M, D and $\ell\ell$, we can follow Figures 37 and 38 and apply the conditions of Rankine-Hugoniot and those of a slipstream. The former determine by themselves the situation in C_u and in C_ℓ, i.e. on both sides of D. The slipstream condition then requires

that the substance velocity on both sides of D must be parallel to D and that the pressure must be the same on both sides of D. Thus we obtain three equations.

If the orientation of $\ell\ell$ is unknown, we can eliminate it, and still have two equations. If the strength of I is unknown (but the "undisturbed" state in A - p,v, but not the velocity Z* - is known), we can eliminate it, too, and still have one equation.

We call the solutions for the immediate neighborhood of T - according to Figure 38, and with the assumption of continuity - the three shock solutions.

Thus measurements made on a shadow photograph of the type of Figure 32 provide data which can be fitted to a three-shock solution only if they fulfill one equation. If the strength of the incident shock I is known, they must even fulfill two equations. Thus a determination of all three-shock solutions allows for a direct empirical verification.

The best specific instance for such a determination is that one of air at moderate pressures (1 to 5 atmospheres), i.e. of an ideal gas with $\gamma = 1.4$. Actually the algebra of this case is rather cumbersome, but a numerical approach is practicable. A numerical survey of three-shock solutions was obtained by S. Chandrasekhar[14], K. Friedrichs[15], and H. Polachek and R. J. Seeger[16].

---

(14) S. Chandrasekhar "On the Conditions for the Existence of Three Shock Waves", Ballistic Research Laboratory, Aberdeen, Report No. 367 (1943).

---

(15) K. Friedrichs, "Remarks on the Mach Effect", Div. 8 and Applied Math. Panel, NDRC (1943).

---

(16) H. Polachek and R. J. Seeger: Reg. Reflect. of Shocks in Ideal Gases AM-524 (1944).

Experiments show disagreements with three-shock solutions.

Thus a conflict between theory and experiment exists at the point T which seems to justify our dropping the assumption of continuity.

In dropping the assumption of continuity we must try to introduce point discontinuities at T. As pointed out an angular rarefaction in C_u would seem to be the most natural solution, but preliminary investigations indicate that this device produces no solution - not even for a weak shock in an ideal gas.

Thus far we have been discussing an infinitesimal region of the shock configuration due to the reflection of a plane shock from a plane surface in the range of irregular reflection. This was a discussion of the boundary conditions designed to indicate the direction the solution of the partial differential equation of compressible fluid flow would take. The essential result is that the nature of the boundary conditions is not yet understood.

Our real interest, however, is not, except in an exploratory sense in the case of an irregularly reflected plane wave but in the irregular reflection of a spherical wave. The discussion for a regular reflection is equally valid in both cases. The theory of the irregular reflection phenomenon is even less understood in this more complicated spherical case. We are therefore forced in our present state of knowledge to rely on certain qualitative notions about the Mach effect coupled with experimental information. The experimental observations on the reflection of spherical blast waves from a plane surface are discussed in the next section.

10.4 EXPERIMENTAL DETERMINATION OF THE HEIGHT OF BURST

The data on which the following discussion is based was obtained from TNT explosions, not nuclear explosions. Therefore, inasmuch as the free air pressure distance curve after taking $W^{1/3}$ scaling into account differs in these two classes of explosions, the results discussed below are not applicable to the blast produced by nuclear bombs. However, it is found that in the range of interest, i.e. 5 to 10 pounds per square inch overpressure a suitable value of W can be found to make the ratio of the peak overpressure produced in the nuclear

explosion to the overpressure produced in the "equivalent" TNT explosion nearly unity. We will be interested in peak pressure only, since this determines the damage caused by large bombs (cf. Section 10.1). For TNT explosions the free air pressure, p (pounds per square inch), in the range of interest is given by

$$p = \frac{206}{(r/W^{1/3})^{1.5}} \qquad (33)$$

for W pounds of TNT
r = distance from explosion feet

Nuclear explosions as calculated on the IBM have a free air pressure distance dependence which can be represented in the region 5 to 10 pounds per square inch to within 7 per cent by

$$p = \frac{c}{(r/W^{1/3})^{1.5}} \qquad (34)$$

If we choose c = 206, then W is the "equivalent" tonnage for the pressure range 5 to 10 pounds per square inch. There is no equivalent tonnage in the sense that the pressure-distance curves for TNT and a nuclear explosion can be made everywhere identical by the choice of an appropriate value of energy released in the form of blast. With this in mind we will now proceed to construct tables of heights of burst by scaling experimental data on the reflection of blast waves due to TNT explosions. The following discussion refers to 1 pound of TNT; lengths and durations are greater for an explosion of W pounds of TNT by a factor $W^{1/3}$.

10.4-1 Determination of Triple Point Trajectory[17] (See Figure 39)

[17] The experimental data summarized by Halverson is used here, OSRD Report 4899. The reader is also referred to A. H. Taub, OSRD Report 6660 " The Effect of Height of Burst on the Blast from Explosives" Confidential, 1946, and OSRD Report 4945 "Airburst from Blast Bombs" Symposium, 1945.

In the region of regular reflection $D < D_0$ ($\alpha < \alpha$ extreme), the sphericity of the shock front introduces no deviations from the results obtained for plane waves because of the local character of the reflection phenomenon.

Figure 39

Spherical shock reflected from rigid wall

$\alpha_{ext} = f\left[p\left(\frac{q}{wv_s}\right), \frac{d}{wy_s}\right]$, given by theory of regular reflection

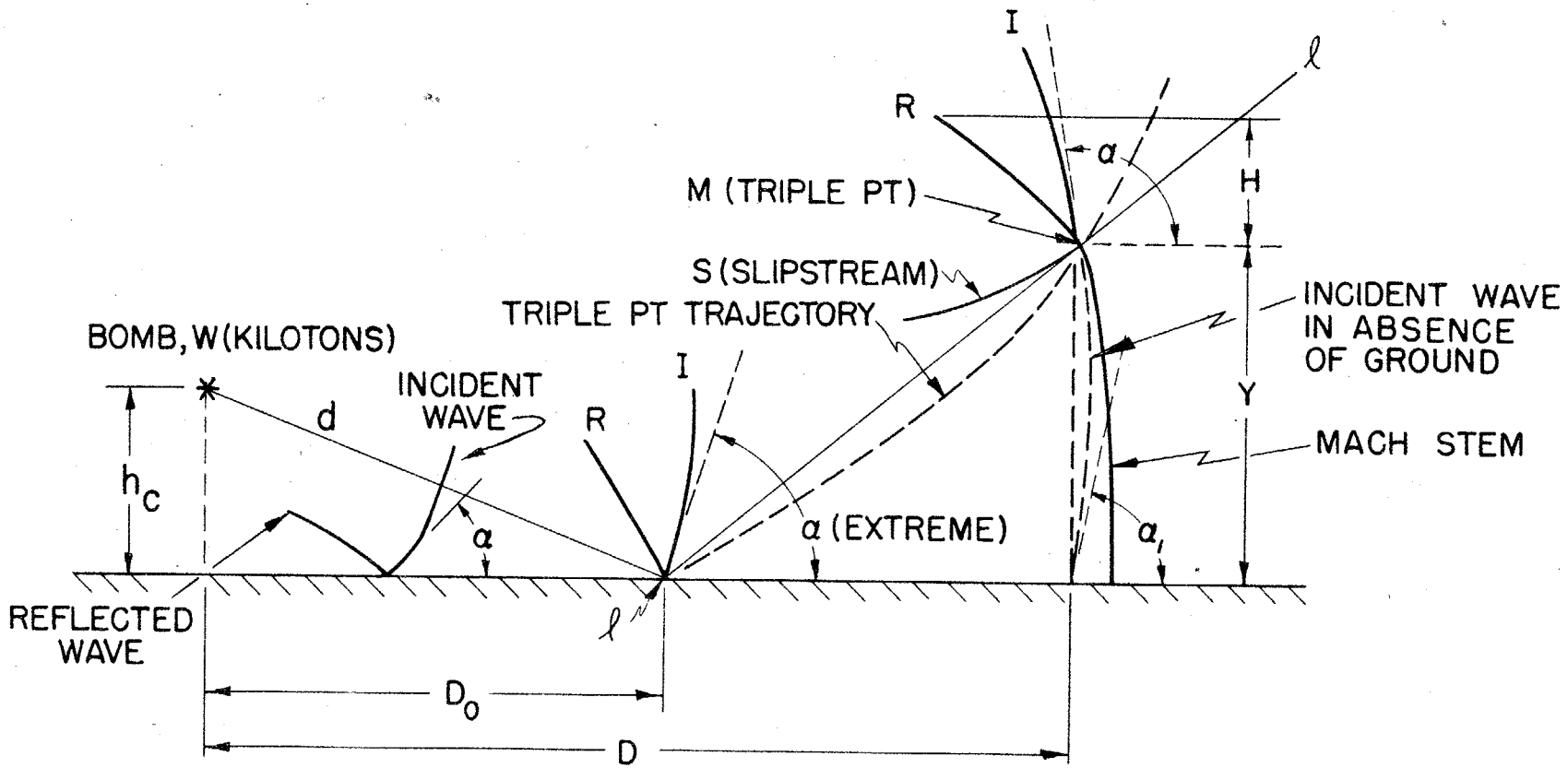

Therefore, we can use regular reflection theory and shock tube experiments to determine the dependence of D_o on the height of burst (Figure 40).

For the case of irregular reflection the situation was studied experimentally. In particular, the triple point was located as follows: gages were placed at various heights (H + Y) and a fixed horizontal distance, D, from the explosion and the differences in the time of arrival between the direct (I) and reflected (R) shocks were noted. An extrapolation of this time to zero gave the height of the triple point for each height of burst. By repeating the procedure for various heights of burst and then scaling the results down to 1 pound of TNT curves of Y versus h_c for various values of D were obtained (Figure 41).

It is more convenient to have a plot of the height of burst h_c as a function of the horizontal distance from the explosion for various selected stem heights y (Figure 42). The stem heights were so chosen that they scaled up to 30 and 100 feet for various tonnages of TNT.

10.4-2 Optimum Height of Burst for Peak Pressure

Knowing the geometry of the Mach effect, the next problem is to connect it with a choice of the heights of burst which maximize the area over which the pressure exceeds a chosen set of values.

Suppose we are interested in the height of burst, h_c , which makes the peak overpressure, p, on the ground, occur at the greatest horizontal projected distance, D. The procedure would be to measure p (D) for each value of h_c and then to plot $D(h_c)$ for selected values of p. Such experiments have been performed using TNT[18] and the results $D(h_c)$ for selected values of p, are

(18) Various reports of Division 2 NDRC, by A. H. Taub and W. T. Read.

incorporated in Figure 42. That h_c, for which $D = D_{max}$, is then the height of burst which yields the greatest distance to a point on the ground for which

Figure 40

Theoretical limits for regular reflection versus charge height

(w = 1 lb TNT) (after Halverson)

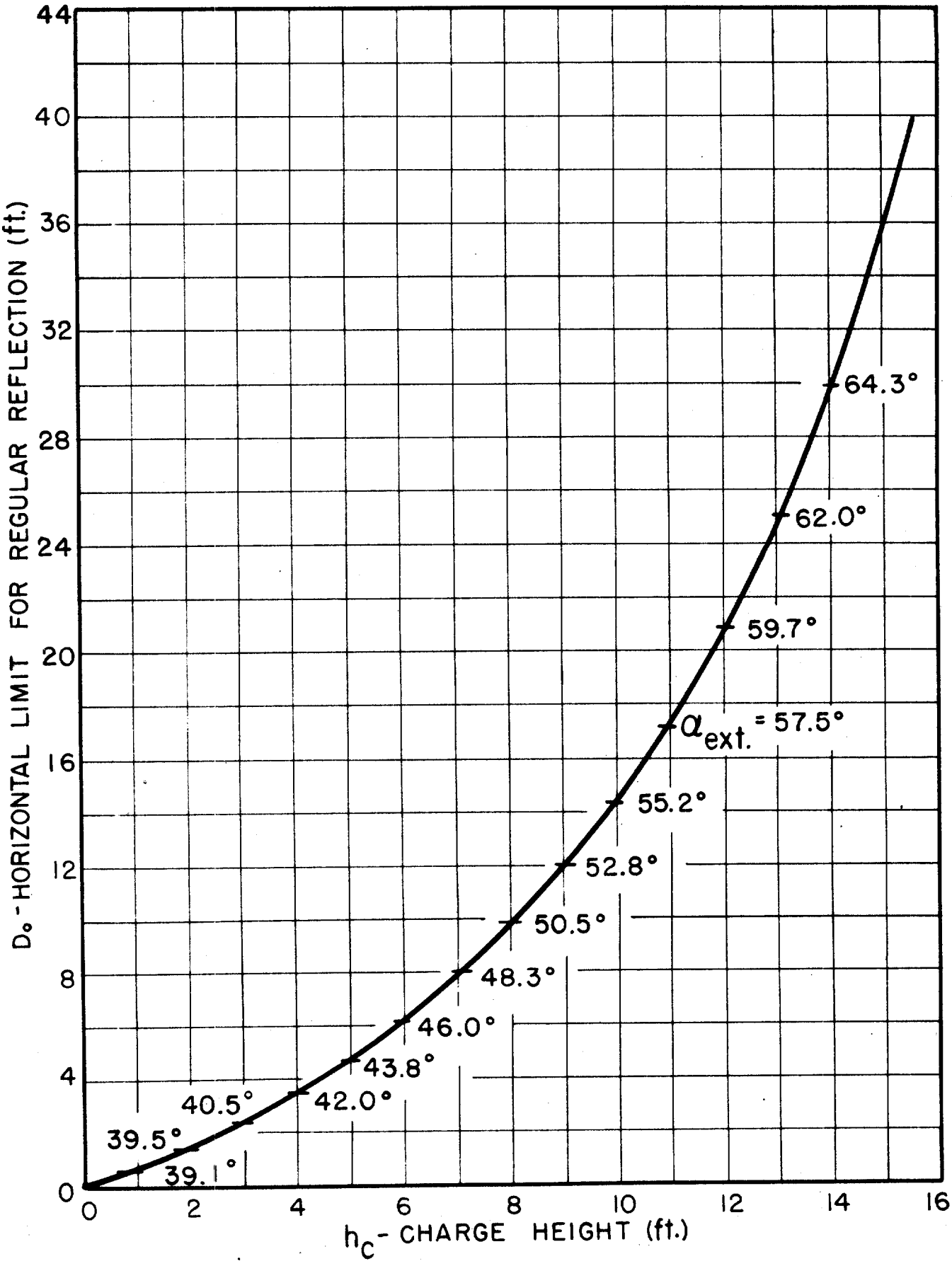

Figure 41

Stem height versus horizontal distance for a given charge height (h_c) (W = 1 lb TNT) after Halverson

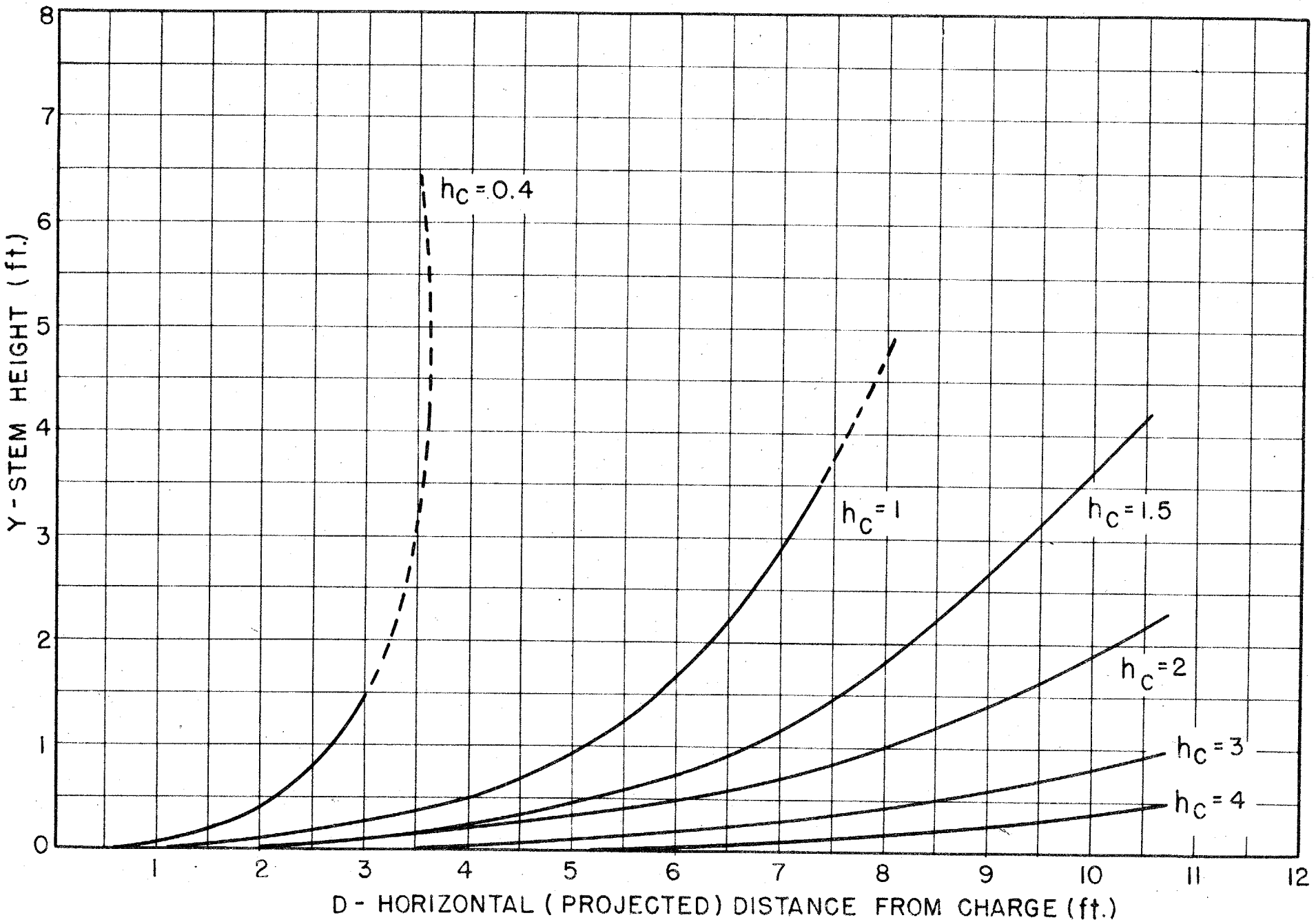

Figure 42

Height of burst versus horizontal distance for a given stem height and overpressure

W = 1 lb TNT
D = horizontal projected distance (feet)
h_c = charge height (feet)

a = 1.00 ft	f = .33 ft
b = .80	g = .29
c = .63	h = .25
d = .46	i = .20
e = .37	j = .15
	k = .08

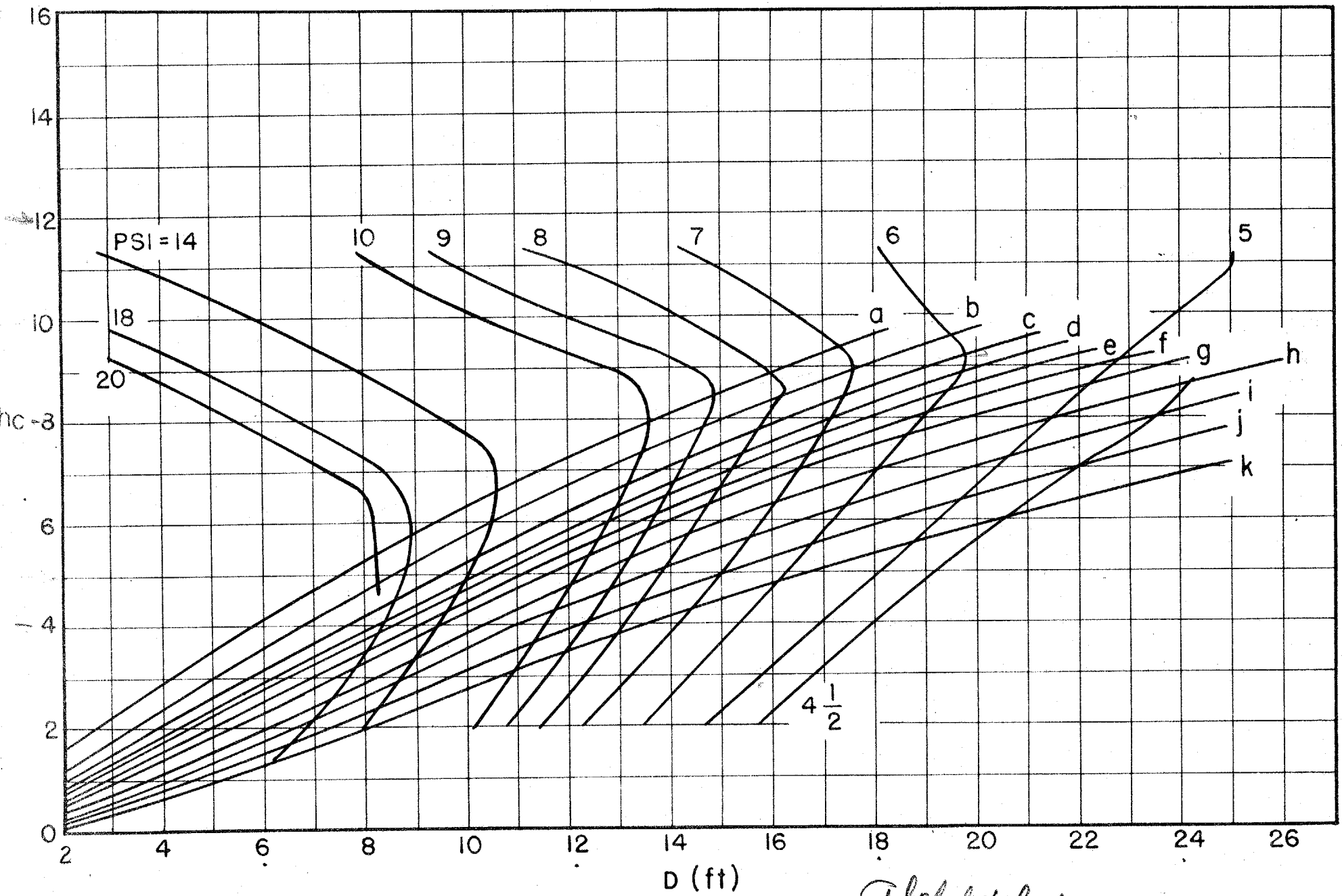

Alphabet backwards

APPROVED FOR PUBLIC RELEASE

the peak pressure has a prescribed value.[19] This value will, in general, be

---

(19) It might be stated that a better scheme now exists than that which was used for obtaining the pressure (on the ground) versus distance curves for an elevated nuclear bomb. The idea is to first deduce the reflection coefficients for chosen overpressures and angles of incidence from the measurements made on TNT and then apply these results to the free air blast curve from the nuclear bomb. The main reason this was not done in determining the height of burst is that the IBM runs which give the free air overpressure, distance curves for the nuclear bomb were not yet carried out when the height of burst tables were made up.

---

in the region of Mach reflection. If we choose, instead, to determine the height of burst by requiring that the stem of the Mach Y have a prescribed height, y, at a given peak pressure, then for this value of h_c it is, in general, true that $D < D_{max}$. The advantage gained by basing h_c on y is that the pressure is increased, not only on the ground but over a vertical region coinciding with the Mach Y as well. In this way, the average pressure exerted by the blast on a structure is increased, resulting in increased destruction in regions where the pressure is marginal. The problem is somewhat complicated by the variation of pressure along the stem of the Y. A 15 to 25 per cent decrease in pressure occurs in traversing the stem of the Y from the ground to the triple point. Because of this variation the mean pressure along a chosen vertical strip is not rigorously maximized by making the stem of the Y just tall enough to cover it. As a working approximation, however, we will choose the height of burst so as to achieve a desired stem height at a chosen peak overpressure. By using a $W^{1/3}$ scale factor, Tables 10.4-2 (a), 10.4-2 (b) were prepared for various tonnages of TNT. These tables give the heights of burst necessary to obtain stem heights of 30 and 100 feet at various chosen peak overpressures. The distances at which these stem heights are obtained are also listed.

Table 10.4-2 (a)

Y = 30 ft.

Height of Burst and Radius at which Stem of Mach Y = 30 ft. and Overpressure Exceeds Given Values for Various Kilotons of TNT

p (psi)	W = 0.5 Kilotons	W = 1.0	W = 2.0	W = 5.0	W = 10	W = 20	W = 100
20 h_c (ft)	----	----	----	900	1300	1650	3100
d (ft)	----	----	----	1800	2200	2800	4800
18 h_c	350	450	650	950	1400	1750	3400
d	800	1000	1300	1800	2400	3000	5200
14 h_c	400	600	800	1150	1600	2000	3900
d	950	1250	1600	2200	2800	3600	6200
10 h_c	550	750	1000	1450	2000	2500	4700
d	1250	1600	2100	2800	3600	4600	8000
9 h_c	600	800	1000	1550	2100	2700	5000
d	1350	1700	2200	3100	4000	5000	8700
8 h_c	650	900	1150	1650	2300	2900	5200
d	1500	1900	2400	3400	4400	5500	9300
7 h_c	700	950	1250	1800	2400	3100	5500
d	1650	2100	2700	3700	4800	6000	10000
6 h_c	800	1100	1400	2000	2600	3300	5900
d	1900	2500	3100	4200	5300	6600	11000

Table 10.4-2 (b)

Y = 100 Ft.

Height of Burst and Radius at which Stem of Mach Y = 100 ft. and Overpressure Exceeds Given Values for Various Kilotons of TNT

p (psi)		W = 0.5 (Kilotons)	W = 1.0	W = 2.0	W = 5.0	W = 10	W = 20	W = 100
18	h_c (ft)	150	200	300	500	800	1200	2300
	d (ft)	600	800	1100	1500	2000	2700	4900
14	h_c	200	300	450	700	1100	1500	2900
	d	800	1000	1400	1900	2500	3300	5900
10	h_c	300	450	650	1000	1400	1900	3700
	d	1100	1400	1800	2600	3300	4300	7500
9	h_c	350	500	750	1100	1500	2100	3600
	d	1200	1500	2000	2800	3600	4700	8200
8	h_c	400	550	800	1200	1700	2300	4300
	d	1300	1700	2200	3100	4000	5200	9000
7	h_c	450	600	900	1350	1900	2500	4600
	d	1400	1900	2500	3400	4400	5700	10000
6	h_c	500	700	1000	1500	2000	2800	5200
	d	1600	2100	2800	3900	5000	6500	11500
5	h_c	550	800	1150	1700	2300	3100	----
	d	1900	2500	3300	4600	6000	7800	----
4½	h_c	600	900	1250	1900	----	----	----
	d	2000	2800	3700	5200	----	----	----

10.5 CONCLUSION: THE HEIGHT OF BURST

In this concluding section we will bring the material discussed in the preceding four sections to bear on the problem of determining the height of burst which results in the greatest area of blast damage. There are two arguments which favor an air burst quite apart from the influence of oblique reflection. First, a bomb burst close to the ground is accompanied by cratering and melting of the ground and hence a loss of energy to the blast. Second, an air burst avoids much shielding of one structure by another. An undesirable feature of air burst is, of course, the fact that the bomb is further removed from the target than it would be if it were burst on the ground. A compensating feature is the fact that the high pressure region of a bomb burst on or close to the ground would over-destroy the target in the near vicinity of the bomb. This local overdestruction represents an unnecessary expenditure of energy on nearby parts of the target region which decreases the destruction inflicted on more remote structures. The reduction in blast pressure due to elevating the bomb is of course more serious for parts of the target which were in immediate contact with the ground burst bomb -- they become removed by at least the height of burst. For more distant parts of the target the effect of raising the bomb off the ground is less important, and at distances which are two or three times greater than the height of burst the change in distance from bomb to target due to elevating the bomb is completely unimportant in its effect on the pressure at the target.

Judging from the results obtained in the low burst (100 feet) at Trinity, it is possible to set reasonable lower limits on the height of burst required to minimize some of the above blast reducing effects due to the proximity of the ground.

If it is desired to avoid fusing earth and structural materials, then since the radius of the area over which the earth was fused at Trinity was

about 1,000 feet, the height of burst h_f which will avoid such fusing is

$$h_f > 1{,}000 \text{ feet} \qquad (35)$$

This number is for an energy release in the form of radiant energy of 3 kilotons of TNT and, since one may use an inverse square law for such radiative effects, the height of burst which will avoid fusing will be related to the tonnage released as radiant energy W_r (kilotons TNT) by the inequality

$$h_f > 1{,}000 \left(\frac{3}{W_r}\right)^{1/3} \qquad (36)$$

This calculation assumes no attenuation of the beam due to absorption. It is not possible to state what proportion of the nuclear energy will be released as radiant energy without knowing the design details of the bomb. To date no such calculation has been carried out because of the extreme complexity of the problem. However, the Trinity figures give a useful indication of the proportion of energy that appears as radiation.

$$\frac{W_r}{W_b} = \frac{3}{10} \qquad (37)$$

As a rough rule then, to avoid fusing

$$h_f > \frac{10^4}{(10 W_b)^{1/2}} \qquad h_f > 316\, W_b^{\frac{1}{2}} \qquad (38)$$

where h_f = height of burst in feet to avoid fusing,

W_b = blast energy in kilotons TNT.

The available evidence on cratering from air burst bombs is very fragmentary. Indeed, because of the extremely high pressures and great duration of the blast from a nuclear explosion it is not possible in our present state of knowledge to interpret, in any complete way, data on cratering from ordinary explosives so that it will apply to nuclear explosives. The only data on

cratering by a nuclear explosion is that obtained at Trinity where the bomb was detonated at a height of 100 feet: A compression crater 10 feet deep in the center and 500 feet in radius was formed in the close packed sand of the New Mexico desert. Using this point and the data in the Weapons Manual as a guide, it appears extremely unlikely that any cratering at all would have occurred had the charge been detonated at a height of 250 feet.

$$h_{no\ crater} > 250 \text{ feet} \qquad \text{for } W_b = 10 \text{ kilotons TNT}^{(20)}$$

(20) It is not possible to match everywhere the blast from a nuclear explosion by the blast from a suitable quantity of TNT. At small distances the pressures developed in the nuclear explosion greatly exceed any pressures developed in a chemical explosion. In addition, the nuclear explosion is very much more rapid than a chemical explosion and does not feature afterburning of the constitutents so characteristic of the latter. Because of this, and the finite size of the mass of TNT as opposed to that of the nuclear explosive, the shape of the blast wave and hence its decay as it travels outward is also different in the two cases. Despite this, it is possible to find (cf. Section 10.4) a quantity of TNT which is equivalent to the nuclear explosive in the sense that the peak overpressure, distance characteristic is nearly the same over a small range of overpressure, say from 5 to 10 pounds per square inch. The Trinity value $W_b = 10$ kilotons TNT equivalent is for distances where the overpressure is in the range 5 to 20 pounds per square inch. Since the ground was close, the energy effective in producing a crater was greater than 10 kilotons and hence the assumption of 10 kilotons amounts to saying that the ground is easier to crater. The value for $h_{n.c.}$ is therefore probably too high.

scaling for an explosion of blast tonnage W_b (kilotons TNT)

$$h_{n.c.} > 120\ W_b^{1/3} \tag{39}$$

where $h_{n.c.}$ = height of burst in feet to avoid cratering.

From the above considerations the height of burst h_{min} to minimize the reduction in blast due to the proximity of the ground may be estimated as

$$h_{min} > h_{n.c.} \text{ or } h_f, \text{ whichever is greater.} \tag{40}$$

The question of the value of h required to minimize overdestruction of the

target is sensitively dependent on the details of the target. Given the pressure which is considered as the limit beyond which overdestruction sets in, a reasonable value of the minimum height of burst can be obtained from the pressure distance curve in free air (cf. Chapter 7 of this volume), and the multiplication of pressure on reflection from the ground, considering the blast wave to be normally incident on a rigid ground.

Now let us consider the effect of reflection on the pressure in the blast from a bomb burst high ($h > h_c$) in the air. Directly under the bomb a reflection from the ground partly compensates for the loss in overpressure due to the increase in distance from the bomb to the target area which accompanies air burst. The gain in overpressure occasioned by the reflection of a normally incident shock is a factor which would be 2 if the shock were weak, and between 2 and 8 if the shock is of finite strength (cf. Figure 21, Section 10.2). For shock strength in the interesting region, 5 to 10 pounds per square inch, this factor is only a little above 2. This, then, is the effect of head-on reflection. As one departs from the point immediately under the bomb, the increase in the overpressure gets even more favorable because of the properties of oblique reflection mentioned previously. The highest amplification occurs soon after Mach reflection sets in. After this it drops again as incidence becomes more and more glancing. Since the blast decays with distance and the free air peak overpressure drops, it is clearly most advantageous to get the greatest boosting factor where the blast pressure is just marginal for the desired type of damage. One should, therefore, choose the height of burst so that the maximum amplification occurs at that point.

Since the optimum amplification occurs for early Mach reflection the height of burst is to be determined by the requirement that Mach reflection sets in at about the limit of B damage.[21] At this point the amplification

(21) If it is desired to maximize A damage, the height of burst should be modified so that Mach reflection starts correspondingly earlier.

factor for overpressure can be as high as 3 (cf. Section 10.3), but it seems safer to count on a somewhat smaller value and consider higher values of peak overpressure, because of various dissipative mechanisms (cf. Section 10.1). The method by which the optimum amplification is properly positioned requires some further discussion. Actually, when the target, for example the wall of a house, is struck, it receives two blows if there is regular reflection by the ground in its vicinity: one by the direct and one by the reflected blast wave. If these two waves are close together they both act as one blast. If they are far apart, i.e., the angle of reflection is far from 90°, then these two shock waves hit the larger part of the wall with a considerable lag between their times of arrival. (As long as the reflection is regular the two shocks would arrive simultaneously at the ground but would be separate at all points above the ground. The separation between shocks increases with distance off the ground.) In this case dissipative and other unfavorable effects may act between the two shocks. Clearly, the best situation from this point of view is one in which the two shocks are merged together, which happens in the stem of the Y. Hence the house should be hit by this stem. As was pointed out, it is desirable to have the Mach effect in its early stages just as the distance at which the type of damage under consideration ceases. Now if one wishes to destroy a wall, then the stem of the Y should cover the entire wall. Consequently the height of burst should be so chosen that the stem is about as high, or higher than the target, about at the distance B damage ceases.

In view of these considerations and the validity of the peak pressure criterion (cf. Section 10.1) we determine the proper height of burst as follows:

(1) The peak pressure required to inflict a given type of damage, B damage, for example, is known: from 3 to 9 pounds per square inch.

(2) An amplification in the overpressure of at least 2 can be expected.(22)

---

(22) This is approximate; the actual amplification is determined experimentally, as described in Section 10.4.

---

(3) The stem of the Mach Y should be about equal to the target height.

By 1, 2 the bomb must be burst at a distance where the peak pressure is something less than half of the peak pressure required according to the above. The height of burst is determined by 1, 2 in conjunction with requirement 3 according to the procedure described in Section 10.4.

We can now proceed to a statement of the height of burst and the damage radius in a few selected cases. On the basis of the Trinity test and the combat drop at Nagasaki we may assume an equivalent blast tonnage of 10 and 20 kilotons. The peak pressures required for B damage may vary according to the structures involved, and even for typical residential property from country to country. In Japan 3 pounds per square inch may be critical; in the U.S.A., England, and Germany, 6 to 9 pounds per square inch might be required. If one is conservative one may use a higher value.(23)

---

(23) In connection with the planning of this project, values of between 3 and 6 pounds per square inch were usually talked about. The height of burst was finally determined on the basis of a 6 pounds per square inch estimate, partly in order to be conservative and partly because we were not certain what the tonnage of the blast would be. The uncertainty in tonnage was due to the probability of predetonation and general uncertainties necessarily affecting the first trials.

The following table gives the heights of burst consistent with the pressure levels of 10 and 6 pounds per square inch and stem heights of 30 and 100 feet. The table is obtained from experiments as discussed in Section 10.4. Table 10.5

gives the heights of burst for 10 and 20 kilotons TNT which should be used if two heights (30 and 100 feet) are to be attained by the stem of the Mach Y at the positions, R, where the peak overpressures are 10 and 6 pounds per square inch. A more complete table can be found in Section 10.4.

Table 10.5

W = 10 kilotons

Overpressure Pr (psi)	Distance R (ft)		Height of burst H (ft)	
	Y = 30 ft.	Y = 100 ft.	Y = 30 ft.	Y = 100 ft.
10	3600	3300	2000	1400
6	5300	5000	2600	2000
W = 20 kilotons				
10	4600	4300	2500	1900
6	6600	6500	3300	2800

On the basis of such considerations it was found that a nuclear bomb in the 10-20 kiloton range should be burst at an altitude of 1500-3000 feet to maximize blast damage. Such heights of burst would, in addition, avoid both fusing and cratering the earth.

10.5-1 Accuracy of Height of Burst

It is appropriate here to insert a few remarks about the accuracy to which it is desirable to fix the height of burst since this requirement is immediately reflected in the complexity of the fusing apparatus required. An accuracy of ± 50 feet, for example, dictates a radar activated fuse whereas an accuracy of ± 250 feet might be attained by a relatively simple clock mechanism which could be pre-set in the airplane, assuming that the bomb is

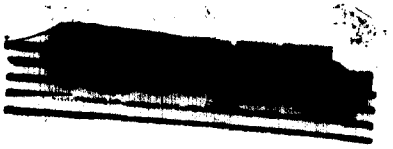

carried by airplane.

There are several factors which limit the accuracy to which the bomb should be fused. They are:

(1) Experimental errors in measuring triple point trajectories and pressures in the blast configuration.

(2) Lack of criteria as to the precise height the stem of the Mach Y should attain at the limiting pressure which it is desired to enhance by irregular reflection.

(3) Imperfect knowledge of the target configuration and hence of the pressure which is required to produce marginal destruction.

(4) The variable nuclear and hence blast performance of the bomb. It can be stated with reasonable certainty, say with a probability of 0.95, that the nuclear efficiency will be greater than 1/2 the rated efficiency.(24)

(24) This was calculated by R. F. Christy for a Christy type gadget, but is not sensitively dependent on the specific implosion design.

One feature which makes the choice of the heights of burst less seriously dependent on the above facts is the relative insensitivity of the value of the area over which the pressure exceeds a certain prescribed value to the height at which the bomb is burst. A variation in height of burst of ± 450 feet, for example, produces no more than a 20 per cent variation in the area defined above in the pressure region 5 to 10 pounds per square inch for blast tonnages of 10 to 20 kilotons. In view of this fact, and those cited above, a very conservative limit on the accuracy to which the bomb should be burst when used in area attack is ± 250 feet.

UNCLASSIFIED

UNCLASSIFIED